Investigating the Interactions Between Bone Marrow Macrophages and Acute Myeloid Leukaemia

By

Jamie Aaron Moore, BSc, MSc.

A thesis submitted for the degree:

Doctor of Philosophy

Norwich Medical School
Department of Molecular Haematology
The University of East Anglia, Norwich, UK

Date of submission: 16th September 2022

Declaration

I declare that the contents of this thesis entitled “Investigating the Interactions Between Bone Marrow Macrophages and Acute Myeloid Leukaemia” was undertaken and completed by myself, unless otherwise acknowledged and has not been submitted in an application for another degree or qualification in this or any other university or institution.

This thesis is approximately 57,000 words in length.

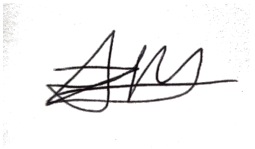

Jamie Aaron Moore

Acknowledgments

It's funny, the journey of my PhD, no, my journey in science, is akin to the simple motion of walking. Once you get going, all you need is put one foot in front of the other, each step takes you further towards your goal, whether you know what that is or not before you set out on the journey is another question. That path is not absolute, and many twists and turns, dead ends and retracing steps may need to be trodden. But that notion – putting one foot in front of the other - moves you forward. It is at this point, in my scientific journey, I take one step to the side and peer back at the path I have walked. I no longer see the start, but I know where it was. That is the most humbling notion for me, knowing that each step I have taken is a step of progression. 'A man cannot discover new oceans unless he has the courage to lose sight of the shore.' Alas, the journey doesn't stop here, just another path appears and a direction taken.

Foremostly, I wish to share my sincere gratitude to all the AML patients, their families and NHS staff, without them, this research would have not been possible. To my amazing supervisors, Stuart and Kris, thank you for everything. You are great leaders, understanding humans and such a joy to be around. The special night, 'flossing,' in Florida will always be in my vault. To my fantastic colleagues who I've had a pleasure to work with - Jayna, Charlotte, Aisha, PK, David, Rebecca, and Kat. I collected many great memories with you, from realising Charlotte should actually open her own bakery (those brownies!), to getting caught listening to some awful music while performing a Seahorse (N-Dubz). There are many more memories, but I want to thank you for the great teamwork that made my research not only possible, but enjoyable.

I am, at heart, a family man. So, none of this would be possible without my wonderful family. I may provide the feet to take the steps, but you are my heart, my drive, and the reason I want to better myself to keep moving forward. I am a lucky person to have you all, especially to point out the directions overlooked by me. Without that support, those first steps may never have been taken. Thank you.

Abstract

Acute myeloid leukaemia (AML) is a heterogeneous and lethal malignancy that currently has no cure. Even in patients that can undergo intensive chemotherapies often relapse due to minimal residual disease sequestered within the bone marrow (BM) microenvironment. The BM microenvironment is a highly complex organ to allow support of haematopoiesis via regulation of the haematopoietic stem cells (HSC). HSC reside in specific niches and are regulated by many cell types, such as BM macrophages. In AML, BM macrophages interact with leukaemic cells to promote AML progression, via regulation of phagocytosis. Phagocytosis in macrophages can occur through LC3, termed LC3 associated phagocytosis (LAP). Impairment of LAP has been shown to supress solid tumour growth, however, the role of LAP in AML has not been defined. In this thesis, I investigated the role of LAP in BM macrophages within the BM microenvironment of AML.

This research shows that depletion of BM macrophages increased AML growth and that LAP is the predominate method that is used to phagocytose dying cells in the AML microenvironment. Inhibition of LAP led to accumulation of apoptotic debris in the BM, resulting in accelerated leukaemic growth. Mechanistically, LAP of AML apoptotic bodies (ABs), by BM macrophages, resulted in STING activation. Mitochondria from AML ABs were processed by BM macrophages via LAP. Moreover, mitochondrial DNA from AML ABs was responsible for the induction of STING activation in BM macrophages. STING activation suppressed AML growth via increased phagocytosis potential in BM macrophages. Furthermore, the phosphatidylserine recognition receptor TIM4 is required for the control of AML growth and the expression of TIM4 in LAP deficient BM macrophages is reduced. Together, these findings show how BM macrophages interact with apoptotic AML cells to supress AML growth in a LAP dependent mechanism.

TABLE OF CONTENTS

List of publications and conference papers

Moore JA, Mistry JJ, Hellmich C, Horton RH, Wojtowicz EE, Jibril A, Jefferson M, Wileman T, Beraza N, Bowles KM, Rushworth SA. LC3-associated phagocytosis in bone marrow macrophages suppresses AML progression through mitochondrial DAMP induced STING activation. (2022) Journal of Clinical Investigation

Moore JA, Mistry JJ, Rushworth SA. Mitochondria and the Tumour Microenvironment in Blood Cancer. In: Birbrair A. (eds) Tumor Microenvironment. Advances in Experimental Medicine and Biology, vol 1329. Springer, Cham (2021) DOI: 10.1007/978-3-030-73119-9_10

Johnson BB, Reinhold J, Holmes TL, **Moore JA**, et al. Modelling Metabolic Shifts during Cardiomyocyte Differentiation, Iron Deficiency and Transferrin Rescue Using Human Pluripotent Stem Cells. Metabolites 2022,12,9.

Mistry JJ, Hellmich C, **Moore JA**, Jibril A, Macaulay I, Moreno-Gonzalez M, Di Palma F, Beraza N, Bowles KM, Rushworth SA. Free fatty-acid transport via CD36 drives β-oxidation-mediated hematopoietic stem cell response to infection. Nature Communications 12, 7130 (2021 Dec). DOI: 10.1038/s41467-021-27460-9

Mistry JJ, Hellmich C, Lambert A, **Moore JA**, Jibril A, Collins A, Bowles KM, Rushworth SA. Venetoclax and Daratumumab combination treatment demonstrates pre-clinical efficacy in mouse models of Acute Myeloid Leukemia. Biomark Res 9, 35. (2021 May) DOI: 10.1186/s40364-021-00291-y

Kumar PR, **Moore JA**, Bowles KM, Rushworth SA, Moncrieff MD. Mitochondrial oxidative phosphorylation in cutaneous melanoma. Br J Cancer. (2020 Nov) DOI: 10.1038/s41416-020-01159-y

Mistry JJ, **Moore JA**, Kumar P, Marlein CR, Hellmich C, Pillinger G, Jibril A, Di Palma F, Collins A, Bowles KM, Rushworth SA. Daratumumab inhibits acute myeloid leukaemia metabolic capacity by blocking mitochondrial transfer from mesenchymal stromal cells. Haematologica. (2020 Mar) DOI: 10.3324/haematol.2019.242974.

Hellmich C, **Moore JA**, Bowles KM, Rushworth SA. Bone Marrow Senescence and the Microenvironment of Hematological Malignancies. Front Oncol. (2020 Feb) DOI: 10.3389/fonc.2020.00230.

Mistry JJ, Marlein CR, **Moore JA**, et al. ROS-mediated PI3K activation drives mitochondrial transfer from stromal cells to hematopoietic stem cells in response to infection. PNAS 116 (49). (2019 Dec) DOI:10.1073/pnas.1913278116.

American Society of Hematology 2021: Abstract # 3441 LC3-Associated Phagocytosis in Bone Marrow Macrophages Suppresses AML Progression through Mitochondrial DAMP Induced Sting Activation
Awarded ASH Abstract Achievement Award

American Association for Cancer Research Annual Meeting 2021: Abstract # 2752 LC3-associated phagocytosis in bone marrow macrophages suppresses AML progression through TIM-4 mediated STING
Awarded the Scholar-in-Training Award

American Association for Cancer Research Annual Meeting 2020: Abstract # 3951 Acute myeloid leukemia export vesicles containing mitochondria which induces a senescent phenotype in bone marrow macrophages

American Society of Hematology 2019: Abstract # 1427 Acute Myeloid Leukemia Export Mitochondria in Extracellular Vesicles Which Induces Pro-Tumoral Changes in Bone Marrow Macrophages
Awarded ASH Abstract Achievement Award

List of figures

List of tables

List of abbreviations

AAM	AML associated macrophages
AB	Apoptotic bodies
AC	Apoptotic cells
ALL	Acute lymphoblastic leukaemia
AML	Acute myeloid leukaemia
APAF1	Apoptotic peptidase activation factor 1
ara-C	Cytosine arabinoside
ARG-1	Arginase-1
ATP	Adenosine triphosphate
BafA1	Bafilomycin A1
BM	Bone marrow
BMDM	Bone marrow derived macrophages
BMM	Bone marrow macrophages
BMSC	Bone marrow stromal cell
BSA	Bovine serum albumin
BSG	Basigin
C/EBPα	CCAAT/enhancer-binding protein
CCD	Coiled-coil domain
cGAMP	2′3′ cyclic GMP-AMP
cGAS	cyclic GMP-AMP synthase
CGRP	Calcitonin gene-related peptide
CL	Clodronate liposomes
CLL	Chronic lymphoblastic leukaemia
CLP	Common lymphoid progenitor
CML	Chronic myeloid leukaemia
CMP	Common myeloid progenitor
CPT1a	Carnitine palmitoyltransferase 1a
Ct	Cycle threshold
DAMPs	Damage associated molecular patterns
ddC	2′,3′-dideoxycytidine

DiI	Vybrant-DiI
DISC	Death-inducing signalling complex
DLS	Dynamic light scattering
DMEM	Dulbecco's Modified Eagle's Medium
DMU	Disease modelling unit
DNA	Deoxyribose Nucleic Acid
DPP4	Dipeptidyl peptidase 4
ECM	Extracellular matrix
EGFR	Epidermal growth factor receptor
ER	Endoplasmic reticulum
ERGIC	ER/Golgi intermediate compartment
EtBr	Ethidium bromide
EV	Extracellular vesicle
FABP4	Fatty-acid binding protein 4
FACS	Fluorescence activated cell sorting
FADD	Fas associated death domain
FAS	Fas cell surface death receptor
FASL	FAS ligand
FcγR	Fc segment of Ig-G
FFA	Free-fatty acids
FLT3	Flt-3 ligand
FMO	Fluorescence minus one
G-CSF	Granulocyte-colony stimulating factor
GAPDH	Glyceraldehyde 3-phosphate dehydrogenase
GBP2	Guanylate-binding protein 2
gDNA	Genomic DNA
Gfi1	Growth factor independence 1
GFP	Green fluorescent protein
GJC	Gap junction channels
GMP	Granulocyte-macrophage progenitor
GOI	Gene of interest
HEA	Haematopoiesis enhancing activity

HSC	Haematopoietic stem cell
HSPC	Haematopoietic stem and progenitor cell
IAP	Inhibitor of apoptosis proteins
IFIT3	IFN-induced protein with tetratricopeptide repeats 3
IFN	Interferon
Ig	Immunoglobulin
IL	Interleukin
IP	Intraperitoneal
IRF	Interferon regulatory factor
IRGB10	Interferon response gene B10
ISG	Interferon-stimulated genes
ITIM	Immunoreceptor tyrosine-based inhibition motifs
IV	Intravenous
LAP	LC3 associated phagocytosis
LCN2	Lipocalin 2
LIF	Leukaemia inhibitory factor
Lin	Lineage
LMPP	Lymphoid-primed multipotent progenitor cell
LPC	Lysophospholipids lysophosphatidylcholine
LPS	Lipopolysaccharide
LSK	Lin-Sca+c-Kit+
LT-HSC	Long Term haematopoietic stem cell
M-CSF	Macrophage-colony stimulating factor
MACS	Magnetic activated cell sorting
mCherry AML cells	mCh-AML
mCherry AML-derived AB	mCh-AB
MDS	Myelodysplastic syndrome
MEM	Minimum Essential Medium Eagle
MEP	Megakaryocyte-erythroid progenitor
MFG-E8	Milk fat globule epidermal growth factor 8
MFI	Mean fluorescence intensity
MHC-II	Major histocompatibility complex II

MIF	Macrophage inhibitory factor
MM	Multiple myeloma
MMP-2	Metalloproteinase-2
MOMP	Mitochondrial outer membrane permeabilization
MPP	Multipotent progenitor
MPT	Mitochondrial permeability transition
MSC	Mesenchymal stem cell
mtAB	Mitochondria containing AB
mtDNA	Mitochondrial DNA
MTG	MitoTracker Green
MTR	MitoTracker Red
NFκB	Nuclear factor-κB
NK Cell	Natural killer cell
NNUH	Norfolk and Norwich University Hospital
NO	Nitric oxide
NOS-2	NO synthase-2
NOX2	NADPH oxidase 2
NP-1	Neuropillia-1
NPTN	Neuroplastin
NSG	NOD SCID Gamma
NTRK3	Neurotrophic receptor tyrosine kinase 3
OCN	Osteocalcin
OSX	Osterix
OXPHOS	Oxidative phosphorylation
PB	Peripheral blood
PBMC	Peripheral blood mononuclear cells
PBS	Phosphate buffered saline
PD-ECGF	Platelet-derived endothelial cell growth factor
PI3KC3	Phosphatidylinositol-3-kinase class III
PI3P	Phosphatidylinositol 3-phosphate
PPARy	peroxisome proliferation-activated receptor
PRR	Pattern recognition receptors

PtdSer	Phosphatidylserine
RANK	Receptor activator of nuclear factor κ-B
RANKL	Receptor activator of nuclear factor κ-B ligand
RIPKI	Receptor interacting serine/threonine kinase 1
RNA	Ribose Nucleic Acid
ROS	Reactive oxygen species
RT	Room temperature
RT-qPCR	Real time quantitative polymerase chain reaction
RTKs	Receptor tyrosine kinases
S1P	Sphingosine-1-phosphate
SCF	Stem cell factor
SCID	Severe combined immunodeficient
SHBG	Sex hormone-binding globulin
SIRPα	Signal regulatory protein-α
SMAC	Secondary mitochondrial activator or caspases
SNP	Single nucleotide polymorphism
SP	Substance P
SPHK1	Sphingosine kinase 1
ST-HSC	Short term haematopoietic stem cell
STING	Stimulator of interferon genes
TAMs	Tumour associated macrophages
TAM receptors	TYRO3, AXL and MER
TBK1	TANK-binding kinase 1
TCA cycle	Tricarboxylic acid cycle
TCR	T cell receptor
TGF	Transforming growth factor
TIM4	T cell immunoglobulin and mucin domain-containing molecule
TLR-4	Toll-like receptor-4
TNF	Tumour necrosis factor
TNT	Tunnelling nanotube
TP	Thymidine phosphorylase
TPO	Thrombopoietin

TRAIL	TNF superfamily member 10
VCAM-1	Vascular cell adhesion molecule 1
VEGF	Vascular endothelial growth factor
VIC	2′-chloro-7′phenyl-1,4-dichloro-6-carboxy-fluorescein
XIAP	X-linked inhibitor of apoptosis
$\Delta\Psi m$	Mitochondrial membrane potential

1. Introduction

1.1 The bone and bone marrow

Two types of bone tissue exist, cortical and cancellous bone. The combination of which gives bone its unique density properties vital to the strength and flexibility of bone. It is within the bone that bone marrow (BM) is located. BM is a soft, spongy tissue that resides within cavities of bones and is the primary source of haematopoiesis. Specifically, BM located in the mid-section of peripheral bone generally consists of adipose tissue, commonly referred to as yellow marrow. Whereas BM situated in the axial skeleton houses both the yellow marrow and the haematopoietic tissue. Due to the high content of haem chromogen in the haematopoietic tissue, it gives the BM a red colour and as such is often called red marrow (Figure 1.1A) [1]. It is here in the red marrow that the primary function of the BM, haematopoiesis, is performed giving rise to ~$5x10^{11}$ blood cells each day and is responsible for the generation of mature blood cells [2]. The BM contain a dense neurological and vesicular network that is innervated with nerves as well as arterioles, capillaries and sinuses. It also contains cells of a heterogeneous population and together they are either directly involved in haematopoiesis or act to support it [3]. The supporting cells within the BM microenvironment are all needed to provide the correct stimuli for the maintenance of normal haematopoiesis.

In flat bone, BM acquires nutrients by numerous blood vessels entering the BM via small and large nutrient canals. In long bone, nutrients are supplied to the BM via nutrient canals which consists of nutrient veins and the main nutrient artery that enters the BM cavity, running longitudinally throughout the centre of the bone. It then branches out to the periphery of the surrounding bone via thin-walled arterioles and capillaries where they accumulate to specialist vascular formations called sinuses or sinusoids [1]. These sinusoids undergo drainage via collecting venules that lead back towards the centre of the cavity and finally to the nutrient veins. Additionally, capillaries from the nutrient artery extend into Haversian canals, returning back to the BM cavity before opening into the sinusoids. As such, blood flow within the BM cavity

occurs in a circular pattern, from the centre of the bone towards the periphery of the BM cavity, finally flowing back towards the centre [4].

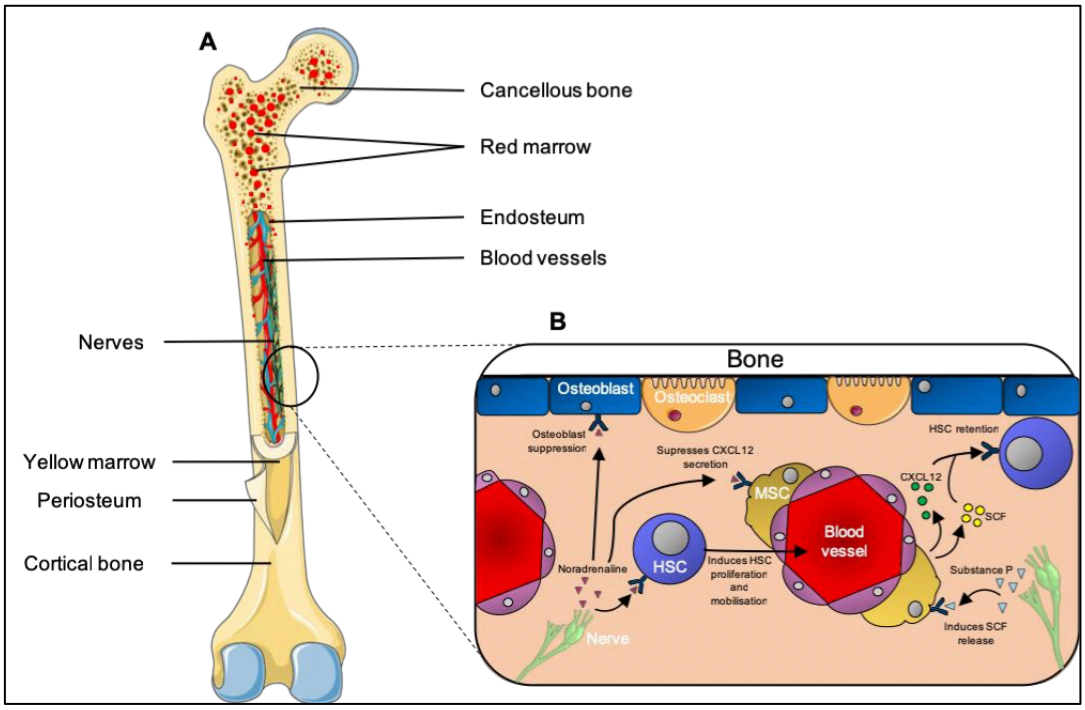

Figure 1. 1 Cross-section of the bone marrow

(A) The bone anatomy, cancellous and cortical bone, make up the unique properties of the bone. The endosteum encases the blood vessels, nerve fibres and red marrow. The periosteum encases the yellow marrow. (B) Nerve fibres release noradrenaline and Substance P, which acts upon haematopoietic stem cells (HSC), osteoblasts and mesenchymal stem cells (MSC) in various ways, leading to HSC retention, proliferation, and mobilisation. SCF – Stem cell factor.

All adult haematopoietic stem cells (HSCs) reside in BM niches that are highly specialised and support HSCs via influencing their different fates such as retention, mobilisation into the peripheral blood and differentiation. These niches are closely linked to the neurovascular network and contain several stromal elements, such as endothelial cells and mesenchymal stem cells. Further cells such as macrophages, adipocytes, and osteoprogenitor cells all influence the fate of HSCs. The diversity in cell types provides essential signals to the HSCs and their progenitors in the form of cell-surface ligands, cell to cell contact and a multitude of soluble factors [1]. Thus, the BM is one

of the largest and most complex organs in the body, with the primary role of the BM, haematopoiesis, giving rise to every blood cell needed for survival.

Innervation of the BM by autonomic and sensory nerve fibres results in neurological regulation of fundamental physiological processes, such as haematopoiesis and bone formation [5]. For example, activation of ß2 adrenergic receptors via noradrenaline leads to reduction of an HSC retention factor, CXCL12, acting to suppress osteoblast function and promoting HSC motility. Ultimately, terminals of sympathetic nerve fibres regulate the efflux of haematopoietic stem and progenitor cells (HSPC) from the BM into the circulation. Mobilisation of HSPC into the peripheral blood allows direct relocation of HSC to sites of need, such as in a tissue injury. Specifically, differentiation into macrophages polarised towards an anti-inflammatory phenotype (M2) has been shown to facilitate wound healing [6]. Moreover, the neuropeptides Substance P (SP) and Calcitonin gene-related peptide (CGRP) released from sensory nerve terminals have been shown to be involved in the stimulation of HSPC, with CGRP acting upon granulocyte-macrophage precursor cells directly while SP mediates the production of SCF and IL-1, important in HSC retention [7, 8]. Collectively, it demonstrates a hardwired process where autonomic and sensory nerve fibres are major influencers on HSC activity, retention and release within the BM (Figure 1.1B).

1.2 Haematopoiesis

At the heart of haematopoiesis is the HSC. HSCs are defined by their self-renewal capacities and pluripotency, having the ability to generate any of the diverse range of haematopoietic cell types. Initially, haematopoiesis starts in embryogenesis with the emergence of the first HSC appearing within the aorto-gonado-mesonephros region [9]. Haematopoiesis then switches to the foetal liver before locating to the BM where HSCs remain located for the life of the organism [10]. Though BM is the location where the majority of haematopoiesis occurs, during times of haematopoietic stress, haematopoiesis can occur in the spleen and liver [11]. In adults, long-term HSCs are found in specific niche microenvironments, closely associated with the endosteum and existing in hypoxic conditions [12, 13]. It is here that long-term HSCs reside in a mainly non-replicative and quiescent state [14]. However, in situations where the haematopoietic system is stressed, such as in infections, the quiescent HSCs are pushed towards cell cycling, leading to an increase in downstream progenitor cells and expansion of immune cells to target the infection [15].

Traditionally, haematopoiesis had been shown in a hierarchal differentiation tree, with long-term HSCs existing at the apex and branching off towards more terminal fated, mature cells. HSCs exist in a heterogeneous pool that is functionally and molecularly diverse, allowing for early lineage specification [16, 17]. Long-term, intermediate and short-term HSCs as well as multipotent progenitor cells (MPP) are thought to all be contained within the HSC pool, where different states of HSCs are more heterogeneous in terms of both self-renewal and differentiation properties [18]. Identification of HSPC can be determined by cell surface markers. Specifically, immature multipotent cells lack markers found on mature cells (lineage$^-$) while they express stem cell antigen (Sca)-1 and CD117 (c-Kit). All HSC activity happens within the Lineage$^-$/Sca-1$^+$/c-Kit$^+$ (LSK) fraction, with approximately one in 30 cells being a HSC [19]. Isolation of HSCs from LSK fractions can be achieved by the use of CD150$^+$/CD48$^-$/CD34^{LOW} markers [20].

From this pool, HSCs give rise to the common myeloid progenitor (CMP) and the lymphoid-primed multipotent progenitor (LMPP). Both subset of progenitors contributes towards the heterogenous population of granulocyte-monocyte progenitors (GMP) which ultimately forms the granulocytes; eosinophils, basophils and neutrophils, as well as monocytes that give rise to macrophages [21]. CMPs further differentiate to the megakaryocyte-erythrocyte progenitor (MEP) that produce megakaryocytes (for thrombocyte production) and erythrocytes. The LMPP also gives rise to the common lymphoid progenitor (CLP) and it is this progenitor that differentiates towards T-lymphocytes, natural-killer (NK) cells or B-lymphocytes that can further differentiate towards antibody producing plasma-cells and memory B-lymphocytes (Figure 1.2). Excluding erythrocytes and megakaryocytes, cells from both LMPP and CMP give rise to all cells of adaptive and innate immunity.

However, the complexity involved in haematopoiesis cannot be simplified completely, as bypass of traditional pathways from HSC to mature cells may occur. As such, more direct pathways, from HSC to mature cells, can coexist in unison with existing progenitor hierarchies [22]. Thus, the traditional differentiation tree view has evolved towards a continuum of differentiation, where fated cells emerge from low- primed undifferentiated HSPC without major transitions through multipotent or even bipotent steps [23-25]. This may have advantages in rapid response towards stress, such as in infections and malignancies.

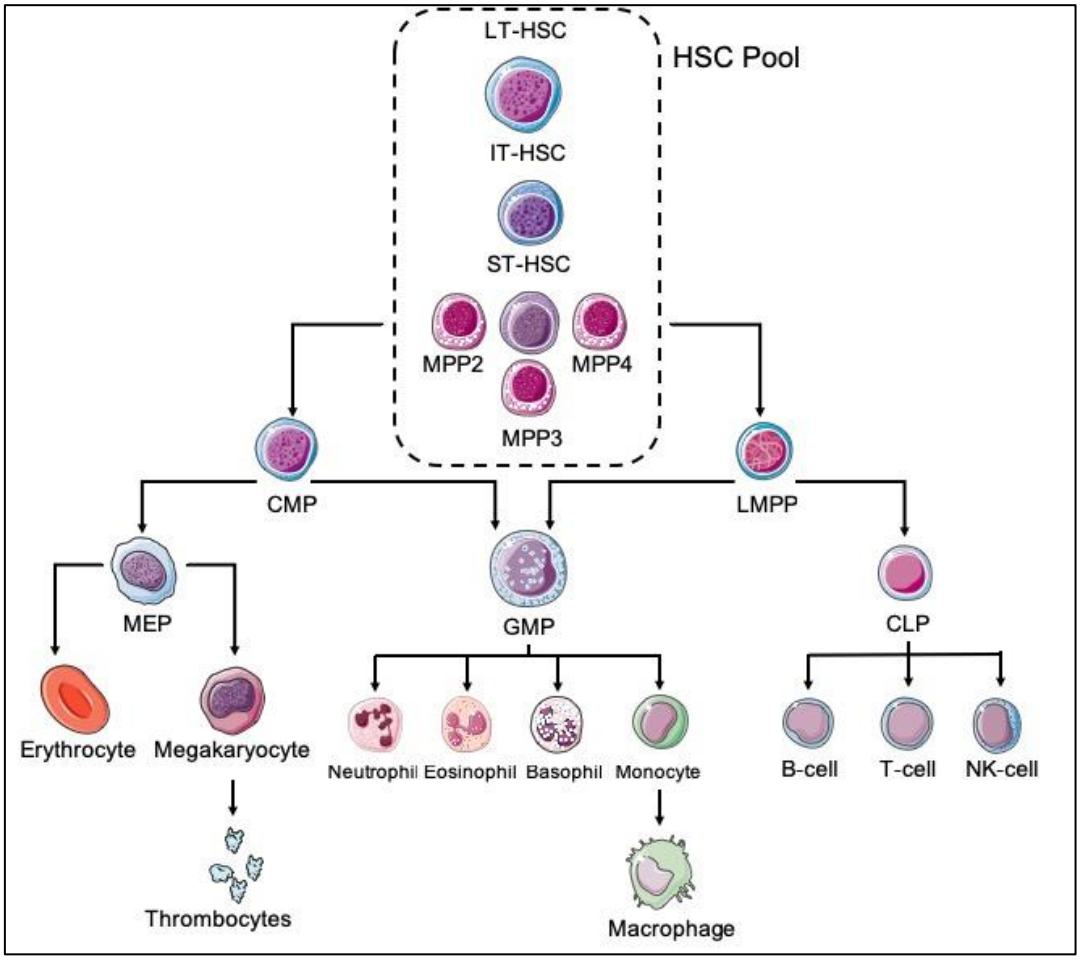

Figure 1. 2 Haematopoiesis diagram

Haematopoiesis is the continued self-renewal and production of mature blood cells from immature haematopoietic stem cells (HSC). Traditionally, long term (LT) HSC are quiescent cells and rarely differentiate down the haematopoietic lineage. They are contained within a pool of HSC that include more mature HSC, including intermediate (IT) and short term (ST) HSC, as well as multipotent progenitor cells (MPP). These cells then have the ability to further differentiate towards certain progenitors, such as the common myeloid (CMP) and common lymphoid (CLP) progenitors, which go on to develop the various types of blood cells. It is envisioned that in times of stress, the multi-step differentiation pathway can be bypassed to meet demands. LMPP - lymphoid-primed multipotent progenitor, GMP - granulocyte-monocyte progenitors, MEP - megakaryocyte- erythrocyte progenitor, NK-cell – natural killer cells.

1.3 Cells of the BM microenvironment

HSPCs are supported by many cell types that may not be directly involved in haematopoiesis, but research has established that many of these cells are needed within the HSPC niche for correct maintenance and differentiation of HSPCs (Figure 1.3).

1.3.1 Bone marrow stromal cells

Bone marrow stromal cells (BMSCs), also classed as BM mesenchymal stem cells, have many roles, for instance the regeneration of tissues such as adipose, bone, cartilage and muscle via differentiation towards certain lineages including osteoblasts, osteoclasts and adipocytes [1, 26]. Importantly, BMSCs are responsible for creating a supportive microenvironment for HSCs. Secreted cytokines and growth factors, such as stem cell factor (SCF-1), interleukins (IL-1, -6, -7, -8, -11, -14 & -15) and leukaemia inhibitory factor (LIF), are produced by BMSCs that have autocrine and paracrine effects upon HSCs [27, 28]. The multipotency of BMSCs allows differentiation towards cells within the BM microenvironment, thus supporting HSC regulation. Markers of BMSCs, such as CD146, have not only allowed identification of BMSCs but have also helped to establish that they are predominantly located near blood vessels and sinusoids within the BM [29, 30].

Importantly, BMSCs are the major producers of SCF-1 and CXCL12, critical factors for HSC maintenance [31]. Studies that have deleted SCF or CXCL12 led to the elimination of HSCs in the BM, consequently highlighting BMSCs as important cells in supporting the HSC niche [32, 33]. BMSCs can further regulate HSCs according to which subset they belong to and which local niche they are attributed to. $NG2^{+}$ $LepR^{-}$ BMSCs are located toward small arteriole regions and maintain HSCs in a quiescent state within the arteriolar niches. $NG2^{-}$ $LepR^{+}$ BMSCs on the other hand are located adjacent to sinusoids and contribute to perisinusoidal niches driving HSC proliferation [34]. The distribution of HSCs between these two niches is dependent on HSC cell cycling activation [31]. Other stromal cells generated from BMSCs are also

thought to be key players in haematopoiesis, specifically forming HSC microenvironments. Together, this information highlights the importance of BMSCs in the support, maintenance and differentiation of HSCs.

1.3.2 Osteoblast lineage cells

The lineage of osteoblasts is a set of BMSC derived cells and include immature osteoblasts, mature osteoblasts and osteocytes [31]. The development of mature osteoblasts from their BMSC precursors requires certain transcription factors, such as RUNX2 to be switched on. Though the primary function of matrix synthesising osteoblasts is the formation of bone, they also have a role in haematopoiesis. Early osteoblast progenitors have been found to support B-lymphocyte differentiation via Osterix positive (OSX+) osteoprogenitor release of IL-7 [35, 36]. Mature Osteocalcin positive (OCN+) osteoblasts producing DLL4, a Notch ligand, has been shown to be essential for CLP development towards T-lymphocytes [37]. However, studies looking at the maturation stage of osteoblasts have indicated that immature osteoblasts with high levels of RUNX2, common in more immature osteoblasts, mediated haematopoiesis-enhancing activity (HEA) specifically HSC regulation via CD166 [38, 39]. Together, these studies suggest that immature osteoblasts may have a role in HSC expansions and maintenance while mature osteoblasts assist with the development of mature lymphocytes.

Osteocyte differentiation occurs when osteoblasts become embedded in newly formed bone matrix. Osteocytes are important in detecting mechanical stress, triggering signals to osteoblasts and osteoclasts in accordance with situational needs. Although embedded in bone, osteocytes are important in haematopoiesis regulation. Osteocytes have been shown to be vital for mobilisation of HSPC in response to granulocyte-colony stimulating factor (G-CSF) [40]. Furthermore, osteocytes may have a critical role in supporting the stroma within the BM [41]. This indicates that osteocytes may influence haematopoiesis in the support and mobilisation of HSCs and down-stream differentiated cells of the haematopoietic system.

1.3.3 Adipocytes

Adipocytes arise from BMSCs, with peroxisome proliferator-activated receptor gamma (PPARγ) and CCAAT/enhancer-binding protein alpha (C/EBPα) believed to be important transcription factors in their differentiation [31]. In adult BM, approximately 70% of the volume is made up of BM adipose tissue [42]. It is thought that BM adipocytes act as a negative regulator of haematopoiesis, with studies showing adipocytes supressing haematopoiesis, specifically in stressed or ageing conditions [43, 44]. Moreover, cell-to-cell contact is a key method adipocytes employ in the regulation of haematopoiesis. Adipocytes can block downstream differentiation of HSCs into granulocytes via neuropilia-1 (NP-1) interactions [45]. Further, adipocytes can cause HSC arrest and apoptosis via cell-to-cell contact [46].

Not only has cell-to-cell contact been shown to regulate haematopoiesis, but the secretion of cytokines and various factors have an important effect on HSPC. Transforming growth factor beta-1 (TGF-ß1) secreted from adipocytes acts as an inhibitor of haematopoiesis, while Lipocalin 2 (LCN2) and Dipeptidyl peptidase-4 (DPP4) both act to negatively regulate haematopoiesis via inhibition of erythroid progenitor differentiation and cleavage of important haematopoietic cytokines, respectively [47-49]. Thus, the role of adipocytes in haematopoiesis focuses on the negative regulation of HSPC.

1.3.4 Endothelial cells

Vascular forming endothelial cells are major regulators of metabolism, oxygen distributing and homeostasis by forming extensive connecting networks [50]. Additionally, the endothelial cellular network is instrumental in haematological cell trafficking. Importantly, endothelial cells have been shown to interact directly and via secreted factors with stem and progenitor cells to regulate organ regeneration and homeostasis [51]. BM specific endothelial cells not only form a physical barrier preventing circulation erythrocytes and thrombocytes entering the BM but are also responsible for regulating haematopoiesis [12]. As well as supporting HSC niches they also provide

angiocrine signals that have roles in haematopoiesis directly and HSC development [32].

Endothelial cells form a network of blood vessels within the BM, these blood vessels contribute to HSC regulation due to the permeability of the specific blood vessel subtype. As such, less permeable arterial blood vessels are responsible for HSC quiescence by keeping HSCs in a low reactive oxygen species (ROS) state, where sinusoids that are more permeable stimulate HSC activation as well as being the site for both immature and mature lymphocyte trafficking [50]. Consequently, having increased blood vessel permeability exposes haematopoietic and progenitor cells to blood plasma which leads to increase ROS levels, as such the long-term renewal and survival of HSCs are compromised whilst their migration and differentiation capacities are enriched. Hence, endothelial cells have an influence on HSCs regulation and their location dictates which state HSCs are retained in.

1.3.5 Megakaryocytes

Megakaryocytes (MKs) are derived from HSCs and are the largest cell in the BM. Accounting for 0.05-0.1% of cells within the BM, MKs are one of the rarest. The primary role of MKs are to produce thrombocytes to prevent bleeding and to reduce blood vessel damage. In the BM, MKs are located centrally near sinusoidal cells, allowing for thrombocyte dissemination into the circulation [2]. Further to this, MKs are significant influencers of bone formation as well as HSC maintenance and quiescence, with CXCL4 identified as a major factor supporting this role. Their location has been demonstrated to be adjacent to HSCs where a functional relationship occurs regulating HSC quiescence and HSC pool size. The removal of MK also causes HSC proliferation, further suggesting MK maintain HSCs in a quiescent state within the niche [52, 53]. Moreover, factors released from MKs allows HSC binding at specific sites within the BM, this maintains HSC quiescence through HSC proliferation and differentiation inhibition [54]. Additionally, indirect regulation of haematopoiesis can occur via MK interactions with osteoblasts, specifically via increase expression of adiponectin [55]. Together, MKs can act as a negative

regulator of haematopoiesis, specifically in the maintenance of HSCs in a quiescent state.

1.3.6 Macrophages

Macrophages are mononuclear, phagocytic cells derived from monocytes of the CMP and have critical roles in immunity and tissue homeostasis, with a diverse range of function in both the innate and adaptive immune system. In most tissues, circulating monocytes differentiate into macrophages for phagocytic purposes, that is, the engulfment and digestion of cellular debris, apoptotic cells, pathogens, malignant cells and a range of other targets. Macrophages interact with B and T lymphocytes via cell-to- cell interactions as well as via cytokine, chemokine and reactive radical signalling [56]. Further, macrophages can be either pro-inflammatory or anti-inflammatory activated, resulting in tissue regeneration, destruction and wound healing [57].

BM macrophages were first identified in murine models as supportive cells in the formation of erythrocytes as well as clearance of expelled nuclei from the maturation of erythrocytes [58, 59]. Erythroblastic island macrophages, specifically $CD169^{+}$ macrophages, are regulators of erythropoiesis [60]. Furthermore, $CD169^{+}$ macrophages maintain HSPC localisation [61]. Moreover, BM macrophages can be found centrally in the marrow as well as on the bone lining, in which they support osteoblast function [6]. Though BM macrophages express many surface proteins dependent on their subtyping, the expression of F4/80 or vascular-adhesion molecule-1 (VCAM-1) can be found on the majority of macrophages [62]. The expression of different surface markers has been shown to coordinate with macrophages identification, location and function. Functionally, $CD11b^{+}$ macrophages have been shown to participate in the clearance of necrotic and apoptotic cells, while $VCAM\text{-}1^{+}$ macrophages play a role in adhesion [63, 64]. Moreover, $F4/80^{+}/CD169^{+}/CD11ß^{INT/LOW}$ macrophages are not only found to locally support BMSC but to support the expression of HSC retention factors [62]. It is the support of BMSC functions within the HSC niche that has been studied

widely, however, the specific BM macrophages dependent factors are still to be fully identified [6, 61, 65].

BM macrophages can also play a role in the regulation of circulating HSPC. Within the BM, HSPC homing and attachment is facilitated via CXCL12 binding to their receptor CXCR4, CXCL12 being a chemokine highly expressed in the BM [66]. Macrophage depletion has been shown to increase the number of circulating HSPC [6, 61]. Accordingly, macrophage depletion correlates with the reduction of HSC retention factors, such as VCAM-1 and CXCL12, suggesting BM macrophage depletion increases HSPC efflux from the BM to the circulation [62]. Furthermore, G-CSF can act as a driver in $CD68^{+}$ macrophage lineage cells to promote HSPC mobilisation [67]. Additionally, the clearance of neutrophils by macrophages is crucial in the BM, spleen and liver to main homeostasis of the blood [68]. Phagocytosis via BM macrophages also regulates granulopoiesis and HSPC trafficking. Specifically, macrophages and dendritic cells can supress IL-23 production, an important cytokine for G-CSF and IL-12-dependent neutrophil differentiation and survival via the phagocytosis of senescent neutrophils [69]. Moreover, this process induces HSPC cell mobilisation via the reduction of niche-specific CXCL12 by circadian rhythms and LXR signalling [70]. Taken together, BM macrophages influence haematopoiesis by regulation of granulopoiesis and HSCP trafficking.

Macrophages are a diverse cell type which can be polarised dependent on situational needs, as such macrophages are also central regulators in stressed haematopoiesis. It is the involvement of BM macrophages in the recycling of dying cells and waste products from cells within a stressed haematopoietic microenvironment, such as in haematopoietic malignancies, that this study attempts to understand. First, we explore how cells undergo cellular death and how macrophages deal with this process.

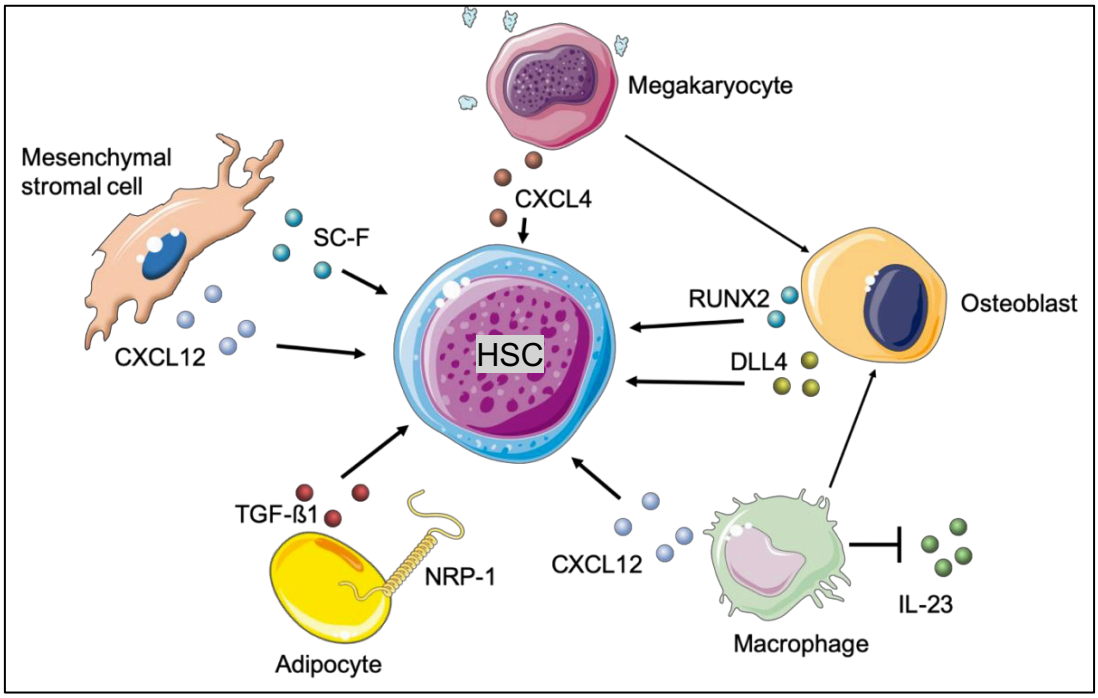

Figure 1. 3 The interaction between haematopoietic stem cells and cells from the bone marrow microenvironment

BMSC can produce CXCL12 and stem cell factor (SC-F) that regulate HSC maintenance. Megakaryocytes release CXCL4 and interact with osteoblasts via adiponectin expression which regulate HSC quiescence. Macrophages secrete CXCL12 that help maintain HSC state, interact with osteoblasts and supress IL-23 for HSC mobilisation. Immature osteoblasts express RUNX2 which mediated haematopoiesis-enhancing activity and DLL4 which has a role in T-lymphocyte differentiation. Adipocytes can directly interact with HSC via nuropilin-1 (NRP-1) to inhibit down-stream differentiation of HSC and the increased release of TGF-ß1 acts to negatively regulate haematopoiesis.

1.4 Cellular death

An average person produces a vast amount of long- and short-lived cells, a consequence of which is the generation of more than 10^{10} dead cells daily [71]. To maintain homeostasis, it is imperative that the disposal of dead and dying cells, along with potentially harmful cells, is achieved efficiently. Though accidental cell death, the sudden and catastrophic death of cells, occurs via the exposure of a multitude of cellular insults (such as temperature change, extreme pH changes and shear forces), the predominant method to deal with the elimination of cells in an organised way is via programmed cell death [72, 73]. Recent research has altered the perspective of cell death from an inevitable process and a consequence of normal cellular life, to a mechanism which allows targeted removal of harmful or damaged cells [74-76].

Necrosis, is not generally seen as a method of programmed cell death, in part because of the lack of any hallmarks of organised cell death, such as cell shrinkage and DNA fragmentation, while exhibiting cellular swelling and ruptured plasma membranes [77]. As such, necrosis is considered a harmful process due to internal cell content exposure and its association to promote local inflammation that can be harmful, such as its ability to facilitate tumour cell growth [78]. Even so, recent research studying the molecular mechanism of necrosis has identified sub classifications of necrosis. For example, mitochondrial permeability transition (MPT)-driven necrosis is triggered by disruptions of the intracellular microenvironment, such as increased oxidative stress, leading to a necrotic phenotype [79, 80]. MPT refers to the loss of permeability of the intra-mitochondrial membrane leading to rapid loss of the mitochondria membrane potential and the breakdown of both mitochondrial membranes and cell death [81].

Since the classification of the 3 types of cell death were reported; type I apoptosis, type II autophagy and type III necrosis [77], the field has progressed to allow more detailed classifications of cell death to include such processes as ferroptosis, NETotic cell death and pyroptosis [80]. The interest in the

following research relies on the process of apoptosis, as such, further information regarding the apoptotic process of cell death are discussed below.

1.4.1 Intrinsic apoptosis

Apoptosis can be initiated intrinsically by a variety of cellular stresses, such as DNA damage, growth factor deprivation, mitotic defects and increased ROS [82-84]. This pathway is also recognised as the mitochondrial, or BCL-2, regulated apoptotic pathway. Cells that undergo apoptosis retain the integrity of their plasma membrane which allows clearance by phagocytotic cells, such as macrophages, in a process known as efferocytosis [85].

The induction of intrinsic apoptosis leads to the widespread and irreversible mitochondrial outer membrane permeabilization (MOMP) [86]. This process is controlled by regulation of pro-apoptotic and anti-apoptotic protein members of the BCL-2 protein family, these groups of proteins share one to four BCL-2 homology (BH) domains (BH1-BH4) [83, 87]. After the induction of the apoptotic stimuli, MOMP is regulated by BCL-2 associated X, apoptosis regulator (BAX) and BCL-2 antagonist/killer 1 (BAK) in which they contain a conserved transmembrane domain and four BH domains [88]. In normal physiological conditions, both BAX and BAK are kept in inactive forms by the pro-survival BCL-2 protein family members, such as BCL-2 and BCL-x [89]. However, during apoptosis, BAX and BAK become activated. This is due to the increased expression and activity of pro-apoptotic BH3-only proteins, which bind with high affinity to pro-survival BCL-2 proteins resulting in their neutralisation [83, 89]. These pro-apoptotic BH3-only proteins include PUMA (p53-upregulated modulator of apoptosis), BIM (BCL2-interacting mediator of cell death) and NOXA (phorbol-12-myristate-13-acetate-induced protein 1) which are primarily activated via transcription upregulation, while BID (BH3 interacting domain death agonist) undergoes post transcriptional activation [90-94]. This allows BAX and BAK to pool mitochondrially, leading to their oligomerisation and assembly into structures that allow pore formation to occur on the outer mitochondrial membrane, thereby inducing MOMP [95, 96].

MOMP is responsible for the release of apoptogenic factors that normally localises within the mitochondrial intermembrane space to the cytosol of the cell [86, 97]. One such factor, cytochrome c, binds directly to apoptotic peptidase activating factor 1 (APAF1) and pro-caspase-9 in a deoxyATP-dependent manner to form the complex known as the apoptosome and leads to activation of caspase-9 [98]. Activated caspase-9 further leads to the proteolytic activation of caspase-3 and caspase-7 which are responsible for the deconstruction of the cell and are known as executioner caspases [99]. The executioner caspases exhort their catalytic activities to destroy cellular components in a controlled manner and are responsible for many of the biochemical and morphological process of apoptosis, including fragmentation of DNA, the production of apoptotic bodies as well as the exposure of phosphatidylserine (PtdSer) on the cell surface [100-103].

Another factor release from the permeabilised mitochondria by BAX/BAK driven MOMP is second mitochondrial activator of caspases (SMAC). SMAC is able to block the activities of X-linked inhibitor of apoptosis (XIAP), which is one of the inhibitors of apoptosis proteins (IAPs) [104, 105]. XIAP is the only IAP member that can offset the apoptotic cascade by binding and physically blocking caspases, such as caspase-3 and caspase-7 [106, 107]. SMAC facilitates apoptosis by allowing the executioner caspases to be functionally active by the blockade of XIAP. The combination of the caspase cascade and the inhabitation of XIAP allows apoptosis to occur more effectively.

The exposure of PtdSer via a caspase dependent manner is essential for apoptotic clearance and acts as an ‘eat-me’ signal for phagocytes. Under normal conditions PtdSer is maintained in the inner membrane of the plasma membrane via the flippases ATP11A and ATP11C [108, 109]. These flippases need a chaperone, such as CDC50A, to retain their location at the plasma membrane and cells that have loss of CDC50A lose their flippases activity and constitutively expose PtdSer externally [108, 110]. However, during apoptosis and the activation of caspase-3, ATP11A and ATP11C cleavage by caspase-3 leads to their inactivation [108, 111]. This inactivation is not sufficient by itself to expose PtdSer on the surface of the cell as the inner to outer

transmembrane exchange requires energy, approximately 15-50 kcal per mol, and as such does not occur freely [112, 113]. To achieve PtdSer externalisation, caspase-3 also cleaves XKR8, a member of the XKR family, which undergoes dimerization to work as a scramblase [114]. Another type of scramblases, those of the transmembrane protein 16 (TMEM16) family, can be utilised via Ca^{2+} activation [115, 116]. The inactivation of ATP11A and ATP11C, along with the activation and dimerization of XKR8 with basigin (BSG) or neuroplastin (NPTN), works to allow translocation of phospholipids between the membrane bilayers and results in the exposure of PtdSer on the cell surface [117]. Exposure of PtdSer at the surface of an apoptotic cell has been shown to be a primary way phagocytes, such as macrophages, recognise and distinguish apoptotic cells from healthy cell to facilitate their engulfment and processing [118-120]. The process of apoptotic cell engulfment, termed efferocytosis, will be discussed later in this section.

1.4.2 Extrinsic apoptosis

Extrinsic apoptosis is initiated by cues from the extracellular microenvironment and driven by plasma membrane receptors [121, 122]. Primarily, extrinsic apoptosis is initiated via two types of receptors: death receptors, which require ligand binding for their activation, or dependence receptors, in which threshold reductions of their ligands results in their activation [123-125].

A number of death receptors have been identified, such as Fas cell surface death receptor (FAS), TNF receptor superfamily member 1A (TNFR1), 10a (TRAILR1) and 10b (TRAILR2) [124, 126-128]. The ligation of the death receptor induces the assembly of dynamic multiprotein complexes localised at the receptors intracellular tail. These include DISC (death-inducing signalling complex), complex I and complex II, which allows activation and functional regulation of caspase-8 or, to a lesser extent, caspase-10 [129, 130].

In regards to FAS and TRAILRs, the ligation of their ligands, FAS ligand (FASLG) and TNF superfamily member 10 (TRAIL) respectively, allows receptor stabilisation to form homotrimers to induce intracellular conformational changes enabling the death domain-dependent association of

FADD (Fas associated via death domain) [131-134]. This allows FADD to drive DISC assembly via the promotion of the death effector domain-dependent recruitment of caspase-8, or caspase-10, and several isoforms of cellular FLICE inhibitory protein (c-FLIP) which is a close relative to capase-8, however, is catalytically inactive [135]. Investigations into the mechanisms regulating caspase-8 activity after death receptor stimulation has provided great insight into this process. Binding of procaspase-8 to FADD at the DISC permits a cascade of events and allows the assembly of a linear filament of procaspase-8 molecule, dependent on their death effector domains, which leads to homodimerization and caspase-8 activation by autoproteolytic cleavage, in which caspase-8 further activates executioner caspases, resulting in cell death [136-139].

Evidence also supports c-FLIP as a key modulator in this process, specifically identification that the short variation of c-FLIP (c-FLIPS) and the long variation (c-FLIPL) can inhibit and activate caspase-8, via modulation of caspase-8 oligomerization [140, 141]. c-FLIPL can act both as a pro-apoptotic, as well as an anti-apoptotic modulator at the DISC [141, 142]. Its pro-apoptotic function is facilitated by the generation of active caspase-8 and c-FLIPL heterodimers where c-FLIPL allows stabilisation of the active centre of caspase-8 [142, 143]. Furthermore, the pro-apoptotic role of c-FLIPL is dependent of the levels of c-FLIPL localisation at the DISC and as such the number of caspase-8 and c-FLIPL heterodimers formed. Though intermediate levels of c-FLIPL leads to sufficient formation of caspase-8 and c-FLIPL heterodimers which promotes caspase-8 activity, high concentrations of c-FLIPL leads to anti-apoptotic effects via the replacement of caspase-8 from the death effector domain filament [144]. On the other hand, c-FLIPS at the DISC act in an anti-apoptotic manner by blocking caspase-8 activation by disrupting the caspase-8 filaments at the DISC [145]. It was also reported that c-FLIPS incorporated into death effector domain filaments inhibit caspase-8 activation via the formation of inactive heterodimers [146]. As such, the relative levels of c-FLIP localisation at the DISC allows control of apoptotic signals.

Extrinsic apoptosis driven by death receptors, as described above, can follow two pathways. So called ‘type I’ cells, such as mature lymphocytes, follows caspase-8 activation and proteolytic maturation of executioner caspases leading to apoptosis [147, 148]. Whereas in ‘type II’ classified cells, such as pancreatic β cells and cancer cells, the activity of caspase-3 and caspase-7 is inhibited by XIAP [149]. As such, this pathway requires the proteolytic cleavage of BH3 interacting domain death agonist (BID) by caspase-8 to form a truncated BID (tBID) which translocates to the OMM where it functions as a BH3-only activator to drive BAX and BAK dependent MOMP formation, which leads to caspase-9 driven cell death [150, 151]. Consequently, death receptors are a potent method for programmed cell death, however, it should be noted that death receptor ligation is a complexed process and does not necessarily lead to apoptosis. Several studies have identified differential outcomes upon death receptor ligation, such as TNFR1 activation leading to the assembly of pro-survival complexes dependent on ubiquitinate receptor interacting serine/threonine kinase 1 (RIPK1) status [152, 153]. Additionally, death receptor activation has been identified to active NF-κB which can result in cell survival associated with a strong inflammatory response [127]. Taken together, though death receptors can have, in certain situations, pro survival effects they are primarily responsible for a robust molecular process to induce cellular apoptosis.

The other type of receptors responsible for extrinsic apoptosis are the family of dependency receptors, such as the netrin 1 receptors; deleted in colorectal cancer (DCC); unc-5 netrin receptor A (UNC5A), UNC5B, UNC5C, and UNC5D; the neurotrophin receptor neurotrophic receptor tyrosine kinase 3 (NTRK3); and the sonic hedgehog receptor patched 1 (PTCH1) [123, 154, 155]. Under normal physiological conditions, when their ligands are available at normal levels, dependency receptors promote cell survival, differentiation, and proliferation. However, once these ligands fall below certain thresholds, caspase activation can occur [155]. For example, in the absence of netrin 1, DDC is cleaved by caspase-3 leading to the promotion of its association to the adaptor, protein phosphotyrosine interacting with PH domain and leucine

zipper 1 (APPL1) and caspase-9, leading to the caspase-9 activated caspase-3 cascade [155, 156].

The process of intrinsic and extrinsic apoptosis destroys the cell in a process that ultimately allows organised clearance of the apoptotic cells by phagocytic cells that avoids potential harmful intracellular components or pathogens being exposed to the microenvironment of the cell (Figure 3). An important process in cellular apoptosis, is the generation of apoptotic bodies.

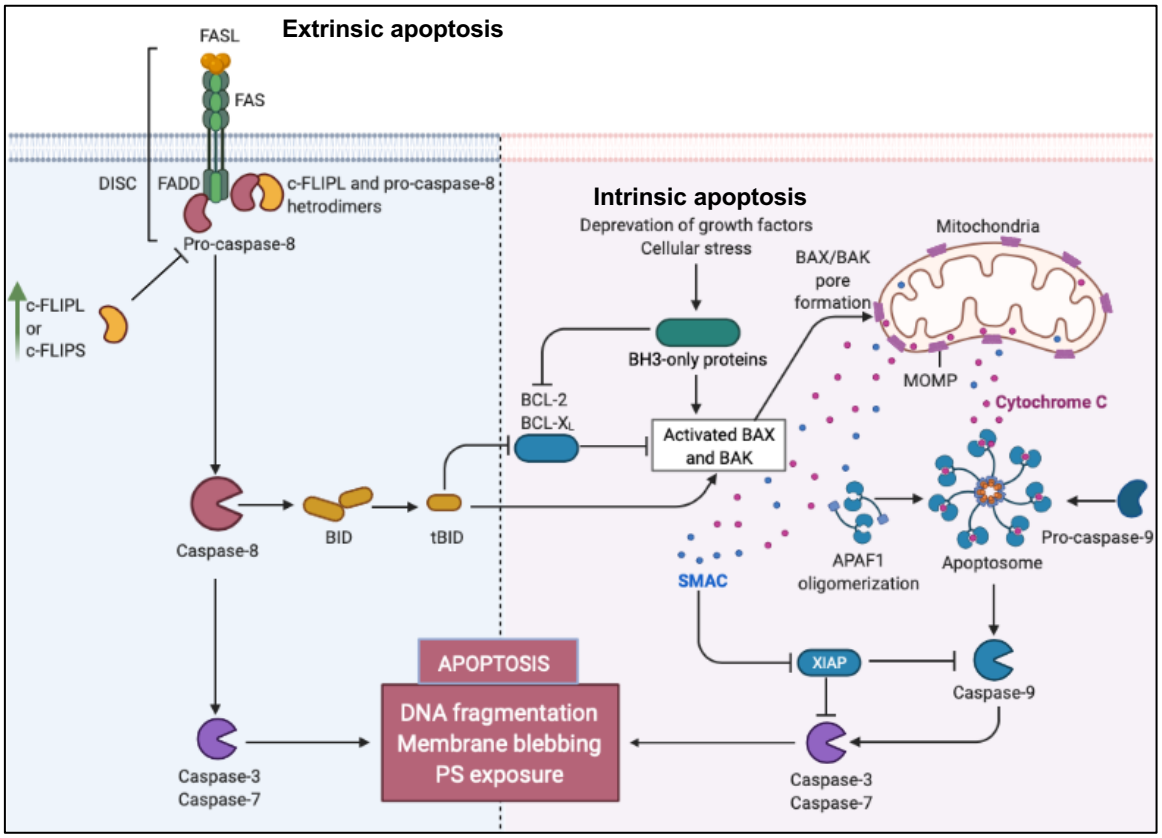

Figure 1. 4 The intrinsic and extrinsic molecular pathway of apoptosis

Extrinsic apoptosis, or death-receptor induced apoptosis (left; blue) is initiated by the activation of death receptors, such as FAS activation by FASL. This leads to the recruitment of pro-caspase-8 to the inner cellular component of the death receptor via the adaptor protein, FAS associated via death domain (FADD). This results in the formation of the death inducing signalling complex (DISC), which leads to the catalytic activation of caspase-8. Caspase-8 can activate effector caspases, leading to apoptosis directly or activated the BH3-only protein BID to tBID, initiating an alternative way to activate the intrinsic apoptosis pathway. c-FLIPS at the DISC act in an anti-apoptotic manner by blocking caspase-8 activation by disrupting the caspase-8 filaments at the DISC or via the formation of inactive heterodimers. The intrinsic apoptotic pathway (right; grey) is activated through different stress stimuli (e.g., reduced growth factors or DNA damage). This induces pro-apoptotic members of the BCL2 family, known as BH3-only proteins, which include BIM, PUMA, NOXA or BAD. These proteins inhibit pro-survival BCL-2 proteins, such as BCL-2 and BCL-XL, which in turns facilitates activation of the critical effectors of apoptosis, BAX and BAK. BAX and BAK form large complexes that causes pore formation in the mitochondria, leading to mitochondrial outer membrane permeabilization (MOMP). MOMP leads to the release of apoptogenic factors, such as SMAC and Cytochrome C. Cytochrome C, upon binding to APAF1, forms the apoptosome, which activates initiator caspase-9. Caspase-9 leads

to the proteolytical cleavage and activation of effector caspase 3 and 7. Effector caspases from either pathway leads to cleavage of multiple intracellular protein in order to induce apoptosis and its characteristics, such as membrane blebbing, PtdSer exposure and DNA fragmentation. Created using BioRender.

1.4.3 Apoptotic bodies

A major component of apoptosis is the production of apoptotic bodies (ABs). During apoptosis, cells undergo extensive plasma membrane blebbing as a result of increased hydrostatic pressure after actomyosin mediated contraction of the cell [157, 158]. The progression of AB formation allows the blebs to be packed with cellular material, such as organelles and condensed chromatin [159]. ROCK1 kinase, an actomyosin regulator, has been shown to be important in the production of membrane blebbing and ABs [103, 160]. Inactive ROCK1 is cleaved by activated caspase-3 at its C-terminus leading to a truncated and active form of ROCK1, which is needed for not only membrane blebbing but also facilitating the re-localisation of fragmented DNA into ABs [103].

Investigations regarding the role and importance of ABs has shown that inhibiting membrane blebbing leads to impaired apoptotic clearance by phagocytes, such as macrophages [161, 162]. Moreover, this impairment could be rescued by the PtdSer bridging protein, milk fat globule epidermal growth factor 8 (MFG-E8) [163]. These studies not only identify the importance of ABs in efferocytosis but PtdSer exposure as a mechanism linking phagocytosis and ABs. As previously discussed, PtdSer at the surface of the cell membrane acts as a signal for phagocytes to process apoptotic cells. It has been identified that externalised phospholipids, such as PtdSer, become highly enriched in ABs, which allows ABs to become a focal point for macrophage recognition and clearance [164]. Not only this, externalisation of intracellular proteins and glycan groups facilities the binding of serum proteins, such as C1q and MFG-E8 [165, 166]. The modifications on the apoptotic cell surface allow rapid clearance by acting as signals for phagocytes, such as CD91 expressing macrophages, to dispose of the apoptotic cell/body [64, 167].

ABs are classified as extracellular vesicles, generally having a diameter in the range of 50-5000nm, with micro-vesicles and exosomes also being classified as extracellular vesicles [168-170]. Several studies have also identified a sub classification of ABs, apoptotic micro-vesicles, being less than 1μm in diameter and having greater membrane integrity than traditional ABs, allowing for molecular exchanges [171-174]. Moreover, recent studies have investigated the occurrence of apoptotic exosomes and their implications in potential pathophysiological conditions, as such the term apoptotic extracellular vesicles has been used to describe all the variations of extracellular vesicles derived from apoptotic cells [175-177]. These studies show that ABs, along with apoptotic micro-vesicles and apoptotic exosomes, are released from the apoptotic cell during cell death.

In contrast to necrosis, which frequently induces an immune response, apoptosis and AB release has been seen as a form of silent cell death. This notion has somewhat changed as apoptosis has been identified as a method of communication with cells of the microenvironment to induce remodelling of the surrounding environment [178]. Specifically, studies have provided evidence that ABs from dying cells may be a major contributor to immune regulation, even with the ability to transport cellular cargo, further identifying apoptotic extracellular vesicles as a key messenger in cellular microenvironments [179-182]. In support of this, apoptotic cells and bodies have been shown to release mitochondria, in which immune cells, such as macrophages, can respond to accordingly, primarily through immune activation [183]. As such, the combination of ABs containing cargo which are released from cells, and that they are highly enriched with ‘eat me’ signals, means further investigations are required to study what effects ABs have upon macrophages as a messenger signal. Exactly how macrophages recognise, process and deal with dying cells will now be discussed.

1.5 How macrophages deal with cell death

1.5.1 Finding dead cells

Macrophages can be located within tissues that have high apoptotic cell turn over, such as regions of the brain, or where apoptotic cells are transported to macrophages by the circulation, such as macrophages located in the spleen [184-186]. However, other macrophages, such as blood borne macrophages, can be recruited and migrate to the area of apoptosis via signal cues. As such, it has been shown that macrophages can respond to array of 'find-me' signals which are released by dying cells and migrate towards them [187, 188]. Of these 'find-me' signals, lysophosphatidylcholine (LPC), sphingosine-1-phosphate (S1P) and the nucleotides ATP, AMP and UTP are the most studied [189-192]. Moreover, the chemokine CX_3CL1 has been shown to mediate the chemotaxis of macrophages to apoptotic B lymphocytes [193]. The majority of studies looking at the 'find-me' signals have been primarily investigated in an in vitro setting, as such the biological implications of these signals in an in vivo setting remain to be fully clarified.

To act upon the 'find-me' signals, it has been shown that macrophages express a range of so called 'find-me' receptors [188]. For example, the G protein-coupled receptor, G2A, has been indicated to play a role in the chemotaxis of macrophages through LPC engagement, however, the exact mechanisms of the binding and signal transduction remains unclear [194]. Additionally, macrophages have been shown to recognise nucleotides via P2Y purinoceptors which are G protein-coupled receptors able to bind to ATP, ADP, UTP and UDP [195, 196]. For instance, the P2Y12 receptor, which has high expression on central nervous system microglia, plays a vital role in early chemotaxis and microglia process extension [196, 197]. Once again, the ability of the 'find-me' receptors, expressed on macrophages, to facilitate migration has not been fully assessed in vivo. As such, questions remain on how exactly the various receptors may work to respond to find-me signals to allow the migration in a gradient dependent manner or how these find-me signal gradients work within complex tissue architectures.

1.5.2 Avoidance of phagocytosis

To avoid phagocytosis, a so called ‘don’t eat me’ signal, has been shown to act as a negative regulator of engulfment from macrophages. This function has been identified to occur through the transmembrane, immunoglobulin-related cell surface protein, CD47 [198]. CD47 has been found to bind to signal regulatory protein-α (SIRPα) on macrophages which can inhibit phagocytosis. It has also been identified to interact with integrins and thrombospondin 1 for the migration of neutrophils, T-cell co-stimulation, and the growth of neuronal axons [199, 200]. In regards to its inhibitory function of phagocytosis it is understood that CD47, after binding to SIRPα, induces phosphorylation of immunoreceptor tyrosine-based inhibition motifs (ITIMs) located in the SIRPα cytoplasmic domain leading to SHP1/2 phosphatases activation [201]. It is still unclear how the exact mechanism of inhibition works, as such, further research is needed to establish this.

CD47 has been found to be frequently overexpressed in tumour cells, specifically in myeloid malignancies, to act as a method of immune-evasion [202, 203]. Furthermore, the disruption of the CD47-SIRPα interactions via blocking antibodies have shown to be effective therapeutics in pre-clinical mouse cancer models, this has led to these antibodies being used in clinical trials for haematological malignancies [204-208]. CD47 as a ‘don’t eat me’ signal maybe balanced by ‘eat me’ signals, however, how the balance is managed and how the relative power of one signal may have over the other to allow or inhibit phagocytosis has not yet been investigated.

1.5.3 Apoptotic uptake receptors

As previously discussed, apoptotic cells present so called ‘eat-me’ signals for phagocytes to recognised and thus processing of the dying cells. Macrophages express a variety of different receptors on their surface that allows apoptotic recognition. Though receptor exist for the recognition of certain plasma proteins displayed on apoptotic cells, such as CR3 and CR4 that are able to recognise C3b on apoptotic surfaces, the majority of research has investigated the exposure of PtdSer on apoptotic cells and the recognition

of PtdSer in macrophages [64, 209, 210]. For example, the αvβ3 and αvβ5 integrins in conjunction with the soluble extracellular matrix MFGE8, which binds PtdSer, allows recognition of apoptotic cells [211]. Their expression has been shown to be present in macrophages and strongly promotes efferocytosis [211]. Furthermore, the single immunoglobulin-domain type I transmembrane protein, CD300b, binds directly to PtdSer and is localised on the phagocytic cup of macrophages [212]. However, the most researched apoptotic recognition receptors are the transmembrane receptors of the TYRO3, AXL and MER (TAM receptors) as well as the T cell immunoglobulin and mucin domain-containing molecule (TIM) families (Figure 1.5) [213, 214].

1.5.4 TAM receptors

The three TAM receptors TYRP3, AXL and MER are cell surface receptor tyrosine kinases (RTKs) [215]. Unlike the TIM4 receptor (discussed later), TAM receptors do not directly bind to PtdSer but rely on their ligands, growth arrest – specific 6 (GAS6) and protein S (PROS1), for their binding activities to PtdSer [215-217]. The amino-terminal γ-carboxyglutamic acid (GLA) domains of GAS6 and PROS1 bind to PtdSer while their carboxy-terminal sex hormone-binding globulin (SHBG) domains bind to the extracellular domains of the TAM receptors [213, 216, 218]. Both ligands function as positive activators of the TAM receptors tyrosine kinase activity to allow phagocytosis when the simultaneous binding of the GLA domain to PtdSer and SHBG domain to the TAM receptor occurs, acting as a bridge between PtdSer and the phagocyte [216, 219]. This binding is dependent on carboxylation of the γ-carbons of glutamic acid residues in the GLA domains in vitamin K-dependent manner as well as binding of 6-7 divalent cations, such as Ca^{2+}, to the GLA domains [216, 219].

In macrophages, TAM receptors and their ligands are the most broadly expressed PtdSer recognition system, as such MER is expressed on all phagocytic macrophages, even at steady state [220, 221]. The MER receptor has been identified as essential mediator of efferocytosis by many macrophages throughout the body in many studies [185, 222-225]. AXL has a more restricted expression under normal conditions, normally limited to

Kupffer cells and alveolar macrophages [226]. However, AXL upregulation has been shown to occur in all macrophages upon inflammatory stimulation, such as lipopolysaccharide (LPS) and IFN-γ exposure [223, 226]. Additionally, in vivo, AXL has a significant upregulation in macrophages after viral infection, trauma or disease [185, 223]. As such, it is thought that MER is responsible for the bulk of macrophage apoptotic cell clearance in regard to homeostasis and continuous tissue turnover, while AXL participates in the phagocytic clearance of apoptotic cells in the context of inflammation during infection, disease and trauma [223, 226]. TYPO3 seems to have limited expression on macrophages but are expressed in certain dendritic cells for the suppression of type II immunity [227]. The importance of the TAM receptors is evident in studies that involves the loss of function mutations in the *Mertk* gene, the gene encoding the TAM receptors. The loss of function of TAM receptors lead to accumulation of apoptotic cells in multiple tissues as well as the development of splenomegaly, lymphadenopathy, rheumatoid arthritis, and autoimmune diseases [228-231]. These studies highlight not only the importance of TAM receptors in the clearance of apoptotic cells, but that the removal of apoptotic cells is critical in maintaining homeostasis and in the prevention of a range of conditions.

As the TAM RTKs carry strong tyrosine kinases, they do not need any intracellular signal transduction to allow macrophage phagocytosis [226, 232]. As such, the kinase activities of the TAM receptors, specifically MER and AXL, is a requirement for the stimulation of apoptotic cell phagocytosis in macrophages [226]. However, the TAM receptors kinase activity alone is not sufficient enough for efferocytosis, accordingly the RTK can be activated by artificial extracellular domain antibodies that allows crosslinking in the absence of GAS6 or PROS1, but this does not allow phagocytosis of apoptotic cells in macrophages [213, 226]. Consequently, it is envisioned that to allow TAM receptor systems to function in efferocytosis it must be present in its entirety. That is, apoptotic PtdSer exposure, ligand and TAM receptor bridging between the macrophage and apoptotic cell as well as the activation of the TAM RTK in the macrophage [213]. Moreover, several studies have identified MER and AXL activation in macrophages and dendritic cells to act potently as an

immunosuppressive, which is a feature of efferocytosis and the noting of immunological silent process of dying cells [229, 232-234]. Together, this data shows that TAM RTKs are an important mechanism in the process of phagocytosis of apoptotic cells and ABs.

1.5.5 TIM4 receptor

The TIM gene family have eight members belonging to the mouse genome and three in the human genome [214]. In respect to efferocytosis in macrophages, the most studied member is TIM4. Unlike the other members of the TIM family, TIM4 is largely expressed on antigen presenting cells, such as macrophages, but not on T-cells [235]. It is highly expressed in peripheral lymphoid tissues, such as the lymph nodes and thymus, but the expression is much less in other tissues, such as the kidneys, lungs and liver [235-237] Furthermore, TIM4 has been shown to be expressed on certain tumour cells in which it can promote tumour growth [238-240]. Structurally, TIM4 is a single-transmembrane protein which includes an immunoglobulin variable region-like (IgV) domain, a mucin-like region, a short cytoplasmic tail and is heavily glycosylated [241]. It has been identified that the level of TIM4 expression can be regulated by various stimuli's, such as LPS, cholera toxins and damage associated molecular patterns (DAMPs) [242-245]. Additionally, TIM4 expression can be downregulated by certain conditions, such as the probiotic *Bifidobacterium infantis* or vitamin D, highlighting the influence environmental factors can have on TIM4 expression [246, 247].

TIM4 has been identified as the natural ligand of TIM1 and can modulate the proliferation of T-cells, which has involvements in immune conditions [248, 249]. Moreover, TIM1 and TIM4 bind to PtdSer in which PtdSer acts as a bridge between the two TIM molecules [241]. TIM4 binds tightly and directly, without the need of a ligand bridge, to PtdSer with low nanomolar affinity in a reaction dependent on Ca^{2+} [213].

TIM4 has been shown to strongly support efferocytosis of apoptotic cells and debris, needing a secondary intracellular signalling transducer due to the short cytoplasmic domain and lack of tyrosine activation residues of TIM4 [241]. As

such, the use of TAM receptor tyrosine kinase activities has been presumed to be used for TIM4 signal transduction, as when TAM receptors aren't present, cells are unable to support efferocytosis [250]. Further, TIM4 enhances TAM receptor associated efferocytosis in macrophages that express TIM4 but not in macrophages that do not [250]. Accordingly, investigations exploring the downstream pathway of TIM4 binding of PtdSer showed that it was independent from the ELMO1/Dock180/Rac pathway and GULP-mediated pathway, the known engulfment signalling pathways [251].To this effect, it has been suggested that TIM4 can use β1, β3 and β5 integrins as co-receptors and as such their cytoplasmic signalling proteins, such as SRC kinases, as downstream effectors [252]. It was identified that integrin bound to TIM4 and acted as a co-receptor to induce the transduction cascade signal needed for efferocytosis [252]. More recently, Fibronectin was shown as a TIM4 associated protein where it acts as a scaffold allowing complex formation between TIM4 and integrins to mediate phagocytosis [253]. These studies identify the interactions that occur with TIM4 to allow it to function effectively as a mediator of apoptotic cell clearance.

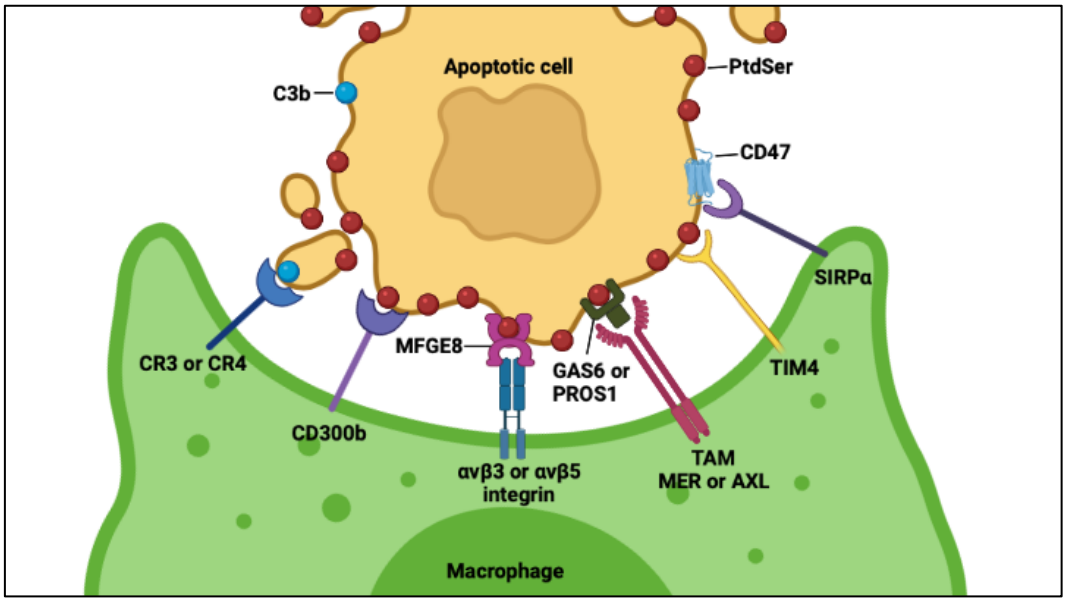

Figure 1.5 Cell surface receptors on macrophages that interact with apoptotic cells

Apoptotic cells and apoptotic bodies universally display externalised phosphatidylserine (PtdSer; red). PtdSer is one of the most potent 'eat-me' signal for apoptotic cell efferocytosis. PtdSer binds directly to cell surface receptors on macrophages that detect PtdSer directly, such as CD300b and TIM4. PtdSer can also be recognised by soluble, bridging proteins, such as GAS6, PROS1 and MFGE8. These soluble proteins carry a PtdSer binding domain and a domain that binds to the macrophage's phagocytic receptor. The TAM receptor kinases MER and AXL bind to GAS6 and PROS1, while avβ3 and avβ5 integrin dimers bind MFGE8. Complement proteins, such as C1q and C3b are found on apoptotic surfaces and are recognised by complement receptors, such as CR3 and CR4. Some cells, including apoptotic cells, express CD47, which binds SIRPα, which acts as a negative regulator of phagocytosis. Created using BioRender.

1.5.6 TIM4 in diseases

The relationship between TIM4 and immune regulation highlights it as potentially important receptor in a multitude of diseases.

1.5.6.1 TIM4 and allergies

There have been a few studies trying to establish the roles TIM4 may have in allergies and allergic reactions. The pathophysiology of asthma is thought to occur through the mis-regulation of helper T-cells and previously studied have shown that single nucleotide polymorphisms (SNPs) of TIM1 has a link to the susceptibility of asthma in certain populations [254, 255]. To this extent, there is an important relationship between TIM4 and the 1419 G>A SNP when investigating childhood susceptibility to asthma [256]. Another allergen, Bla g 7, enhances the TIM4 expression in dendritic cells which suggests this antigen is capable of inducing Th2 polarisation via TIM4 in dendritic cells [257]. In allergic rhinitis, deficiencies in vitamin D may support its pathogenesis via the increased expression of TIM4 in dendritic cells [247]. Further evidence to support TIM4 involvement in allergies has identified that the simultaneous exposure of peanuts and cholera toxin resulted in increased expression of MHC II and TIM4 in dendritic cells, cumulating in the activation and differentiation of peanut specific T-cells [258]. However, blocking the interaction between TIM4 and TIM1 with antibodies inhibited the allergic reaction. These studies provide evidence that TIM4 has a role in the pathogenesis of different allergies.

1.5.6.2 TIM4 and autoimmunity

Many factors have been shown to contribute towards autoimmune disease, including the defective clearance of apoptotic cells and debris [259]. Rheumatoid arthritis (RA) and systemic lupus erythematous (SLE) have been linked to occur due to the defective clearance of apoptotic cells with TIM4 playing a vital role in the macrophage clearance of apoptotic cells and autoimmune diseases [260, 261]. In several different human populations, the SNP rs7700944 *tim-4* has shown to have an association with RA [262-264]. It has been reported that the gene expression of TIM4 from peripheral blood

mononuclear cells (PBMCs) was increased in SLE patients, with TIM4 being positively correlated with SLE [265]. Studies in mice that lacked *tim-4* and *MFG-E8* showed increased levels of autoantibodies, a process that was accelerated in the presence of an anti-TNF-α antibody or by inducing a type I IFN response [266]. However, the same study showed that mice that lacked solely *tim-4* or *MFG-E8* had little to no autoimmunity. Contrastingly, a significant development of autoantibodies was found in TIM4-deficient mice [267]. The differences seen between studies may, in part, be explained by environmental differences, even with the mice being kept in sterile conditions [268]. Further, studies looking at blocking TIM4 showed an effect on the pathology of some autoimmune diseases, such as autoimmune encephalomyelitis and collagen-induced arthritis [248, 249]. Hence, it seems TIM4 may play a role in autoimmunity, but the complexities are still not fully understood.

1.5.6.3 TIM4 and tumours

The expression of TIM4 has been shown to be highly expressed on macrophages within a tumour environment [245, 269, 270]. More specifically, TIM4 expression was shown to be high in macrophages and dendritic cells upon stimulation of apoptotic tumour derived DAMPs post chemotherapy, which mediated TIM4-AMPKα1 mediate degradation and reduced antigen presentation [245]. Furthermore, studies in mice showed that overexpression of TIM4 on antigen presenting cells acted as a negative regulator in antitumour immunity via promoting tumour immune tolerance by limiting the T-cell response and T-cell numbers [269]. Moreover, a subset of $TIM4^+$ and $CD163^+$ macrophages were identified as the driving factor to promote the metastasis of ovarian cancer cells [271].

Targeting TIM4, in combination with TIM3, via antibodies in melanoma models was shown to increase the efficiency of current therapeutic of melanoma vaccines, highlighting it as a potential tumour target [272]. More recently it was show that TIM4, as a phagocytic receptor for lung dendritic cells in mouse models, was important in early immune surveillance and is downregulated in later tumour stages resulting in an impaired immune response [273].

Additionally, it was shown that TIM4^{+} cavity-resident macrophages directly inhibit and reduce CD8^{+} T-cells, important in the antitumour response, while TIM4 blockade resulted in enhanced antitumour efficiency and adaptive T-cell therapy in vivo [274]. Together, these studies provide conflicting data on the role of TIM4 in the tumour response. While studies have identified that high expression of TIM4 as a promotor of tumour immune tolerance, others have shown that TIM4 expression was important for immune surveillance of tumours. Further investigations are needed to provide more evidence of the role TIM4 in macrophages has on tumour progression, as such the differences seen in previous studies may be attributed to the tumour type and its microenvironment, as well as the staging and progression of the disease during experimentation, this information needs to be established.

TIM4, with the other apoptotic recognition receptors, are an important part of cellular immunity. The recognition of apoptotic cells and ABs by macrophages leads to downstream processes, such as cytoskeleton rearrangements to facilitate engulfment. We will now discuss the processes that occur upon activation of apoptotic recognition receptors in macrophages.

1.6 Phagocytosis

Phagocytosis can be found to occur in almost all cell types of multicellular organisms; however, only professional phagocytes are able to perform phagocytosis with high efficiency [275]. Dendritic cells, monocytes, osteoclasts, neutrophils, and macrophages full within this category. Professional phagocytes are responsible for the removal of microorganisms, removal of dying cells and antigen presentation to lymphocytes for adaptive immunity [276]. The process of phagocytosis involves sensing and taking in flagged particles. Upon binding to the particle via detection receptors, the initiation of signal pathways leads to actin cytoskeleton remodelling, this results in the membrane covering the particle [277]. The membrane then closes at the outermost ends, thus creating the phagosome. The phagosome changes the structure of its membrane and the composition of its cargo through a process known as phagosome maturation [278]. Thus, the particle gets internalised inside the phagosome. The fusion of the phagosome and

lysosomes changed the composition of the cargo in what is called the phagolysosome. The fusion releases certain enzymes that allows for degradation of the ingested particle [275]. In the context of clearance of apoptotic cells by phagocytes, the engulfment and clearance of cells undergoing apoptosis is termed efferocytosis.

1.6.1 Efferocytosis

Several approaches have revealed that efferocytosis is a distinct process from classical phagocytosis [279]. As previously described (1.5), the clearance of apoptotic cells and ABs requires expression of receptors that recognise apoptotic specific ligands. This leads to the reorganisation of the macrophages cytoskeleton to engulf debris and induction of phagosome to lysosome fusion for cargo degradation [280]. The process of efferocytosis has been shown to lead to the production of anti-inflammatory mediators and as such is deemed to be an immunologically silent mechanism of clearance when compared to phagocytosis, where proinflammatory cytokines can be produced [281, 282]. Defects in efferocytosis may lead to rupture and subsequential leakage of unprocessed ABs which can lead to the exposure of harmful contents, such as caspases and enzymes, upon neighbouring cells [283, 284]. This process, known as secondary necrosis, can lead to inflammation resulting in cell and tissue damage [285, 286]. However, efferocytes, such as macrophages, cannot simply be classed as anti-inflammatory, this is because the complex polarity and transcriptional landscape of macrophages means they may occupy a distinct space within macrophage classification, which is discussed later (1.7).

Following recognition via receptors, apoptotic cells are engulfed by the macrophage into a plasma membrane vacuole, sometimes referred to as an efferosome [287]. Like phagosomes that contain engulfed pathogens, efferosomes undergo a regulated sequences of progressive fusions with endosomes and lysosomes [288]. These fusions are controlled by proteins such as Rab GTPases, such as Rab5 and Rab7, and SNAREs, with fusion events transporting enzymes which degrade the apoptotic contents within the efferosome [289-291]. Similar to phagocytic maturation, these fusion events

are termed efferosome maturation [287, 292]. Rab5 is recruited to efferosomes as the apoptotic contents are engulfed, in which Rab5 mediates the fusion of the early endosomes with efferosome, initiating the degradation process [289]. Rab5 is exchanged for Rab7 later in the efferosome formation process, with Rab7 facilitating the fusion of late endosomes and lysosomes to the efferosome. This allows the generation of the highly hydrolytic environment responsible for apoptotic cell degradation [293]. However, this process can be less effective in the clearance of apoptotic cells, as the maturation of efferosomes is not as efficient as enhance processes of phagocytosis and efferocytosis, such as LC3 associated phagocytosis (LAP).

1.6.2 LC3 associated phagocytosis

Efferosomes have also been shown to employ LAP, which is a noncanonical form of autophagy. LAP involves the recruitment of autophagy mediators, such as the class III phosphatidylinositol-3-kinase (PI3KC3) [294, 295]. The efferosome recruits Rubicon which mediates the activity of the PI3KC3 complex, resulting in the generation of phosphatidylinositol 3-phosphate (PI3P) association on the efferosome [296, 297]. Consequently, this process is required for the stabilisation of the NADPH oxidase 2 (NOX2) complex allowing the sustained production of reactive oxygen species (ROS) [298]. This is a critical component for the recruitment of the LC3 conjugation machinery components, such as ATG3, 5, 7, 12 and 16. Following this, LC3 lipidation occurs and localised to the efferosome which is termed the LAPosome. LAPosomes enhances the degradation of apoptotic cargo via the promotion of lysosomal fusion (Figure 1.6) [298].

It has been shown that the dysregulation or impairment of LAP leads to an inhibitory effect in the clearance of apoptotic cells. Specifically, in the absence of LAP, phagocytosis of ABs still occurs but they remain unprocessed by the phagocytic cell, highlighting the importance of LAP in the finalising the processes of degradation of ABs [299]. Furthermore, LAP has been shown to be dependent on Rubicon, in which it is a negative regulator of canonical autophagy with downregulation of Rubicon resulting in an increase in autophagosome numbers [300, 301]. As such, deletion of Rubicon in mice

models of autoimmune diseases increases vulnerability in the development of systemic lupus erythematosus-like features, possibly owing to altered apoptotic cell processing [302]. Moreover, it has been demonstrated that LAP deficiencies inhibit tumour immunosuppression via efferocytosis [303]. Another mice model with altered ATG16L1 protein showed that it was important for functional LAP, while allowing autophagy to occur, highlighting the ATG16 and LC3 conjugated machinery as an important mechanism in LAP formation [304].

After the resolution of LAP and the apoptotic content is digested in LAPosomes, the phagocyte becomes burden with the macromolecular digested components. The phagocytes can either use digested components in biosynthetic processes or exported to the extracellular environment [298]. In certain situations, an overload of degraded products, such as cholesterol, can act to stimulate downstream effectors resulting in altered regulation of the phagocyte. One such example is the stimulation of nuclear receptors (liver X receptor (LXR) and PPARy) which leads to the reduction of inflammatory signals after the removal of apoptotic components [305, 306]. Even so, the inability to process internalised apoptotic debris due to LAP deficiencies can lead to the accumulation of undigested apoptotic cells. These cells have been shown to exhibit different macrophage polarisation, increase in pro-inflammatory mediators, enhanced anti-tumour response and the Stimulator of Interferon Genes (STING)-dependent type I IFN responses (see 1.10) [303, 307, 308]. Further, apoptotic debris that contain DNA can activate STING which can mediate immune recognition of tumour cells [309]. This suggests that LAP processing of apoptotic tumour DNA can counter the initiation of inflammation, it can also supress the anti-immune response. Additionally, this raises the question of how phagocytic cells deal with an overload of different degraded products. As such, the high cellular turnover in malignant environments may lead to an overload of tumour derived products after LAPosome degradation, the effect upon the phagocyte is currently not fully understood, thus further investigations are required. Even so, the activation of phagocytes, specifically macrophages, is a complexed paradigm which will now be discussed.

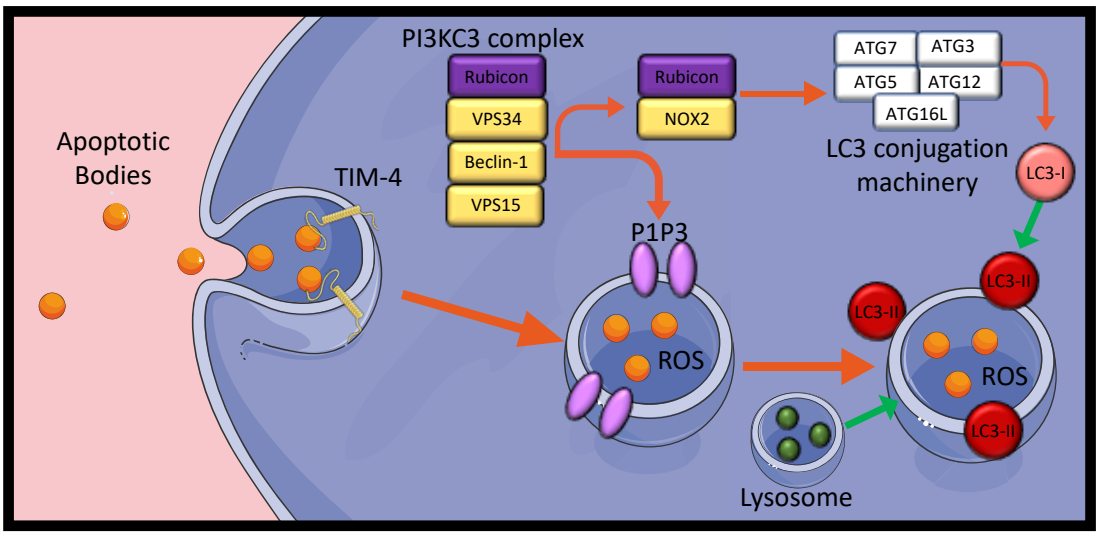

Figure 1.6 LC3 associated phagocytosis (LAP)

LAP is triggered to allow for degradation of the phagocytosed apoptotic debris following efferosome maturation. Apoptotic bodies are recognised by cell surface receptors, such as TIM4, which are engulfed into phagosomes. The process of LC3 tagging to phagosomes (LAPosomes) requires recruitment of the PI3KC3 complex (which includes Rubicon, vps34, vps15 and beclin-1) which enables PI3P to be located to the phagosome. This stabilises the NOX2 complex which produces ROS, in which ROS is required for the recruitment of LC3-II to the phagosome, forming the LAPosome. LAPosomes allow for lysosome recruitment and sequential fusion, leading to degradation of apoptotic cargo.

1.7 Macrophage activation

T lymphocytes were identified early as the major organiser of the immune response, with their cytokine production profile of interferon gamma (IFNγ) and IL-4 allowing subdivisions of Th1 and Th2 cells respectively [310]. Further, these cytokines are cross-regulatory and allow control of two essentially opposite immune reactions, type-I and type-II [311]. Though macrophages are not included in this paradigm, their role in immune response organisation is still vital. Specifically, macrophages can secrete IL-12 leading to IFNγ production and Th1 development, alternatively they can secrete IL-10 leading to IL-4/IL-3 production for the proliferation of Th2 cells [56, 57]. It is the production of IL-12 or IL-10 that sets the bases for the M1 and M2 activated macrophages. Accordingly, M1 or classically activated macrophages are obtained by stimulation with LPS alone or in combination with IFNγ. Meanwhile M2 activation is mainly associated with antiparasitic activities and tissue repair, where M2 macrophages are further subdivided into M2a or alternatively activated macrophages; M2b or type-II activated macrophages; and M2c, which can be classed as macrophages with deactivated stimuli [312].

1.7.1 Classically activated macrophages

Macrophages are stimulated towards M1 activation via IFNγ and microbial products, such as LPS. IFNγ is mainly secreted by Th1 and $CD8^+$ cytotoxic lymphocytes as well as NK cells and antigen-presenting cells [57]. The outer membrane of gram-negative bacteria is mainly composed of LPS and is recognised by LPS-binding protein which is presented to cell surface receptor complexes composed of CD14, the transmembrane signalling receptor toll-like receptor-4 (TLR-4) and MD2 [313]. Classically activated macrophages are known to produce vast quantities of proinflammatory cytokines such as TNFα, IL-1ß, IL-12, IL-15 and IL- 18 [57, 314]. Additionally, they secrete various chemokines, such as CXCL13, CCL15, CCL20 as well as the angiostatic IFNγ response chemokines CXCL9, CXCL10 and CXCL11 [315-317]. These secreted factors induce Th1 and NK cell recruitment to a type-I immune response via their activity on CXCR3.

The function of M1 macrophages are generally characterised by their enhanced ability for endocytosis as well as their enhanced intracellular pathogenic response [57]. The increase in microbial activity is achieved by different mechanisms, including acidification of phagosomes, restriction of nutrients to pathogens, synthesis of reactive oxygen intermediates and the release of nitric oxide (NO) [318, 319]. Innate activation of macrophages possesses many similarities to M1 activated macrophages. Directed recognition of microbial Pathogen-Associated Molecular Patterns (PAMPs) via Pattern Recognition Receptors (PRR), such as toll-like receptors, can lead to macrophage activation with secretion of proinflammatory cytokines matching the M1 macrophage activated profile [320, 321]. However, innate activation of macrophages differs from M1 macrophages as they show no increased ability in phagocytic properties and can be identified by novel innate activated macrophage markers, such as MARCO receptors [322]. Typically, innate activated macrophages are unable to fully develop to an M1 macrophage as TLR ligation induces only low-level expression of p40 which is insufficient to produce activated IL-12 seen in M1 macrophages [314]. Even so, pathogens are able to induce IL-12 heterodimers, as such microbial stimulation of innate macrophages can share similar properties to M1 macrophages. Hence, subdivision of M1 activated macrophages may be necessary to allow differentiation between innate and classically activated macrophages. Together, classically activated macrophages are essential for microbial defence and are polarised to allow for a strong response for such activities.

1.7.2 Alternatively activated macrophages

As oppose to classically activated macrophages, alternatively activated macrophages (M2 macrophages) were first shown to be activated by IL-4 [323]. M2 macrophages are phenotypically and functionally similar cells important in type-II inflammation and tissue repair [57]. M2 macrophages are subdivided into three broad categories; M2a, M2b and M2c.

M2a macrophages are activated by stimulation of IL-4 or IL-13, of which they are produced largely by Th2 cells, mast cells and basophils [323]. Both IL-4

and IL-13 downregulate proinflammatory mediators, such as TNFα, IL-1ß, IL-6 and IL-8, as such the action of IL-4 and IL-13 on macrophages act for anti-inflammatory properties [57]. Additionally, IL-4 has been shown to decrease important immune membrane proteins such as CD14 and CCR5 [57, 324]. Studies have also provided evidence that IL-4 and IL-13 regulate important molecules, such as major histocompatibility complex II (MHC-II) and ß2 integrins as well as chemokines CCL22 and CCL18 [312, 325]. Furthermore, M2a macrophages express fibronectin-I (FN-I), ßIG-H3, the coagulation factor XIII and IGF-1, which promotes tissue repair and proliferation [326, 327]. Further studies in mice have demonstrated that M1 macrophages but not M2a macrophages express NO synthase-2 (NOS-2), however they produce large amounts of arginase-1 (ARG-1) which alters the production of NO to proline, as such M2a macrophages fail to produce NO hindering their ability for microbial processing [328, 329]. Moreover, M2a macrophages production of proline and polyamine stimulate collagen formation, cellular growth and tissue repair. M2a macrophages also express high levels of chemokines CCL8, CCL13 and CCL26 which are important in the recruitment of basophils, eosinophils and Th2 cells via CCR3 interactions [57]. Therefore, macrophages activated towards M2a have enhanced compacities to facilitate repair and growth mechanisms.

Macrophages can be stimulated towards M2b cells via LPS or IL-1ß through immune complexes recognised for the Fc segment of Ig-G (FcγR) and TLR4 or IL-1R [330, 331]. As to oppose to the function of M1 macrophages, M2b cells express low levels of IL-12 and high expression of IL-10, this cytokine profile is indicative of favourable development of a type-II adaptive immune response [332]. Furthermore, M2b play a role in B-cell response via proficiently sustaining antibody production [57]. Comparing M2a and M2b cells, M2b cells differ as they produce higher levels of IL- 10 as well as TNFα, IL-1ß and IL-6. Moreover, the distinction between M2a and M2b cells can be made upon the expression of the enzyme sphingosine kinase 1 (SPHK1) in M2b cells, where SPHK1 may play a role in preserving cell viability of endotoxin-stimulated macrophages [333]. Additionally, the expression of SPHK1 could be important in the negative-regulation of inflammatory

mediators in M2b cells [334]. As such, M2b cells are suited to type-II immune activation and immunoregulation.

The stimulation of macrophages with TGFß, IL-10 or glucocorticoids induces the M2c category of macrophages. Generally, M2c cells are classified as a type of deactivated macrophage, in the sense that there is downregulation of proinflammatory cytokines while there is an increase in activities such as healing function and scavenging for debris [57]. TGFß is a cytokine that mediates a variety of responses such as cell proliferation, activation and differentiation. In macrophages, TGFß regulates cytokine production, host defences as well as chemotaxis. Furthermore, TGFß acts to negatively regulate the expression of CD163 in macrophages as well as inhibiting the production of LPS inducing macrophage proinflammatory cytokines IL-1α, IL-18 and TNFα [335]. IL-10 is produced by a vast range of cells as part of the response to infection and inflammation, playing an important role in limiting the intensity and duration of such responses. IL-10 is a key regulator important for M2c macrophages by downregulating antigen presentation via lowering the expression of MHCII as well as inhibiting the production of proinflammatory cytokines TNFα, IL-6 and IL-12 [57]. Glucocorticoids are released during times of stress, for example during starvation and infection as well as playing an important role in maintaining homeostasis. Recognition of glucocorticoids takes place via the glucocorticoid receptor located in the nucleus and leads to the repression of proinflammatory factors, such as IL-1, IL-4, IL-8, IL-12 and TNFα. Further, it down regulates proinflammatory mediates NOS2 and cyclooxygenase 2 [336]. Additionally, glucocorticoids act to increase the expression of IL-10 and the scavenger receptor CD163 which further inhibits the inflammatory response.

1.7.3 Tumour-associated macrophages

The tumour microenvironment produces signals that allows the recruitment and differentiation of various lymphocytes and are major influences in the activation of precise transcriptional programmes displayed on tumour-associated macrophages (TAMs) [312, 317]. The expression of factors such

as TGFß, IL-10 and PGE2 by, not only malignant cells but by TAMs, leads to a suppression of antitumor activities. IL-10 is an important factor in the differentiation of monocytes to macrophages, while inhibiting dendritic cell maturation [337]. Moreover, IL-10 pushes TAMs towards a more M2c like cell, carrying out various functions such as debris scavenging, angiogenesis and tissue repair advantageous to the tumour [338]. TAMs have a hindered ability to produce NO, with specific studies identifying macrophages positive for NOS2 to be at a relatively low percentage within the tumour and generally only found at the periphery of the cancer [339]. Furthermore, TAMs are poor producers of ROIs, given further evidence that TAMs are polarised towards a M2 macrophages and not a M1 macrophages [57]. In support of this, TAMs express low levels of proinflammatory cytokines IL-1ß, IL-6, IL-12 and TNFα as well as being poor antigen presenting cells [312].

An important factor in cancer growth and progression, as well as in the function of M2 macrophages, is angiogenesis and the production of factors to support angiogenesis, such as VEGF and platelet-derived endothelial cell growth factor (PD-ECGF) [312, 340]. Further to this, TAMs produce the angiogenic factor thymidine phosphorylase (TP), whose expression has been shown to correlate with the formation of tumour vascularisation [341]. Hypoxic conditions trigger the release of the pro-angiogenic factors, so it is not surprising that TAMs can be found in hypoxic regions, where they can support tumour-associated angiogenesis. Hypoxic conditions are especially important in haematological malignancies within the BM, for example hypoxic conditions are important in the regulation of leukaemia blasts [342]. Overall, TAMs are able to supress other immune cells, promote angiogenesis and metastasis.

Taken together, macrophages are a very complex cell type, with stimulation of certain cytokines, interaction with host and non-host intermediates as well as stress stimuli polarising macrophages to allow them to act specifically to the situational needs (Figure 1.7). The sub-categorisation of macrophages is still an oversimplification of how macrophages can interact and become polarised towards many different macrophage types. Still, TAMs seem to be more closely associated towards an anti-inflammatory phenotype of an M2 cell,

which supports the growth and progression of the malignancy. A lot of questions remain, such as whether macrophage that are exposed to high levels of apoptotic cells are polarised towards an anti-inflammatory phenotype. Additionally, how important the local microenvironment is in regulating macrophages and how the macrophages adapt to specific microenvironment cues are largely unknown. In regards to this study, how BM macrophages interact with apoptotic AML cells to shape the tumour microenvironment to support or inhibit disease progression is investigated.

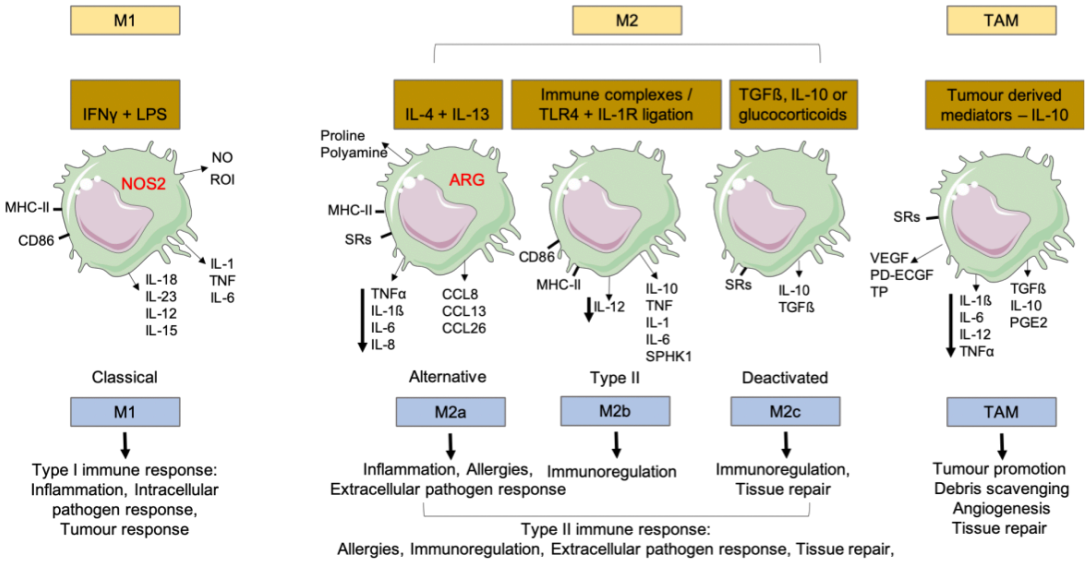

Figure 1.7 Selected inducers and functional properties of the different types of polarisations in macrophages

Macrophages become polarised and carry out a range of functions dependent on environmental stimuli. M1 macrophages are induced by IFNy and LSP and are responsible for cytotoxic and anti-tumour properties, where M2 macrophages are generally more prone to protumour and immunoregulatory activities. M2a (polarised by IL-4 and IL-13) and M2b (polarised by a combination of immune complexes and TLR or IL-1R agonists) are responsible for type II immune response and immunoregulatory functions. M2c (polarised by IL- 10) are responsible for tissue remodelling and suppression of immune responses. TAMs - Tumour associated macrophages (polarised by IL-10 and other tumour derived mediates such as TGFB) are functionally similar to M2 macrophages, promoting angiogenesis as well as tissue remodelling which supports the malignancy.

1.8 Haematological malignancies

Blood malignancies represent a range of different cancers. These include cancers of the blood, BM and lymphatic system. The most common types are lymphomas, which affect the lymphatic system and myelomas and leukaemia's, which are generated within the BM. Lymphomas typically arise within lymph nodes and can interfere with the body's ability to defend itself against infections. Myeloma and leukaemia growth occurs within the BM and as such can affect the normal function of the BM and haematopoiesis leading to a decrease in functional erythrocytes, lymphocytes and thrombocytes.

1.8.1 Multiple Myeloma

Multiple myeloma (MM) is the malignancy of plasma cells in the BM, specifically initiating from mutations in memory B cells [343]. MM produce excessively abnormal antibodies that can lead to kidney failure and viscus blood. The microenvironment within the BM can act to support MM, such as supporting its survival, proliferation, metastasis and resistance to anti-cancer therapies [344]. BMSC have shown to protect MM via adherent contact which leads to upregulation in anti-apoptotic pathways as well as cell cycle regulatory proteins [345]. Osteoblasts may have a role in MM pathogenesis by supporting its survival and growth, via IL-6 secretion and blockage of TRAIL-mediated cell death via osteoprotegerin secretion [346]. Endothelial cells have also shown to support MM proliferation, growth and expansion via the secretion of several growth factors, including IL-6 [347]. As such, the microenvironment plays a supportive role for MM.

1.8.2 Leukaemia

Leukaemia is classed by the invasion of abnormally differentiated and non-functioning haematopoietic blasts to the BM, blood, haematopoietic organs such as the spleen and other tissues [348]. It is the rapid and uncontrolled growth of leukaemia cell that causes a displacement of normal haematopoietic cells and the haematopoietic system, leading to complications such as anaemia and immunodeficiency, which could be life-threatening. The

classification of leukaemia depends on whether it is chronic or acute and dependent on the progenitor affected, myeloid or lymphoid, even so, the genetic variability in leukaemia is very heterogeneous [349]. Acute forms of the disease develops from immature haematopoietic cells and the disease progresses rapidly whereas the chronic forms of leukaemia develop from more mature haematopoietic cells and the development is generally slow and less rapid. Although this study focuses on acute leukaemia, chronic leukaemia can still develop into the acute form of the disease.

1.8.3 Acute Lymphoid Leukaemia

Acute lymphoid leukaemia (ALL) is a malignancy of immature lymphoid cells arising from either B-cell (B-ALL) or T-cell (T-ALL) progenitors. Studies have indicated ALL has a dependence on its microenvironment. ALL cells are able to adhere to MSCs which induces changes in cell morphology and cell cycling in ALL cells, potentially providing a protective change toward therapies [350]. Specifically, BMSC are able to express high levels of asparagine synthetase while ALL do not, which allows protection against apoptosis in ALL treated with asparaginase, a treatment used in ALL patients [351]. ALL also express functional CXCR4 receptors which have been shown to facilitate their homing to the BM microenvironment [352]. Furthermore, the expression of TNFα, IL-1ß, IL-12 and GM-CSF by B-ALL cells can contribute to a proinflammatory microenvironment that can affect the normal haematopoiesis within ALL BM [353]. Thus, the BM microenvironment can be important to the progression of leukaemia and the interaction from ALL can shape the microenvironment to be advantageous for the leukaemia's survival.

1.8.4 Acute Myeloid Leukaemia

Acute myeloid leukaemia (AML) is a lethal malignancy that predominantly effects elder patients, with poor survival rates of between 5-15% in patients that are older than 60 years. Approximately 3,100 people are diagnosed with AML every year in the UK [354]. Even younger patients able to successfully undergo intensive chemotherapy can often relapse due to a small number of malignant cells that reside in protective niches within the bone marrow [3]. As

such, more targeted treatments are needed. The molecular heterogeneity of AML is vast and as such, understanding the genomic landscape, identification of prognostic factors as well as understanding the microenvironment involved in the disease progression is envisioned to benefit new treatment strategies and better patient outcomes. AML is a malignancy of the elderly, the median age at diagnosis is 71 with AML not commonly diagnosed in patients less than 45 [355]. There are poor survival rates in AML patients, with only 27% of patients surviving 5 years post diagnosis. Males have higher incidence rates of AML, with 5.2 cases per 100,000 in males compared to 3.6 cases per 100,000 in females [356].

Using improved genomic techniques, such as next-generation sequencing, the frequency and spectrum of specific mutations related to AML are emerging. Mutations in the *FLT3* gene confers a proliferative advantage through mutated class III tyrosine kinase receptors, specifically via P13K-AKT, RAS-RAF and JAK-STAT signalling pathways. Impairment of haematopoietic differentiation can also occur via chromosomal rearrangements such as *RUNX1:RUNX1T1*. Further, cohesion complex gene mutations, for example *STAG2* and *RAD21*, can inhibit accurate segregation of chromosomes and impair transcriptional regulation. Moreover, mutations in tumour suppressor genes, such as *TP53*, can lead to the deregulation of transcription as well as inhibiting degradation through MDM2 and PTEN [348-353, 357]. Not only is AML a multi-gene disease it also has complex and varied sub- clonal populations. It is the heterogeneity in the leukaemic clones that allows selection of those capable of activating mechanisms towards chemotherapy resistance and is a contributing factor for the high rate of relapse in AML [358].

1.8.4.1 AML classification

Due to the heterogenetic nature of AML, the French-American-British (FAB) classification was created in 1976. The classification was initially based on the cell type that the leukaemia developed from and the degree of maturity, it was split into six subtypes (M0-M6) [359]. Updates to this system were introduced which added two more classifications, M7 and M0 [360, 361]. An M9

classification was also purposed in 1999 for acute basophilic leukaemia, however this is not widely accepted [362]. Table 1.1 contains information about the FAB AML classification system.

Table 1.1 FAM classification system of AML.

Adapted from cancer.org [363].

FAB subtype	Name
M0	Undifferentiated acute myeloblastic leukaemia
M1	Acute myeloblastic leukaemia with minimal maturation
M2	Acute myeloblastic leukaemia with maturation
M3	Acute promyelocytic leukaemia (APL)
M4	Acute myelomonocytic leukaemia
M4 eos	Acute myelomonocytic leukaemia with eosinophilia
M5	Acute monocytic leukaemia
M6	Acute erythroid leukaemia
M7	Acute megakaryoblastic leukaemia

While the FAB classification is useful, recently the World Health Organization (WHO) proposed an alternate classification system. The main reason was to allow more clinically useful and prognostic information that the FAB system didn't provide [364]. An updated version of this classification was published in 2016 and tries to better classify AML. The current WHO classification of AML is presented in Table 1.2.

Table 1.2 The WHO classification of AML.

Adapted from cancer.org [363].

Major Classification	Minor Classification
AML with certain genetic abnormalities (gene or chromosome changes)	• AML with a translocation between chromosomes 8 and 21 {t(8;21)} • AML with a translocation or inversion in chromosome 16 {t(16;16) or inv(16)} • APL with the *PML-RARA* fusion gene • AML with a translocation between chromosomes 9 and 11 {t(9;11)} • AML with a translocation between chromosomes 6 and 9 {t(6:9)} • AML with a translocation or inversion in chromosome 3 {t(3;3) or inv(3)} • AML (megakaryoblastic) with a translocation between chromosomes 1 and 22 {t(1:22)} • AML with the *BCR-ABL1* (*BCR-ABL*) fusion gene* • AML with mutated *NPM1* gene • AML with biallelic mutations of the *CEBPA* gene (that is, mutations in both copies of the gene) • AML with mutated *RUNX1* gene*
AML with myelodysplasia-related changes	
AML related to previous chemotherapy or radiation	
AML not otherwise specified	• AML with minimal differentiation (FAB M0) • AML without maturation (FAB M1) • AML with maturation (FAB M2) • Acute myelomonocytic leukaemia (FAB M4) • Acute monoblastic/monocytic leukaemia (FAB M5) • Pure erythroid leukaemia (FAB M6) • Acute megakaryoblastic leukaemia (FAB M7) • Acute basophilic leukaemia • Acute panmyelosis with fibrosis
Myeloid sarcoma (also known as granulocytic sarcoma or chloroma)	
Myeloid proliferations related to Down syndrome	

1.8.4.2 AML symptoms, diagnosis, and treatment options.

Symptomatically, variations in the signs of AML vary between patients, with symptoms such as chronic fatigue, bruising, weakness, and bleed being present demonstrated in a range on AML patients [365]. However, with

symptoms varying from person to person, diagnostics are needed to confirm AML in patients. Initially, a blood test is required to investigate blood cell levels, with very low or abnormal lymphocyte counts allowing an early indicator of AML [354]. Confirmation of AML is achieved by collection of a bone marrow sample where the combination of flow cytometry and Wright-Giesma staining are used to diagnose AML [348, 366]. Greater than 20% of the bone marrow containing AML blasts leads to a diagnosis of AML [367].

Treatment for AML has predominately remained unchanged for over 40 years, with the main strategy to treat the patient reliant on intensive chemotherapies to reduce the overall AML blast count to less than 5%. Unfortunately, the current treatments of AML are highly aggressive and not well tolerated by the elderly patients, resulting in the poor 5-year survival rate. Different variations of a 7+3 treatment strategy are the standard chemotherapy treatment, where an infusion of cytarabine is given for 7 days (this can vary, such as a 10 day treatment) and an anthracycline agent given on day 1, 2 and 3 [368]. However, even though approximately 70% of patients treated this was enter remission there are a number of those who have disease relapse [348]. As such, allogenic haematopoietic stem cell transplant (HSCT) is commonly administered as a consolidation therapy for AML patients. Donor HSCs that have been matched to have the same human leukocyte antigen (HLA) are administered to myeloablated AML patients, thus patient bone marrow is replaced with donor HSCs reducing the chances of relapse [369]. Due to the common relapse rates new research is required to investigate the biology of the disease to develop new treatments which can be tolerated much better in the demographic effected by this disease, which could result in increased patient survival.

Even though the treatment for AML has remained largely unchanged, the issue of the effected demographic remains largely elderly individuals who cannot undergo insensitive chemotherapy regimens, recent years has seen some developments in alternative treatments. Specifically, targeted drugs have been developed to work on a certain pathway or target within the cancer cell. There therapies can be used in combination with chemotherapy but also

offers the potential to be beneficial when chemotherapy would be ineffective, or the patient is unable to undergo traditional therapies [370]. One such development is FLT3 inhibitors, where the drug target blocking the produced FLT3 protein and its interactions and have shown to also be beneficial for patients where traditional therapies haven't worked, or they have relapsed [371, 372]. Another class of drugs that have shown good response in AML patients are BCL-2 inhibitors, which targets the anti-apoptotic BCL-2 protein within the mitochondria. Importantly, patients who cannot undergo the intensive chemotherapies, such as patients that are 75 years of age, can use BCL-2 in combination with lower doses of chemotherapies to have positive outcomes [373]. As such, the FDA has approved venetoclax, a BCL-2 inhibitor, as combination therapy newly diagnosed AML patients ≥75 years of age [370]. The development of new targeted drugs is allowing hard to treat patients to have alternative therapies that can be well tolerated in these patients. A number of new drugs are summarised in table 1.3.

Table 1.3 Recently approved AML drugs

Drug	Indication	Administration	Findings in trials	Issues needing attention
Midostaurin Rydapt®	Newly diagnosed *FLT3* mut AML in combination with intensive therapy (FDA, EMA)	Oral	Phase 3 trial (RATIFY): intensive chemotherapy + midostaurin vs placebo: 4-year OS: 51.4% midostaurin vs 44.3% placebo	Careful administration of comedications with strong CYP3A4 inhibitory activity
CPX-351 Vyxeos®	Newly diagnosed tAML, AML-MRC (FDA, EMA)	IV	Phase 3 trial: median OS 9.6 (CPX-351) vs 6.0 months (standard chemotherapy)	Side effects similar to standard chemotherapy but less alopecia
Venetoclax Venclexta®	Newly diagnosed AML in patients ≥75 years or with comorbidities precluding intensive therapy; in combination with LDAC or HMA (FDA)	Oral	VIALE-A trial: VEN-AZA vs placebo: median OS 14.7 (venetoclax) vs 9.6 months (placebo) VIALE-C trial: LDAC-VEN vs placebo: median OS 8.4 (venetoclax) vs 4.1 months (placebo	Hematological toxicity (follow recommended dose adjustments), neutropenic fever, dose adjustments if comedications with strong CYP3A4 inhibitory activity, tumor lysis syndrome (but much rarer than in CLL)
Gilteritinib Xospata®	R/R *FLT3* mut AML as monotherapy (FDA, EMA)	Oral	Phase 3 (ADMIRAL) trial: gilteritinib vs salvage chemotherapy: CR/CRi 34% (gilteritinib) vs 15.4% (salvage therapy); OS 9.3 (gilteritinib) vs 5.6 months (salvage therapy)	Check *FLT3* mutational status at time of R/R disease
Enasidenib Idhifa®	R/R *IDH2* mut AML as monotherapy (FDA)	Oral	Phase 1/2 trial: OR in 40.3% of patients, OS 9.3 months	Check *IDH2* mutational status at time of R/R disease, *IDH* differentiation syndrome, indirect hyperbilirubinemia

Table data adapted from [370].

Improving understanding of the biology of AML has allowed the development of these alternative therapies. Interactions with the other cells within the AML microenvironment will also be important area to explore for therapies. Like HSCs that reside in BM niches, it is thought that leukaemia initiating cells (AML blasts) are located in a similar stem cell like compartment, having the ability to have long-term self-renewal compacities and maintain the AML phenotype. Additionally, this protective environment is expected to be a major cause of AML relapse [374]. Like its non-malignant counterpart, AML blasts are supported by a microenvironment where several cell types are manipulated to support the growth and progression of AML. Some of which will now be discussed.

1.8.4.3 AML microenvironment

BMSC act as key supports of HSC growth and are manipulated by leukaemic cells via changes in chemokine and cytokine expression. IL-8, a chemokine important in chemotaxis, as well as it's receptor CXCR2 are upregulated by myelodysplastic syndrome (MDS) $CD34^+$ cells, a pre-AML disorder [375]. IL-6, a cytokine involved in inflammation, acts to protect leukaemic cells, specifically by the activation of pro- survival pathways such as the JAK/STAT pathway [376]. Further, studies looking at co-culture with cancer related BMSC and cancer cells found increase resistance to anti-cancer drugs and proliferation via cell-to-cell contact or secreted factors [377-379]. In terms of AML, studies have shown that BMSC can inhibit AML blast drug- induced and spontaneous apoptosis via direct cell-to-cell contact [380, 381]. Furthermore, activation of c-Myc in AML cells by BMSC promotes chemotherapy resistance while the chemokine macrophage inhibiting factor (MIF) induces BMSC to express IL-8, creating an environment that supports AML [378, 382]. Additionally, deletion of PTEN, a tumour suppressor gene, in both HSC and BM cells leads to malignant cell proliferation, while deletion of PTEN in HSC alone leads to HSC depletion, not a malignant profile highlighting the importance of BMSC in the initiation of AML [383]. Together, BMSC are critical cells in the survival, protection and progression of AML cells.

Adipocytes are found in abundance and in close proximity to leukaemic niches within the BM, as such it is envisioned that AML cells may deregulate energy mechanics to be advantageous for their proliferation and growth. It has been identified that adipose tissue can act as a reservoir for HSPC [384]. Adipocytes and the release of free-fatty acids (FFA) via lipolysis governs a survival advantage for leukaemic cells via metabolic transition towards an adipocyte enriched niche [385, 386]. It has been identified that FFA from adipocytes in the BM are able to activate transcriptional programmes that support the survival of leukaemic cells [386, 387]. Furthermore, the inhibition of fatty acid oxidation via carnitine palmitoyltransferase 1a (CPT1a) and avocation B, leads to an impaired apoptotic protective effect of BM adipocytes on AML and the inhibition of AML survival, respectively [387, 388]. Adipocytes can also

promote chemotherapy resistance in cancers, with sub-populations of leukaemic cells protected from chemotherapy within BM adipose tissue niches [387, 389, 390]. In regards to AML, studies have shown a reliance of BM adipocytes for AML survival and proliferation. Specifically, the importance of fatty-acid binding protein 4 (FABP4), a chaperone protein for FFA, in the support and protection of AML, while the release of FFA can be used by leukaemia cells for energy production [387, 391]. Thus, the support adipocytes can exhibit upon AML cells relies on the switch of metabolic processes in AML cells to utilise FFA.

Other cells that support the AML microenvironment include endothelial cells. Their location allows them to act as regulators between the BM and circulation, as such they can provide a protective environment for AML as well as a route for dissemination and the initiation of metastasis [392]. Moreover, they can support AML blast retention, proliferation and survival as well as providing protection of AML blasts from chemotherapy cytotoxicity via cell adhesion to the tumour supporting endothelial cells [3, 393]. Another cell shown to be a factor in AML are megakaryocytes. The manipulation of leukaemic cells on megakaryocytes allows suppression of normal HSPC proliferation via mechanisms such as TGFß1/*Erg3* signalling and as such allows a growth advantage in AML [394].

Several studies have identified specific ways AML interact with macrophages to benefit AML survival and immune-avoidance. One of the main phagocytic signals, calreticulin, has been shown to be expressed by many forms of malignancies [395]. To counter this, AML cells have an increased expression of CD47, as previously discussed, which inhibits macrophage phagocytosis of AML cells by interaction with SIRPα which is needed for the morphological changes in macrophage phagocytosis [203]. In support of this notion, it was found that patients with MDS had increased monocytes but an impaired ability to induce macrophages. Further, the phagocytic function of MDS macrophages was reduced, while the levels of NOS2 was increased, as such the macrophages in MDS are impaired [396]. Furthermore, it has been reported that AML leads to the invasion of AML-associated macrophages into

the BM and spleen of both AML patients and mice. Moreover, the survival of mice *in vivo* correlated with the amount of macrophage infiltration with the role of the transcriptional repressor, growth factor independence 1 (Gfi1) playing a critical role in macrophage polarisation towards a TAMs phenotype [397]. In regard to TAMs, their expression is much higher in acute leukaemia patients when compared to control patients. Additionally, overall survival rates in leukaemia patients that have higher levels of TAMs is significantly worse when compared to patients that have low levels of TAMs [398]. Thus, macrophages and TAMs may play a significant role in reshaping the AML microenvironment to support its development by decreased phagocytotic capacities, support of metastasis and immune suppression. However, further research is needed to identify specific mechanisms that AML and BM macrophages use to either allow AML proliferation or to control its growth.

1.9 Energy production in normal and malignant haematopoiesis

It is important to understand the differences in energy production between non-malignant and malignant cells, especially in regards to AML, as it may allow therapeutic targets to exploit weaknesses in the malignancy. Quiescent HSC reside in BM niches, of which are typically located in hypoxic conditions. Additionally, quiescent HSC energy demands are relatively low [12]. As such, quiescent HSC rely upon anaerobic glycolysis for the production of adenosine-5'-triphosphate (ATP) [399]. Glycolysis converts glucose to pyruvate and then to lactate, anaerobically, which generates a relatively low amount of ATP. A benefit of glycolysis is the reduced need for mitochondrial functions and as such the limitation of the production of ROS. HSC are sensitive to oxidative stress and high levels of ROS, which leads to the exit of HSC from their quiescent state and the potential of HSC exhaustion and loss of their self-renewal potentials [12, 400].

During HSC differentiation, the energy demands on the cell increases. Moreover, down-stream progenitor cells can be located to vascular endothelial cells which changes the location of the HSC from a hypoxic niche to a more oxygenated environment as it differentiates [401]. This coincides with a switch

in metabolic energy production from glycolysis to oxidative phosphorylation (OxPHOS), where the production of ATP is much more efficient [402]. Pyruvate from glycolysis and the breakdown of FFA can be fed into the tricarboxylic acid (TCA) cycle and as well as the generation of four ATP molecules, results in the production of NADH and $FADH_2$. During OxPHOS, it is the electrons from NADH and $FADH_2$ that combine with O_2 to produce the energy required to drive ADP synthesis to ATP via the electron transport chain (ETC) (Figure 1.8).

In AML, unlike the notion proposed by Warburg that cancer cells rely on glycolysis for their energy production, OxPHOS is the primary method of ATP production [403, 404]. OxPHOS and the ETC occurs within the mitochondria. In comparison to non- malignant HSC, AML cells have an increased content of mitochondria, supporting the evidence that AML cells use the mitochondria for ATP production [405, 406]. Mitochondria are dynamic and complex organelles, having key roles in not only energy production, but maintaining the homeostasis of the cell, inflammation and even initiate apoptosis via cytochrome-C release. The conversion of pyruvate to acetyl-CoA through the TCA cycle is the main source of mitochondrial OxPHOS [407]. The health of the mitochondria is maintained by its membrane potential ($\Delta\Psi m$), which is needed for ATP production as well as preventing signals that induce apoptosis [408, 409]. Furthermore, the loss of $\Delta\Psi m$ can lead to senescence in cells as well as inhibiting cell division [410]. The reliance of AML cells on OxPHOS for ATP production requires the $\Delta\Psi m$ to be in tacked, as such dysfunctional mitochondria in AML cells would be required to be removed to ensure AML survival or lead to eventual cell death.

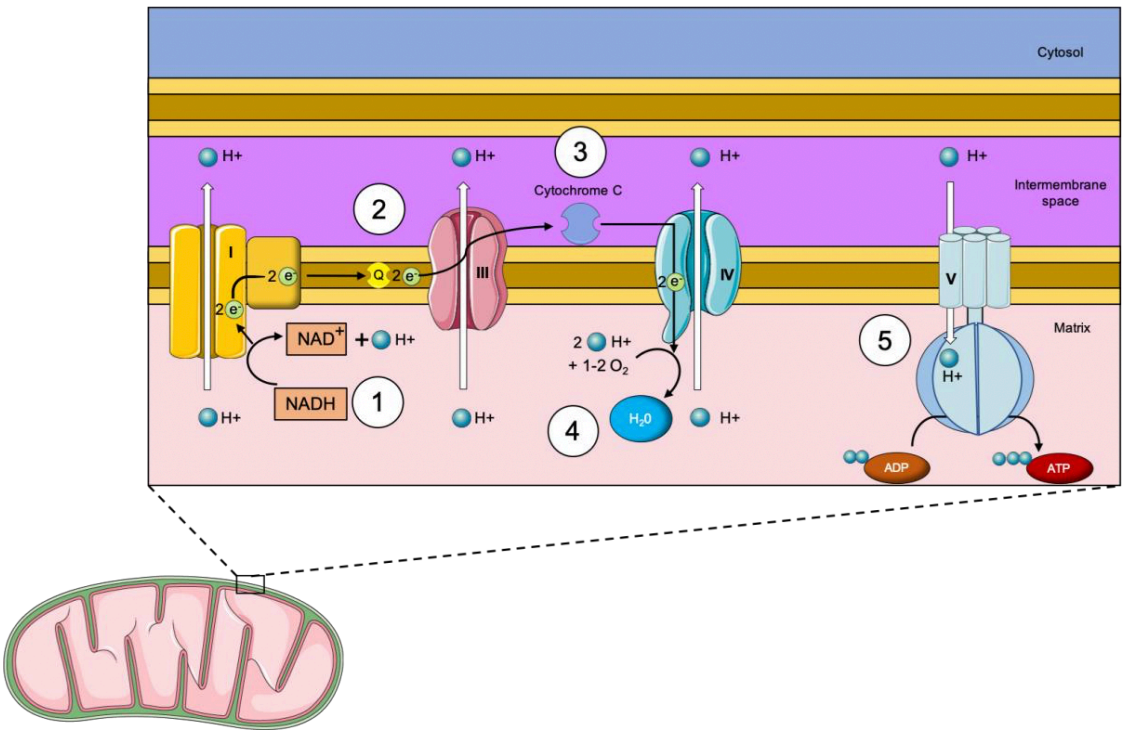

Figure 1.8 The electron transport chain

Mitochondria are an essential component in the regulation of cell survival but more importantly the generation of adenosine-5'- triphosphate (ATP). **1.** Pairs of electrons enter the electron transport chain donated from either NADH or $FADH_2$ to complex I. **2.** The electrons are transferred to coenzyme-Q (Q), carrying the electrons through the membrane of complex III. **3.** The peripheral membrane protein, cytochrome c, further transports the electrons to complex IV. **4.** Complex IV facilitate the transfer of electron to molecular oxygen. **5.** The process of electron transfer in complexes I, III and IV allows a decrease in free energy, this in turn leads to protons to be pumped from the cell's matrix to the intermembrane space. This creates a proton gradient which drives ATP synthesis via proton flow back to the matrix via complex V, converting ADP to ATP.

The increase in mitochondrial content in AML suggests a series of potential issues that the malignant cells must overcome. First, the energy demands on AML cells are high and as such the generation or import of additional mitochondria is needed to support these demands. It has been shown that AML cells require functional mitochondria through tunnelling nanotubules (TNTs) from the surrounding BMSC via the generation of superoxide which supports its growth [411]. Second, the high number of mitochondria present in

the cell can lead to excess and dysfunctional mitochondria, both of which can lead to an increase level of ROS and initiator signal cascades for apoptosis as the potentially toxic by-product of OxPHOS is ROS. It is envisioned that AML cells would need to remove these excess or dysfunctional mitochondria to avoid cell death. Furthermore, the increase in apoptosis via increased dysfunctional mitochondria, may lead to an accumulation of apoptotic cells with excess mitochondria. Studies have identified that cells can export dysfunctional mitochondria, specifically to macrophages, for their degradation [412, 413]. What impact this has on BM macrophages in AML is unknown. Moreover, the impact of the accumulation of apoptotic AML cells and dysfunctional mitochondria as a potential activator of the immune system has not been researched. Ultimately, these are the aims of this study.

1.9.1 Mitochondrial transfer in acute myeloid leukaemia

With the BM microenvironment playing a crucial part of HSC and malignant cell survival, it is not surprising that malignant cells utilise intercellular communications, such as mitochondrial transfer. Interestingly, studies have shown transfer of mitochondria from BM microenvironment to leukaemic cells which is then utilised to increase mitochondrial metabolisms and chemotherapy resistance [411, 414]. Unlike vertical transfer, transfer from parent to daughter cell during mitosis, intercellular horizontal transfer of lysosomes, vesicles and mitochondria can happen between different cell types. Mitochondria transfer is of particular importance due to the function of the organelle in energy production and apoptotic initiation. It was first described in cancer cells lacking mitochondria DNA (mtDNA), which were unable to produce the subunits needed in ETC and as such were not able to use OxPHOS for ATP production. Recovery of respiration was achieved after mitochondrial transfer from BMSC, which was further shown by fluorescently labelled mitochondria from donor mice tissue to the cancer cells lacking mtDNA [415, 416]. Mitochondria transfer in AML has been shown, specifically AML cells have acquired functional mitochondria from BMSC [411]. It has been shown that in a co-culture system that mimics the AML microenvironment, that AML can acquire functional mitochondria from murine

or human BMSC, leading to increase in mitochondrial mass and mitochondrial produced ATP. The transfer was also observed *in vivo.* The same study demonstrated that AML cells were less prone to mitochondria depolarisation due to chemotherapy, adding a survival advantage [414]. This is supported by research that found that NOX2 in AML drives the production of superoxide, the production of which stimulate BMSC to transfer mitochondria through TNTs from AML cells. The inhibition of NOX2 also showed the prevention of mitochondria transfer, which was detrimental to the AML cells [411]. Other studies have also shown the process of mitochondrial transfer in non-malignant cells, for example astrocytes have been shown to release functional mitochondria via CD38 and cyclic ADP ribose signalling, which is transferred to neurons, while others have shown similar mitochondrial transfer from MSCs and renal cells [417, 418].

TNTs are a method of mitochondrial transfer that can occur both in normal and malignant cells. TNTs are tubes or channels that are open at the extremities and allow direct contact with the cytoplasm between two or more cells [419]. It has been shown that TNTs are capable of carrying proteins, lipids, organelles, viruses, ions and RNA between the interacting cells [420, 421]. In a bladder cancer model, TNT mediated mitochondrial transfer was shown to be linked to the increased invasiveness of the cancer [422]. Differences in their cytoskeleton structure, their size and functional properties mean TNTs can be categorised into two classes [423, 424]. Type I TNTs are larger and longer than type II TNTs and contain microfilaments as well as microtubules, where type II TNTs lack any tubulin [419]. As such, organelle transfer only occurs in type I TNTs, which includes mitochondrial transfer [423]. Due to the tubulin needed to transfer mitochondria, studies have shown that blockage of mitochondrial transfer can be achieved by such interventions as alkaloids and actin inhibition via cytochalasin-B, which led to reduced mitochondrial transfer [411, 425]. Moreover, Mitochondrial Rho GTPase-1 (Miro-1) has been shown to be important in mitochondrial transfer, with knockdown showing decrease transfer, while overexpression of Miro-1 increased organelle transfer [426]. It has also been shown that mitochondrial transfer is reliant on calcium

exchange via gap junction channels (GJCs) [427]. The collection of type-I TNTs, Miro-1 and GJCs appear to work in unison for mitochondria transfer.

However, the notion that dysfunctional mitochondria can be transferred intercellular for external mitophagy has been shown to occur via extracellular vesicles (EVs), such ABs. The study showed that oxidative stress and dysfunctional mitochondria are managed by MSCs by targeting dysfunctional mitochondria to the cell membrane via arrestin domain-containing protein 1-mediated microvesicles, which are further phagocytosed by macrophages and re-utilised to increase their bioenergetics [412]. Together, this information shows that mitochondrial transfer occurs and can support the recipient cell by receiving healthy mitochondria or by exporting potentially toxic mitochondria. The mechanism of mitochondria transfer seems to be varied and dependent of whether the mitochondria are functional or not. In the case of dysfunctional mitochondria, EVs are a method of transporting them to phagocytes, which is true for apoptotic cells and ABs.

EVs are a heterogeneous population of lipid bilayer particles that range in size from 15 nanometres (nm) to 10 micrometres (μm) and are produced by nearly all types of malignant and non-malignant cells types [168]. They are further classified dependent on their size from exosomes (<150 nm), to microvesicles (MV, >200 nm) and then to the largest, oncosomes (can reach 1-10 μm, produced by cancer cells) [419]. ABs also fall within these categories, as previously discussed (1.4.3). They can encase a range of cellular components and transport them extracellularly over large distances. In terms of mitochondrial transfer, some EVs are large enough to facilitate their transfer. Two studies identified that astrocytes were able to produce EVs containing mitochondria, the size of the EVs ranging from 300 to 1100 nm, indicating that they are contained within MVs [417, 428]. Further, MSCs outsource dysfunctional mitochondria in MVs which are taken up by macrophages. Additionally, the MSCs release EV containing microRNA's that inhibit macrophage suppression via TLR signalling, which facilitates macrophage desensitisation to the phagocytised mitochondria [412]. This suggests EVs are a method used for mitochondrial trafficking and dysfunctional mitochondria

may be contained within EVs and taken up by macrophages. Importantly, it shows a proof of principle mechanism that macrophages can uptake these EVs, such as ABs, and process them in a way that the cargo contained within them can impact the function of the macrophage.

Even though there has been studies showing the interplay between EVs, such as ABs, and the cross-talk between malignant cells and their microenvironment, specifically in myeloma and leukaemia [429, 430], limited literature has looked at the effect of ABs containing mitochondria on leukaemic cells or their microenvironment. Interestingly, EVs are significantly elevated in haematological cancers and can lead to the modification of the BM microenvironment towards a cancer supporting environment, interfere with anti-cancer immune processes and help facilitate treatment resistance [431-434]. This highlights a potential target in AML that may be targeted, however, further research is needed.

1.10 Stimulator of Interferon Genes (STING)

A critical element of immunity can be attributed to the detection of foreign DNA and in mammalian cells this is largely orchestrated by the cyclic GMP-AMP synthase (cGAS) - stimulator of interferon genes (STING) pathway [435]. The binding of DNA to cGAS allows activation of its catalytic activity and to the production of 2′3′ cyclic GMP-AMP (cGAMP) which is a second messenger molecule and potent agonist of STING [436-438]. cGAMP is detected in the endoplasmic reticulum (ER) by the STING protein [439]. STING is comprised of a cytosolic N-terminal segments, a transmembrane domain, a connector region, and a ligand binding domain (with a C-terminal tail). Unbound STING forms a domain swapped homodimer, which upon binding of cGAMP undergoes significant conformational changes, allowing for side-by-side oligomerisation of STING dimers [440, 441]. The oligomerisation of STING dimers confers an activational change in STING which is responsible for downstream effector functions. Before the initiation of the downstream functions, STING is translocated from the ER to the ER/Golgi intermediate compartment (ERGIC) and then onto the Golgi [442]. Once there, STING recruits TANK-binding kinase 1 (TBK1) which confers downstream signalling

events. Further to this, STING's translocation promotes $LC3^{+}$ vesicles formation, highlighting a link between STING activation and regulation of LC3 association (Figure 1.9) [443].

The most studied and prominent downstream function of cGAMP – STING signalling is the production of type I interferons (IFN) and gene related outcomes [444]. For example, the activation of interferon regulatory factor 3 and 7 (IRF3 and IRF7) can lead to the activation of type I IFN interferon-stimulated genes (ISGs), which ultimately can lead to T-cell recruitment and adaptive immunity. As such, recruitment and activation via dimerization of IRF3 by STING signalling can lead to IRF3 translocation to the nucleus to induce target genes [445, 446]. In addition, IRF3 can also induce many other genes aside from type I IFN and ISGs, such as inflammatory mediators *IL6* and *IL12* [447]. As such, the influence of IRF3 and IRF7 on gene products largely depends on several factors, such as what type of cell interactions are occurring, the specific STING trigger and the exact in vivo context [448]. Moreover, activation of the cGAS – STING pathway can promote NF-κB responses through various pathways, such as initiation of p52–RELB nuclear translocation [449]. This can act as a negative regulator of STING downstream mechanisms, consequently having an effect upon cancer immune escape and metastasis [450]. But STING activation is not limited to the activation of these specific genes, studies have demonstrated that STING activation and type I IFN expression leads to the upregulation of guanylate-binding protein 2 (GBP2), IFN-induced protein with tetratricopeptide repeats 3 (IFIT3) and interferon response gene B10 (IRGB10) which confers several effects, such as inflammation and TBK-1 regulation as well as antiviral activities [451-453].

Although STING activation can convey type I IFN response, it has been shown that STING activation is responsible for a multitude of other effectors. One such mechanism is the cGAS–STING initiation of autophagy [448]. The ULK complex and TBK1 has been shown to be critical in the STING activation of canonical autophagy and STING related autophagic vesicle formation [443]. Further research has identified that STING activation can also trigger non-canonical autophagy responses, involving selective components, such as the PI3P effector WIPI2 as well as the ATG5-12-16L1 conjugated complex [443,

454-456]. In regards to apoptotic uptake and activation of STING, it has been identified that impairment of apoptotic cell debris regulation can also trigger cGAS–STING activity. An example of this involves deficiency in DNase II, the DNase contained in lysosome required for the degradation of DNA from apoptotic cells, which has been associated with the accumulation of apoptotic cells in macrophages [457]. Moreover, studies have highlighted that further upstream factors that play a role in the regulation of the degradation of apoptotic DNA contents and thus prevent activation of STING, with LAP required for effective clearance of apoptotic cells [448, 458]. Specifically, it has been identified that LAP deficiencies can promote STING activation within myeloid cells in solid tumours [303]. Furthermore, release of mitochondria can act as a cell-intrinsic trigger, similar to that of antiviral signalling, via cGAS–STING signalling [459]. Additionally, TIM4 deficiency has been shown to replicate a similar phenotype, as such it may suggest that dedicated apoptotic receptor pathways enables DNA degradation in an immunologically silent process [448]. It also presents a mechanism that links TIM4 recognition and LAP processing of apoptotic cells and the activation of STING. Further, activation of the cGAS–STING by DNA in an environment where the mechanism becomes overwhelmed, such as in infections and malignancies, may lead to increased STING activation. Given that DNA damage, DNA export and uptake from either extracellular sources or via phagocytic uptake are major factors underlying many malignant phenotypes, a better understanding of the molecular processes taken by extracellular DNA and apoptotic cell DNA processing will be of importance. Thus, while studies have identified certain pathways that STING activation is a prerequisite for, there are still unknowns regarding STING activation and its downstream targets, and as such, warrant further investigations.

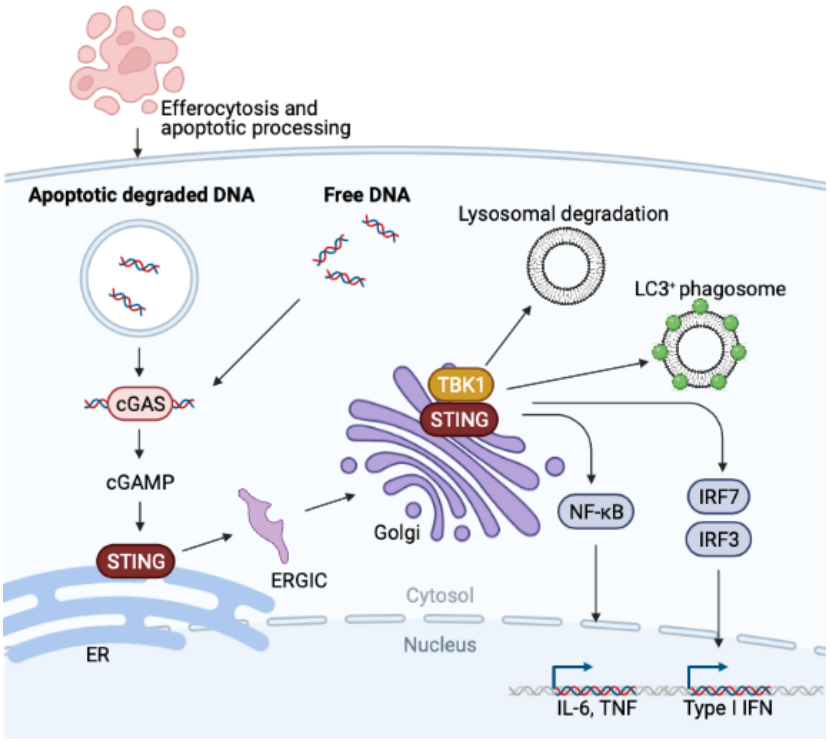

Figure 1.9 The cGAS-STING signalling pathway overview

A schematic overview showing DNA activation of cytosolic cyclic GMP–AMP synthase (cGAS), which can occur via free cytosolic DNA and via uptake and processing of apoptotic cells containing DNA. On binding of DNA, cGAS leads to the synthesis of 2′3′ cyclic GMP–AMP (cGAMP). cGAMP binds to stimulator of interferon genes (STING) dimers found at the endoplasmic reticulum (ER). Significant conformational changes occur in STING that allows STING oligomerisation, which primarily allows STING to be released from the ER and integration with trafficking factors. STING passes through the ER–Golgi intermediate compartment (ERGIC) and Golgi, where it recruits TANK-binding kinase 1 (TBK1), leading to STING phosphorylation and recruitment of interferon regulatory factor 3 and 7 (IRF3/7). Activated IRF3 and IRF7 can translocate to the nucleus and induce different gene expression, for example expression of type I interferons, interferon-stimulated genes (ISGs), chemokines, inflammatory mediators and pro-apoptotic genes. Activation of STING can also lead to NF-κB stimulation and the formation of $LC3^{+}$ phagosomes. STING is eventually degraded within autophagosomes and lysosome, the latter being transported from the Golgi. Created using BioRender.

1.11 Rationale

AML is currently an incurable malignancy with low survival rates even with intensive treatment strategies. Moreover, these treatment strategies largely remain unchanged over recent decades, even with novel therapeutics emerging. As such, more research and the identification of novel therapeutic interventions are needed for the improved survival outcomes of AML patients. Recent studies have identified that interactions within the BM microenvironment, specifically cell interactions with AML cells, as having an important impact on the control of AML growth. Thus, it is envisaged that new therapies will be generated by understanding the biological processes that underpin AML biology. AML has been shown to rely heavily on their microenvironment not only for proliferative capacities but the evading of current chemotherapy strategies. AML interactions with BM macrophages has been shown to be important in AML regulation, and as such highlights a potential mechanism that can be exploited for AML treatments.

In this study, AML interactions with BM macrophages will be investigated in terms of the phagocytic capacities of BM macrophages and how that may contribute to the progression of AML. Research will focus on whether LAP dependent mechanisms are important in the clearance of apoptotic AML cells with the aim to identify how this process may contribute to AML growth and survival.

1.12 Hypothesis

I hypothesise that during AML apoptosis, BM macrophages efficiently process AML ABs via LAP dependent mechanisms. The increased AML turnover, their reliance on OxPHOS and increased mitochondrial load leads to increased ABs that contain mitochondrial contents. I also hypothesise that LAP of AML ABs containing mitochondrial DNA leads to STING activation in BM macrophages which supports the phagocytic capacities via increased TIM4 expression or increased $LC3^{+}$ phagosome formation.

1.13 Aims and Objectives

1. To investigate the impact of LC3 associated phagocytosis in BM macrophages and explore how deficiencies in this process effects AML progression.
2. To determine what mechanisms BM macrophages, through LC3 associated phagocytosis, deploy to process apoptotic AML cells and their apoptotic cargo and how that influences BM macrophages phenotypically.
3. To investigate what role TIM4 in BM macrophages has upon AML progression and if this is linked to LC3 associated phagocytosis.

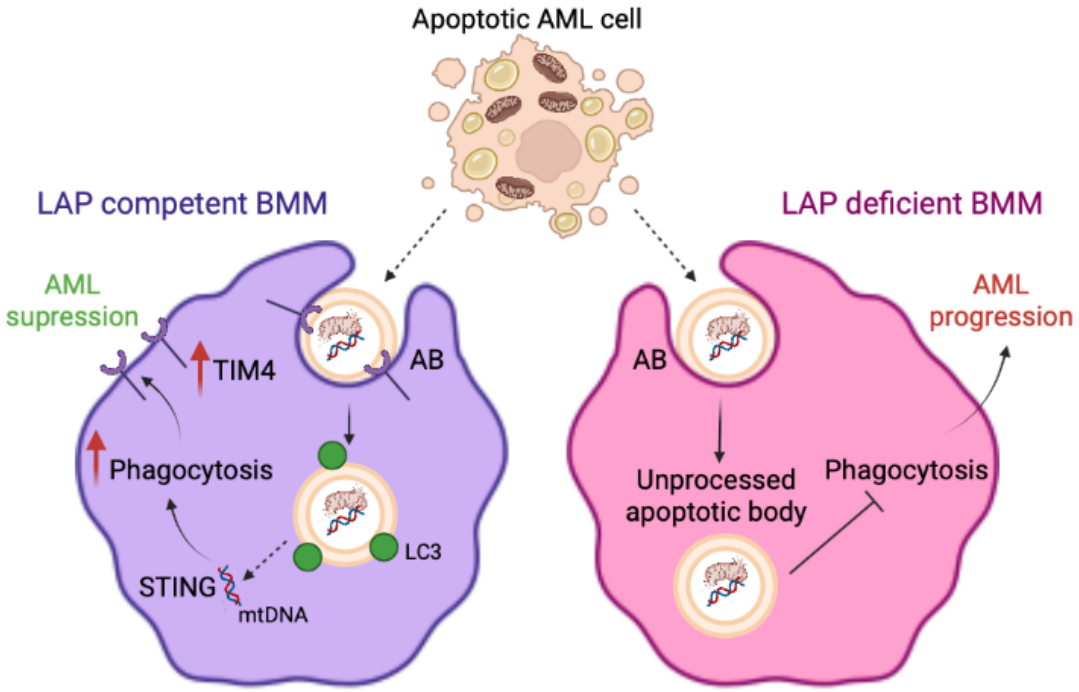

Figure 1.10 Graphical representation of research hypotheses

AML apoptotic bodies (ABs) containing mitochondria are taken up by LC3 associated phagocytosis (LAP) competent bone marrow macrophages (BMM). The processing of apoptotic cargo leads to sensing of AML mitochondrial DNA (mtDNA) via STING, which allows changes to occur in the BMM to increase its phagocytic potential, such as increase in TIM4 expression. In LAP deficient models, apoptotic cargo is not processed correctly and as such no stimulation of increased phagocytosis occurs.

2. Materials and methods

2.1 Materials

The reagents and materials used in this study are described in the methods below. The reagents were obtained from the manufacturers as indicated below.

Table 2.1 Reagents used, with manufacturer and catalogue number.

Product	Manufacturer	Catalogue Number
µ-Plate 24 Well Black Plates	Thistle Scientific	82406
1.0 µm microshperes CML Latex Beads, 4% w/v	Fisher Scientific	11540136
26G Butterfly Needles	Fisher Scientific	12349169
2',3'-Dideoxycytidine (ddC)	Abcam LTD	AB142240
26G Needles	Fisher Scientific	12349189
Alexa Fluor® 488 Anti-LC3B antibody	Abcam LTD	AB225382
APC Annexin V Apoptosis Detection Kit	Biolegend	640932
Annexin V Apoptosis Detection Set PE-Cyanine7	ThermoFisher	15531207
Bafilomycin A1 (BafA1)	Merck Life Science	B1793-2UG
Bovine Serum Albumin	Fisher Scientific	BP1600-100
Busulfan	Sigma Aldrich	B2635
Cellometer SD100 counting chamber	Nexcelom Bioscience	CHT4-SD100-002
CellTrics 30/40/50µm filter	Wolf Labortatories	04-0042-2316
CD117 MicroBeads, mouse	Miltenyi Biotec	130-091-224
CD14 MicroBeads, human	Miltenyi Biotec	130-050-201
CD34 Microbeads, human	Miltenyi Biotec	130-046-702
Combo: Clophosome®-A and Control Liposomes	Stratech Sceintific	F70101C-AC-FOR
D-Luciferin	Fisher Scientific	8829
DAPI	ThermoFisher	62248
DMEM Medium	ThermoFisher	10566016
DMSO	Fisher Scientific	BP231-100
EDTA	Sigma Aldrich	E9886
Fetal Bovine Serum	ThermoFisher	105000056
Fetal Bovine Serum, exosome-depleted	ThermoFisher	A2720803
FIX & PERM Cell Fixation & Cell Permeabilization Kit	ThermoFisher	GAS004
FlouroBrite DMEM	ThermoFisher	A1896701
GenElute Mammalian Genomic DNA Miniprep Kit	Sigma Aldrich	G1N70
H-151 STING inhibitor	SAS Invivogen	INH-H151
Heparin	Sigma Aldrich	H3393
Histopaque-1077	Sigma Aldrich	10771
Hoechst 33342 Solution	ThermoFisher	62249
Human IL3	PeproTech	200-03
Human IL6	PeproTech	200-06

Human TPO	PeproTech	200-07
IsoFlo - Isoflurane	DMU - in house	-
L-Glutamine	Sigma Aldrich	G7513
LS columns	Miltenyi Biotec	130-042-401
MEM Medium	ThermoFisher	11095080
MethoCult	STEMCELL	4434
MitoTracker Green FM	ThermoFisher	M7514
MitoTracker Red FM	ThermoFisher	M22425
Mouse IL3	PeproTech	213-13
Mouse IL6	PeproTech	216-16
Mouse Lineage Cell Depletion Kit	Miltenyi Biotec	130-110-470
Mouse mCSF	PeproTech	315-02
Mouse SCF	PeproTech	250-03
MS columns	Miltenyi Biotec	130-042-401
ND1 Taqman Gene Expression Assay Mouse	ThermoFisher	4331182_Mm042252
OneComp eBeads™ Compensation Beads	ThermoFisher	01-1111-42
Opti-MEM	ThermoFisher	31985062
PCRBIO 1-Step Go RT-PCR Kit	PCR Biosystems	PB10.53-10
Penicillin-Streptomycin	GE-Healthcare	SV30010
pHrodo™ Red, succinimidyl ester (pHrodo™ Red, SE)	Fisher Scientific	10676983
pHrodo(TM) E. COLI BIOPARTICLES(R) CONJUGATE	Fisher Scientific	10581135
Proteome Profiler Mouse XL Cytokine Arrays	R&D Systems	ARY028
qPCRBIO SyGreen Mix	PCR Biosystems	PB20.12-51
ReliaPrep RNA Cell Miniprep System	Promega	Z6012
rLV.EF1.AcGFP-Mem9	Clontech	0019VCT
rLV.EF1.mCherry-Mito-9 lentivirus	Clontech	0024VCT
RMT4-54 Ultra-LEAF™ Purified Tim-4 Antibody	Biolegend	130016
RPMI Medium	ThermoFisher	11875093
Sodium Pyruvate	Fisher Scientific	11501871
StemMACS HSC expansion Medium	Miltenyi Biotec	130-101-526
TaqMan Human Tert	ThermoFisher	4403316
Taqman Mouse Tert	ThermoFisher	4458368
TaqPath ProAmp MasterMix	ThermoFisher	A30865
Tris Base	Fisher Scientific	BP152-1
Trypan Blue Solution	Sigma Aldrich	T8154
Trypsin-EDTA	ThermoFisher	25200056
Tween-80	Fisher Scientific	T164-500
VECTASHIELD® mounting media	Vector Laboratories	H-1400-10
Zymosan A (S. cerevisiae) BioParticles™, Texas Red™ conjugate	Fisher Scientific	11580896

BioLegend (San Diego, CA, USA), Clontech Takara Bio, Saint-Germain-en-Laye, France), Fisher Scientific (Hampton, New Hampshire, USA), GE Healthcare (Little Chalfont, UK), Ibidi (Munich, Germany), Machery-Nagel, Duren, Germany), Merck Millipore (Burlington, MA, USA), Miltenyi Biotec (Bergisch Gladbach, Germany), New England BioLabs (Ipswich, MA, USA), PCR Biosystems (London, UK), Peprotech (Rocky Hill, NJ, Promega (Madison, WI, USA), USA), Qiagen (Hilden, Germany), Sigma Aldrich (St Louis, MO, USA), ThermoFisher (Waltham, MA, USA) and Vector Laboratories Ltd (Peterborough, UK).

2.2 Animals

All animal research attributed to in this thesis was carried out in accordance with regulations set by the UK Home Office and the Animal Scientific Procedures Act 1986 under project license 70/8814 (Prof. Kristian Bowles) and PP0023671 (Dr. Stuart Rushworth). All procedures were carried out by me, under UK Home Office personal license ID99A0852, with assistance from Dr Jayna Mistry (I2777C6D5), Dr Charlotte Hellmich (and Dr Stuart Rushworth (ICD3874DB). Full training was conducted by Mr Richard Croft (IGEBEFB87) and Mrs Anja Croft (L8A2ACED) before undertaking procedures. Animals were housed in a pathogen free, containment level 3 laboratory in the Disease Modelling Unit (DMU) at the University of East Anglia. The mice were maintained and bred in the "barn" of the DMU. Breeding pairs were kept together for 6 months before separation and the offspring weaned 3 weeks post birth. Mice used were at age 8-12 weeks of age and both genders were used for experiments. Non-obese diabetic (NOD) severe combined immunodeficiency (SCID) Il2rg knockout (NOD.Cg.Prkd^{scid}IL2rg^{tm1Wji}/SzJ (NSG) mice were purchased from The Jackson Laboratory (Bar Harbour, ME, USA). C57BL/6J mice were purchased from Charles River (Massachusetts, United States). Atg16l^{E230-} and Atg16l^{E230+} mice were provided by Prof. Thomas Wileman. LysMcreAtg16l^{E230-}mice were provided by Prof. Thomas Wileman and Dr. Naiara Beraza.

2.2.1 NSG mice

NSG mice are deficient of B and T cell as the scid mutation is located in Prkdc, a DNA repair complex protein. Additionally, they are deficient in functional NK cells due to the IL2rgnull mutation. This severe immune deficiency allows for the human xenograft experiments. As such, NSG mice were used for human AML and human CD34^{+} haematopoietic stem cell engraftment in this study to identify uptake of AML mitochondria in cell populations. The mice were not irradiated before transplantation, as such the animals were relatively healthy.

2.2.2 C57/BL6 mice

The C57/BL6 is a commonly and widely used inbred mouse strain. The C57/BL6 mice are long-lived and breed well. They have a functioning immune system so all experiments requiring engraftment of murine AML (MN1 or MEIS1/HOXA9) required pre-treatment with busulfan. Busulfan was intraperitoneally injected into C57/BL6 mice 2 days before murine AML injection. The schedule of busulfan treatment required 2 days of injection with 25mg/kg busulfan each day. The C57/BL6 mice were used in this study for the depletion of macrophages to study the effect of AML growth in a macrophage deficient environment with the use of clodronate liposomes (2.2.8). C57/BL6 mice were used for the derivation of bone marrow derived macrophages and bone marrow stromal cells for in vitro experiments. Furthermore, C57/BL6 mice were used in STING inhibiting experiments with the use of H-151 and TIM4 inhibiting experiments using RMT4-54.

2.2.3 Atg16l^{E230} and LysMcreAtg16l^{E230} mice

Atg16l^{E230-} mice were generated by Prof. Thomas Wileman's group. LAP requires the E3 ligase-like activity of the LC3 conjugated machinery (ATG12–ATG5-ATG16L1 complex). ATG16L1 has a N-terminal domain that binds the ATG12–ATG5 conjugate, this is followed by a coiled-coil domain (CCD) that binds WIPI2, which facilitates the complex to the phagosome membrane. At the CCD, a linker region attaches a large C-terminal WD containing several WD repeats which is required for LAP. As such, 2 stop codons were inserted in the frame at the end of the CCD of the *Atg16L1* gene, resulting in the generation of Atg16l^{E230} mutation conveying the ability to undergo autophagy but not LAP. Mice lacking the WD and linker domain of ATG16L1 were generated by homologous recombination in embryonic stem cells.

LysMcreAtg16l^{E230} mice were generated by Dr. Naiara Beraza's group. Heterozygous floxed LysMcre mice were mated with homozygous lox-P flanked Atg16 mice to generate homozygous lox-P flanked Atg16 and LysMcre mice. These mice were then mated with Atg16L1^{E230-} to generate LysMcreAtg16l^{E230-} mice. The resulting Atg16L1$^{E230f/f}$ Cre^{+} mice were LAP deficient specifically in myeloid cells, such as macrophages.

2.2.4 Schedule 1

Mice were monitored daily and humanely sacrificed at the first sign of illness (weight loss, reduced motility, severe over grooming, hind limb paralysis, hunched posture, and piloerection) using schedule 1 methods. Additionally, the end point of experiments, animals were sacrificed via schedule 1 methods. Mice were sacrificed via gradual CO_2 asphyxiation followed by neck dislocation.

2.2.5 Animal injections

Busulfan, Clodronate, H-151, RMT4-54 and D-luciferin were all administered using an intraperitoneal (IP) injection. The mice were restrained using a scruff technique and 150-200µl of the compounds were injected with a sterile 26-gauge needle into the peritoneum. In the case of where daily IP injections were needed, the mice were IP injected in alternate flanks. For humanised and human AML NSG models, the donor cells ($1x10^6$ of either $CD34^+$ cells isolated from cord blood or human AML blasts) were administered to recipient NSG mice via intravenous (IV) tail vein injection. For murine AML models using MN1 and MEIS1/HOXA9 cells, $1x10^6$ cells were administered to the busulfan treated recipient mice via IV tail vein injection. The mice were placed in a 37℃ heat box for 10 minutes for tail vein vasodilation prior to injection. The mice were then placed in a benchtop holder and 200µl of $1x10^6$ cells suspended in PBS was injected into the lateral tail vein with a sterile 26-gauge needle. Mice were transferred to their home cage after injection for recovery.

2.2.6 Bone marrow isolation

Isolation of bone marrow was achieved by isolating the femur and tibia from each mouse. Each bone was cut centrally and placed in a 0.5ml microcentrifuge tube containing a hole, this allowed removal of the bone marrow from the bone. The 0.5ml microcentrifuge tube was placed in a 1.5ml microcentrifuge tube and centrifuged for 6 seconds to allow collection of bone marrow cells. The bone marrow pellet from each mouse was collected and washed in 1ml of MACS buffer (1XPBS, 0.5% BSA, 2mM EDTA, filtered) before being passed through a 40µm CellTrics filter (Sysmex, Japan).

2.2.7 Bone marrow cell counts

After isolation of bone marrow, the automated cell counter Cellometer Auto T4 Bright field Viability Cell Counter (Nexcelom Bioscience LLC Lawrence, MA, USA) was used. The Auto T4 utilises bright field microscopy with pattern recognition software to count single live, dead, and total cells. Isolated bone marrow cells were diluted 1 in 10 in MACS buffer (10µl in 90µl). The cell aliquots were then diluted in a 1:1 ratio with Trypan Blue (100µl and 100µl), and 20µl was loaded onto a Cellometer SD100 counting chamber (Nexcelom Bioscience LLC Lawrence, MA, USA). The cell concentration was calculated accounting for dilution factors (total dilution factor 20).

2.2.8 Clodronate liposome experiment

C57/BL6 mice were treated via intraperitoneal (IP) injection of 25mg/kg of busulfan on day -2 and day -1 prior to tail vain injections of $1x10^6$ MEIS/HOXA9-luci cells or MN1-GFP cells on day 0. 19 days post injection animals were imaged via in vivo bioluminescent imaging (2.2.11, Bruker, Coventry) and then injected IP with either 150µl of clodronate liposomes or control liposomes (Clophosome®-A, Stratech, UK). Animals were imaged again and scarified at day 23 post murine AML injection. Bioluminescence levels of MEIS/HOXA9-luci cells was analysed via ImageJ (Fiji). The BM was harvested from the tibia and femur of both hind legs from each mouse and the macrophage number (GFP^-, $CD45^+$, $GR1^-$, $CD115^{LOW/INT}$, $F4/80^+$) and engraftment (GFP^+) was analysed via flow cytometry.

2.2.9 In vivo STING inhibition

C57/BL6 mice or $Atg16l^{E230}$ mice were treated via IP injection of 25mg/kg of busulfan on day -2 and day -1 prior to tail vain injections of $1x10^6$ MN1-GFP cells on day 0. At day 7, 9, 11 and 13 post MN1-GFP injection, mice were IP injected with 200µl of H-151 (750nmol, Invivogen) or vehicle (200µl of PBS with 0.1% TWEEN80). The animals were sacrificed at day 14 post injection and the BM isolated as previously described. The BM was analysed using flow cytometry for MN1 engraftment (GFP^+), live MN1 cells (GFP+, annexin V-) and T-cell activity (GFP^-, $CD45^+$, $NK1.1^-$, $B220^-$, $CD4^+/CD8^+$, $CD8^+$-IFN-γ^+). The bone marrow macrophages (GFP^-, $CD45^+$, $GR1^-$, $CD115^{LOW/INT}$, $F4/80^+$) were

sorted via FACS (FACSMelody, BD) into RNA lysis solution (250µl of BL+TG buffer), and the RNA was extracted (2.7.1). Gene expression analysis was carried out using qPCR for *GBP2, IRF7, IFIT3, IL1ß* and *IL6* and normalised against *GAPDH.*

2.2.10 In vivo TIM4 inhibition

C57/BL6 mice were treated via IP injection of 25mg/kg of busulfan on day -2 and day -1 prior to tail vain injections of $1x10^6$ MN1-GFP cells on day 0. At day 7, 9, 11 and 13 post MN1-GFP injection, mice were IP injected with 150µl of RMT4-54 TIM4 inhibitor (250µg, Ultra-LEAF™ Purified anti-mouse Tim-4 Antibody, Biolegend). The animals were sacrificed at day 14 post injection and the BM isolated as previously described. The BM was analysed using flow cytometry for MN1 engraftment (GFP^+), AML debris (SSC^{LOW}, FSC^{LOW}, GFP^+) bone marrow macrophages (GFP^-, $CD45^+$, $GR1^-$, $CD115^{LOW/INT}$, $F4/80^+$), AML associated macrophages (GFP^-, $CD45^+$, $Lys6G^-$, $CD11b^+$) and T-cell activity (GFP^-, $CD45^+$, $NK1.1^-$, $B220^-$, $CD4^+/CD8^+$, $CD8^+$-IFN-γ^+). The AML associated macrophages were sorted via FACS (FACSMelody, BD) into RNA lysis solution (250µl of BL+TG buffer), and the RNA was extracted (2.7.1). Gene expression analysis was carried out using qPCR for *GBP2, IRF7, IFIT3, IL1ß, TNFa* and *IL6* and normalised against *GAPDH.*

2.2.11 Live in vivo imaging

To analyse AML tumour burden and location, bioluminescent imaging of live mice was performed. This was enabled as murine AML cells (MEIS1/HOXA9) expressed the luciferase construct (2.3.7). MEIS1/HOXA9-luci engrafted mice were intraperitoneally injected with 150mg/kg of D-luciferin (Invitrogen). The mice were then left for 10 minutes at room temperature for optimal detection of the luciferase signal. The mice were then anaesthetised using isoflurane (IsoFlo, DMU in house) during the last 5 minutes using a chamber filled with isoflurane with a flow rate of 2-4%. After confirmation of loss of consciousness, the mice were transferred to the Bruker In-Vivo Xtreme (Bruker, Coventry, UK) and imaged. The imaging was preformed via a pre-set method of 1 minute exposure bioluminescent image, x-ray and light image. Mice were transferred to their home cage after imaging for recovery. Tumour burden and location

was visualised by the detection of light produced by the formation of Oxyluciferin from luciferin, which is catalysed by the luciferase in the modified MEIS1/HOXA9-luci cells. Images captured were edited using ImageJ, specifically bioluminescent images and X-Ray images were merged. Bioluminescence analysis was carried out using ImageJ software.

2.2.12 Engraftment of human CD34$^+$ and AML cells in to NSG mice

For the humanised CD34$^+$ haematopoietic progenitor cell model, 6-8 week old NSG mice were treated with 3 doses of 25mg/kg of busulfan via IP injection on day -3, day -2 and day -1 before injected non-malignant CD34$^+$ on day 0. NSG mice were then IV injected with 1x10^6 isolated CD34$^+$ cord blood cells. The BM was also analysed for human cell engraftment by human CD45$^+$ cells. For human AML NSG models, 1x10^6 primary AML blasts, with and without rLV.EF1.mCherry-mito9 lentivirus transduction (2.3.3) were injected IV into non-treated 6-8 week old NSG mice. At pre-defined humane end points animals were sacrificed, bone marrow isolated and engraftment determined using expression of human CD45. Mouse bone marrow cells were examined via flow cytometry for bone marrow stromal cells (CD45$^-$/CD105$^+$) and bone marrow macrophages (CD45$^+$, GR1$^-$, CD115$^{LOW/INT}$, F4/80$^+$). The MFI mCherry intensity of each population was analysed via FlowJo (TreeStar, Ashland).

2.3 Cell culture

Culture of cells was carried out in 5% CO_2 at 37°C.

2.3.1 Primary human cells

Non-malignant and malignant human haematopoietic cells were collected at the Norfolk and Norwich University Hospital by Dr Charlotte Hellmich. Studies were performed following approval from the United Kingdom Health Research Authority research ethics committee (LRCEref07/H0310/146). Bone marrow aspirates were obtained in collection tubes containing 5ml of Dulbecco's Modified Eagle's Medium (DMEM) and 100 units of Heparin. Umbilical cord blood was obtained in collection tubes containing 15ml of DMEM and 500 units of Heparin. Primary AML blasts were obtained from the bone marrow of AML patients after informed consent and under approval from the UK National

Research Ethics Service (LRCEref07/H0310/146). AML cells and $CD34^+$ haematopoietic stem cells were isolated via density gradient centrifugation. Density gradient centrifugation was achieved via the use of Histopaque-1077 (Sigma-Aldrich). Cells differentially migrate through the Histopaque-1077 allowing for fractionation of cell populations. Briefly, 10ml of Histopaque per 15-20 mL of bone marrow was added to a 50ml falcon tube. The bone marrow was then carefully layered on top of the Histopaque and centrifuged at 300xg for 20 minutes with no brakes or acceleration. After centrifugation, the red cells along with heavy granulocytes are pelleted at the bottom with a layer of Histopaque atop. The 'buffy coat' (containing mononuclear cells) is located on top of the Histopaque layer with the final layer on top of that being the plasma. The 'buffy coat' was removed with a pasture pipette and washed with PBS by the addition of PBS up to 50ml in a new falcon tube and centrifugation at 300xg for 5 minutes with brakes and acceleration on.

Isolated cells from cord blood were further processed to isolate $CD34^+$ cells. The $CD34^+$ cells were enriched using magnetic-activated sorting (MACS) and magnetically labelled CD34 microbeads (Miltenyi Biotec, Germany). The CD34 magnetic microbeads were added to the isolated cells and incubated at 4˚C for 30 minutes according to the manufacturers protocol. The cells were then centrifuged at 300xg for 5 minutes and resuspended in 3ml of MACS buffer. The cells were loaded onto a LS column (Miltenyi Biotec, Germany) prewashed with MACS buffer attached to a magnet. The column was washed three times with MACS buffer and the $CD34^+$ cells were flushed from the LS column by removal from the magnet and plunging the column. The cells were then used directly for experiments or cryopreserved. AML cells were cultured in Dulbecco's Modified Eagle Media (DMEM) containing 10% foetal bovine serum (FBS) plus 1% penicillin-streptomycin. $CD34^+$ cells were cultured in StemMACS™ HSC Expansion Medium (Miltenyi, Biotec, Bergisch Gladbach, Germany) supplemented with stem cell factor (SCF, 10ng/ml), Flt-3 ligand (FLT3, 10ng/ml), thrombopoietin (TPO, 10ng/ml), interleukin (IL) 3 and IL 6 (10ng/ml). Supplementation was sourced from PeproTech, Inc. (Rocky Hill, NJ, USA).

2.3.2 Primary CD14 monocyte isolation

Peripheral blood (PB) samples taken from healthy and AML patients was performed by Dr Charlotte Hellmich under informed consent approval from the UK National Research Ethics Service (LRCEref07/H0310/146). Between 5-10ml of PB was collected in EDTA blood collection tubes. Mononuclear cells were isolated via Histopaque as described above. AML peripheral blood samples were also thawed from previous samples as described in 2.3.7. Cells were counted via Trypan Blue exclusion (2.4.1) to determine cell number. The $CD14^+$ cells were isolated using MACS and magnetically labelled CD14 microbeads (Miltenyi Biotec, Germany). The appropriate amount of CD14 microbeads was added to the cells according to the manufacturer's instructions. The labelled cells were incubated at 4˚C for 30 minutes and were centrifuged at 300xg for 5 minutes. The cells were resuspended in 1ml of MACS buffer. The cells were loaded onto a MS column (Miltenyi Biotec, Germany) prewashed with MACS buffer attached to a magnet. The column was washed three times with MACS buffer and the $CD14^+$ cells were flushed from the MS column by removal from the magnet plunging the column. $CD14^+$ cells were then fixed and permeabilised via Invitrogen™ FIX & PERM™ Cell Permeabilization Kit (ThermoFisher, MA, USA) according to the manufacturers protocol. Briefly, $CD14^+$ cells were spun at 300xg for 5 minutes and resuspended in 200µl of MACS buffer. 100µl of reagent A was added for 15 minutes at room temperature after which cells were washed with MACS buffer. Cells were resuspended in 100µl of MACS buffer with the addition of 100µl of reagent B as well as 1µl of LC3-FITC and 1µl of DAPI for 20 minutes at room temperature protected from light. The $CD14^+$ cells were washed once with MACS buffer and resuspended in appropriate volumes to allow 100,000 cells/10µl. 10µl of $CD14^+$ cells were added to µ-Plate 24 well black plates (Ibidi) in duplicate and covered with a cover slip. $CD14^+$ cells were imaged using confocal microscopy (Zeiss LSM 800 Axio Observer.Z1 confocal microscope, Carl Zeiss) to assess LC3-FITC signals between AML and healthy $CD14^+$ cells. LC3 density was calculated using ImageJ software.

2.3.3 rLV.EF1.mCherry AML generation

To generate mCherry mitochondria in primary AML cells (mCh-AML), primary AML cells were seeded at a density of $5x10^4$ in 500µl of DMEM supplemented with 10% FBS. AML cells were transduced with 0.5µl of rLV.EF1.mCherry-Mito-9 lentivirus ($0.5x10^6$ virus particles, Clontech Takara Bio Europe, France). 1ml of DMEM medium was added after 24 hours and AML cells were cultured for an additional week to ensure no residual lentivirus remained. Transduction was confirmed by the detection of mCherry fluorescence in AML cells by fluorescent microscopy.

2.3.4 Murine bone marrow macrophages

Mouse bone marrow derived macrophages (BMDM) were isolated via cultured mouse bone marrow in RPMI-1640 (Gibco) containing 20% FBS (Gibco) plus 1% penicillin-streptomycin (Gibco) supplemented with 20ng/ml of macrophage CSF (Peptrotech, NJ, USA). Briefly, $1\text{-}2x10^7$ bone marrow cells in 10ml of fresh media were plated onto 10cm plastic dishes. The addition of 5ml of fresh media was added at day 3. At day 6-7, cells were washed with 1xPBS, cold PBS was added, and cells were removed by cell scraping. After cell number was established, BMDM were plated in RPMI-1640 containing 20% FBS plus 1% penicillin-streptomycin for 24 hours before experimental use. For longer survival, BMDM were cultured in RPMI-1640 containing 20% FBS plus 1% penicillin-streptomycin supplemented with macrophage CSF (10ng/ml). Mouse BMDM markers were confirmed by flow cytometry for $F4/80^+$, $GR1^-$. Isolation of $F4/80^+$ from BM samples were isolated using positive selection for F4/80 microbeads using the protocol described in 2.3.1 (Miltenyi Biotec, Germany) or via FACS sorting using anti-F4/80-FITC antibody and the FACSMelody (BD, Franklin Lakes, NJ, USA). $F4/80^+$ cells were sorted into RPMI-1640 media containing 20% FBS plus 1% penicillin-streptomycin.

2.3.5 Murine bone marrow stromal cells

The bone marrow of mice was cultured in Minimum Essential Medium Eagle (MEM) supplemented with 20% FCS, and 1% penicillin-streptomycin for 96 hours. The media was removed, and non-adherent and non-viable cells were then washed off with PBS. Fresh MEM media was added to the remaining

adherent cells in the flask. The media was replaced twice a week until BMSC colonies were visible. The BMSC were characterised by their adherence to cell culture plastics and the expression of the cell surface markers CD105 and CD140a but not CD45 and CD31. To disassociate cells, Trypsin-EDTA was used. Briefly, BMSC cells were growth to a confluence of 70-80%, the media was removed, and the cells washed with PBS to remove residue media containing FBS. Trypsin-EDTA was added and incubated for 2 minutes. Disassociation was confirmed by light microscopy, the cells were resuspended in fresh media before BMSC cells were plated at the correct density. The cells were then used directly for experiments.

2.3.6 LSK cell isolation

Mouse LSK cells were isolated from the bone marrow of mice using the mouse direct lineage cell depletion kit (Miltenyi Biotec, Germany) according to the manufacturers protocol and as described in 2.3.1. The flow through was collected containing lineage negative cells (Lin^-). Lin^- cells were further enriched with CD117 microbeads (Miltenyi Biotec, Germany) and then sorted for SCA1-APC (Miltenyi Biotech, Germany) on a FACSMelody (BD, Franklin Lakes, NJ, USA). The LSK cells were expanded in DMEM containing 10% FBS plus 1% penicillin-streptomycin supplemented with mSCF (100ng/ml), mIL3 (10ng/ml) and hIL6 (10ng/ml) (Peptrotech, NJ, USA).

2.3.7 MN1 and MEIS1/HOXA9 cells

MN1 and MEIS1/HOXA9 cells were generated as previously described [460]. Briefly, Lin^- cells from C57BL/6J were isolated as previously described. Lin^- cells derived from C57BL/6J were retrovirally infected by coculture with GP+E86 cells (ATCC) transfected with pSF91MN1iGFP, or MIH-HA-HoxA9 in the presence of polybrene (10 µg/mL, Sigma-Aldrich) for 3 days. MIH-HA-HoxA9 transfected cells were then cocultured with GP+E86 packaging MIY-HA-Meis1a to generate MEIS1.HOXA9 and MN1 overexpressing cells. Cells were maintained in DMEM 10% FBS plus 1% penicillin-streptomycin supplemented with mSCF (100ng/ml), mIL3 (10ng/ml) and hIL6 (10ng/ml) (Peptrotech, NJ, USA). MEIS1/HOXA9 cells were infected with pCDH-luciferase-T2A-mCherry for in vivo imaging, kindly provided by Professor

Irmela Jeremias, (Helmholtz Zentrum München, Munich, Germany). MEIS1/HOXA9 cells were plated at $5x10^4$ per well in 12-well plates and expanded. Transduced MEIS1/HOXA9 cells (MEIS1/HOXA9-luci) were sorted using mCherry fluorescence on a BD FACSMelody (BD Bioscience).

2.3.8 mCherry AML co-culture with BMDM and BMSC

A co-culture system was used to determine mitochondrial movement from mCherry AML (mCh-AML) to bone marrow derived macrophages (BMDM) and bone marrow stromal cells (BMSC). BMDM and BMSC were seeded in a 24-well plate at a density of 5×10^5 in normal culture media. The media was replaced 24 hours after seeding and mCh-AML cells were added at 4:1 ratio for 6 hours. BMDM and BMSC were then washed 3 time with PBS to remove mCh-AML cells and fixed and permeabilised via Invitrogen™ FIX & PERM™ Cell Permeabilization Kit (ThermoFisher, MA, USA) as per manufacturer's instruction with the addition of DAPI. Cells were then imaged via confocal microscopy using the Zeiss LSM 800 Axio Observer.Z1 confocal microscope (Carl Zeiss). BMDM and BMSC cells in mono-culture were used as controls.

2.3.9 Cell Cryopreservation

Primary AML samples taken from patients were cryopreserved upon AML cell isolation. MN1 and MEIS1/HOXA9 cells were cryopreserved for long term storage. AML cells, MN1 and MEIS1/HOXA9 cells frozen at a $5x10^6$ cells/ml concentration in FCS supplemented with 10% DMSO. Cells were then transferred to cryotubes and slowly preserved in a Mr. Frosty™ Freezing Container (ThermoFisher, Waltham, MA, USA) in a -80˚C freezer. The Mr. Frosty™ Freezing Container cools at -1˚C/minute, which is optimal for cell cryopreservation.

To thaw cells, first culture media was pre-warmed to 37˚C. The cryotubes were then removed from the -80˚C freezer and placed at 37˚C until partially defrosted, with a small amount of cell mixture frozen. Prewarmed media was added to the cryovial slowly and then the cells were transferred into a 15ml falcon tube with 10ml of warm media. This was again done slowly to dilute the DMSO. The cells were centrifuged at 300xg for 5 minutes, the supernatant

discarded, and the pellet was resuspended in the relevant media and cultured accordingly.

2.4 Cell viability assays

2.4.1 Cell counting via Trypan Blue

The Trypan Blue exclusion assay is a commonly used methodology that allows determination of viable cell numbers. Viable cells passively exclude Trypan Blue due to the intact cellular membrane, whereas non-viable cells without an intact membrane rapidly take up Trypan Blue. A 10µl aliquot of the cell suspension was mixed in a 1:1 ratio with Trypan Blue. The cell mixture was then pipetted onto a haemocytometer, and the healthy cells were counted. The four outer quadrants were counted, averaged, and the cells/ml was calculated by the calculation below (Figure 2.1).

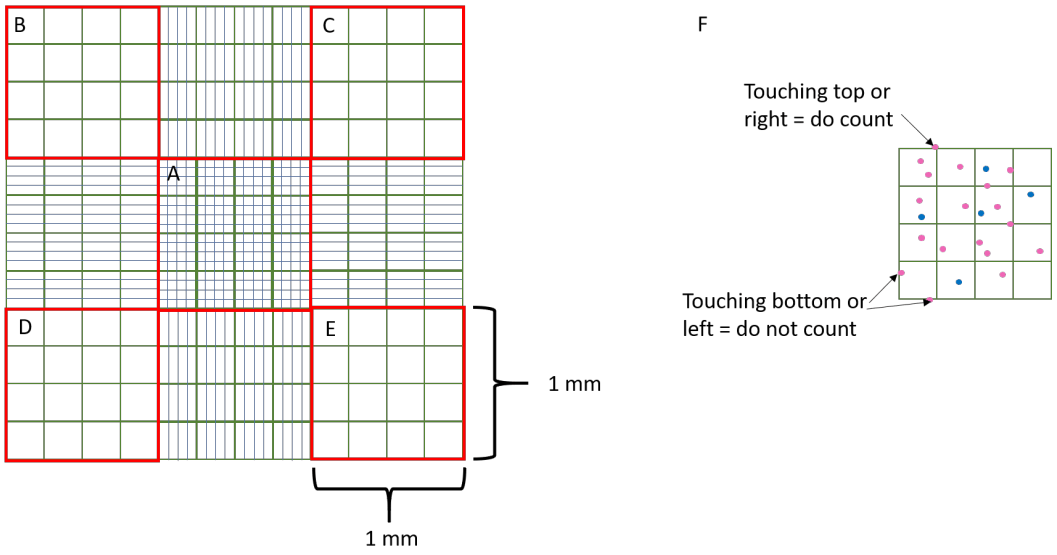

$$\text{Cell number (cells/ml)} = \left(\frac{\text{Viable cell number}}{\text{Number of quadrants counted}}\right) \times \text{Dilution factor} \times 10^4$$

Figure 2. 1 Trypan Blue cell counting

Viable cell numbers using the haemocytometer and Trypan Blue method with calculation. B, C, D and E quadrants are counted. F represents counting strategy.

2.4.2 Apoptosis

The generation, detection and isolation of apoptotic cells and ABs was achieved by the following protocols. Additionally, characterisation of ABs size profile was carried out by Dynamic Light Scattering (DLS) by Adam Pattinson.

2.4.2.1 Apoptosis induction and apoptotic body isolation

To induce apoptosis, cells were treated with 5μM cytosine arabinoside (ara-C) for 24 hours. To determine apoptosis, Annexin V was used. The Annexin V antibody preferentially binds to phosphatidylserine, which under normal condition is in the inner plasma membrane of the healthy cells. However, during cellular apoptosis, phosphatidylserine translocates to the extracellular plasma membrane. As such, this can be used as a marker for cellular apoptosis by the detection of phosphatidylserine by fluorescently labelled Annexin V. Apoptosis was determined by Annexin V-PE-Cy7 (Invitrogen) by flow cytometry. Briefly, cells were washed twice by PBS, once in 1x binding buffer, pelleted by centrifugation and resuspended in 200μl of 1x binding buffer. 5μl of Annexin V-PE-Cy7 antibody was added to the buffer and left to incubate in the dark for 10 minutes. The cells were then washed in 1x binding buffer before being resuspended in 200μl of 1x binding buffer. Apoptotic cells were analysed via flow cytometry (Sysmex Cube 6, BD FACSCanto II and BD FACSMelody).

The isolation of ABs was achieved via centrifugation as previously described [461]. This was achieved by washing apoptotic cells with 1xPBS. Apoptotic cells were then spun at 500xg for 10 minutes. This pellets all large components such as the cells and apoptotic fragments. The supernatant was carefully placed in a new size appropriate tube and the supernatant was spun at 10000xg for 10 minutes. This process pellets ABs, while smaller micro vesicles are retained in the supernatant (Figure 2.2). Confirmation of ABs by the binding of annexin V was achieved via flow cytometry. The ABs pellet was resuspended in either PBS or appropriate media and used in experiments immediately.

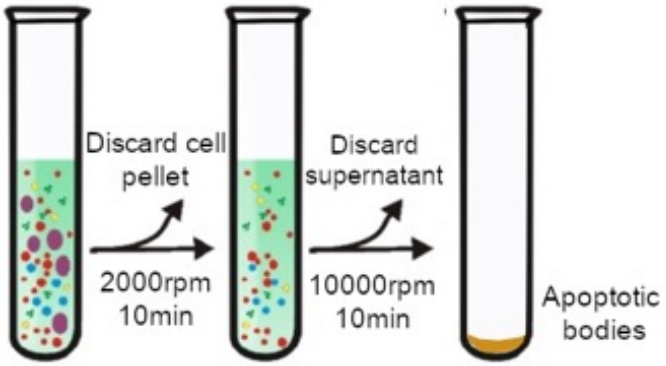

Figure 2.2 Isolation of apoptotic bodies from apoptotic cells via differential centrifugation.

2.4.2.2 Dynamic Light Scattering

To assess the size profile of isolate ABs, Dynamic Light Scattering (DLS) was used. DLS is a biophysical tool which can be used to infer the physical properties of particle-based solutions. Briefly, a laser is passed through a suspension and the light fluctuates over time due to Brownian motion which is detectable by a sensor. This information is used to produce a graphical representation of size profiles within a solution. Before apoptotic induction in MN1 cells, cells were cultured in exosome-depleted FBS (ThermoFisher Scientific) for 1 week. ABs were isolated as previously described, washed twice in PBS before being resuspended in 500µl of PBS. A Malvern ZetaSizer ZS with a solid-state helium-neon laser (λ = 632.8 nm) and detector (placed at 173°) was used to infer the physical profile of ABs. Samples were vortexed for 30 seconds prior to transfer of 450µl of ABs solution to a semi-micro cuvette. ABs were equilibrated for 30 seconds at 25°C prior to analysis which consisted of 3 runs (11 reads per run). A 1:1000 dilution was performed with 1µm microspheres (Invitrogen) and PBS and used as a control for size profile analysis. Microspheres were analysed via DLS as described above. Information generated was exported to Microsoft Excel and displayed via GraphPad Prism 7.

2.5 Microscopy

Microscopy was carried out on EVOS™ M5000 Imaging System (Invitrogen) or Zeiss LSM 800 Axio Observer.Z1 confocal microscope (Carl Zeiss). Morphological images of BMDM as well as MN1-GFP and MEIS1/HOXAP-luci florescence were captured on EVOS™ M5000 Imaging System (Invitrogen). ImageJ by Fiji was used to process all captured images and GraphPad Prism 7 used for analysis.

2.5.1 Phagocytic assays

For phagocytic studies, isolated F4/80$^+$ BM macrophages were plated at a density of 2x10^5 on µ-Plate 24 well black plate (ibidi) in 500µl of RPMI-1640 containing 20% FBS plus 1% penicillin-streptomycin supplemented with macrophage CSF (10ng/ml) until required or FluoroBrite™ DMEM containing 10% FBS plus 1% penicillin-streptomycin for immediate use. Zymosan A (S. cerevisiae) BioParticles™, Texas Red™ conjugate (Invitrogen) were incubated with the BM macrophages according to the manufacturer's instructions for 2 hours. Cells were washed 2x with PBS before being fixed and permeabilised (ThermoFisher, MA, USA) as previously described in 2.3.2 during which LC3-FITC and DAPI was incubated with the BM macrophages for 20 minutes. Cells were washed 2x with PBS and 500µl of FluoroBrite™ DMEM added. Cells were observed under EVOS™ M5000 Imaging System under 40x magnification (Invitrogen) and Zeiss LSM 800 Axio Observer.Z1 confocal microscope with a 63x water objective (Carl Zeiss).

BMDM were plated at a density of 2x10^5 on µ-Plate 24 well black plate (ibidi) in 500µl of RPMI-1640 containing 20% FBS plus 1% penicillin-streptomycin for 24 hours. MN1 ABs were generated and isolated as previously described with the exception that MN1 apoptotic cells were incubated with pHrodo™ Red, SE (Invitrogen) according to the manufacturer's instructions for 30 minutes before ABs isolation. The media was removed from the BMDM and 500µl of FluoroBrite™ DMEM added and the STING inhibitor H-151 (10µM, InvivoGen), TIM4 inhibitor RMT4-54 (30µg/ml, Biolegend) or vehicle (PBS with 0.1% TWEEN80) added for 2 hours. ABs were then cultured with the BMDM for 3 hours. For lysosomal inhibition, 1µM of Bafilomycin A1 (BafA1) was

added to BMDM 1 hour before the addition of pHrodo ABs. Cells were fixed and permeabilised as previously described during which LC3-FITC and DAPI was incubated with the BMDM for 20 minutes. Cells were washed 2x with PBS and 500µl of FluoroBrite™ DMEM added. Cells were observed under EVOS™ M5000 Imaging System under 40x magnification (Invitrogen) and Zeiss LSM 800 Axio Observer.Z1 confocal microscope with a 63x water objective (Carl Zeiss).

BMDM were plated at a density of $2x10^5$ on µ-Plate 24 well black plate (ibidi) in 500µl of RPMI-1640 containing 20% FBS plus 1% penicillin-streptomycin for 24 hours. mCherry AML (mCh-AML, 2.3.3) were used to generate mCherry ABs (mCh-AB) as previously described. The media was removed from the BMDM and 500µl of FluoroBrite™ DMEM added and the TIM4 inhibitor RMT4-54 (30µg/ml, Biolegend) or vehicle (PBS) added for 2 hours. For LAP deficient BMDM, RMT4-54 was not used. mCh-AB were then cultured with the BMDM for 4 hours and 24 hours. Cells were washed 2x with PBS and 500µl of FluoroBrite™ DMEM added. Cells were observed under Zeiss LSM 800 Axio Observer.Z1 confocal microscope with a 63x water objective (Carl Zeiss).

Sorted F4/80$^+$ BMM (2.3.4) were plated at a density of $1.5x10^5$ on µ-Plate 24 well black plate (ibidi) in in 500µl of RPMI-1640 containing 20% FBS plus 1% penicillin-streptomycin for 24 hours. The media was changed to 500µl of FluoroBrite™ DMEM (Thermo Scientific) containing 10% FBS plus 1% penicillin-streptomycin and BMM were cultured with the STING inhibitor H-151 (10µM, InvivoGen) or vehicle (PBS with 0.1% TWEEN80) for 2 hours. BMM were then incubated with pHrodo™ Red *E. coli* BioParticles™ (Invitrogen) for 2 hours before being imaged on Zeiss LSM 800 Axio Observer.Z1 confocal microscope with a 63x water objective (Carl Zeiss).

2.5.2 Human AML microscopy

Human AML cells that were transduced with a rLV.EF1.AcGFP-Mem9 lentivirus (Clontech Takara Bio Europe, Saint-Germain-en-Laye, France) for plasma membrane expression of GFP (AML-GFP). AML-GFP cells were plated at a density of $1.5x10^5$ on µ-Plate 24 well black plate (ibidi) and were stained with MitoTracker™ Red (Invitrogen) according to manufactures

protocol and 1µl of Hoechst 33342 (Thermo Scientific) in FluoroBrite™ DMEM (Thermo Scientific) containing 10% FBS plus 1% penicillin-streptomycin for 20 minutes. Images were captured on Zeiss LSM 800 Axio Observer.Z1 confocal microscope with a 63x water objective (Carl Zeiss). The BM of NSG mice engrafted with human AML cells was isolated and spread onto a microscope slide. May-Grunwald Giemsa staining was used and performed by Prof. Kris Bowles. Stained bone marrow smear slides were imaged via Olympus BX51 light microscope (Olympus UK).

2.6 Flow Cytometry and Cell Sorting

Flow cytometry in this study was utilised for the identification of cell populations by surface receptors and intracellular markers with antibodies conjugated to a detectable fluorophore. Additionally, flow cytometry was used to sort cellular populations based upon cell surface receptors. Different flow cytometers were used dependent on the number of lasers required for the number of fluorophores detection and the ability to sort cells. All antibodies were purchased from Miltenyi Biotech (Bergisch Gladbach, Germany) or BioLegend (San Diego, CA, USA). Details regarding antibody panels can be found at table 2.2 and table 2.3. All flow cytometry data was analysed using FlowJo 10 for Mac (TreeStar, USA).

2.6.1 Sysmex Cube 6

The Sysmex Cube 6 (Sysmex, Germany) is a 2-laser flow cytometer (488nm and 633nm) and can of detect FITC, PE, PERCP and APC fluorophores. Whilst the Sysmex Cube 6 is capable of this detection it lacks the ability to do colour compensations, as such it cannot account for colour cross-over. Therefore, this machine was only used for single colour flow cytometry. The Sysmex Cube 6 was primarily used for the detection of MN1-GFP engraftment via FITC detection and the detection of apoptosis in cells (and ABs) using Annexin-V-APC.

The flow cytometer was run through a full clean cycle before use to ensure the fluidics were clean and no blockages were present. For apoptosis detection, annexin-V was used as previously described. The annexin-V labelled cells were washed by centrifugation at 300xg for 5 minutes and resuspended in 1ml

of MACS buffer and transferred into a flow tube. The samples were processed on the Sysmex Cube 6 with $1x10^4$ events captured in a pre-defined gated region. The flow cytometer was cleaned after use and data was exported as FCS files. The data was analysed using FlowJo 10 software (FlowJo, LLC, USA).

2.6.2 FACSCanto II

The FACSCanto II (BD, Franklin Lakes, NJ, USA), located in the Pathology Laboratory at the Norfolk and Norwich University Hospital, is maintained by Dr Allyson Tyler. This flow cytometer has three-lasers (488, 633 and 405nm) being able to detect 7 fluorophores simultaneously - FITC, PE, PE Cy5, PE Cy7, APC, APC Cy7, BV421 and BV510. The FACSCanto II was used for the majority of experiments which required multiple colour detection, apart from cell sorting. Before experimental runs, compensation for each antibody panel was preformed to measure emission cross-over using either UltraComp eBeads™ Compensation Beads (ThermoFisher, Waltham, MA, USA) or unlabelled control cells (brilliant-violent antibodies) for each marker. The compensation was linked to each experiment before running the samples. Furthermore, fluorescent minus one (FMO) was utilised to allow specification of gating strategies, which required the removal of one antibody from each panel for each fluorophore used. The samples were all run on the FACSCanto II utilising the automated carousel capturing $1x10^5$ events.

Antibody cocktails were prepared in MACS buffer where 1µl of each antibody per sample was added to the cells ($5x10^6$ BM cells per sample). Following a 30-minute incubation at 4°C in the dark, the cells were then centrifugated again at 300xg for 5 minutes and re-suspended in 200 µL of MACS buffer. In experiments using MitoTracker™ Green or MitoTracker™ Red (Invitrogen), the cells were stained with the dyes in 500µl of MACS buffer for 20 minutes in the dark, washed 2x in PBS, and centrifuged at 300xg for 5 min before adding any additional antibodies. For detection of mitochondria in the ABs of human $CD34^+$, human AML and MN1 cells, apoptotic cells were stained with the MitoTracker™ Red (Invitrogen) in 500µl of MACS buffer for 20 minutes in the dark, before isolation of ABs was performed. After completion of use, FCS files were downloaded and data was analysed using FlowJo 10 software

(FLowJo for Mac, USA). All gating was set by using FMO controls to establish positive and negative gates for each cell marker.

2.6.3 The FACSMelody

The FACSMelody (BD, Franklin Lakes, NJ, USA), located at the Earlham Institute (Norwich, UK), has the same capabilities as the FACSCanto II, however, it can additionally sort cells via FACS. This flow cytometer was used to sort the F4/80^{+} bone marrow macrophages, bone marrow macrophages (CD45^{+}, GR1^{-}, CD115$^{LOW/INT}$, F4/80^{+}) and AML associated macrophages (CD45^{+}, Lys6G^{-}, CD11b^{+}). It was also used to sort the mitochondrial containing ABs from MN1 cells.

To sort macrophage populations, isolated BM cells were incubated with antibody cocktails for 30-minutes as previously described. The cells were centrifuged at 300xg for 5 minutes and resuspended in 1ml of MACS before being passed through a 40um filter. The samples were processed by the FACSMelody and sorted into lysis buffer for RNA analysis by qPCR or into culture media for culture. The positive and negative gating for the sorting of macrophage populations was set by FMO controls.

For the sorting of mitochondrial containing ABs, apoptosis was induced as previously described. Apoptotic cells were incubated with MitoTracker™ Red (Invitrogen). The cells were stained with the dyes in 500µl of MACS buffer for 20 minutes in the dark, before the isolation of ABs as previously described. ABs were resuspended in 1ml of MACS buffer and run the FACSMelody and sorted into culture media ready for co-culture. The use of 1µm biospheres were used as positive selection for particle size of ABs along with the detection of MitoTracker™ Red.

2.6.4 Amnis ImageStream^{x} Mk II

Amnis ImageStream^{x} Mk II (Luminex), located at the Quadram Institute (Norwich, UK) and combined the capabilities of a multi-colour flow cytometer and a microscope. The ImageStream^{x} Mk II System is a multispectral imaging flow cytometer allowing the acquisition of up to 12 channels. The flow cytometer can capture fluorescence intensity measurements as with a conventional flow cytometer; however, it to locate and quantitate the

distribution of signals on, in or between cells. The Amnis ImageStream^{x} Mk II was used to detect mitochondrial levels in ABs isolated from MN1and LSK cells. Briefly, before isolation of ABs, cells were stained with MitoTracker™ Green (Invitrogen) and Vybrant™ DiI Cell-Labelling Solution (Invitrogen) according to manufacturer's protocol. ABs were isolated as previously described and resuspended in 1ml of MACS buffer and run on the Amnis ImageStream^{x} Mk II. The use of 1µm biospheres were used as positive selection for particle size of ABs along with the detection of MitoTracker™ Green and Vybrant™ DiI.

Table 2.2 Antibody panel information used in flow cytometry protocols

		Flourophore							
Antibody Panel	Specific	FITC	APC	APC-Cy7	PE	PE-Cy5	PE-Cy7	BV421	BV510
BMM	CD169+	MN1-GFP	CD169	CD115	CD206	GR1	F4/80	CD86	CD45
BMM	TIM4	MN1-GFP	TIM4	CD115	CD206	GR1	F4/80	CD86	CD45
BMM	Diff M1/M2	MN1-GFP	TIM4	CD115	CD206	GR1	F4/80	CD11c	CD45
BMM	Sorted	GR1	F4/80	CD115	CD206	-	CD45	CD86	-
AAM	Flow	MN1-GFP	-	-	CD206	Lys6G	CD45	CD86	CD11b
AAM	Sorted	MN1-GFP	-	-	CD206	Lys6G	CD45	CD86	CD11b
T-cell	-	MN1-GFP	IFN-y	NK1.1	Gran. B	CD8	CD4	B220	CD45
BMSC	-		CD105	CD140a	-	CD31	-	-	CD45
Engraftment	MN1	MN1-GFP	-	-	-	-	-	-	-
Engraftment	Live MN1	MN1-GFP	Annexin-V	-	-	-	-	-	-
Engraftment	NSG AML		hCD38	hCD90	-	hCD45RA	hCD49f	hCD34	mCD45
Lineage cells	-	MN1-GFP	-	CD48	-	CD34	CD117	Lin Cocktail	CD16/32
Apoptosis	-	MN1-GFP	Annexin-V	-	-	-	-	-	-
Image flow AB	-	MTG	-	-	VybrantDil	-	-	-	-

Table 2.3 Antibody specific information

Antibody	Clone	Manufacturer	Antibody	Clone	Manufacturer
Annexin V-APC	-	Biolegend	CD49f-PE-Cy7	REA518	Miltenyi
Annexin V-PE-Cy7	-	Fisher Scientific	CD8-PerCP	53-6.7	Biolegend
B220-BV421	RA3-6B2	Biolegend	CD86-BV421	GL-1	Biolegend
CD105-APC	MJ7/18	Biolegend	CD90-APC-Cy7	DG3	Miltenyi
CD115-APC/Fire™ 750	AFS98	Biolegend	F4/80-APC	BM8	Biolegend
CD117-PE-Cy7	REA791	Miltenyi	F4/80-PE-Cy7	BM8	Biolegend
CD11b-BV510	M1/70	Biolegend	GR1-FITC	RB6-8C5	Biolegend
CD140a-APC-Cy7	APA5	Miltenyi	GR1-PerCP	RB6-8C5	Miltenyi
CD16/32-BV510	93	Biolegend	Granzyme B-PE	QA16A02	Biolegend
CD206-PE	C068C2	Biolegend	IFN-y-APC	XMG1.2	Biolegend
CD31-Pe-Cy5	WM59	Biolegend	Ly6G-PerCP	1A8	Biolegend
CD34-BV421	561	Biolegend	NK1.1-APC-Cy7	PK136	Biolegend
CD38-APC	IB6	Miltenyi	Pacific Blue™ anti-mouse Lineage Cocktail	17A2	Biolegend
CD4-PE-Cy7	GK1.5	Biolegend		RB6-8C5	
CD45-Alexa Fluor® 700	I3/2.3	Biolegend		RB6-8C6	
CD45-APC	30-F11	Biolegend		RB6-8C7	
CD45-BV510	30-F11	Biolegend		RB6-8C8	
CD45RA-PE-Cy5	T6D11	Miltenyi	TIM4-APC	REA999	Miltenyi

2.7 Real time quantitative PCR

2.7.1 RNA extraction

The gene expression levels in the bone marrow macrophages were determined using real time, quantitative PCR (RT-qPCR). For gene expression in macrophages after treatment of ABs, macrophages were cultured as previously described with the addition of specified ABs for 24 hours. To analyse the gene expression, the RNA was extracted from the cells. To extract the RNA from macrophages the ReliaPrep™ RNA Cell Miniprep Kit (Promega, USA) was used following the manufacturer's protocol. Cells were washed twice with PBS to remove residue media and ABs. 250µl of BL+TG buffer was added to cells and pipetted up and down 10 times. Cell lysates were placed into 1ml microcentrifuge tubes and plates were checked under a light microscope to confirm cell lysis. Cell lysate solutions then had 85µl of Isopropanol added and vortexed for 5 seconds to mix. The cell lysate was loaded onto a ReliaPrep™ mini-column and centrifuged at 13000xg for 30 seconds. The flow through was discarded and 500µl of RNA wash solution was added to the column and centrifuged at 13000xg for 30 seconds. The flow through was discarded and 30µl of premade DNase I incubation mix was incubated on the column membrane for 15 minutes at room temperature. 200µl of column wash solution was added and the column spun at 13000xg for 30 seconds. The flow through was discarded and 500µl of RNA wash solution was added and the column was centrifuged again using the same parameters. A second wash step with 300 µl of RNA wash solution was carried out after that. The column was then centrifuged at 16000 xg for 2 minutes and left to dry at RT for 2 minutes. To elute the RNA, 20µl of nuclease free water was added to the column and centrifuged for 1 minute at 13000xg. The RNA was placed on ice for immediate used or stored at -20^{o}C for long term storage.

2.7.2 DNA extraction

To detect the levels of mitochondria DNA in cells after p0 cell generation and mitochondrial copy number in CD34^{+} and AML samples RT-qPCR was used. DNA was extracted using the GenElute Mammalian Genomic DNA Miniprep Kit (Sigma Aldrich, USA) using the manufacturer's protocol. Briefly, cells were

washed in PBS and then resuspended in 200µl of resuspension solution. Cell lysis was achieved by the addition of 20µl of Proteinase K and 200µl of Lysis Solution C. This lysate was vortexed briefly and incubated in a heat block at 70℃ for 10 minutes. 200µl of absolute ethanol was then added to the lysate, which was then loaded onto a column. The column was centrifuged at 13000xg for 1 minute, the flow through was discarded. 500µl of wash solution was added to the column and centrifuged at 13000xg for 1 minute, the flow through was discarded. A further 500µl of Wash Solution was added to the column and centrifuged at 16000xg for 3 minutes. To elute the DNA,100µl of Elution Solution was added directly to the column and centrifuged for 1 minute at 13000xg. DNA was placed on ice for immediate use or stored at -20℃ for long term storage.

2.7.3 RNA/DNA quantification

RNA and DNA was quantified using the NanoDrop spectrophotometer (ThermoFisher, Waltham, MA, USA). The NanoDrop was cleaned and blanked using 1µl of elution buffer (nuclease free water or Elution Solution) before use. 1µl of the sample was loaded onto the NanoDrop and RNA/DNA concentration (ng/µl) was determined. Purity of the sample was determined using the A260/230 ratio, with a ratio of between 1.7 and 2.3. deemed sufficiently pure.

2.7.4 cDNA synthesis

In order to analyse the gene expression of macrophages, extracted RNA was converted to cDNA. This was achieved using two methods. Firstly, using reverse transcription with the qPCRBIO cDNA synthesis kit (PCR Biosystems, UK), according to the manufacturers protocol. For a 10µl reaction, 2µl of 5X cDNA Synthesis Mix was added with 0.5µl of 20X RTase and 2µl of RNA. The remaining volume was made up to 10µl with nuclease free water. PCR specific tubes were placed in a Thermocycler (Bio-Rad, UK) and run using a cycling program of an initial 42℃ incubation for 30 minutes followed by a 85℃ incubation for 10 minutes. The cDNA samples were held at 4℃ before a dilution in nuclease free water ready for RT-qPCR. The samples were stored on ice or at -20℃ until further use. Another method employed utilised one-step PCR using one-step SYBR-green technology (PCRBIO 1-Step Go RT-PCR

Kit, PCR biosystems, UK) with QuantiTect Primer Assays (Table 2.6, Qiagen, Germany). A master mix of 0.1µl of RTase Go 1-Step, 2.5µl of SYBR-green and 0.4µl of PCR primer was added directly to a 384-well plate with the addition of 2µl of RNA. The plate was placed in a Roche Lightcycler 480 (Roche, Basel, Switzerland) for RT-qPCR (see below for details).

2.7.5 Gene expression

cDNA synthesised using the qPCRBIO cDNA synthesis kit was used to perform qPCR to determine gene expression of macrophages. The qPCRBIO SYBR-green Mix (PCR Biosystems, UK) was used to carry out qPCR on 384 well Roche Lightcycler reaction plates. A master mix was created containing 2µl of SYBR-green Mix, 0.5µl of QuantiTect Primer and 0.5µl nuclease free water. 2µl of the diluted cDNA was added to the PCR wells along with 3µl of the master mix. PCR plates were sealed and centrifuged at 100xg for 1 minute before loading into the Lightcycler. qPCR was run using a pre-programmed method described below (Table 2.4 and table 2.5). As cDNA is amplified, SYBR-green incorporates into newly synthesised DNA and detected in the form of fluorescence.

Table 2.4 qPCRBIO SYBR-green Lightcycler programming

Process	Cycles	Temperature	Time
Pre-amplification	1	95˚C	2 mins
Amplification	45	95˚C	15 secs
		60˚C	10 secs
		72˚C	10 secs
Melt Curve	1	95˚C	5 secs
		65˚C	1 min
		97˚C	Cont
Cooling	1	40˚C	30 secs

Table 2.5 PCRBIO 1-Step Go RT-PCR SYBR-green Lightcycler programming

Process	Cycles	Temperature	Time
Reverse transcription	1	45°C	10 mins
Polymerase activation	1	95°C	2 mins
Amplification	40	95°C	10 secs
		60°C	10 secs
		72°C	30 secs
Melt Curve	1	95°C	5 secs
		65°C	1 min
		97°C	Cont
Cooling	1	40°C	30 secs

The raw values extracted from the Lightcycler are known as the cycle threshold (Ct) values. Genes of interest were normalised to a housekeeping gene, Glyceraldehyde 3-phosphate dehydrogenase (GAPDH), which is present in every cell and expression is unaffected by cellular treatments or genetic alterations. To analyse the results, ΔCt values for specific genes was quantified by calculation of Ct of specific gene – the Ct of the housekeeping gene. The ΔΔCt value was then calculated by the ΔCt control – the ΔCt experiment conditioning. The fold change in expression was then determined relative to untreated cells by 2-ΔΔCt. Each sample was replicated at least three times.

Table 2.6 QuantiTect Primers (Qiagen) used in RT-qPCR analysis

Gene	Assay Name	GeneGlobe ID
GAPDH	Mm_Gapdh_3_SG QuantiTect Primer Assay	QT01658692
IL6	Mm_Il6_1_SG QuantiTect Primer Assay	QT00098875
IL1-B	Mm_Il1b_2_SG QuantiTect Primer Assay	QT01048355
TNF-a	Mm_Tnfaip1_1_SG QuantiTect Primer Assay	QT00116564
GBP2	Mm_Gbp2_1_SG QuantiTect Primer Assay	QT00106050
IRF7	Mm_Irf7_1_SG QuantiTect Primer Assay	QT00245266
IFIT3	Mm_Ifit3_1_SG QuantiTect Primer Assay	QT00292159

2.7.6 Taqman® based qPCR

To determine mtDNA levels of p0 generated MN1 cells as well as the mitochondrial copy number in AML and $CD34^+$ cells, Taqman® based qPCR was carried out. In this assay a sequence specific probe, which contains both a 2′-chloro-7′phenyl-1,4-dichloro-6-carboxy-fluorescein (VIC)/ 6-Carboxyfluorescein (FAM) fluorophore and a TAMRA® quencher binds to a gene of interest. During DNA amplification the probe is cleaved which releases the fluorophore and quencher, allowing the fluorophore to be detection. Pre-designed Taqman® assays were obtained from ThermoFisher, encompassing mouse COX3 and ND3 mtDNA, mouse ND1 mtDNA, human ND1 mtDNA and human and mouse genomic DNA (gDNA).

The mouse mtDNA Taqman® assay was run in simplex reactions. For the master mix, 0.25µl of Taqman® reagent, which contained primers and probe was added to 2.5µl of TaqPath ProAmp enzyme (ThermoFisher, USA) and mixed with 1.25µl nuclease free water. 4µl of this master mix was loaded into each well of a 384 well PCR plate and 1µl of extracted DNA was then added. The plate was then sealed, centrifuged for 1 minute at 100xg and loaded onto the Lightcycler 480. The qPCR was run using the method below (Table 2.7).

Table 2.7 Taqman® assay Lightcycler programming

Process	Cycles	Temperature	Time
Pre-amplification	1	60°C	30 secs
		95°C	5 mins
Amplification	50	95°C	15 secs
		60°C	1 min
Cooling	1	40°C	30 secs

The Ct value was determined and mtDNA values were generated. Mouse ND3 mtDNA were normalised against the mouse gDNA Ct to obtain the ΔCt. ΔCt values was determined by Ct mouse ND3 mtDNA – Ct mouse gDNA. The ΔCt value was used to generate mitochondrial DNA values (2-ΔCt) and calculated as a fold change to determine changes in mtDNA levels in p0 MN1 cells compared to untreated MN1 cells.

mtDNA copy number was determined for human mitochondria and normalised to human gDNA. The Ct values for human were obtained and normalised against the human gDNA. To calculate the ΔCt = hmtDNA – Ct hgDNA. The copy number was then calculated by 2-ΔCt.

2.8 In vitro bioluminescence detection of MEIS1/HOXA9-luci cells

To assess whether signal detected from in vivo image with luciferin treatment denoted live MEIS1/HOXA9-luci cells, in vitro analysis was preformed to determine whether apoptotic MEIS1/HOXA9-luci cells produced bioluminescent output after the addition of luciferin. $2x10^5$ MEIS1/HOXA9-luci cells were plated into 96 well plates in 100µl of FluoroBrite DMEM containing 10% FBS plus 1% penicillin-streptomycin and either 5µM of Ara-C or PBS was added. Cells were cultured for 24 hours, after which 150µg of D-luciferin was added to the cells for 10 minutes. The bioluminescence was measured on the FLUOstar Omega microplate reader (BMG LABTECH, Ortenberg, Germany). Data was exported into GraphPad Prism for analysis.

2.9 ρ^0 MN1 generation

The generation of MN1 cells devoid of mtDNA, ρ^0 MN1 cells, was used to study the effects of mtDNA on STING activation. To generate ρ^0 MN1 cells, $5x10^6$ MN1 cells were cultured in DMEM containing 10% FBS plus 1% penicillin-streptomycin supplemented with mSCF (100ng/ml), mIL3 (10ng/ml), hIL6 (10ng/ml), ethidium bromide (1µg/ml), 2′,3′-dideoxycytidine (ddC; 200µM), sodium pyruvate (100µg/ml) and uridine (50µg/ml). Ethidium bromide preferentially intercalates with mtDNA causing shearing and degradation, whilst ddC, a nonazylated dideoxynucleoside analogue, inhibits the replication of mtDNA. As such, pyruvate and uridine supplementation was required for cell survival. Every 7 days, cells were centrifuged at 300xg for 5 minutes and resuspended in fresh media. At 20 days mitochondrial DNA detection was performed using qPCR as previously described (2.7.6) [462]. Briefly, DNA was extracted from MN1 and ρ^0 MN1 cells using the GenElute Mammalian Genomic DNA Miniprep Kit (Sigma Aldrich, USA) according to the manufacturer's protocols. Purified DNA was then analysed via Taqman® probes ND3 for mitochondrial DNA and normalised against Tert for genomic

DNA (ThermoFisher, USA). Relative mtDNA/gDNA ratio was calculated using the ΔΔCt method.

2.10 Cytokine array

For the analysis of cyto- and chemokines with ABs treatment in BMDM from Atg16l^{E230+} and Atg16l^{E230-}, the Proteome Profiler Mouse XL Cytokine Arrays (R&D Systems) was utilised. This allowed the detection of 111 secreted cytokines in BMDM from Atg16l^{E230+} and Atg16l^{E230-} mice treated with and without MN1 derived ABs. It employs capture and control mouse antibodies that have been pre-spotted in duplicates on a nitrocellulose membrane. After a series of incubation steps a measurement of cytokine protein expression in the samples cultured conditioned media. BMDM were isolated from Atg16l^{E230+} and Atg16l^{E230-} mice as previously described and plated at a density of 2.5x10^5 in 24 well plates in 200µl of RPMI-1640 containing 10% FBS plus 1% penicillin-streptomycin. Vehicle (PBS) or ABs from MN1 cells were generated as previously described and added to the BMDM for 24 hours. The supernatant was removed, pooled, and centrifuged at 10000xg for 10mins to remove any debris. The supernatant was placed in a new microcentrifuge tube.

The array membranes were blocked using 2ml of the blocking buffer and incubated for 1 hour at RT with rocking. Next, 0.5ml of array buffer was added to 1 ml of the cell supernatant, which was applied onto each membrane and left overnight at 4℃ with rocking. Each membrane was then removed and place into individual containers and washed with 20ml of 1X Wash Buffer for 10 minutes while rocking. This was repeated two more times after which membranes were removed, excess wash buffer allowed to drain and placed into the 4 well multi-dish containing 30µl of Detection Antibody Cocktail and 1.5ml of 1X Array Buffer 4/6 and covered with the lid. Membranes were incubated for 1 hour at RT while rocking. The membranes were washed again three more times as described above, removed and excess buffer was allowed to drain. The membranes were then placed into the 4 well multi-dish containing 2.0ml of 1X Streptavidin-HRP and covered with the lid. Membranes were incubated for 30 minutes at RT whilst rocking before being washed once as previous described. Each membrane was removed from its wash container and excess Wash Buffer allowed to drain from the membrane by blotting the

lower edge onto paper towels. Membranes were placed on the bottom sheet of a plastic sheet protector with the identification number facing up. 1.0ml of the prepared Chemi Reagent Mix was pipetted evenly onto each membrane and covered carefully with a top sheet of plastic sheet protector, while gently smoothing out any air bubbles. Membranes were incubated for 1 minute. Each membrane was imaged using the G:BOX Chemi XRQ (Syngene) and quantified using ImageJ (Fiji). The optical density of the resulting images was quantified and analysed against reference spots that were used and normalised to background values. GraphPad Prism 7 software was used to generate heatmaps.

2.11 Plasmid source

Table 2.4 Plasmid information

Plasmid name	Use case	Source
pCDH-luciferase-T2A-mCherry	In vivo imaging of MEIS/HOXA9 cells	Irmela Jeremias, Germany
rLV.EF1-mCherry-Mito-9-lentivirus	Mitochondrial tracking	Clontech, 0024VCT

2.12 Statistics

Data produced in this study was analysed using GraphPad Prism software (Version 7.0 Mac OS X, San Diego, CA, USA), BD FlowJo 10 software (FlowJo for Mac OS X, LLC, Ashland, USA), ImageJ 2.0 (Fiji) and Microsoft Excel (Albuquerque, NM, USA). Due to the data variability with in vivo work, statistical comparison of two groups was performed without assumption of normal distribution with the Mann-Whitney U test. For comparison of more than two groups, the Kruskal-Wallis statistical test was used to establish if any statistically differences were evident between the groups which was followed by Dunn's multiple comparisons post-hoc test to identify where the statistical significance was found. Tests were performed with GraphPad Prism software. Differences between the means of each group were determined significant when the probability value, p, was less than 0.05*, 0.01**, 0.001*** and 0.0001****. The results represent the mean ± 1 standard deviation of 3 or

more independent samples. Sample size (n) represents number of biological replicates. No statistical methods were used to predetermine sample size.

3. LC3 associated phagocytosis in bone marrow macrophages is important for AML suppression

3.1 Introduction

The phagocytic function of macrophages is a vital part of the immune response. Specifically, macrophages have key roles in the clearance of pathogens and dying cells. Within the BM, macrophages have diverse functions from regulation of haematopoiesis to the clearance of expelled nuclei from maturating erythrocytes [58, 59, 61]. $CD11b^{+}$ BM macrophages are predominately responsible for the phagocytosis of dying cells [64]. As such, this highlights that a population of macrophages within the BM is responsible for the regulation of apoptotic cells via phagocytosis. However, investigations into how phagocytic macrophages in the BM deal with malignancy, such as AML, are not fully understood. Furthermore, the specific method of this process has not been investigated in AML.

AML is a malignancy that is dependent on the BM microenvironment for its survival and growth. It has been shown that AML can take mitochondria from BMSC as well as having the ability to use and utilise free-fatty acids from adipocytes [385-387, 411, 414]. Further to this, AML blasts are thought to be protected in BM niches, similar to HSCs, which allows for their survival and chemotherapy avoidance [3, 374]. The reliance of AML on BM macrophages seems to be by supressing the function of BM macrophages, such as increased expression of CD47 on AML cells and decreased phagocytic function of macrophages [202, 203]. It is not fully understood what role phagocytosis in BM macrophages has on the regulation of AML cells. Therefore, in this chapter of my thesis, I have investigated the importance of phagocytosis by BM macrophages on AML progression. This is to understand if macrophages need phagocytic functions in an *in vivo* setting to assist with AML suppression.

3.2 Depletion of phagocytic cells in vivo leads to increased AML tumour burden

Firstly, to investigate AML in an *in vivo* setting, two mouse models of AML were used (MN1 or MEIS1/HOXA9). To investigate AML engraftment in the animals, two methods were deployed. The MN1 cells had a GFP tag that allowed identification of MN1 cells via flow cytometry. Also, MEIS1/HOXA9 cells were transduced with an pCDH-luciferase-T2A-mCherry to allow for mCherry tagging as well as being able to visualise MEIS/HOXA9 cells in vivo by bioluminescence imaging. Both these cell types were confirmed to possess their corresponding fluorescent tags by microscopy and flow cytometry (Figure 3.1A).

To understand the importance of phagocytosis in AML progression, C57/BL6 mice were intravenously (i.v) injected with 10^6 of MN1-GFP or MEIS1/HOXA9-luci cells after 2 days of pre-treatment with 25mg/kg of busulfan via intraperitoneal (i.p) injections. After 19 days post injection of AML cells, mice were injected i.p with either 150µl of clodronate liposomes (CL), which selectively causes apoptosis in phagocytic cells such as macrophages, or control liposomes (CNT) (Figure 3.2A). To confirm reduction of bone marrow macrophages (BMM), at day 23 animals were sacrificed and the bone marrow isolated. BMM were defined as $CD45^+$, $GR\text{-}1^-$, $F4/80^+$ and $CD115^{INT}$ (Figure 3.2B). CL treated animals had decreased BMM compared to CNT treated animals (Figure 3.2C).

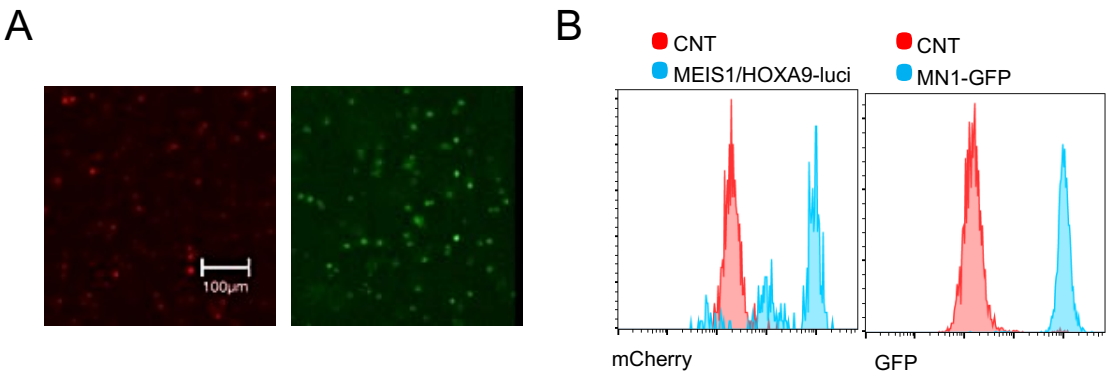

Figure 3.1. Identification of fluorescent characteristics in MN1-GFP and MEIS/HOXA9-luci cells

(A) MEIS1/HOXA9 cells were transduced with an pCDH-luciferase-T2A-mCherry to allow for in vivo imaging, while expressing a mCherry tag (MEIS1/HOXA9-luci, left). MN1 cells with a GFP tag (MN1-GFP, right). Images collected using EVOS™ M5000 Imaging System under 20x magnification. (B) Flow cytometry histogram plots of MEIS/HOXA9-luci (left, mCherry positive) cells and MN1-GFP cells (right, GFP positive) compared to untreated MN1 and MEIS/HOXA9 cells as a negative control (CNT).

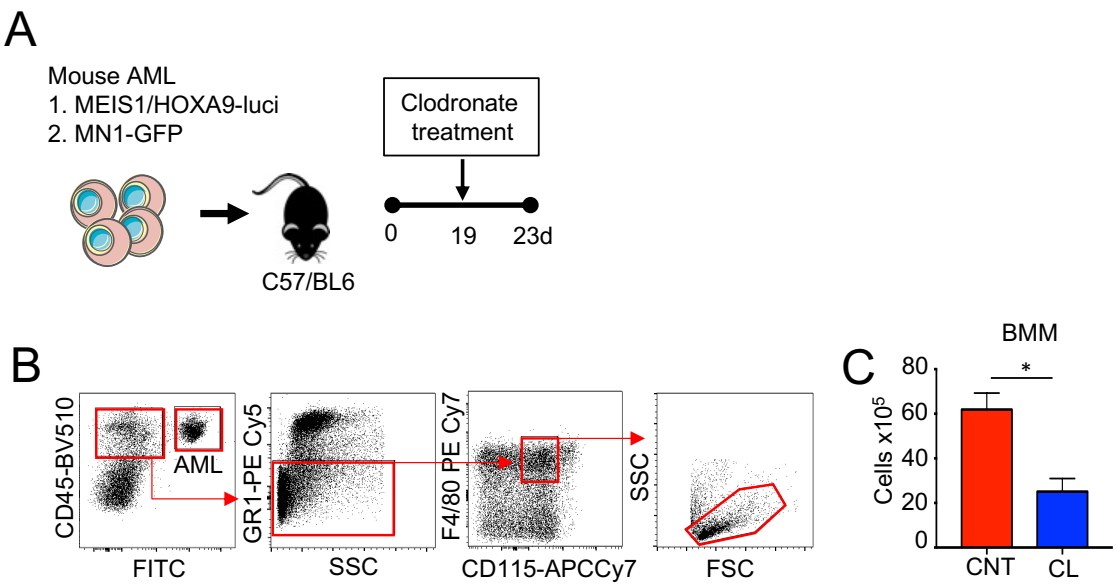

Figure 3. 2. Depletion of bone marrow macrophages in vivo

(A) Schematic diagram of experiment design, MEIS/HOXA9-luci and MN1-GFP cells were I.V injected into 2 groups of animals that were pre-treated with busulfan. After 19 days, animals were treated with clodronate (CL) or control (CNT) liposomes and sacrificed at day 23 and the bone marrow harvested. (B) The gating strategy used during flow cytometry to identify bone marrow macrophages. (C) The number of bone marrow macrophages in CNT and CL treated animals (from flow cytometry plots). n=5 in each group. Data shown are means ± SD *P < 0.05, Mann–Whitney U. See pg. 88 for flow panel information.

MEIS1/HOXA9-luci cells were utilised to investigate AML progression using in vivo imaging to visualise changes between CL treated and CNT treated animals. In vivo imaging was used to identify AML engraftment before (day 19) CL treatment and after (day 23) CL treatment. Animals in both groups had similar levels of AML engraftment at day 19, however, CL treated animals had increased AML progression compared to CNT animals after day 23 (Figure 3.3A). The bioluminescence of each animal was analysed to confirm the increase in AML progression in CL treated animals (Figure 3.3B). To determine if this observation was seen in other AML models and not unique to this AML model, a second murine AML model, MN1-GFP cells, was used. AML progression was investigated after CL treatment, the bone marrow was harvested from the animals and investigated via flow cytometry for AML engraftment via GFP fluorescence (Figure 3.4A). CL treated animals had increased MN1-GFP in the bone marrow compared to CNT treated animals (Figure 3.4B).

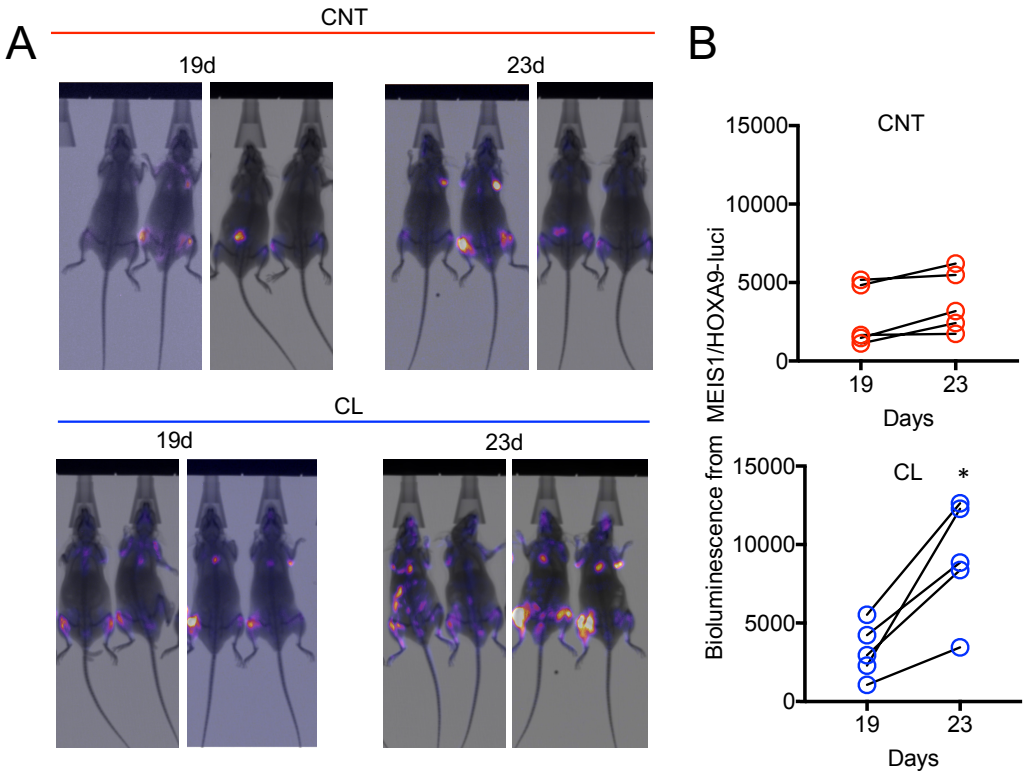

Figure 3.3. Depletion of bone marrow macrophages accelerates MEIS/HOXA9 cell growth in vivo

(A) Animals injected with MEIS1/HOXA9-luci cells were imaged using the in vivo Bruker imaging system. Representative images of AML engraftment at day 19 and day 23 in animals treated with clodronate (CL) or control (CNT) liposomes. (B) Bioluminescence from MEIS1/HOXA9-luci cells of each animal was analysed via imageJ. n=5 in each group. Data shown are means ± SD *P < 0.05, Mann–Whitney U.

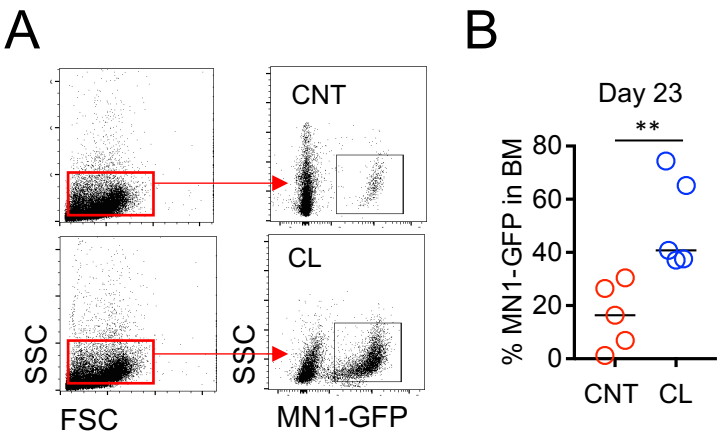

Figure 3.4. Depletion of bone marrow macrophages accelerates MN1 cell growth in vivo

Animals pre-treated with busulfan and injected with MN1-GFP cells were treated with clodronate (CL) and control (CNT) liposomes at day 19 and sacrificed at day 23. (A) Flow plots of mice bone marrow with MN1-GFP engraftment via FITC. (B) Identification of the percentage of MN1-GFP positive cells within the bone marrow of CL and CNT treated animals. n=5 in each group. Data shown are means ± SD **P < 0.01, Mann–Whitney U.

Next, to investigate whether the signals received from both the luciferase in vivo imaging and GFP from flow cytometry was representative of live AML cells, two methods were used. To address whether luciferase signal can be detected in dead MN1/HOXA9-luci cells, the induction of apoptosis in these cells was undertaking via the addition of 5μM of Ara-C (Cytarabine) for 24 hours (Figure 3.5A). Bioluminescence signal was not detectable compared to untreated MN1/HOXA9-luci cells (Figure 3.5B). Next, to identify the absolute amount of live MN1-GFP cells and resident cells *in vivo,* the bone marrow isolated from CL and CNT treated animals was analysed via flow cytometry with annexin V staining (Figure 3.5C). To investigate the affect clodronate treatment had on non MN1-GFP bone marrow cellularity, the annexin V status of GFP negative resident cells was analysed. Treatment of clodronate did not alter the amount of annexin V positive cells compared to control treated animals (Figure 3.5D). Furthermore, data showed that the absolute live MN1-GFP cell counts were higher in the CL treated animals compared to the CNT (Figure 3.5E). Together, these results show that functional bone marrow macrophages are important in the suppression of AML and their depletion leads to increased AML growth.

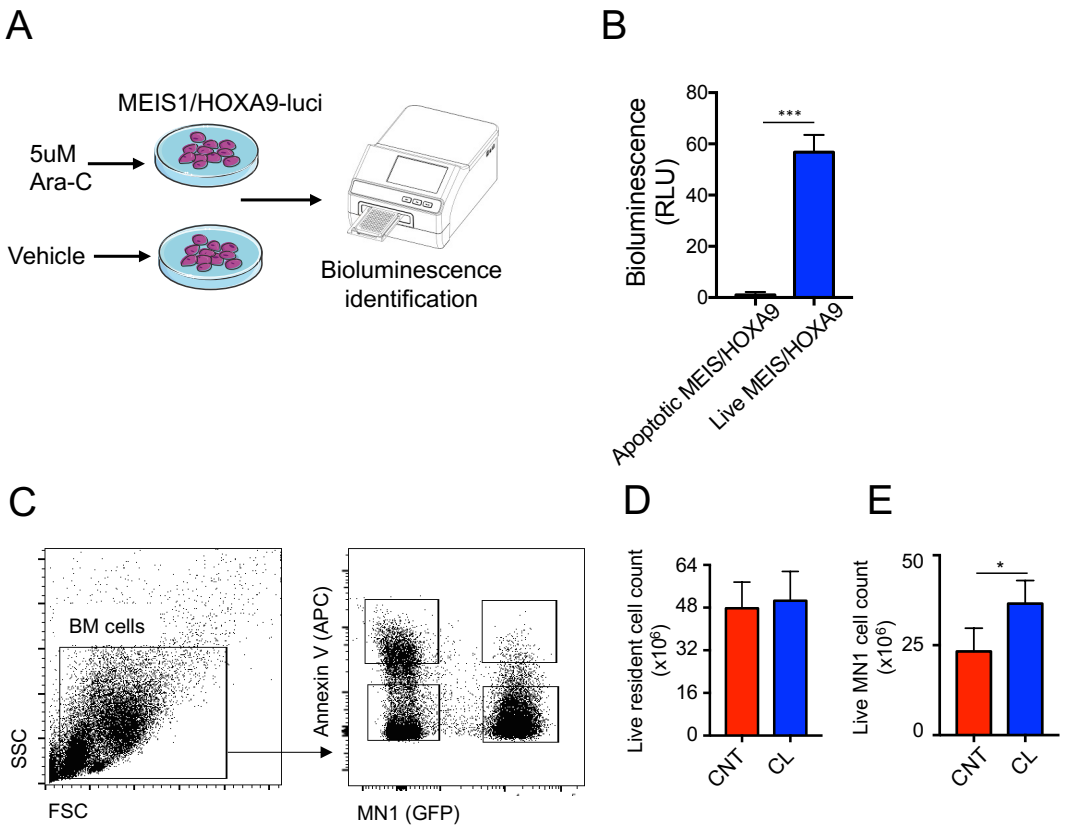

Figure 3.5. Clodronate treatment does not alter the amount of living AML and resident cells

(A) 20,000 MEIS1/HOXA9-luci cells were plated into 96 well plates and either 5μM of Ara-C or PBS was added and analysed via bioluminescence 24 hours later. (B) Bioluminescence readout (n=6). (C) Flow plots of mice bone marrow with MN1-GFP engraftment and annexin V. (D) Total cell count of annexin V negative and GFP negatives cells (live resident cells) from control and clodronate treated animals. (E) Total cell counts of annexin V negative MN1-GFP cells from control and clodronate treated animals. n=5 in each group. Data shown are means ± SD *P<0.05, ***P < 0.00, Mann–Whitney U. See pg. 88 for flow panel information.

As one of the primary functions of macrophages is to phagocytose, including the phagocytosis of cancer cells, this function was investigated in animals that had been engrafted with MN1 cells. To understand phagocytosis in bone marrow macrophage in animals that were engrafted with MN1 cells the bone marrow was extracted and the F4/80$^+$ cells (macrophages) were isolated via magnetic separation. The F4/80$^+$ cells were then incubated with Zymosan particles to analyse their phagocytic potential (Figure 3.6A). F4/80$^+$ cells isolated from animals engrafted with MN1 cells had an increased number of bioparticles associated to them compared to F4/80$^+$ cells from control animals (Figure 3.6B&C). Phagocytosis can occur in macrophages which is either dependent or independent on LC3 [463]. To identify which mechanism is involved in the increased phagocytic capacities in AML associated macrophages, the isolated F4/80$^+$ cells from MN1 engrafted animals were fixed and permeabilised to allow visualisation of LC3 via an LC3 specific antibody (Figure 3.7A). LC3 association to the bioparticles was captured via confocal microscopy (Figure 3.7B). Significantly more bioparticles were LC3$^+$ compared to those that did not have LC3 association (Figure 3.7C). Together, these results show that macrophages isolated from the bone marrow of mice with AML are more phagocytic than mice without AML. Furthermore, the primary method of phagocytosis is dependent on LC3, also known as LC3 associated phagocytosis (LAP).

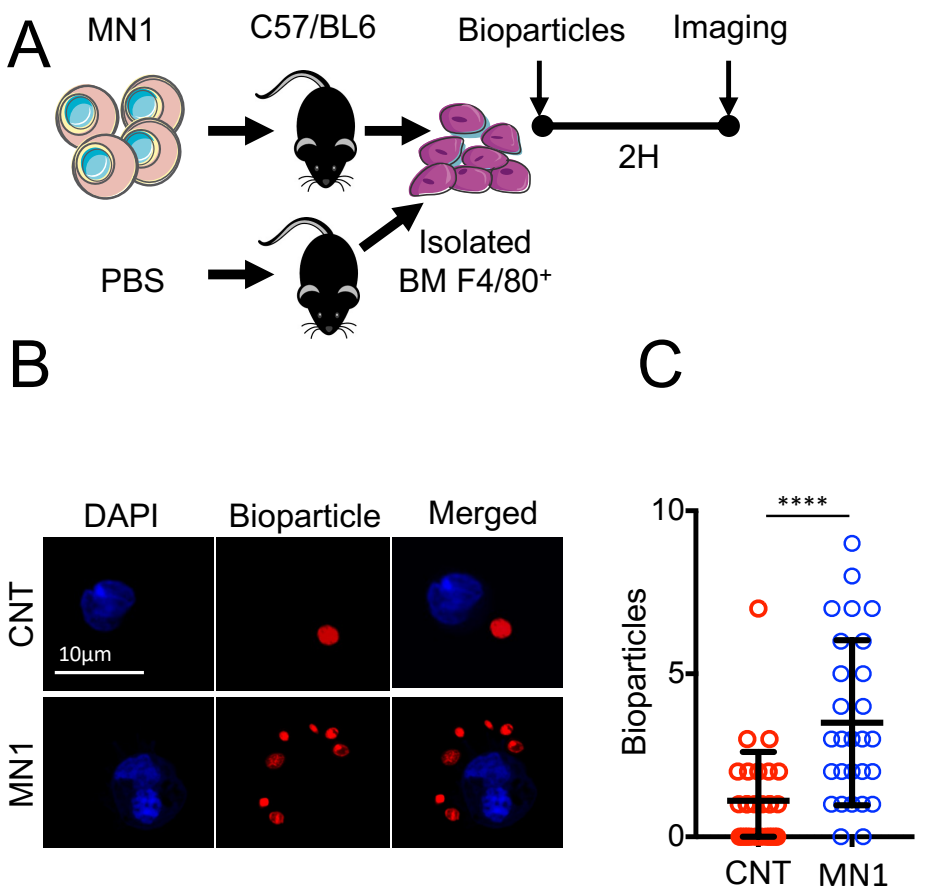

Figure 3.6. AML associated macrophages have increased phagocytic capacities

(A) Experimental design schematic, C57/BL6 animals with and without engrafted MN1 cells were sacrificed and the bone marrow F4/80$^+$ macrophages isolated via MACS magnetic separation. The F4/80$^+$ cells were cultured with Zymosan bioparticles before being imaged by fluorescence microscopy. (B) Representative images of control and MN1 engrafted isolated F4/80$^+$ and bioparticle uptake. (C) Bioparticle counts per macrophage (n=30). Data shown are means ± SD ****P < 0.000, Mann–Whitney U.

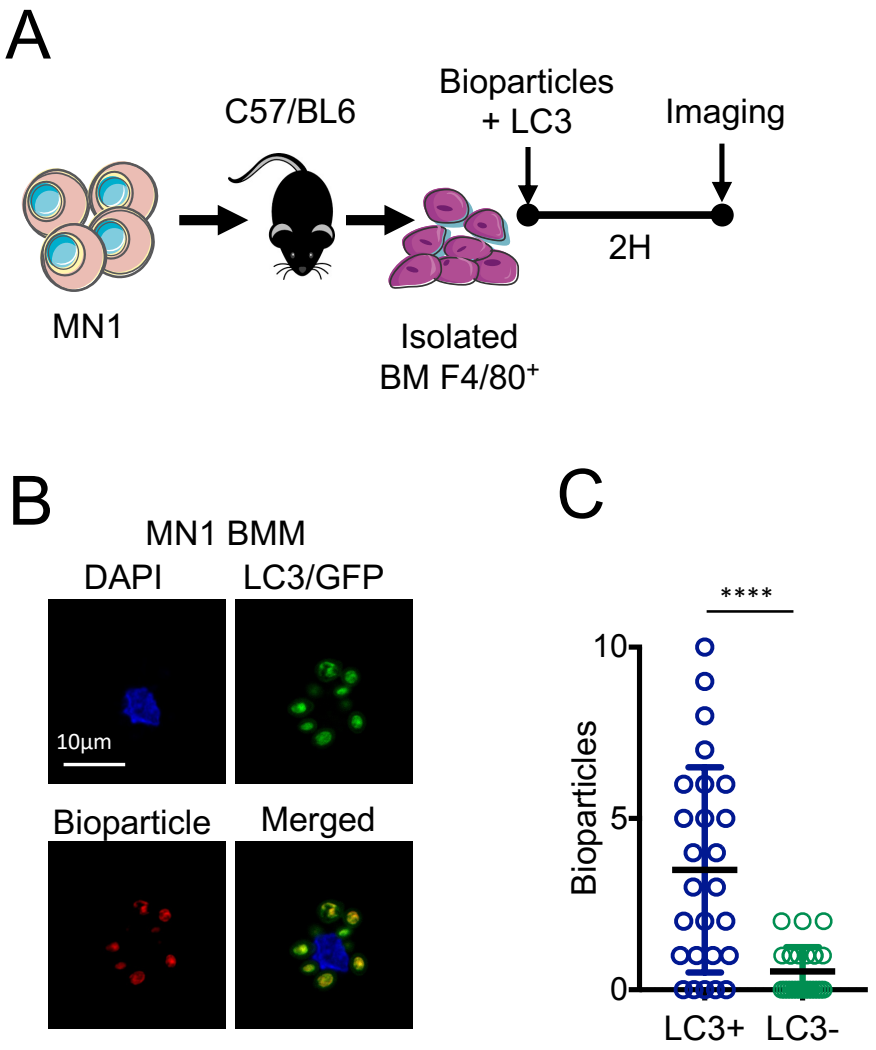

Figure 3.7. AML associated macrophages primarily undergo LC3-associated phagocytosis

(A) Experimental design schematic, isolated F4/80$^+$ macrophages from MN1 engrafted animals were cultured with Zymosan bioparticles, fixed and permeabilised, labelled with anti-LC3 antibody before being imaged by fluorescence microscopy. (B) Representative images of MN1 engrafted isolated F4/80$^+$, bioparticle uptake and LC3 association. (C) Number of LC3$^+$ and LC3$^-$ bioparticles per macrophage (n=25). Data shown are means ± SD ****P < 0.000, Mann–Whitney U.

3.3 LC3-associated phagocytosis in macrophages is required for AML suppression

The identification that macrophages from AML engrafted animals are important for the suppression of AML and that the primary method of phagocytosis is associated to LC3 highlights the potential that the process of LC3-associated phagocytosis (LAP) in BM macrophages may be an important pathway in AML progression. To investigate the importance of LAP within AML disease progression, the generation of a specific LAP deficient mouse model was used Atg16L1^{E230-}. The model utilises the importance of the ATG16L1 protein within the LC3 conjugated machinery to initiate LAP, two stop codons were inserted into exon 6 immediately after glutamine E230, preventing translation of the linker and WD domain (Figure 3.8) [304]. The Atg16L1^{E230-} model was used with wildtype counterparts with intact ATG16L1 genes, Atg16L1^{E230+}.

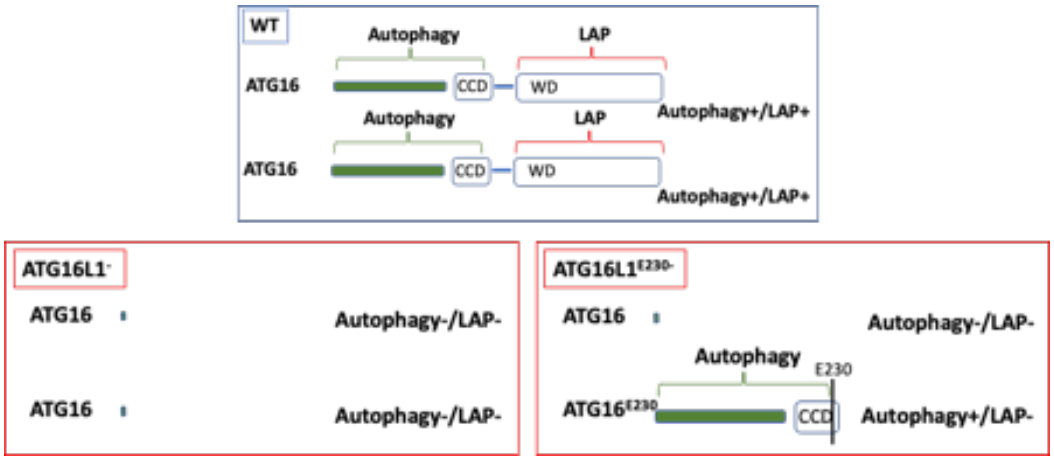

Figure 3.8. Atg16L1^{E230-} mouse model

Schematic diagram of Atg16L1^{E230-} mouse model. Wildtype (WT) mice have intact linker and WD domains allowing for LAP and autophagy. Complete loss of Atg16L1 leads to a deficiency in both LAP and autophagy. Atg16L1^{E230-} mice have two stop codons entered before glutamine E230 which prevents translation of the linker and WD domain resulting in LAP deficiency.

To study the effects of LAP on AML progression, the two mouse models of AML was utilised, MN1 and MEIS1/HOXA9, both having a GFP tag for visualisation via flow cytometry. Atg16L1^{E230-} and Atg16L1^{E230+} mice were i.v injected with 10^6 of MN1-GFP cells after 2 days of pre-treatment with 25mg/kg of busulfan via i.p injections (Figure 3.9A). Atg16L1^{E230-} animals had increased MN1-GFP engraftment in the bone marrow at day 14 and day 20 post injection compared to Atg16L1^{E230+} animals (Figure 3.9B). Furthermore, Atg16L1^{E230-} animals had decreased survival compared to Atg16L1^{E230+} animals (Figure 3.9C). Next, 10^6 of MEIS1/HOXA9-GFP cells were i.v injected into Atg16L1^{E230-} and Atg16L1^{E230+} mice after 2 days of pre-treatment with 25mg/kg of busulfan via i.p injections (Figure 3.10A). Atg16L1^{E230-} animals had increased MEIS1/HOXA9-GFP engraftment in the bone marrow at day 20 post injection compared to Atg16L1^{E230+} animals (Figure 3.10B) as well as decreased survival (Figure 3.10C).

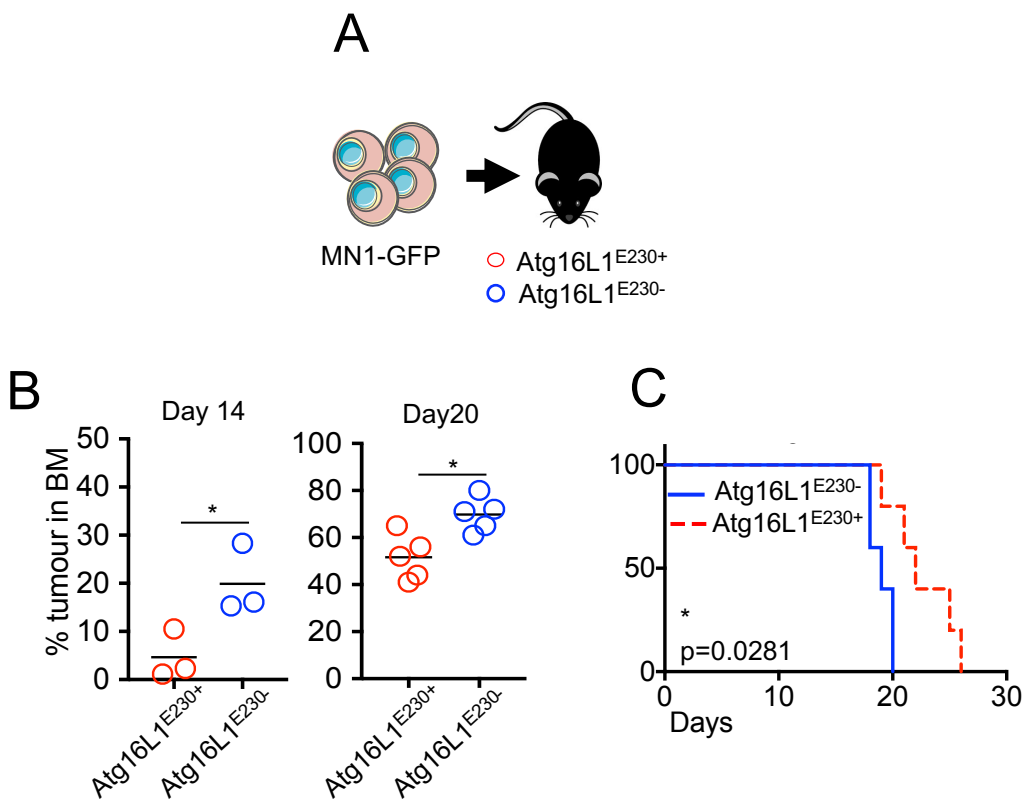

Figure 3.9. LAP deficiency leads to increase MN1 tumour burden and decreased animal survival

(A) 10^6 MN1-GFP cells were injected i.v. into Atg16L1^{E230-} and Atg16L1^{E230+} animals after pre-treatment with 25mg/kg of busulfan. (B) The amount of tumour in the bone marrow was analysed via flow cytometry as a percentage of GFP positive cells in the bone marrow. The bone marrow of Atg16L1^{E230-} and Atg16L1^{E230+} animals was analysed at day 14 (n=3) and day 20 (n=5). (C) The survival of Atg16L1^{E230-} and Atg16L1^{E230+} animals engrafted with MN1-GFP cells was monitored and plotted on a Kaplan Meier graph (n=5). Data shown are means ± SD *P < 0.05, Mann–Whitney U.

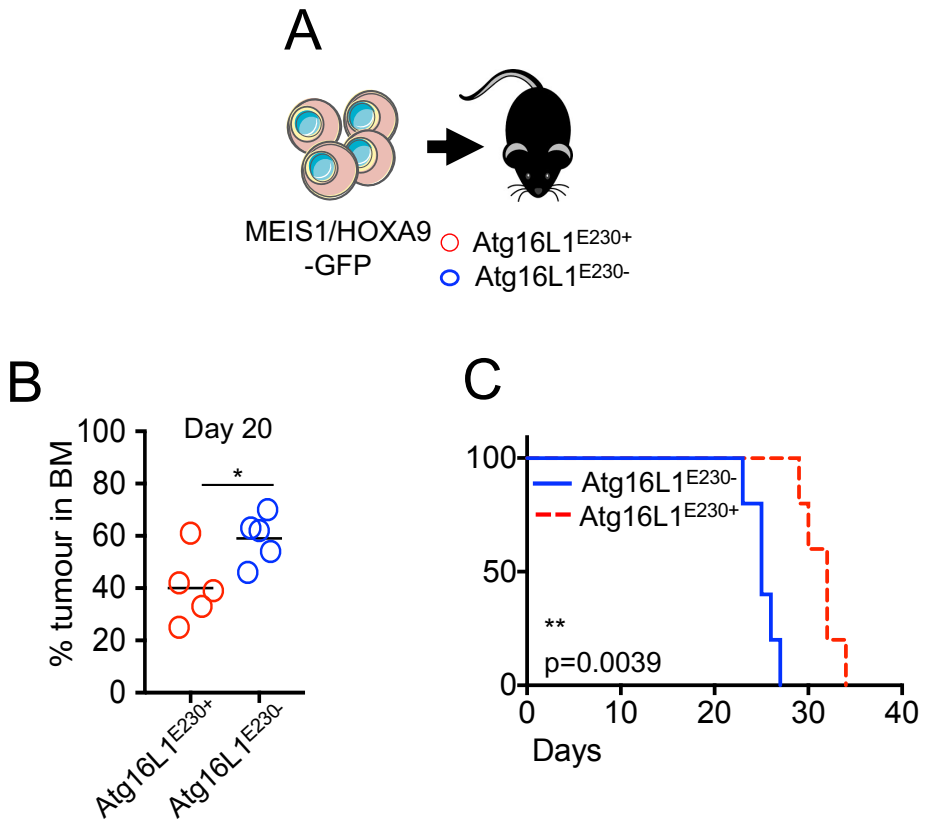

Figure 3.10. LAP deficiency leads to increase MEIS1/HOXA9 tumour burden and decreased animal survival

(A) 10^6 MEIS1/HOXA9-GFP cells were injected i.v. into Atg16L1^{E230-} and Atg16L1^{E230+} animals after pre-treatment with 25mg/kg of busulfan. (B) The amount of tumour in the bone marrow was analysed via flow cytometry at day 20 as a percentage of GFP positive cells in the bone marrow (n=5). (C) The survival of Atg16L1^{E230-} and Atg16L1^{E230+} animals engrafted with MEIS1/HOXA9-GFP cells was monitored and plotted on a Kaplan Meier graph (n=5). Data shown are means ± SD *P < 0.05, **P < 0.01, Mann–Whitney U.

Identification of increased AML progression in Atg16L1^{E230-} mice suggests that LAP is important in the control of AML suppression. However, as the animals are myelosuppressive conditioned with busulfan before injection of AML cells, investigations into how treatment with busulfan effects the cellularity of the bone marrow in the two mouse models was undertaken. The BM from Atg16L1^{E230-} and Atg16L1^{E230+} animals with and without 2 daily doses of busulfan (25mg/kg per dose) were isolated. The BM cells were then counted using trypan blue to identify viable cells counts between groups. Though there was variation in the cell counts, no significant differences were found (Figure 3.11A). The BM was analysed via flow cytometry to further investigate the cellularity between Atg16L1^{E230-} and Atg16L1^{E230+} BM treated with busulfan, with no significant differences evident in BM plots (Figure 3.11B). Next, the BM was analysed for specific cell populations, lineage positive and negative cells as well as macrophages (Figure 3.12A). No significant differences were seen in lineage positive, lineage negative, as well as macrophage populations between Atg16L1^{E230-} and Atg16L1^{E230+} animals treated with busulfan and untreated (Figure 3.12B-D). These results show that AML progression is accelerated in Atg16L1^{E230-} mice compared to Atg16L1^{E230+} mice, with busulfan treatment not altering the overall cellularity of the bone marrow. This suggest that LAP is an important mechanism in the control of AML progression.

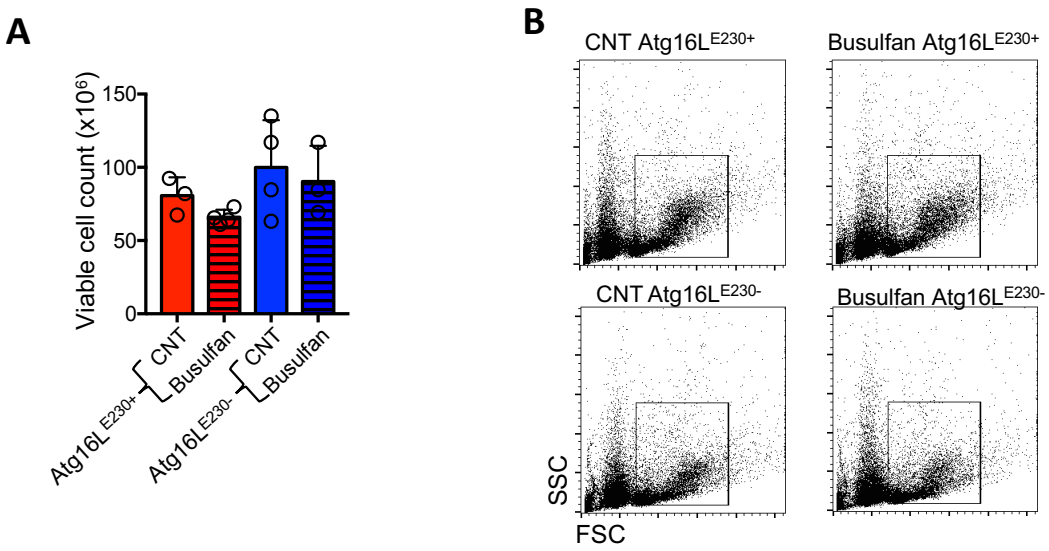

Figure 3.11. Busulfan treatment does not alter viable bone marrow cell numbers from Atg16L1^{E230-} and Atg16L1^{E230+} animals

(A) The bone marrow isolated from Atg16L1^{E230-} and Atg16L1^{E230+} animals either treated with or without 25mg/kg of busulfan for 2 days was analysed for cell viability by trypan blue exclusion 14 days post treatment. (B) Representative flow cytometry plots of the bone marrow cellularity from Atg16L1^{E230-} and Atg16L1^{E230+} animals either treated with or without 25mg/kg of busulfan for 2 days (n=3, 4). Data shown are means ± SD. No significance at $p>0.05$.

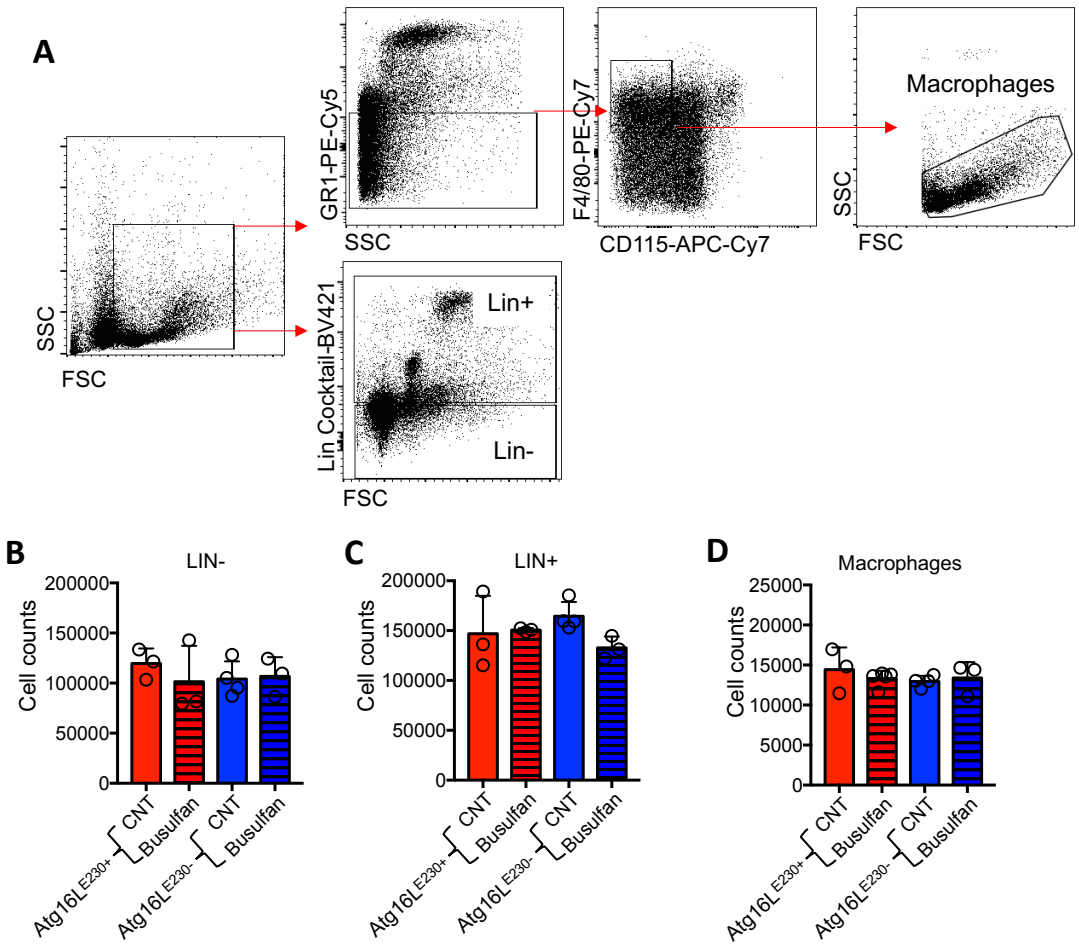

Figure 3.12. Busulfan treatment does not alter cell populations from Atg16L1^{E230-} and Atg16L1^{E230+} animals

(A) The bone marrow isolated from Atg16L1^{E230-} and Atg16L1^{E230+} animals either treated with or without 25mg/kg of busulfan for 2 days was analysed via flow cytometry 14 days post treatment for certain cell populations: lineage^{+}, lineage^{-} and macrophages (GR1^{-}, F4/80^{+}, CD115$^{LOW/INT)}$. (B) Total cell count for lineage^{-} cells. (C) Total cell count for lineage^{+} cells (D) Total cell count for macrophages. (n=3, 4). Data shown are means ± SD. No significance at p>0.05. See pg. 88 for flow panel information.

The accelerated AML progression seen in Atg16L1^{E230-} animals shows that the LAP mechanism plays an important role in AML tumour progression. To understand if this process is specific to macrophages, another mouse model was used. LysMcreAtg16L1^{E230-} mice were generated by crossing mice containing the Lysozyme-M-Cre promoter with mice containing floxed sites flanking exon 2 of ATG16L1 gene. The generation of LysMcreAtg16L1^{E230-} animals allowed for targeted LAP deficiency in monocytes and macrophages (Figure 3.13).

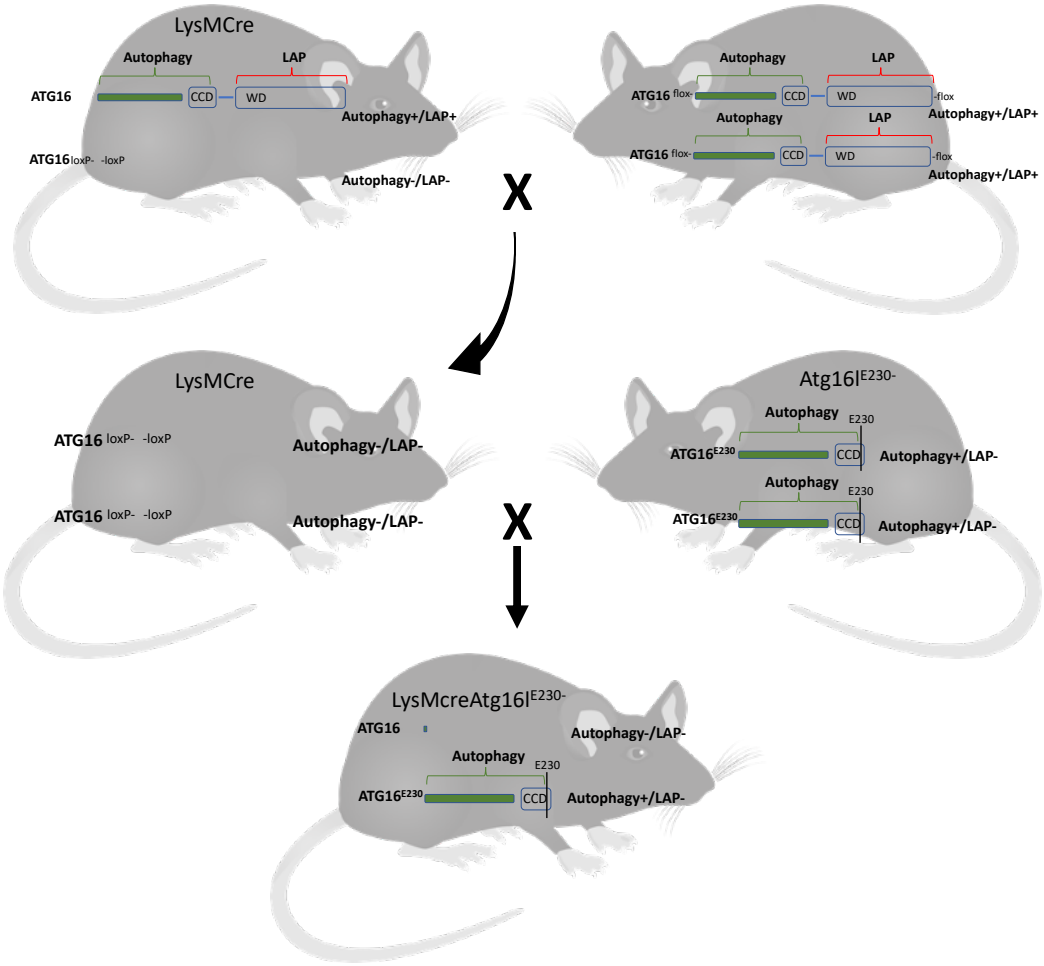

Figure 3.13. LysMcreAtg16l^{E230-} mouse model

Heterozygous floxed LysMcre mice were mated with homozygous lox-P flanked Atg16 mice to generate homozygous lox-P flanked Atg16 and LysMcre mice. These mice were then mated with Atg16L1^{E230-} to generate LysMcreAtg16l^{E230-} mice.

LysMcreAtg16L1^{E230-} and LysMcreAtg16L1^{E230+} mice were injected with 10^6 MN1-GFP cells after busulfan pre-treatment (2 days, 25mg/kg). After 14 days the animals were sacrificed, and the bone marrow was isolated to investigate AML engraftment via GFP fluorescence (Figure 3.14A). LysMcreAtg16L1^{E230-} animals had increased AML engraftment compared to LysMcreAtg16L1^{E230+} animals (Figure 3.14B). Furthermore, analysis of the level of annexin V positive MN1-GFP cells in the bone marrow identified there was no differences in the amount of annexin V positive MN1-GFP cells in LysMcreAtg16L1^{E230-} and LysMcreAtg16L1^{E230+} mice and that most cells were annexin V negative (Figure 3.14C). To identify absolute live cell counts of resident and MN1 cell numbers, the identification of annexin V negative populations was used via flow cytometry (Figure 3.14D). There were no differences in amount of annexin V negative cells between the two groups (Figure 3.14E). Additionally, data showed that the absolute live MN1-GFP cell counts were higher in LysMcreAtg16L1^{E230-} mice compared to LysMcreAtg16L1^{E230+} mice (Figure 3.14F). This data shows that LAP, specifically in macrophages of the bone marrow, is required for the suppression of AML, supporting the previous findings that LAP is an important mechanism in the control of AML progression.

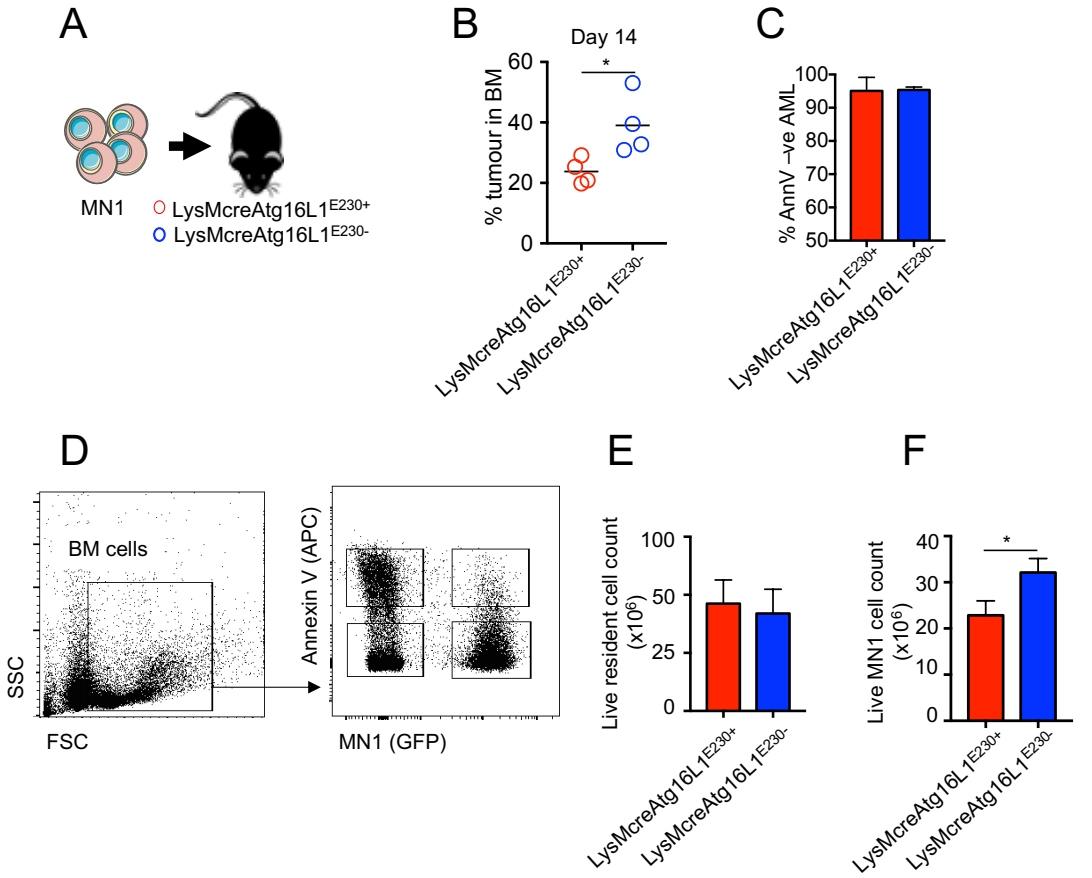

Figure 3.14. LAP deficiency in macrophages leads to increase tumour burden without altering resident cellularity

(A) 10^6 MN1-GFP cells were injected i.v. into LysMcreAtg16L1^{E230-} and LysMcreAtg16L1^{E230+} animals after pre-treatment with 25mg/kg of busulfan (B) The amount of tumour in the bone marrow was analysed via flow cytometry as a percentage of GFP positive cells in the bone marrow. The bone marrow of LysMcreAtg16L1^{E230-} and LysMcreAtg16L1^{E230+} animals was analysed at day 14. (C) The percentage of GFP$^+$ MN1 cells that was negative for annexin V staining via flow cytometry. (D) Flow plots of mice bone marrow with MN1-GFP engraftment and annexin V. (E) Total cell count of annexin V negative and GFP negatives cells (live resident cells) from LysMcreAtg16L1^{E230-} and LysMcreAtg16L1^{E230+} animals. (F) Total cell counts of annexin V negative MN1-GFP cells from LysMcreAtg16L1^{E230-} and LysMcreAtg16L1^{E230+} animals. n=4 in each group. Data shown are means ± SD *P<0.05, Mann–Whitney U.

The increased AML progression seen in LAP deficient animals suggests that LAP in macrophages may play a protective role within a leukaemic microenvironment and hinder the progression of AML. The animal models used relies on the injection of murine AML into host animals after pre-treatment with busulfan. Although I have shown that busulfan treatment does not alter the cellularity of the bone marrow, the injection of AML cells into host animals may not represent to what extend LAP occurs in a setting where AML develops in situ. As such, to investigate whether LAP is important in a setting were AML developed in situ, I looked at LC3 in human AML patient monocytes.

To do this, the peripheral blood of patients with AML and healthy patients was collected. The white cells were isolated via histopaque separation and then the isolation of $CD14^+$ monocytes was achieved via magnetic separation and positive selection using CD14 microbeads. The $CD14^+$ cells were then fixed and permeabilised to investigate the LC3 density of the cells via microscopy (Figure 3.15A). Though variation was seen, $CD14^+$ cells isolated from AML patients showed increased expression of LC3 when compared to healthy patients (Figure 3.15B). This information shows that LC3 is upregulated in human AML patients, as such, AML patient macrophages may be primed for phagocytosis, specifically LAP.

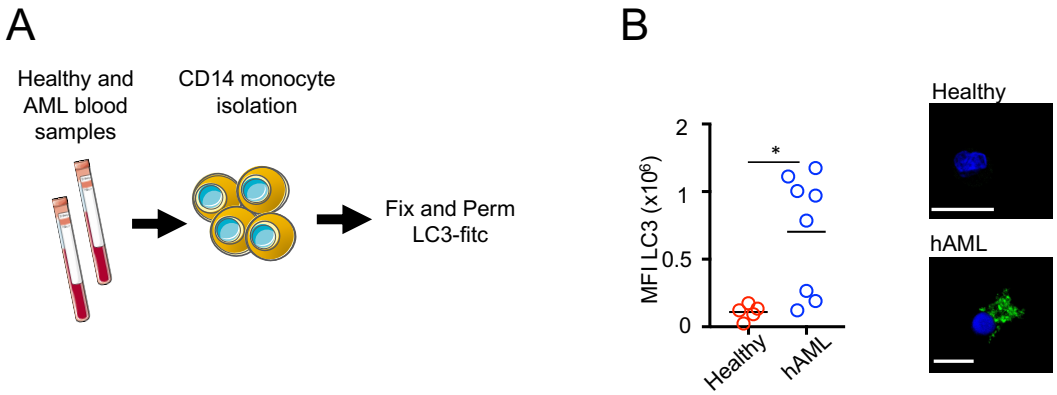

Figure 3.15. LC3 density in human AML and healthy CD14⁺ cells from peripheral blood

(A) Healthy and AML blood samples were collected, and the peripheral blood mononuclear cells were isolated via Histopaque. Cells were labelled with CD14 microbeads before positive selection via magnetic separation using MAC columns. 50,000 $CD14^+$ cells were fixed and permeabilised, labelled with anti-LC3-fitc and DAPI before being plated into black µ-Plate 24 well plates. Images were taken via confocal microscopy, the average of 20 $CD14^+$ cells were collected for each sample (B) LC3 density was assessed via calculation of the MFI of LC3 using ImageJ. Representative microscopy images of healthy and AML $CD14^+$ cells. Scale bar=10µm. Data shown are means ± SD *P<0.05, Mann–Whitney U.

3.4 Summary

In this first chapter, I have investigated the role of macrophages within the leukaemic environment. I have shown that bone marrow macrophages are important cells in the control of AML progression and their depletion leads to increased tumour progression. leukaemic associated macrophages are primed towards a more phagocytotic phenotype, with the primary method of phagocytosis occurring via LC3-dependent mechanisms. Moreover, LC3 associated phagocytosis is required to limit the growth of AML which is shown by engrafting AML into LAP deficient animals and observing a more advanced AML progression and decreased animal survival. Furthermore, animals that have macrophage specific LAP deficiency show increased AML progression. Finally, monocytes from AML patients have an increased LC3 content compared to healthy patients. Taken together, the data presented here shows that LAP is an important mechanism that macrophages use to control the progression of AML within the bone marrow microenvironment.

4. STING activation in bone marrow macrophages occurs via LC3 associated phagocytosis of AML apoptotic bodies containing mitochondrial DNA which promotes AML suppression

4.1 Introduction

I have established that LC3 associated phagocytosis (LAP) in macrophages located in the bone marrow is important for the control of AML growth. It has been shown that LAP is an important immune defence in the regulation of pathogenic infections as well as in dying cells, including cancer cells [298, 299]. Furthermore, research has shown that in models of solid tumours that LAP impairment leads to an anti-tumour response [303]. Specifically, LAP deficiency in tumour associated macrophages leads to STING type I IFN activation and the subsequent activation of a T-cell immune response. While the location of the malignancies of solid tumours allows for infiltration of T-cells and tumour suppression, the microenvironment of the bone marrow in which AML residues is an immuno-privileged site. This is important in order to protect the process of haematopoiesis and as such cytotoxic T-cells are largely excluded [464, 465]. Thus, what role LAP mediated immune activation has upon AML is unknown. Furthermore, what role STING plays in leukaemic associated macrophages is yet to be investigated. In this results chapter I have explored what role LAP in macrophages plays in the regulation of AML growth and whether this is governed by a STING mediated response.

4.2 LAP deficiency does not alter macrophage polarity in an AML microenvironment

First, to investigate whether LAP deficient mice have an altered macrophage phenotype, flow cytometry was used to identify separate macrophage populations and their polarity. To do this, macrophage populations were investigated in C57/BL6 mice with and without AML. C57/BL6 mice were injected with 10^6 MN1-GFP cells or vehicle after 2-day pre-treatment with 25mg/kg of busulfan. After 14 days the bone marrow was isolated and run via flow cytometry with a range of antibodies (Figure 4.1A). AML associated macrophages (AAM) were defined as $CD45^+$, $Lys6G^-$, $CD11b^+$ whilst tissue resident BMM express $CD45^+$, $GR1^-$, $F4/80^+$, $CD115^{INT}$ (Figure 4.1B) [61, 397].

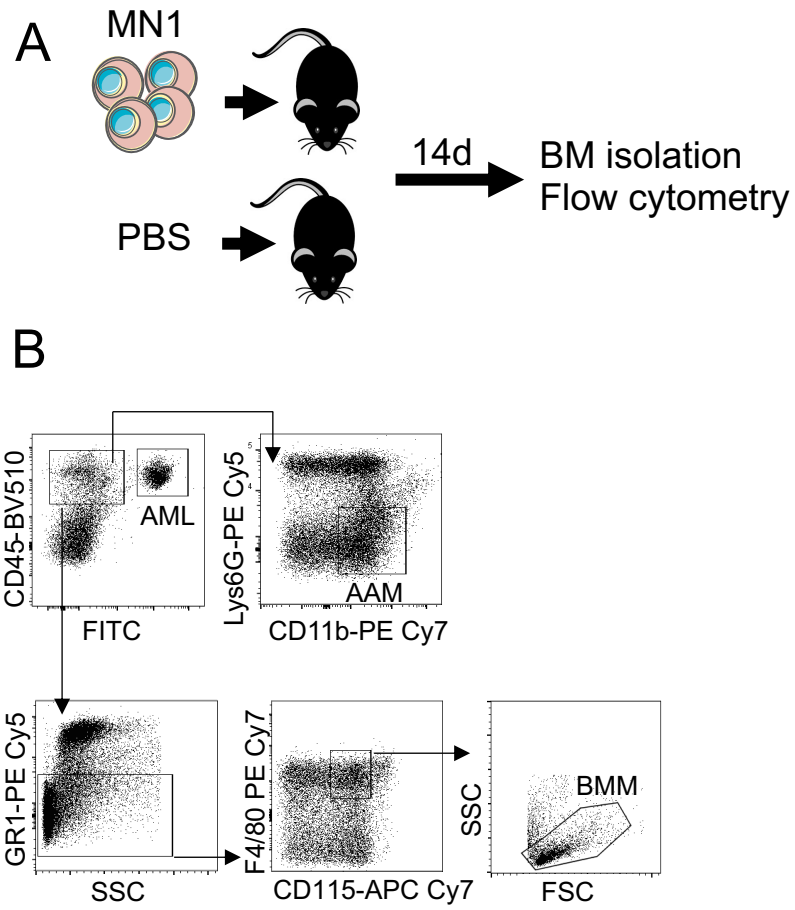

Figure 4.1. Gating strategy for the identification of macrophage populations

(A) Schematic diagram of experiment design, MN1-GFP cells or vehicle was I.V injected into C57/BL6 animals that were pre-treated with busulfan (2 days, 25mg/kg). After 14 days, animals were sacrificed, and the bone marrow harvested for flowcytometry. (B) The gating strategy used during flow cytometry to identify AML associated macrophages (AAM) and resident bone marrow macrophages (BMM). See pg. 88 for flow panel information.

AAM and BMM cell populations and cell numbers were investigated as a percentage of CD45 cells. Furthermore, to investigate the effects of cellular polarity in the macrophage populations, the M1 macrophage marker (CD86) and the M2 macrophage marker (CD206) was used. The percentage of AAM cells was increased in animals with MN1 cell engraftment compared to non-engrafted animals. Additionally, there was a decrease in M1 polarity marker CD86 in MN1 engrafted animals compared to control animals. However, no change was observed between groups in their M2 status (Figure 4.2A). The percentage of BMM cells were increased in mice with MN1 engraftment compared to control animals. When investigating the BMM polarity, both M1 and M2 markers were increased in MN1 engrafted animals compared to non-engrafted mice (Figure 4.2B). This data shows that both AAM and BMM populations of macrophages are increased in an AML environment. Furthermore, AAM cells lose M1 polarity whilst BMM have increased M1 and M2 markers in an AML environment compared to a non-leukaemic environment.

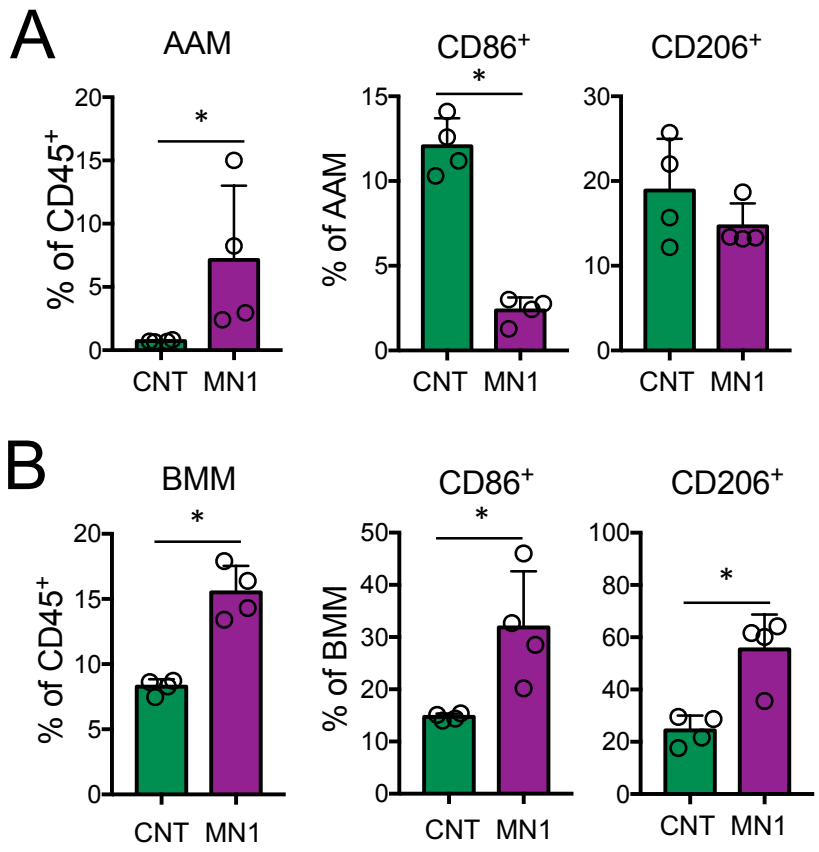

Figure 4.2. MN1 engraftment alters macrophages

(A) AML associated macrophage (AAM) numbers were calculated as a percentage of $CD45^+$ cells between MN1 engrafted and non-engrafted animals. CD86 and CD206 percentage of AAM was calculated between groups. (B) Resident bone marrow macrophage (BMM) numbers were calculated as a percentage of $CD45^+$ cells between MN1 engrafted and non-engrafted animals. CD86 and CD206 percentage of BMM was calculated between groups. n=4 in each group. Data shown are means ± SD. *$p<0.05$, Mann–Whitney U. See pg. 88 for flow panel information.

To investigate whether any difference in macrophage numbers or polarity occurred in LAP deficient animals, Atg16L1^{E230-} and Atg16L1^{E230+} mice were used. Atg16L1^{E230-} and Atg16L1^{E230+} mice were injected with 10^6 MN1-GFP cells after 2-day pre-treatment with 25mg/kg of busulfan. After 14 days the bone marrow was isolated and run via flow cytometry for the identification of macrophages (Figure 4.3A). There were no differences observed in AAM numbers between MN1 engrafted Atg16L1^{E230-} and Atg16L1^{E230+} mice. Additionally, though slight differences were seen in CD86 and CD206 positive AAMs, there was no significant differences seen between MN1 engrafted Atg16L1^{E230-} and Atg16L1^{E230+} mice (Figure 4.3B). Similarly, the number of BMM, as well as their polarity status, was not altered in Atg16L1^{E230-} and Atg16L1^{E230+} mice (Figure 4.3C). Taken together, whilst AML engraftment alters the levels and polarity of both resident and recruited macrophages in the bone marrow, deficiencies in LAP does not alter this observed phenotype to enhance or decrease macrophage activation.

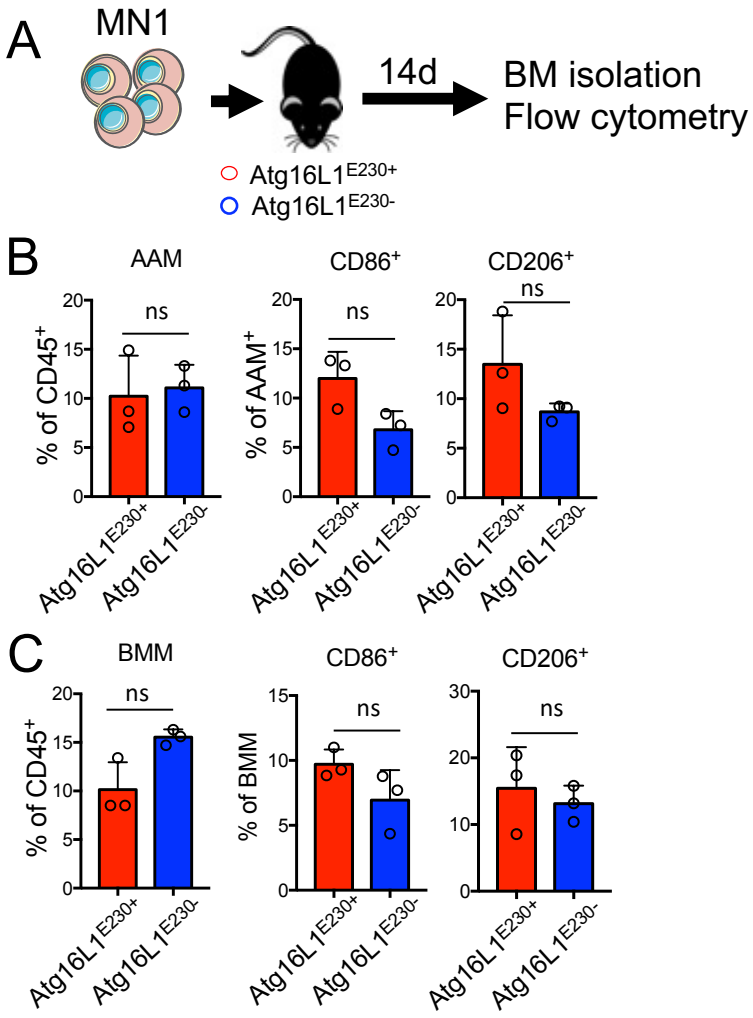

Figure 4.3. LAP does not alter the number or polarity of macrophages after AML engraftment

(A) Schematic diagram of experiment design, MN1-GFP cells were injected into Atg16L1^{E230-} and Atg16L1^{E230+} mice that were pre-treated with busulfan (2 days, 25mg/kg). After 14 days, animals were sacrificed, and the bone marrow harvested for flow cytometry. (B) AML associated macrophage (AAM) numbers were calculated as a percentage of CD45^{+} cells between Atg16L1^{E230-} and Atg16L1^{E230+} mice. CD86 and CD206 percentage of AAM was calculated between groups. (C) Resident bone marrow macrophage (BMM) numbers were calculated as a percentage of CD45^{+} cells between Atg16L1^{E230-} and Atg16L1^{E230+} animals. CD86 and CD206 percentage of BMM was calculated between groups. n=3 in each group. Data shown are means ± SD. No significance at $p>0.05$, Mann–Whitney U. See pg. 88 for flow panel information.

4.3 LAP in bone marrow macrophages mediates AML apoptotic cell clearance and apoptotic body degradation

As LAP deficient mice have increased AML progression and decreased survival, it suggests that LAP is an important regulatory mechanism in macrophages in the control of AML. However, the identification that LAP does not alter the number or polarity of macrophages in a leukaemic environment suggests that the suppressive nature of LAP may occur via a separate mechanism, independently of increased macrophage numbers. As the primary role of macrophages are to phagocytose and that LAP is an important mechanism used to clear apoptotic and dying cells, it was investigated how LAP controls apoptotic uptake in an AML environment. Atg16L1^{E230-} and Atg16L1^{E230+} mice were either injected with 10^6 MN1 cells or vehicle (PBS) after pre-treatment of busulfan (2-days, 25mg/kg). After 14 days the bone marrow was isolated, and the apoptotic status was analysed via annexin-V and flow cytometry (Figure 4.4A). The whole bone marrow was analysed for complete apoptotic status as well as the identification of ABs via gating the cellular debris within the bone marrow gate (Figure 4.4B).

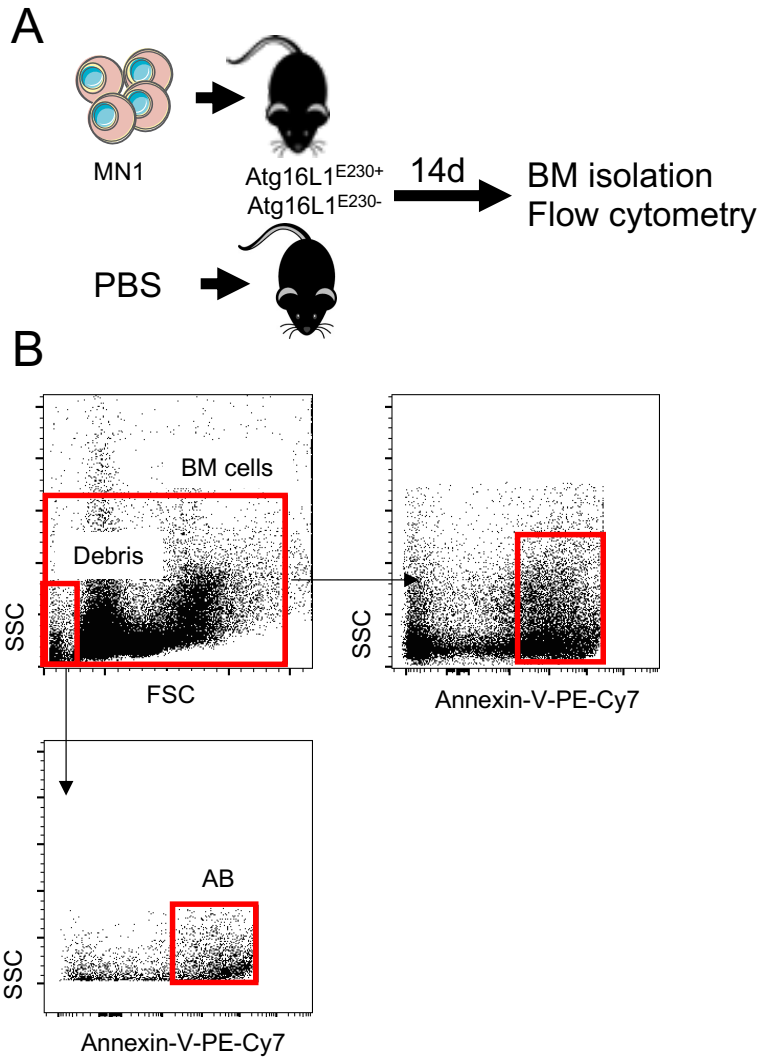

Figure 4.4. Gating strategy for the identification of annexin V positive bone marrow cells and apoptotic bodies

(A) Schematic diagram of experiment design, after pre-treatment with busulfan (2 days, 25mg/kg) MN1 cells or PBS was injected into Atg16L1^{E230-} and Atg16L1^{E230+} mice. After 14 days, animals were sacrificed, and the bone marrow harvested for flow cytometry for analysis of annexin V positivity. (B) Gating strategy used to investigate the bone marrow (BM) and cellular debris annexin V status. Annexin V positive debris was identified as apoptotic bodies (ABs). See pg. 88 for flow panel information.

Atg16L1^{E230-} mice engrafted with MN1 cells had significantly more apoptosis in the bone marrow when compared to Atg16L1^{E230+} mice engrafted with MN1 cells (Figure 4.5A). Animals without MN1 engraftment had comparable annexin V positivity as well as similar levels to Atg16L1^{E230+} mice engrafted with MN1 cells. Comparing the debris of Atg16L1^{E230-} and Atg16L1^{E230+} mice engrafted with MN1 cells, the annexin V positive debris was used as an ABs fold change. Results showed that Atg16L1^{E230-} mice with MN1 engraftment had an increased number of ABs compared to Atg16L1^{E230+} mice engrafted with MN1 cells (Figure 4.5B). This information suggests that animals lacking the ability to undergo LAP have an increased apoptotic burden in a leukaemic environment, with significantly more ABs in the BM.

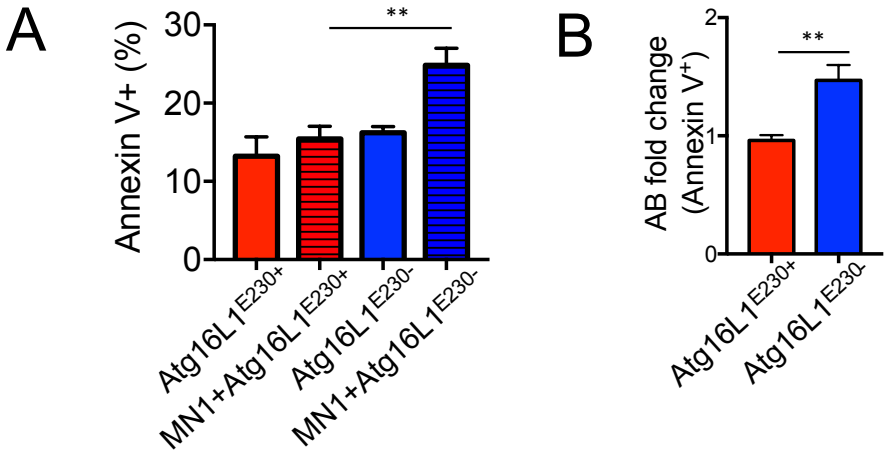

Figure 4.5. LAP deficient mice have increased apoptotic burden and apoptotic bodies after AML engraftment

(A) The percentage of annexin V positive staining in the bone marrow of Atg16L1^{E230-} and Atg16L1^{E230+} mice with and without MN1 engraftment. (B) The fold change of annexin V positive debris (apoptotic bodies, ABs) as calculated as a fold change of ABs between Atg16L1^{E230-} and Atg16L1^{E230+} mice engrafted with MN1 cells. n=4 in each group. Data shown are means ± SD. **p<0.01, (A) Kruskal Wallis with Dunn's post hoc, (B) Mann–Whitney U.

The increased ABs seen in Atg16L1^{E230-} mice engrafted with MN1 cells highlights that LAP is required to clear apoptotic AML cells. Thus, the inability to clear AML debris may be a factor in the AML progression seen in LAP deficient mice. Moreover, the ability to efficiently process AML ABs via LAP may alter the macrophages to allow suppression of AML. To investigate what role AML ABs has on macrophages I generated and classified AML-derived ABs. To do this, MN1 cells were treated with 5μM cytosine arabinoside (ara-C) for 24 hours. To confirm apoptosis in MN1 cells, flow cytometry was used to determine annexin V positivity (Figure 4.6A). To isolate the ABs from the apoptotic MN1 cells I used a centrifugation protocol as previously described [461]. ABs have a diameter of between 800-5000nm making them one of the largest extracellular vesicles. To isolated ABs, apoptotic cells and supernatant were spun at 500xg for 10 minutes. The cells were discarded, and the supernatant was spun at 10000xg for 10 minutes. The supernatant was removed, and the pellet contained the isolated MN1 derived ABs (Figure 4.6B). To confirm the isolate of the ABs fell within the size range previously described for ABs, dynamic light scattering (DLS) was used to confirm the ABs size range. ABs were resuspended in filtered PBS and analysed via DLS in conjunction with pre-defined sized microbeads. The ABs had a diameter of approximately 1000nm, consistent with previously described sizing for ABs (Figure 4.6C) [461].

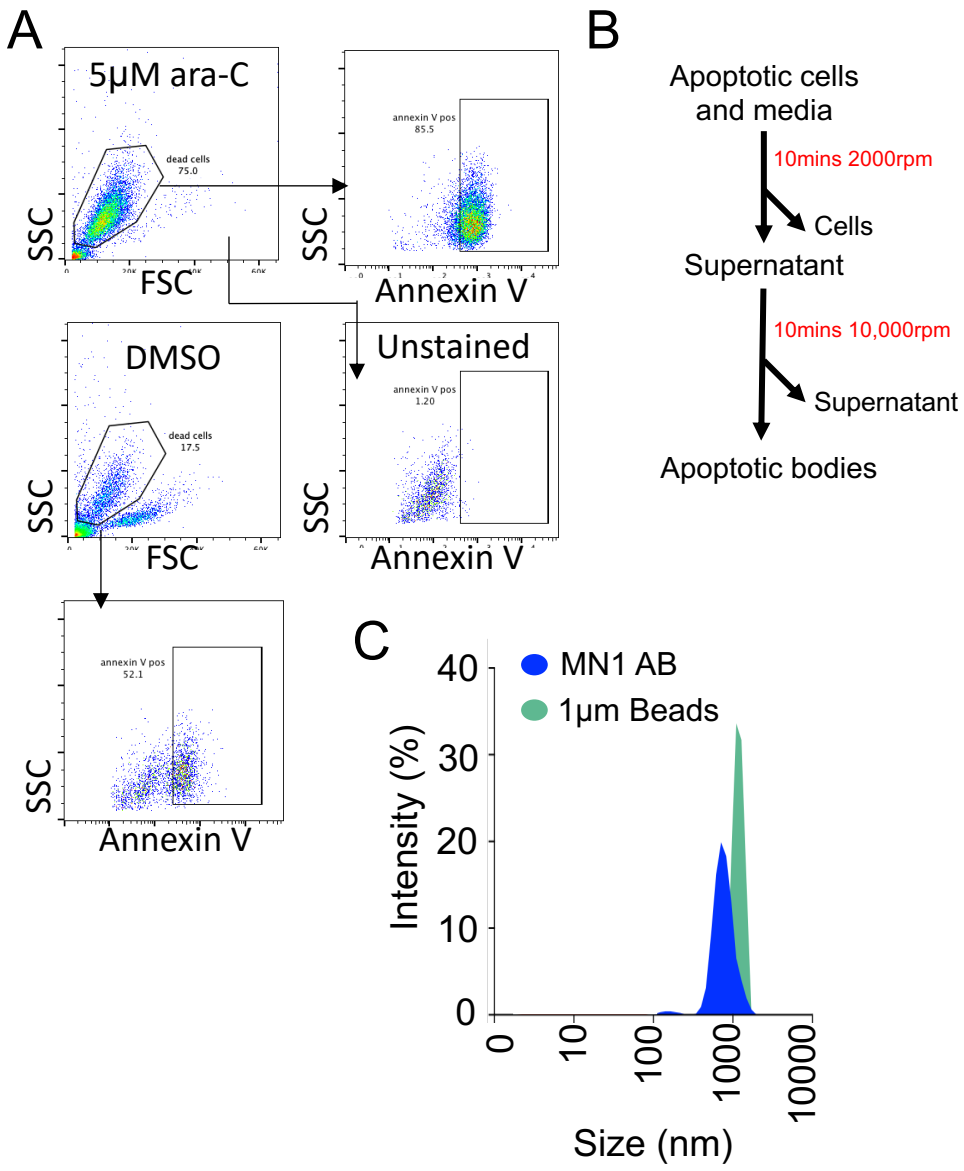

Figure 4.6. Induction of apoptosis and isolation of apoptotic bodies from MN1 cells

(A) MN1 cells were incubated with 5µM cytosine arabinoside (ara-C) or DMSO for 24 hours. The cells were collected and stained with annexin V to determine apoptosis. Gates were used to identify dead cells and annexin V positive cells. Unstained ara-C treated cells were used as controls (unstained). (B) Apoptotic bodies (ABs) were isolated via centrifugation. Apoptotic cells and media were spun at 500xg for 10 minutes. The supernatant was spun at 10000xg for 10 minutes to isolate ABs from the pellet. (C) The identification of the size profile of isolated MN1 ABs was achieved via dynamic light scattering. The vast majority of particles identified as 1000nm and size confirmation was achieved via pre-defined 1µm sized beads.

Next, to study the effects of the MN1 ABs on LAP deficient macrophages, I generated bone marrow derived macrophages (BMDM) (See 2.3.4). To achieved this, the bone marrow from Atg16L1^{E230-} and Atg16L1^{E230+} mice was isolated, filtered, counted, and plated into 10cm tissue culture plates at a density of 10^7 cells per plate in media containing 20ng/ml of macrophage colony-stimulating factor (m-CSF) (Figure 4.7A). After 7 days, confirmation of macrophage differentiation was achieved via microscopy (Figure 4.7B). Furthermore, to confirm macrophage differentiation, the use of flow cytometry identified the specific mature macrophage marker F4/80 (Figure 4.7C).

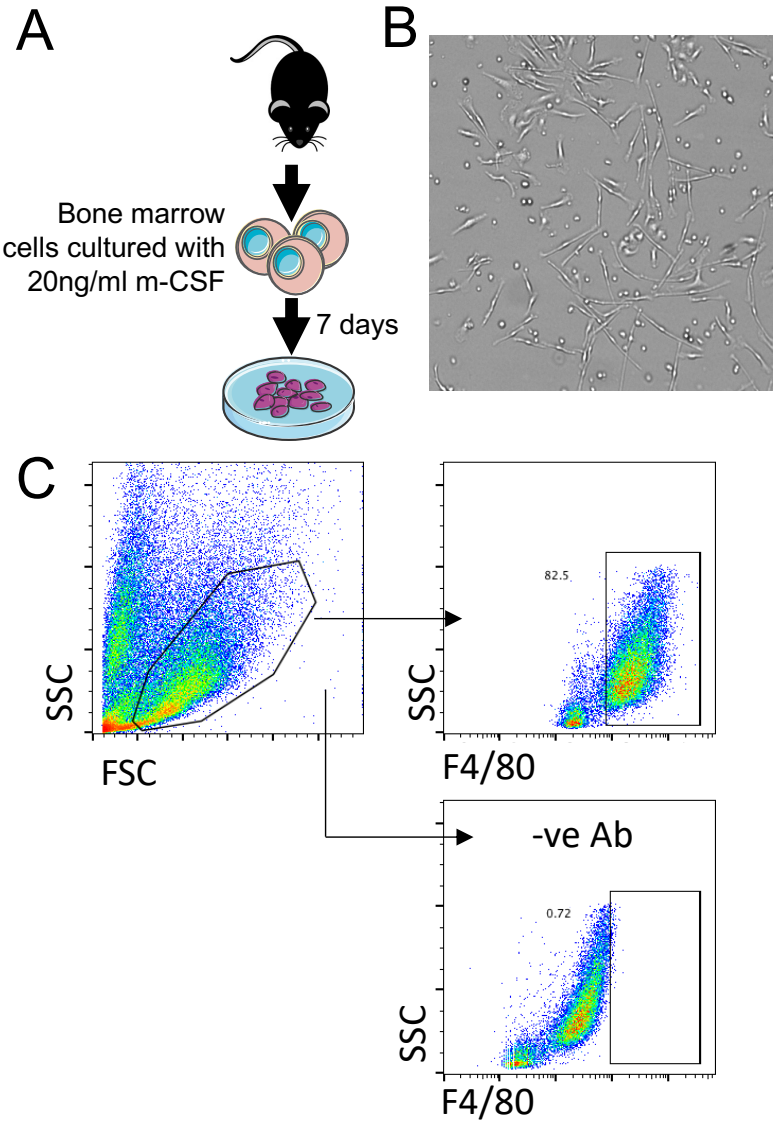

Figure 4.7. Bone marrow macrophage generation and identification

(A) The bone marrow from Atg16L1^{E230-} and Atg16L1^{E230+} mice were harvested and filtered through a 30µm meshed filter. The cells were counted and cultured in the presence of 20ng/ml macrophage colony-stimulating factor (m-CSF). Cells were plated at density of 10^7 cells per 10cm tissue culture plate. (B) Representative light microscopy image of differentiated bone marrow derived macrophages (BMDM) captured at 20x magnification using EVOS™ M5000 Imaging System (Invitrogen). (C) Differentiated BMDM were incubated with an anti-F4/80-FITC antibody for 20 minutes before analysing the expression of F4/80 using flow cytometry. Gating placement was achieved via BMDM without anti-F4/80-FITC antibody as a negative control (-ve Ab).

To investigate the differences between LAP deficient and LAP competent macrophages in the phagocytosis of MN1 derived ABs, the use of pHrodo Red SE allowed for specific tracking of phagocytosis. pHrodo Red SE is a pH sensitive dye that increases in fluorescence as the pH changes from neutral to acidic. As such, the fluorescence remains undetected until lysosomal fusion occurs with the phagosome, allowing for specific detection of phagocytosis. Isolated ABs from MN1 cells were labelled with pHrodo Red SE and cultured with BMDM isolated from Atg16L1^{E230-} and Atg16L1^{E230+} mice for 3 hours (Figure 4.8A). Using confocal microscopy, the identification of ABs specific phagosome per BMDM showed that Atg16L1^{E230-} BMDM had significantly less phagosomes than Atg16L1^{E230+} BMDM (Figure 4.8B).

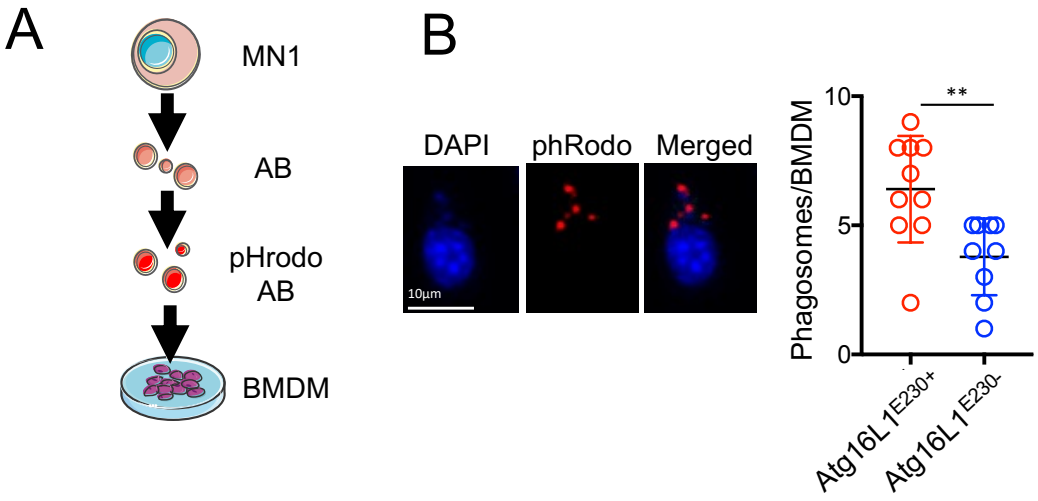

Figure 4.8. LAP is required for enhance phagocytosis of MN1 apoptotic bodies

(A) Apoptotic bodies (ABs) were isolated from apoptotic MN1 cells and labelled with pHrodo Red SE. Labelled pHrodo ABs were cultured with BMDM from Atg16L1^{E230-} and Atg16L1^{E230+} mice for 3 hours before being imaged via confocal microscopy. (B) Representative image of a Atg16L1^{E230+} BMDM with pHrodo Red SE labelled ABs and DAPI (magnification 63X). The number of phagosomes, as identified by pHrodo fluorescence, was counted per BMDM. n=10 BMDM. Data shown are means ± SD. **p<0.01, Mann–Whitney U.

Next, I investigated if LC3 localisation to phagosomes occurred more frequently in Atg16L1^{E230+} BMDM compared to Atg16L1^{E230-} BMDM. ABs from MN1 cells were isolated and labelled with pHrodo Red SE and cultured with BMDM from Atg16L1^{E230+} and Atg16L1^{E230+} animals for 3 hours. The BMDM were then labelled with an anti-LC3-fitc antibody (Figure 4.9A). Using confocal microscopy, the identification of ABs specific phagosome with LC3 localisation in BMDM showed that Atg16L1^{E230-} BMDM had significantly less LC3^{+} phagosomes than Atg16L1^{E230+} BMDM (Figure 4.9B). This data identifies LAP as an important mechanism for enhance phagocytotic clearance of ABs from AML cells. Furthermore, LC3 co-localises with phagosomes for efficient clearance of ABs in LAP competent macrophages.

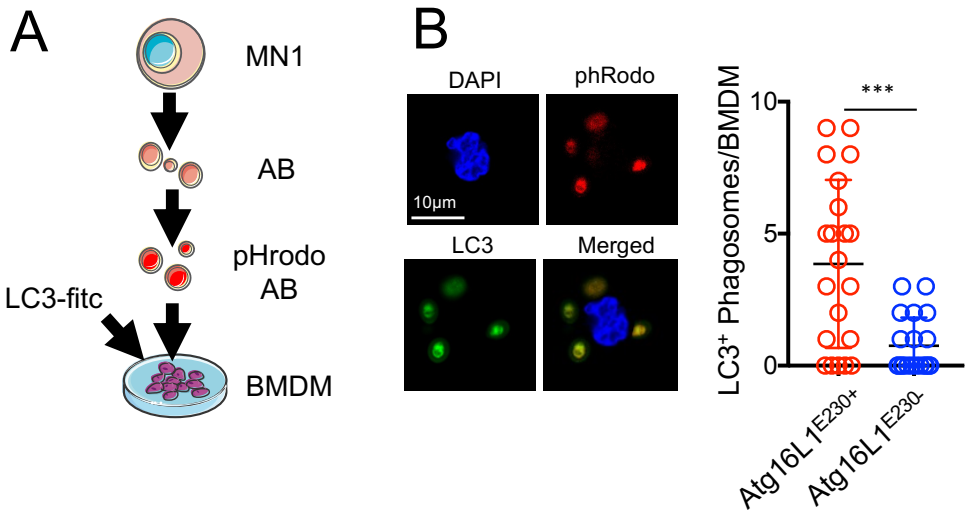

Figure 4.9. LC3 localisation to phagosomes occurs more frequently in LAP competent macrophages

(A) Apoptotic bodies (ABs) were isolated from apoptotic MN1 cells and labelled with pHrodo Red SE. Labelled pHrodo ABs were cultured with BMDM from Atg16L1^{E230-} and Atg16L1^{E230+} mice for 3 hours. BMDM were then labelled with an anti-LC3-fitc antibody before being imaged via confocal microscopy. (B) Representative image of a Atg16L1^{E230+} BMDM with pHrodo Red SE labelled ABs, DAPI and LC3 (magnification 63X). The number of LC3^{+} phagosomes, as identified by pHrodo and LC3 co-localisation, was counted per BMDM. n=25 BMDM. Data shown are means ± SD. ***p<0.005, Mann–Whitney U.

The identification that LAP is required for effective AML ABs clearance by macrophages suggests that LAP is responsible for delivery of apoptotic cargo to lysosomes in macrophages for degradation. To confirm that this was the case, the lysosomal inhibitor, Bafilomycin A1 (BafA1), was used. BafA1 inhibits V-ATPase, which leads to the blockage of late-stage lysosomal fusion as well as lysosomal degradation [466]. This allows the study of lysosomal delivery to the phagosomes containing AML ABs. To do this, Atg16L1^{E230+} and Atg16L1^{E230-} BMDM were generated and cultured with 1μM of BafA1 or vehicle for 1 hour before the addition of pHrodo Red SE labelled MN1 ABs for 2 hours (Figure 4.10A). Using confocal microscopy, the identification of ABs specific phagosome in BMDM showed that BafA1 inhibited lysosomal fusion in Atg16L1^{E230+} BMDM but no differences were seen in Atg16L1^{E230-} BMDM with or without BafA1 (Figure 4.10B). This data shows LAP competent BM macrophages deliver ABs to lysosomes for degradation, which does not occur in LAP deficient BM macrophages.

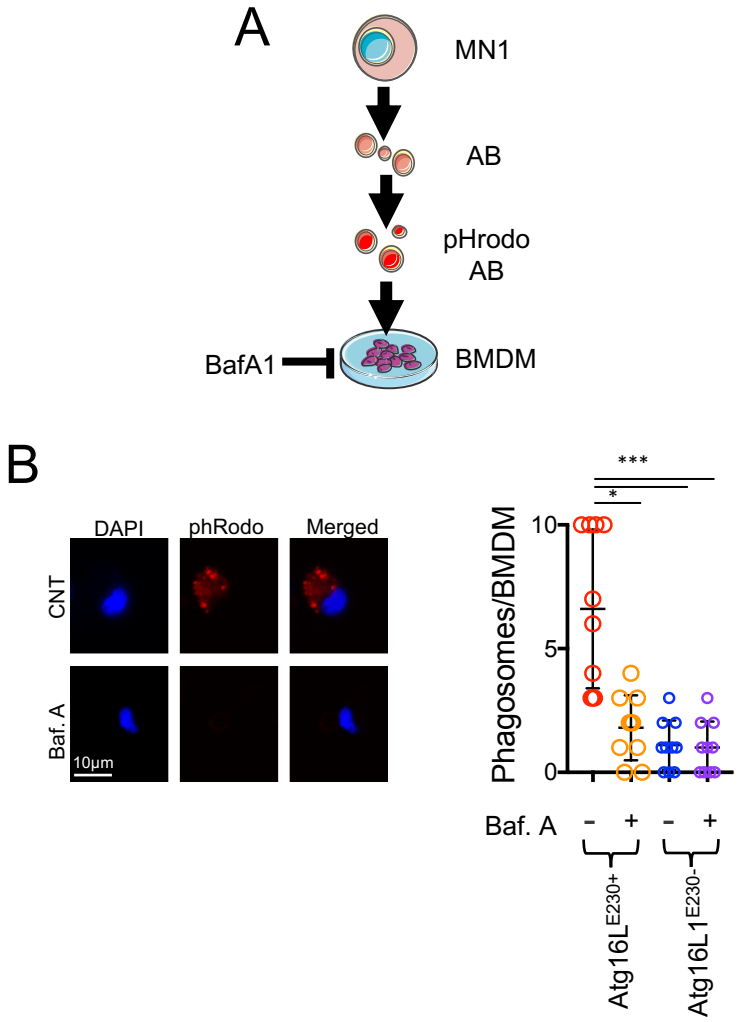

Figure 4.10. LAP is required to deliver phagosomes to lysosomes for apoptotic body degradation

(A) BMDM from Atg16L1^{E230-} and Atg16L1^{E230+} mice were cultured with 1µM of Bafilomycin A1 (BafA1) for 1 hour. Apoptotic bodies (ABs) were isolated from apoptotic MN1 cells and labelled with pHrodo Red SE. Labelled pHrodo ABs were cultured with for 2 hours on treated BMDM before being imaged via confocal microscopy. (B) Representative image of a control and BafA1 treated Atg16L1^{E230+} BMDM with pHrodo Red SE labelled ABs and DAPI (magnification 63X). The number of phagosomes, as identified by pHrodo fluorescence, was counted per BMDM. n=10 BMDM. Data shown are means ± SD. *p<0.05, ***p<0.005, Kruskal Wallis with Dunn's post hoc.

4.4 Uptake of AML apoptotic bodies leads to STING activation which results in reduced AML tumour burden

The uptake and efficient clearance of AML ABs in LAP competent macrophages and their ability to supress AML growth highlights the potential that the uptake of AML ABs by macrophages leads to changes in the macrophages in a LAP dependent way. However, my previous results shows that LAP deficiencies in mice do not alter the polarity or number of macrophages in an AML microenvironment. As macrophages are reliant on environmental signals and can produce vast amount of cyto- and chemokines, I investigated what changes occur between LAP competent and deficient macrophages after exposure to AML ABs.

To study this, I used the Proteome Profiler Mouse XL Cytokine Array which allowed the study of multiple cytokines simultaneously. MN1 ABs were isolated from apoptotic MN1 cells and cultured with BMDM from Atg16L1^{E230-} and Atg16L1^{E230+} animals for 24 hours. The supernatant was isolated from the BMDM and analysed using the cytokine arrays (Figure 4.11A). A large number of cytokines did not appear upon analysis on the cytokine arrays, indicating that the range of cytokines released by BMDM may be more targeted (Figure 4.11B).

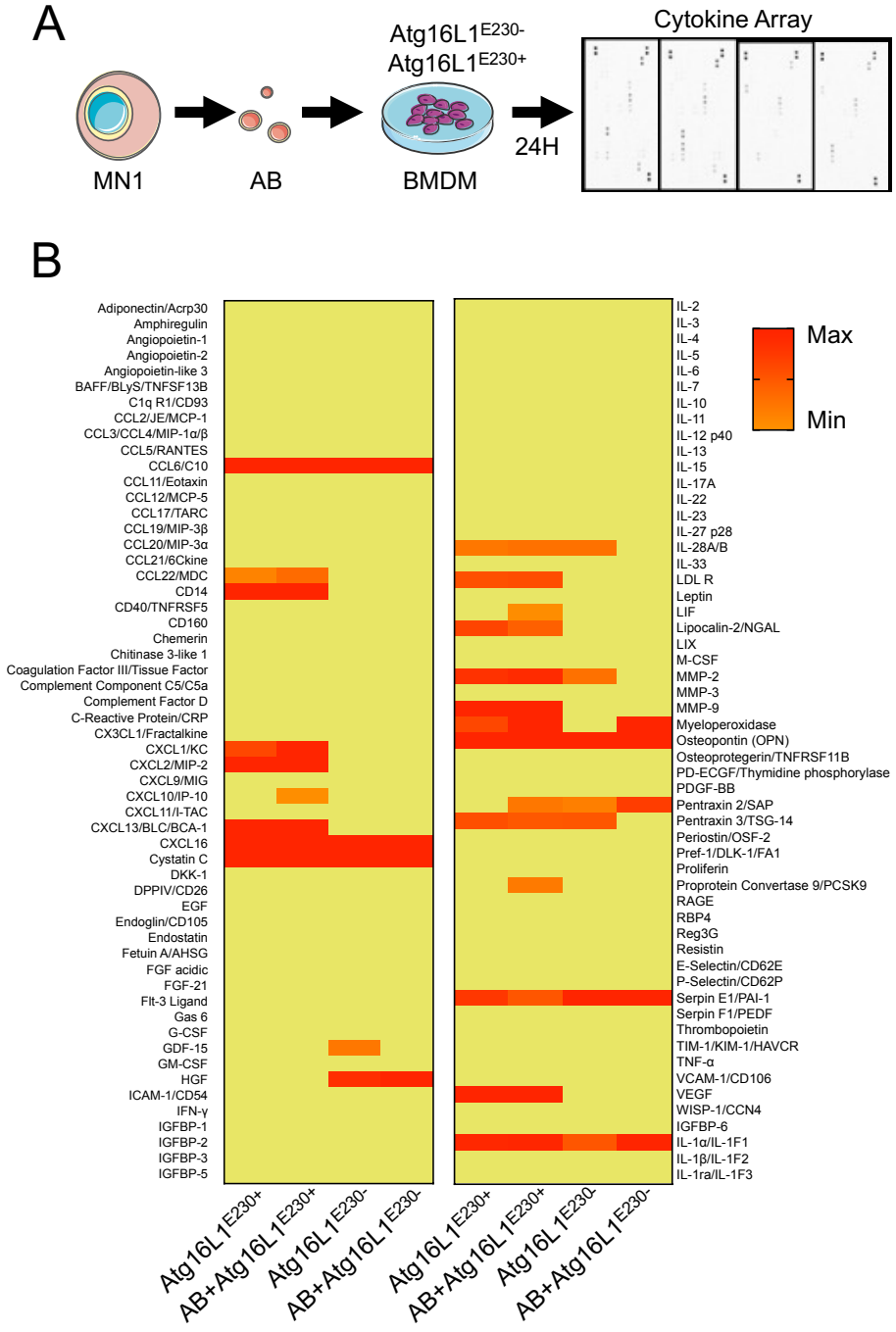

Figure 4.11. Analysis of cytokines from macrophages derived from Atg16L1^{E230-} and Atg16L1^{E230+} mice cultured with MN1 apoptotic bodies

(A) MN1 ABs were isolated from apoptotic MN1 cells and cultured with BMDM from Atg16L1^{E230-} and Atg16L1^{E230+} animals for 24 hours. BMDM from Atg16L1^{E230-} and Atg16L1^{E230+} animals cultured without MN1 ABs was used as a control. The supernatant was isolated from the BMDM and centrifuged at 10000xg for 10mins to remove any debris before performing cytokine arrays. Cytokine membranes were analysed using the G:BOX Chemi XRQ (Syngene)

and quantified using ImageJ software. (B) Complete cytokines analytes from each cytokine array from Atg16L1^{E230-} and Atg16L1^{E230+} BMDM treated with and without ABs from MN1 cells, displayed on a heatmap. n=12 wells per treatment group.

To further evaluate the cytokines from BMDM, specific cytokines that were expressed by the macrophages were grouped together. Cytokines related to inflammation showed varying expression between Atg16L1^{E230-} and Atg16L1^{E230+} BMDM, with some cytokine, such as myeloperoxidase (MPO) and pentraxin 2 (SAP), showing upregulation when ABs were added to the BMDM when compared to untreated BMDM (Figure 4.12A). Furthermore, cytokines relatED to regulatory pathways showed varying expression between LAP competent and LAP deficient BMDM, with only marginal increases in cytokine expression for hepatocyte growth factor (HGF) seen in Atg16L1^{E230-} BMDM cultured with MN1 ABs (Figure 4.12B). However, upon analysis on cytokines relating to the STING pathway, such as CXCL1/2 and MMP-9, no detectable levels were seen in LAP deficient macrophages, even when cultured with MN1 ABs [467, 468]. Moreover, the cytokines relating to STING activation was detectable in LAP competent BMDM, with increased expression of these cytokines when cultured with ABs isolated from MN1 cells (Figure 4.12C). This data suggests that LAP deficient macrophages do not express STING related cytokine, whilst LAP competent macrophages are able to, in which, the addition of AML ABs increases the expression of STING related cytokines.

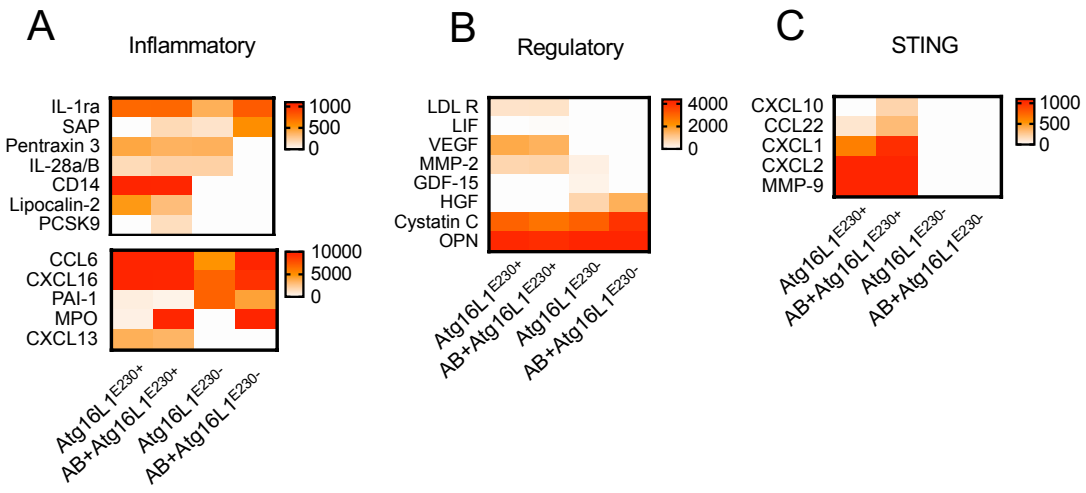

Figure 4.12. Analysis of grouped cytokines from macrophages derived from Atg16L1^{E230-} and Atg16L1^{E230+} mice cultured with MN1 apoptotic bodies

(A) Inflammatory related cytokines displayed on a heatmap from bone marrow derived macrophages (BMDM) with and without 24-hour culture with MN1 apoptotic bodies (ABs). Top and bottom panels represent different expression levels, as shown by the scale bars. (B) Regulatory related cytokines displayed on a heatmap from BMDM with and without 24-hour culture with MN1 ABs. (C) STING related cytokines displayed on a heatmap from BMDM with and without 24-hour culture with MN1 ABs. n=12 wells per treatment group.

The increased expression of STING related cytokines in LAP competent macrophages, along with the lack of cytokine expression relating to STING seen in LAP deficient macrophages, suggests that STING may play a role in the macrophage specific AML suppression seen in LAP competent animals. As such, it was next investigated if there were any differences in STING activation between LAP competent and LAP deficient macrophages in a leukaemic environment. To do this, 10^6 MN1 cells were injected into Atg16L1^{E230-} and Atg16L1^{E230+} mice after busulfan pre-treatment. Atg16L1^{E230+} mice injected with PBS and pre-treatment of busulfan was used as a control. After 14 days, the BM was harvested, filtered and the F4/80$^+$ macrophages were isolated via magnetic separation by F4/80 microbeads. The isolated F4/80 macrophages RNA was extracted, and the gene expression was analysed by RT-qPCR for STING related genes, *Gbp2, Irf7* and *Ifit3* (Figure 4.13A) [303, 469]. Macrophages from MN1 engrafted Atg16L1^{E230+} animals showed increased activation of STING indicated by increased expression of G*bp2, Irf7* and *Ifit3* compared to macrophages from MN1 engrafted Atg16L1^{E230-} animals and non-engrafted Atg16L1^{E230+} animals (Figure 4.13B).

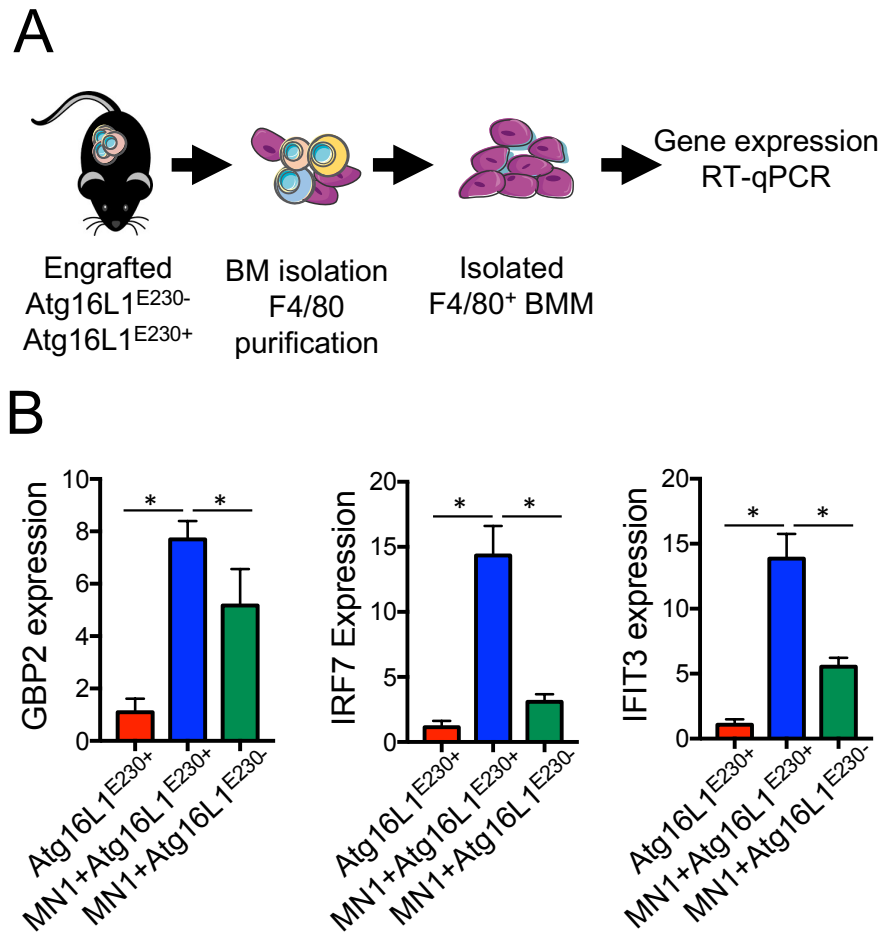

Figure 4.13. LAP in bone marrow macrophages leads to STING activation in AML engrafted mice

(A) MN1 cells ($1x10^6$) or vehicle (PBS) were injected into busulfan treated Atg16L1^{E230+} and Atg16L1^{E230-} mice (25mg/kg for 2 days). Bone marrow macrophage F4/80$^+$ cells were isolated from harvested bone marrow via magnetic separation using F4/80 microbeads and the RNA extracted to be analysed via RT-qPCR. (B) The relative gene expression between untreated, engrafted Atg16L1^{E230+} and Atg16L1^{E230-} from isolated F4/80$^+$ macrophages. n=4 mice in each group. Data shown are means ± SD. *p<0.05, Kruskal Wallis with Dunn's post hoc.

Next, I investigated what role STING has on the progression of AML. First, to confirm that the increased cytokine and gene expression resulted from the activation of STING, C57/BL6 mice were injected with 10^6 MN1-GFP cells after pre-treatment of busulfan. On day 7, 9, 11 and 13 post MN1-GFP injection, animals were treated with the STING inhibitor H-151 or vehicle. The animals were sacrificed at day 14, the BM was isolated and the F4/80$^+$ macrophages were sorted via FACS purification. The RNA from the F4/80$^+$ macrophages was extracted and analysed via RT-qPCR (Figure 4.14A). STING inhibition via H-151 led to decreased G*bp2, Irf7* and *Ifit3* gene expression (Figure 4.14B). Furthermore, H-151 treatment led to an increased in proinflammatory genes *Il1-ß* and *Il6* (Figure 4.14C). Moreover, analysis of the bone marrow from animals showed that mice treated with the STING inhibitor had increased MN1-GFP burden (Figure 4.14D).

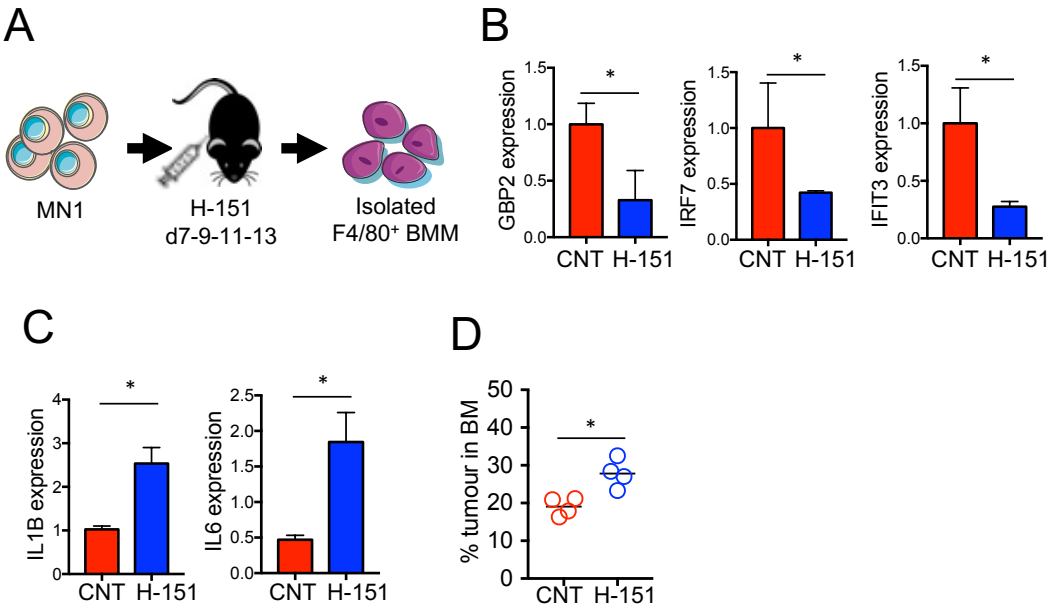

Figure 4.14. STING inhibition leads to altered gene expression and increase AML progression

(A) MN1 cells ($1x10^6$) were injected into busulfan treated $Atg16L1^{E230+}$ and $Atg16L1^{E230-}$ mice (25mg/kg for 2 days). At days 7, 9, 11 and 13 mice were injected with 200µl 750nmol H-151 or 200µl vehicle (PBS with 0.1% TWEEN80). At day 14 the bone marrow was harvested and the $F4/80^+$ macrophages were isolated via FACS. The RNA was extracted to be analysed via RT-qPCR. (B) The relative G*bp2, Irf7* and *Ifit3* gene expression between vehicle treated engrafted C57/BL6 (CNT) and the H-151 treated engrafted C57/BL6 (H-151) isolated $F4/80^+$ macrophages. (C) The relative *Il1-ß* and *Il6* gene expression. (D) Identification of the percentage of MN1-GFP positive cells within the bone marrow of CNT and H-151 treated animals. n=4 mice in each group. Data shown are means ± SD. *p<0.05, Mann–Whitney U.

To confirm the role of LAP in the activation of STING, MN1-GFP engrafted Atg16L1^{E230-} and Atg16L1^{E230+} animals were injected with the STING inhibitor H-151 or vehicle at day 7, 9, 11 and 13 post MN1-GFP injection. The bone marrow was harvested and analysed via flow cytometry for MN1-GFP engraftment (Figure 4.15A). The bone marrow was also analysed for the percentage of live MN1-GFP by identifying the percentage of annexin V negative MN1-GFP population (Figure 4.15B). Data showed that the STING inhibitor enhanced the AML tumour burden in the Atg16L1^{E230+} mice but did not alter the engraftment of Atg16L1^{E230-} mice (Figure 4.15C). Furthermore, the percentage of live MN1-GFP cells was comparable between the two models (Figure 4.15D). Together, this data shows that macrophage LAP in a leukaemic environment is responsible for STING activation which governs AML suppression. Moreover, inhibiting STING in mice leads to increased AML in a LAP dependent manner.

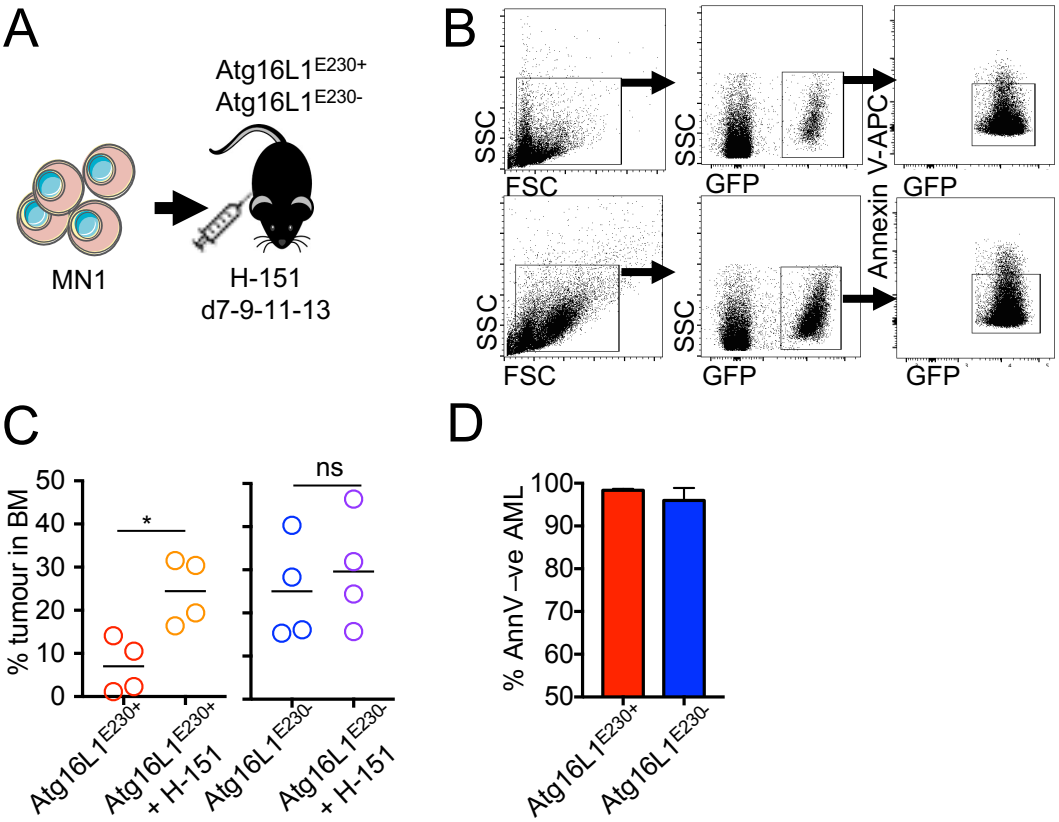

Figure 4.15. LAP is required for AML suppression via STING activation

(A) MN1-GFP cells ($1x10^6$) were injected into busulfan treated Atg16L1^{E230+} and Atg16L1^{E230-} mice (25mg/kg for 2 days). At days 7, 9, 11 and 13 mice were injected with 200µl 750nmol H-151 or 200µl vehicle (PBS with 0.1% TWEEN80). At day 14 the bone marrow was harvested and analysed via flow cytometry for AML engraftment and PtdSer exposure via annexin V. (B) Representative gating strategy for the identification of MN1-GFP engraftment and annexin V negative MN1-GFP cells (Top= Atg16L1^{E230+}, bottom= Atg16L1^{E230+} + H-151). (C) Identification of the percentage of MN1-GFP positive cells within the bone marrow of Atg16L1^{E230+} and Atg16L1^{E230-} mice treated with H-151 or vehicle. (D) The percentage of GFP$^+$ MN1 cells that were negative for annexin V staining via flow cytometry in Atg16L1^{E230+} and Atg16L1^{E230-} mice treated with H-151. n=4 mice in each group. Data shown are means ± SD. *p<0.05, Mann–Whitney U. See pg. 88 for flow panel information.

4.5 STING activation in bone marrow macrophages leads to increased phagocytic capacities but not cytotoxic T-cell activation in AML

As STING activation in BM macrophages via LAP leads to the suppression of AML growth, I investigated by what mechanism this occurs. The STING pathway usually leads to the production of type I IFN and the recruitment of cytotoxic T-cells. To investigate whether this occurred in BM of an AML microenvironment and whether the activation of STING influenced T-cell recruitment and activation, I injected C57/BL6 mice with 10^6 MN1-GFP cells after busulfan treatment. Mice were then treated with H-151 STING inhibitor or vehicle on day 7, 9, 11 and 13 post MN1-GFP injection. At day 14 the BM was harvested and analysed via flow cytometry for $CD4^+$ and $CD8^+$ cells, as well as $CD8^+$ T-cell activation (IFN-γ positive). The mice were compared to control, non-engrafted mice (Figure 4.16A). MN1 engraftment saw an increase in $CD4^+$ T-cells, which when STING was inhibited, reversed the phenotype. However, there was no increases in $CD8^+$ T-cells or the amount of activated $CD8^+$ T-cells (Figure 4.16B).

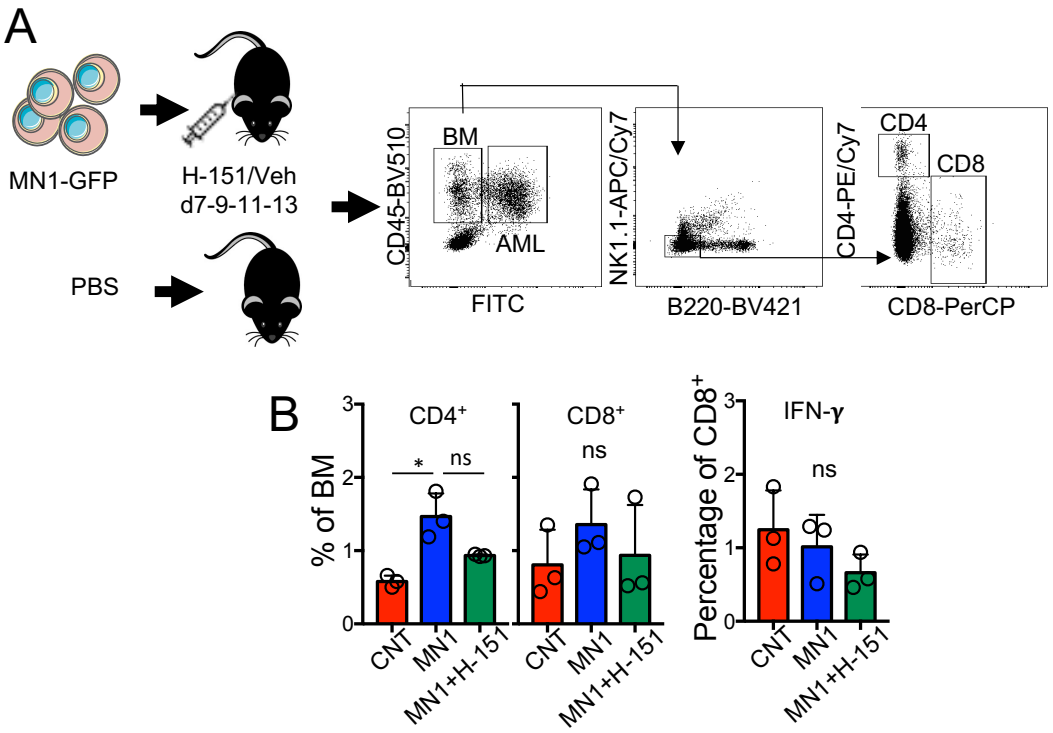

Figure 4.16. STING activation does not lead to cytotoxic T-cell activation in AML

(A) MN1-GFP cells ($1x10^6$) were injected into busulfan treated C57/BL6 mice (25mg/kg for 2 days). At days 7, 9, 11 and 13 mice were injected with 200µl 750nmol H-151 or 200µl vehicle (PBS with 0.1% TWEEN80). Control mice without MN1-GFP injection were used as a comparison. At day 14 the bone marrow was harvested and analysed via flow cytometry for $CD4^+$ cell numbers (GFP^-, $CD45^+$, $B220^-$, $NK1.1^-$, $CD4^+$), $CD8^+$ cell numbers (GFP^-, $CD45^+$, $B220^-$, $NK1.1^-$, $CD8^+$) and $CD8^+$ cell activation (GFP^-, $CD45^+$, $B220^-$, $NK1.1^-$, $CD8^+$, IFN-γ^+). (B) The percentage of $CD4^+$ and $CD8^+$ cells in the BM as well as the percentage of IFN-γ expressing $CD8^+$ cells. n=3 mice in each group. Data shown are means ± SD. *p<0.05, Kruskal Wallis with Dunn's post hoc. See pg. 88 for flow panel information.

Since I have previously shown that AML primed macrophages have increased phagocytic potential compared to naïve macrophages, I next investigated the phagocytic capacities of macrophages following STING inhibition by H-151. To study this, F4/80^{+} macrophages were isolated from the BM of a C57/BL6 mouse by FACS sorting. The macrophages were placed into culture with the STING inhibitor H-151 or vehicle for 2 hours, after which the macrophages were treated with pHrodo bioparticles for 2 hours to study their phagocytic abilities (Figure 4.17A). The macrophages were imaged via confocal microscopy (Figure 4.17B). Treatment of H-151 significantly reduce the phagocytic potential in macrophages compared to control treated macrophages (Figure 4.17C). This data shows that, unlike solid tumours, the effect of STING activation in BM macrophages within leukaemic environment leads to upregulation of phagocytic capacities in BM macrophages and not the activation of cytotoxic T-cells.

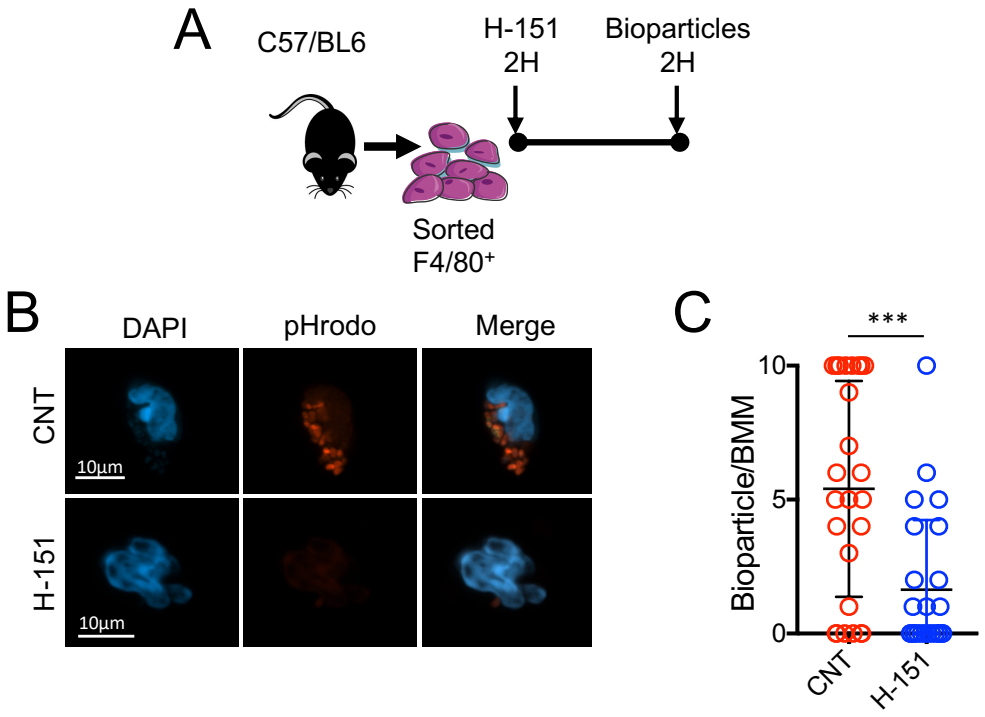

Figure 4.17. STING inhibition reduces bone marrow macrophage phagocytosis

(A) F4/80$^+$ macrophages were sorted via FACS from the bone marrow of a C57/BL6 mouse. The F4/80$^+$ cells were cultured in the presence of 10µM of H-151 or CNT vehicle (DMSO) for 2 hours. Cells were then incubated with pHrodo Red BioParticles at a particle concentration of 100µl/ml for 2 hours before being fixed and permeabilised. DAPI was used for nuclei stain. (B) Representative confocal microscopy images of F4/80$^+$ macrophages from control and H-151 treated macrophages. Image collected at 63X magnification. (C) The number of BioParticles counted per control and H-151 treated bone marrow macrophage (BMM) via microscope. n=25 BMM. Data shown are means ± SD. ***p<0.005, Mann–Whitney U.

4.6 Mitochondrial containing AML derived apoptotic bodies are processed by bone marrow macrophages

So far, the data presented here has shown that AML derived ABs can induce a STING related response in BM macrophages via LAP. I have also shown that STING activation is important in the suppression of AML through a LAP dependent mechanism. This data suggests that the uptake of apoptotic AML cells by LAP in macrophages causes the STING response. As such, to understand what may be triggering a STING response, I examined the contents of AML ABs. First, to see if STING activation via ABs is due to leukaemic cell that produces the ABs, I compared the activation potential of STING in a non-malignant cell type. To do this, the bone marrow from C57/BL6 mice was harvested and the lineage negative cells isolated via MACS magnetic separation using lineage depletion microbeads. The lineage negative cells were then enriched with CD117 microbeads and magnetic separation and further sorted via Sca-1 to produce LSK cells. The LSK and MN1 cells were cultured in the same conditions before apoptosis was induced and the ABs isolated as previously described. The isolated ABs were then cultured on BMDM for 24 hours, after which the RNA was extracted from the BMDM and analysed via qPCR for STING related gene expression (Figure 4.18A). ABs derived from MN1 cells had increased expression in STING related genes, however, ABs derived from LSK cells did not have increased expression in the same gene expression (Figure 4.19B). This suggests there is something contained within the AML ABs and not LSK ABs that caused this response.

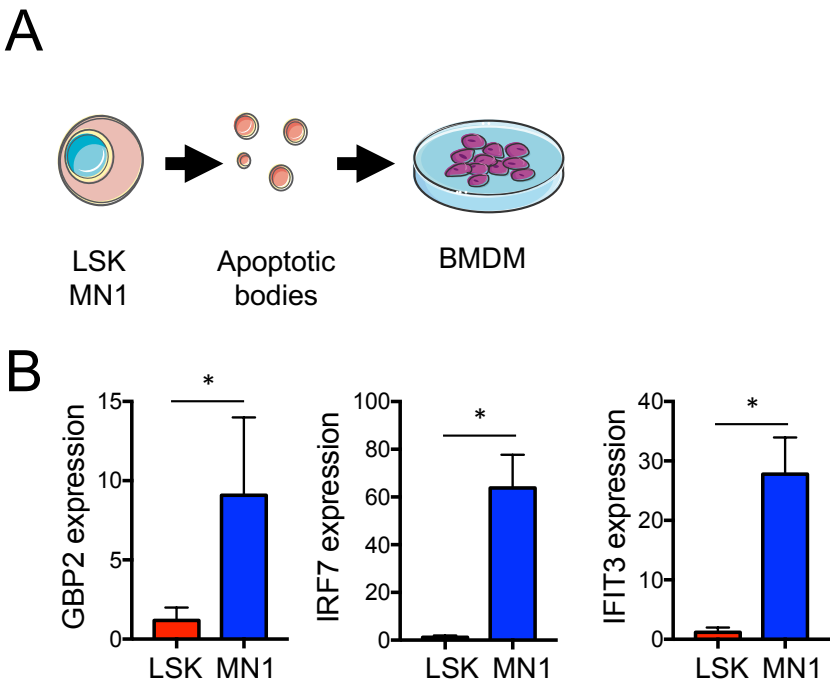

Figure 4.18. AML, but not non-malignant, derived apoptotic bodies induces STING related gene expression in macrophages

(A) Apoptotic bodies isolated from MN1 and LSK cells were cultured with bone marrow derived macrophages (BMDM) from C57/BL6 animals for 24 hours. The RNA was extracted and analysed for *Gbp2, Irf7* and *Ifit3* via qPCR. (B) The relative gene expression of BMDM cultured with LSK and MN1 apoptotic bodies. n=5. Data shown are means ± SD. *p<0.05, Mann–Whitney U.

Understanding the differences in ABs from AML and non-malignant cells may help determine what is responsible for the difference in STING related activation. Previous work looking at differences in AML cellular content compared to non-malignant cells has identified that AML cells have increased mitochondrial content [406, 411]. As STING activation has been shown to be triggered by components of the mitochondria, such as mtDNA, I next investigated whether AML ABs had detectable mitochondrial content, and whether their non-malignant counterparts differed regarding mitochondrial content. To do this, human cord $CD34^+$ non-malignant cells were isolated via CD34 microbead magnetic separation. The $CD34^+$ cells and human AML cells were investigated for their mitochondrial content via TaqMan qPCR quantification (Figure 4.19A). AML cells had higher copy numbers of mitochondria compared to $CD34^+$ cells (Figure 4.19B).

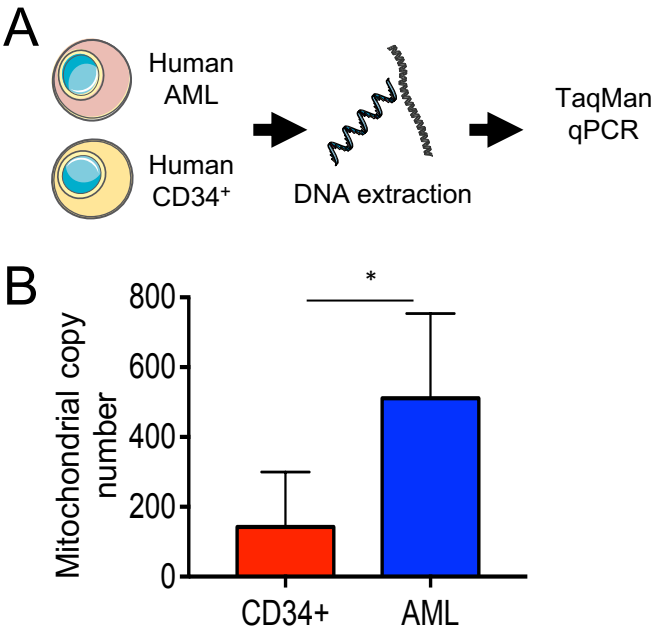

Figure 4.19. AML cells have increased mitochondria

(A) CD34$^+$ non-malignant cells were isolated from human cord blood. Human AML cells were isolated from the bone marrow of AML patients. The DNA was extracted, and the mitochondrial DNA was analysed via qPCR and normalised to genomic DNA for mitochondria copy number. (B) The mitochondrial copy number of CD34$^+$ and AML cells. n=5 AML, n=4 CD34$^+$. Data shown are means ± SD. *p<0.05, Mann–Whitney U.

To investigate whether apoptotic AML cells released mitochondria into ABs, I looked at human AML cells via confocal microscopy. Human AML cells were transduced with a GFP membrane lentivirus to allow identification of the cell membrane. The cells were then stained with MitoTracker Red and Hoechst 33342 to allow visualisation of the mitochondrial and nucleus, respectively. Apoptotic cells were visualised via confocal microscopy at 63X objective for the appearance of ABs blebbing and the co-localisation of mitochondria. Observation on AML cells undergoing extensive membrane blebbing presented blebs containing mitochondria, showing AML cells do produce mitochondrial containing ABs (Figure 4.20). To study if there was a difference in mitochondrial content in AML ABs compared to non-malignant ABs, I isolated ABs from MN1 cells and LSK cells stained with MitoTracker Green and a membrane dye, Vybrant-DiI. I then used image flow cytometry to analyse the mitochondrial content in intact ABs (MitoTracker Green and Vybrant-DiI positive, Figure 4.21A and 4.21B). Images and data collected via image flow cytometry identified that intact ABs from MN1 cells had significantly more mitochondrial content than LSK cells (Figure 4.21C and 4.21D).

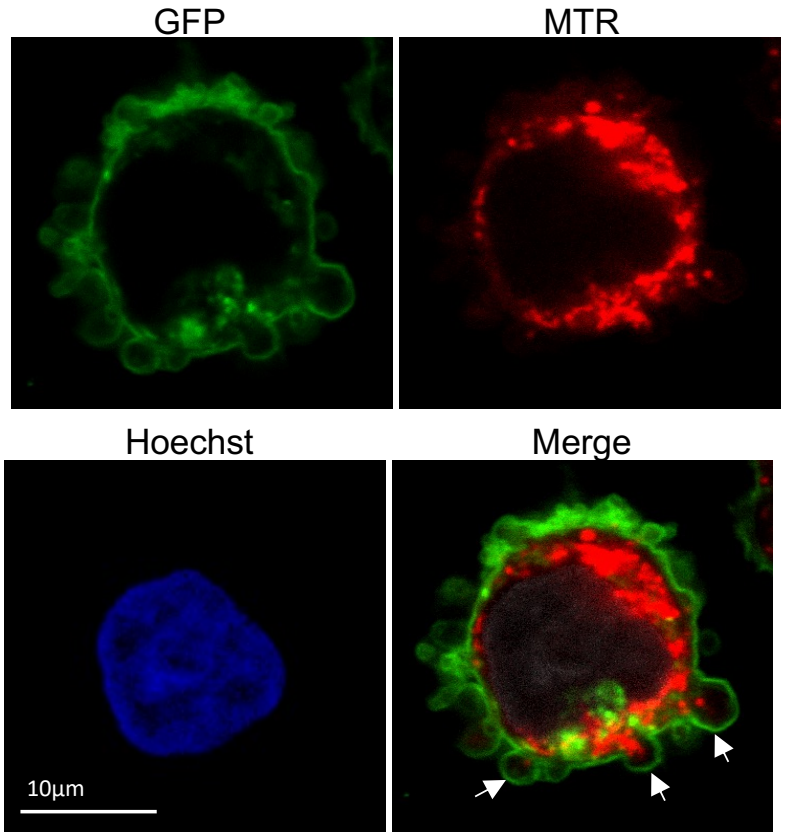

Figure 4.20. AML apoptotic blebs contain mitochondria

Representative image of a human AML cell with extensive membrane blebbing containing mitochondria. Human AML cells were transduced with a GFP-membrane lentivirus to label the membrane with GFP. Cells were incubated with MitoTracker Red (MTR) and Hoechst before imaging for apoptotic cells. Image were collected using confocal microscopy with a 63X water objective. Arrows indicate membrane blebs containing mitochondria.

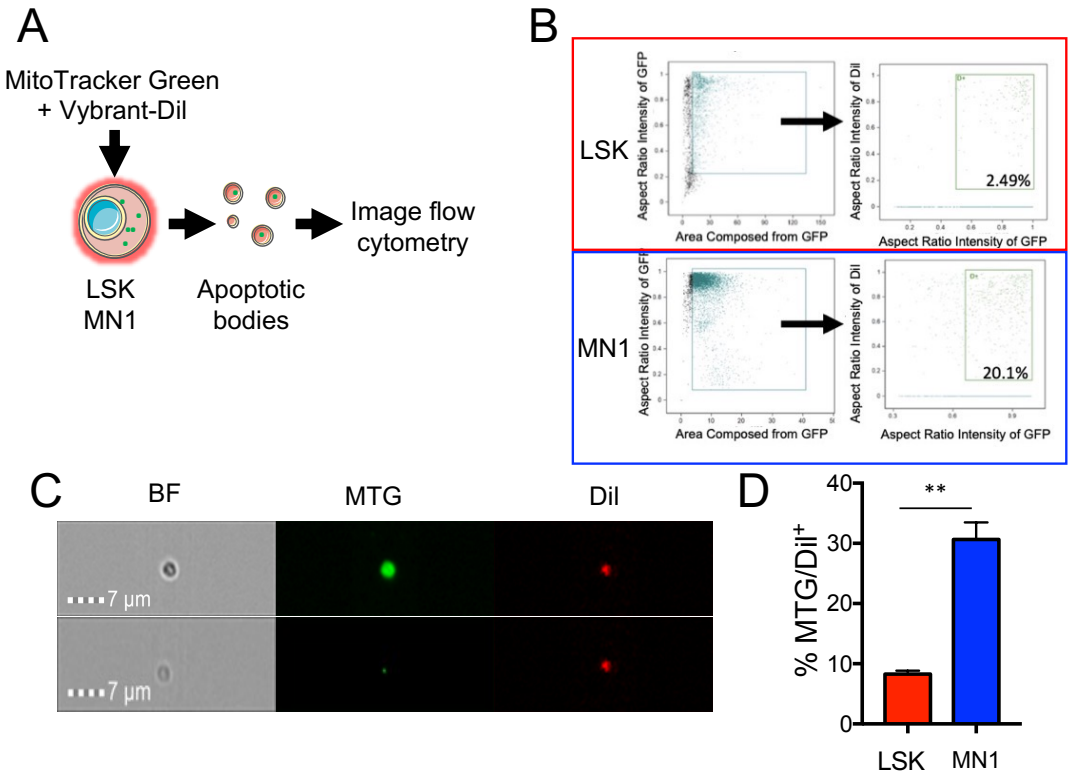

Figure 4.21. MN1 apoptotic bodies have an increased mitochondrial content

(A) LSK and MN1 cells were stained with MitoTracker Green (MTG) and Vybrant-DiI (DiI) before apoptotic induction and isolation of apoptotic bodies (ABs). The ABs were analysed via image flow cytometry. (B) An example of the gating strategy to identify MTG and DiI positive ABs. (C) Representative images of non-malignant LSK (bottom) and MN1 (top) ABs that were stained with MTG and DiI. (D) The percentage of ABs that were positive for MTG and DiI between LSK and MN1 cells. n=5. Data shown are means ± SD. **p<0.01, Mann–Whitney U. See pg. 88 for flow panel information.

To expand on this data, I looked at the mitochondrial content in ABs from MN1 cells, human AML cells and non-malignant $CD34^+$ cells. To do this, I stained each cell type with MitoTracker Red before isolating the ABs. The ABs were then analysed by flow cytometry for the percentage of ABs containing MitoTracker Red (Figure 4.22A and 4.22B). Data showed that both MN1 and hAML derived ABs had increase MitoTracker Red percentage compared to that of $CD34^+$ isolated ABs (Figure 4.22C). Taken together, these data show AML cells produce ABs containing mitochondria. Furthermore, AML ABs contain a greater number of mitochondrial components compared to non-malignant derived ABs.

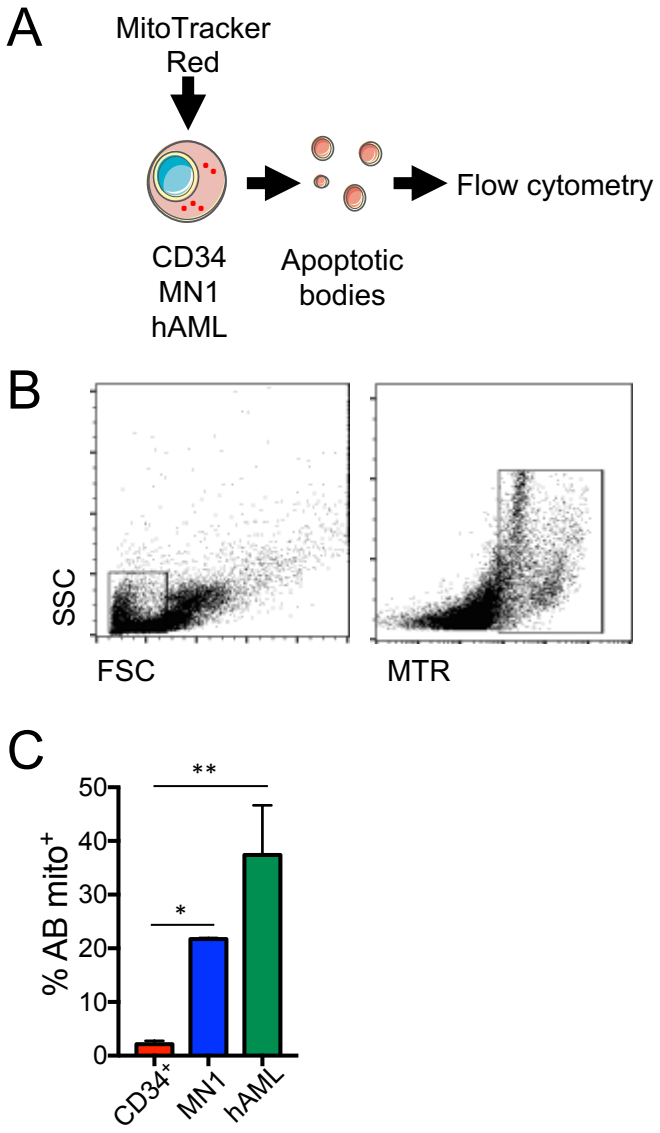

Figure 4.22. Human AML and MN1 apoptotic bodies have increased mitochondria

(A) Human cord blood $CD34^+$, MN1 and human AML cells were stained with MitoTracker Red (MTR) before apoptotic induction and isolation of apoptotic bodies (ABs). The ABs were analysed via flow cytometry. (B) An example of the gating strategy to identify MTR positive ABs. (C) The percentage of ABs that were positive for MTR between $CD34^+$, MN1 and human AML cells. n=5 AML and MN1, n=4 $CD34^+$. Data shown are means ± SD. *p<0.05, **p<0.01, Kruskal Wallis with Dunn's post hoc.

To determine whether BM macrophages were the cells that were responsible for the uptake and processing of ABs containing mitochondria, human AML cells were transduced with a mCherry mito-9 lentivirus, which labelled the mitochondria with a mCherry tag (mCh-AML). mCh-AML, as well as untagged AML cells and $CD34^+$ cells, were injected into NSG mice for 35 days, after which the BM was harvested, and the BM macrophages analysed by flow cytometry for mCherry uptake (Figure 4.23A, 4.23B and 4.23C). BM macrophages from mCh-AML engrafted animals had increased mCherry uptake. Additionally, upon analysis of BM stromal cells, there was no increase in mCherry fluorescence, suggesting BM macrophages are the cells that processed the mitochondrial from AML cells (Figure 4.23D).

Further to these investigations, assessment of whether the engraftment of mCh-AML cells represented AML engraftment and not HSC engraftment was undertaken. This was undertaken to exclude the possibility that non-malignant populations from the AML BM sample were not responsible for the engraftment seen. To do this, NSG mice engrafted with human AML were sacrificed at day 35 and the BM investigated. The BM of these mice were compared to the BM of humanised NSG mice in which human umbilical cord blood $CD34^+$ stem and progenitor cells were transplanted into the NSG mice (Figure 4.24A). Analysis of the BM by flow cytometry showed AML engrafted animals had increased human $CD34^+$ cells, above what is usually expected in non-malignant humanized engrafted models (Figure 4.24B). Additionally, the BM of AML engrafted mice was analysed via light microscopy and May-Grunwald Giemsa staining. Images demonstrated the presence of multiple AML blasts in the BM, confirming engraftment of human AML cells (Figure 4.24C).

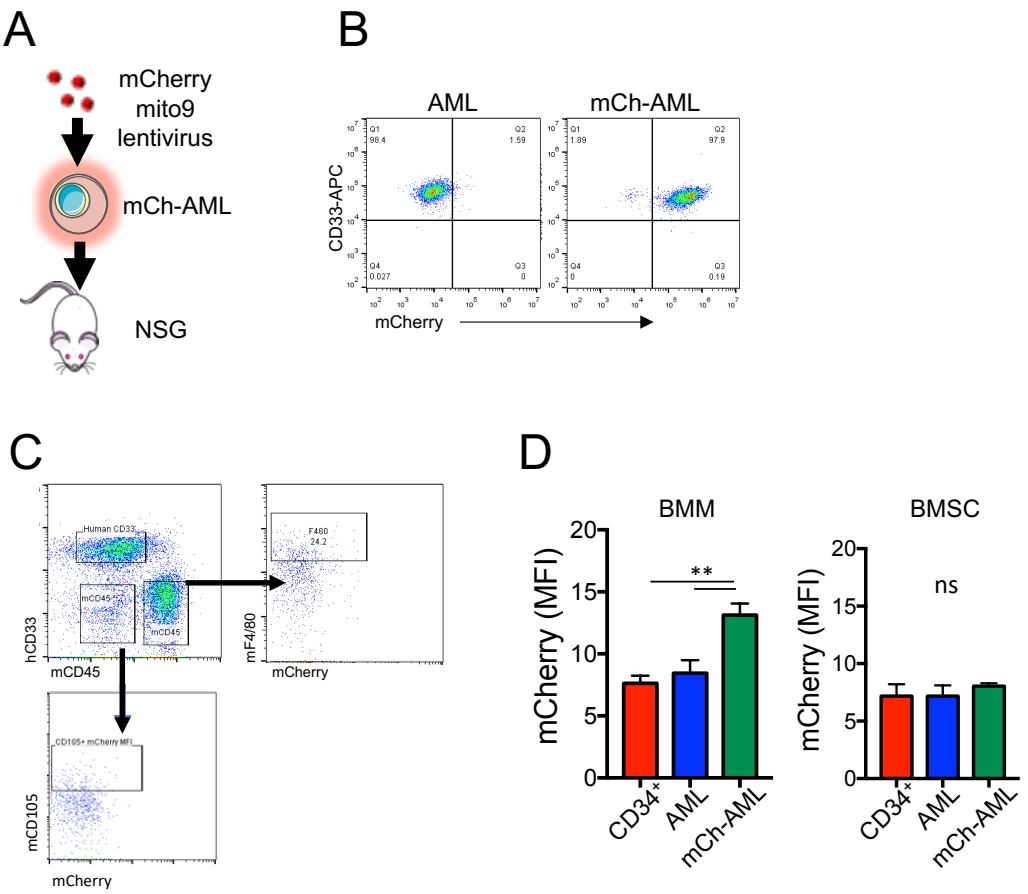

Figure 4.23. BM macrophages uptake mitochondria from AML cells in vivo

(A) Schematic of experimental design. Primary AML cells were transduced with rLV.EF1.mCherry mito9 lentivirus (mCh-AML) and injected into NSG mice for 35 days. The BM was harvested and used for flow cytometry (B) Representative flow plots to identify mCh-AML cells with AML cells without transduction as controls. (C) Gating strategy to identify mouse bone marrow macrophages (BMM, hCD33^{-},mCD45^{+}, mF4/80^{+}) and bone marrow stromal cells (BMSC, hCD33^{-}, mCD45^{-}, CD105^{+}). (D) BMM and BMSC analysis by flow cytometry for mCherry fluorescence. n=4. Data shown are means ± SD. **p<0.01, Kruskal Wallis with Dunn's post hoc. See pg. 88 for flow panel information.

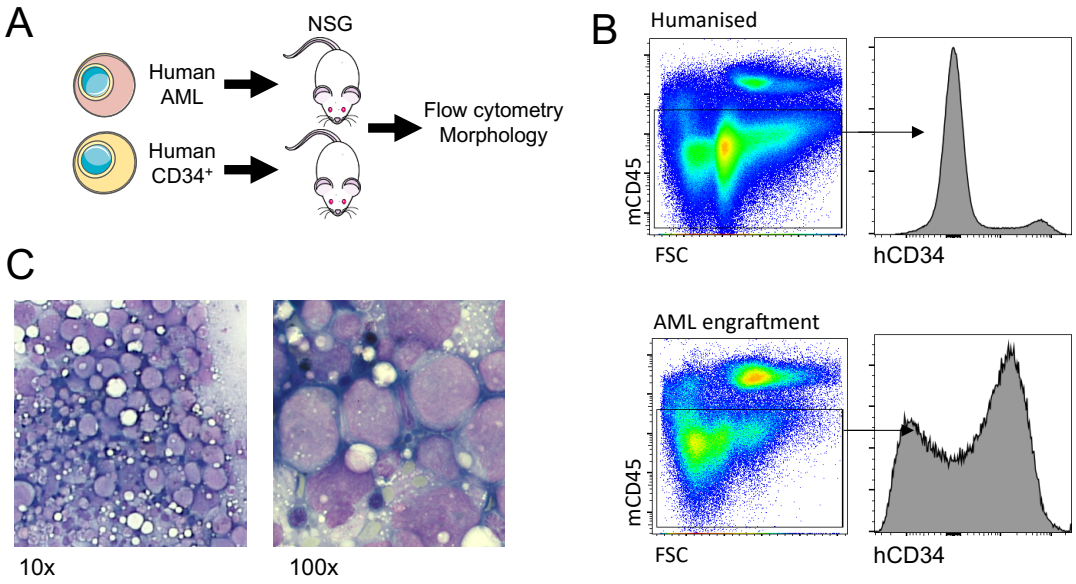

Figure 4.24. Human AML engraftment in mice is different to humanised CD34⁺ mouse models

(A) Schematic of experimental design. Human AML cells and non-malignant CD34 cells were injected into NSG animals. After 35 days, animals were sacrificed, and the BM investigated. (B) Flow cytometry plots of humanised (CD34 injected mice) and AML engraftment (human AML injection) models and the expression of hCD34 cells in the BM. (C) Microscopy and May-Grunwald Giemsa staining images for the identification of AML blasts in the BM of human AML injected animals. n=3. See pg. 88 for flow panel information.

To expand on this research and to confirm this it was the BM macrophages that were phagocytosing the mitochondria, not the stromal cells, BMDM along with BM stromal cells were co-cultured with mCh-AML cells to investigate mCherry uptake via microscopy (Figure 4.25A). BMDM but not BM stromal cells had increased mCherry fluorescence compared to controls (Figure 4.25B and 4.25C). The data presented here shows that BM macrophages are responsible for the uptake of the mitochondrial from AML cells, supporting the data that BM macrophages process AML derived ABs containing mitochondria.

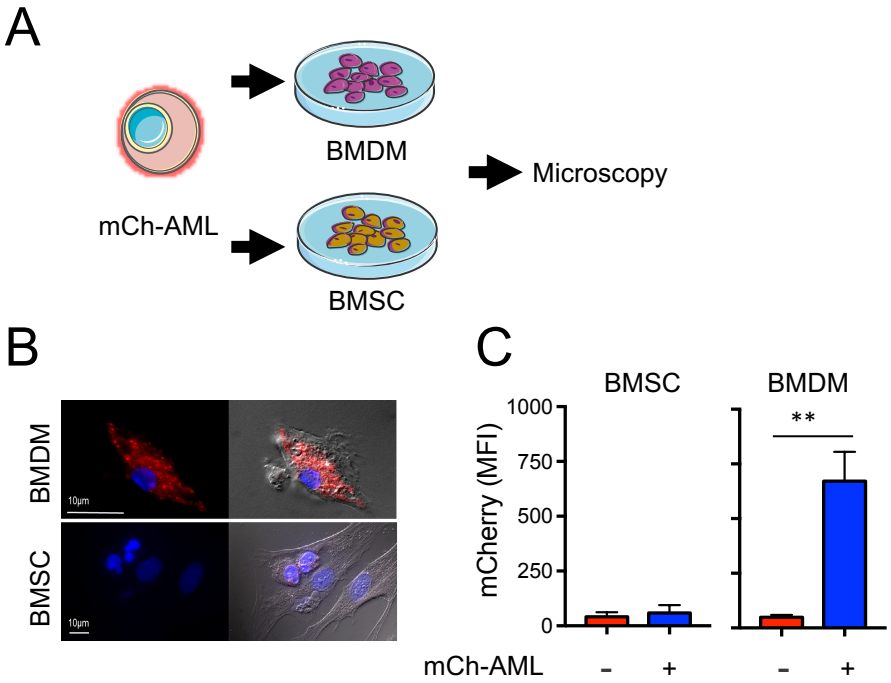

Figure 4.25. BM macrophages uptake mitochondria from AML cells in vitro

(A) Schematic of experimental design. Primary AML cells were transduced with rLV.EF1.mCherry mito9 lentivirus (mCh-AML) and co-cultured with bone marrow derived macrophages (BMDM) or bone marrow stromal cells (BMSC). BMDM and BMSC in mono-culture were used as controls and cells were analysed via fluorescent microscopy for mCherry uptake. (B) Representative images of BMDM and BMSC after co-culture with mCh-AML cells taking with fluorescent microscopy. (C) The mean fluorescent intensity (MFI) of mCherry analysed in BMDM and BMSC cells cultured with and without mCh-AML cells. n=25. Data shown are means ± SD. **p<0.01, Mann–Whitney U.

4.6 AML apoptotic bodies containing mtDNA activates STING in bone marrow macrophages via LC3 associated phagocytosis

So far, I have shown that AML ABs contains mitochondria, and the BM macrophage are the cells responsible for the uptake of AML mitochondria. Furthermore, AML ABs are responsible for STING activation in BM macrophages via LAP, leading to increased phagocytotic potential. To directly identify whether the mitochondria contained within the AML ABs caused STING activation in BM macrophages, mCh-AB were isolated from mCh-AML and cultured with BMDM isolated from Atg16L1^{E230+} and Atg16L1^{E230-} mice. The mCherry fluorescence of BMDM were investigated at 4 and 24 hours by confocal microscopy (Figure 4.26A). While both Atg16L1^{E230+} and Atg16L1^{E230-} mice had increased mCherry fluorescence after 4 hours of culture, only LAP competent BMDM had significantly decreased mCherry fluorescence after 24 hours (Figure 4.26B and 4.26C). This suggests that while both LAP competent and LAP deficient macrophages are able to uptake ABs containing mitochondria, it is only the LAP competent macrophages that are able to efficiently process the ABs for degradation. These observations support my previous findings that shows LAP is required to facilitate the delivery of ABs from the phagosomes to lysosomes for ABs degradation (Figure 4.10).

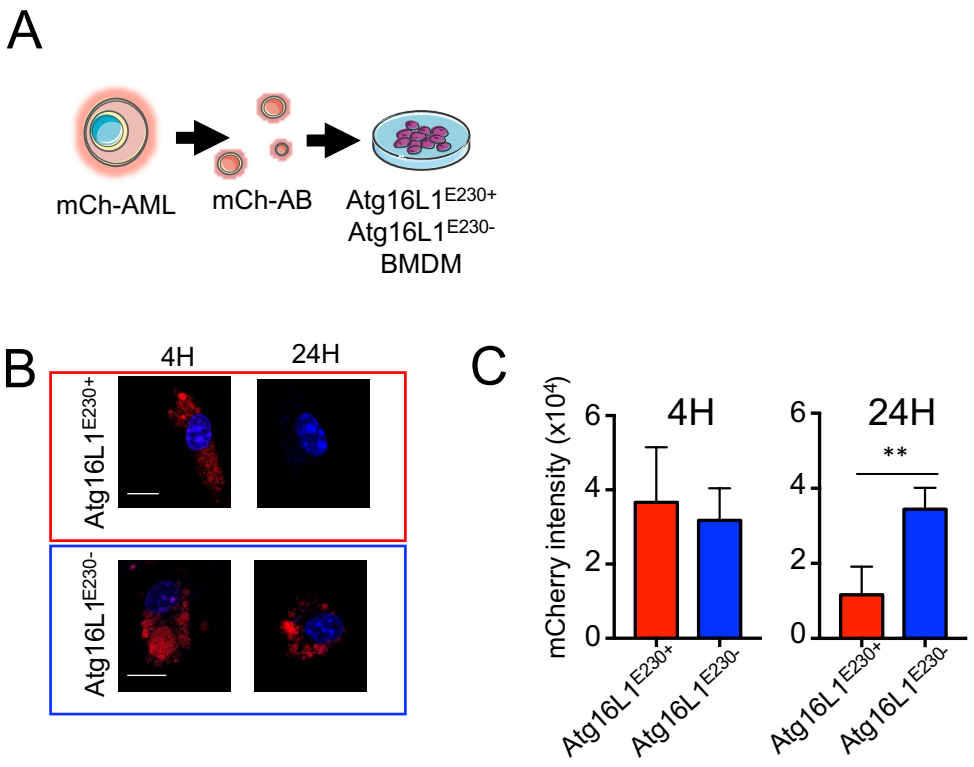

Figure 4.26. LC3 associated phagocytosis in bone marrow macrophages is required for degradation of AML apoptotic bodies containing mitochondria

(A) Schematic of experimental design. Primary AML cells were transduced with rLV.EF1.mCherry mito9 lentivirus (mCh-AML), apoptosis induced, and the apoptotic bodies isolated (mCh-AB). The mCh-AB were cultured with bone marrow derived macrophages (BMDM) isolated from Atg16L1^{E230+} and Atg16L1^{E230-} mice. The BMDMs were observed via confocal microscopy at 4 hours and 24 hours. The fluorescence of mCherry was investigated post capture with ImageJ. (B) Representative images of Atg16L1^{E230+} and Atg16L1^{E230-} BMDM mCherry fluorescence at 4 and 24 hours. (C) The fluorescent intensity of mCherry analysed in BMDM cultured with mCh-AB. n=25. Scale bar 10μm. Data shown are means ± SD. **p<0.01, Mann–Whitney U.

Next, as I have shown that AML ABs containing mitochondria are processed by BM macrophages via LAP, I investigated what it was about the mitochondria that causes activation of the STING pathway. The cGAS-cGAMP sensing of DNA leads to downstream activation of STING [435]. Apoptotic cells, including mitochondria from dying cells, can be phagocytosed and the mitochondria DNA (mtDNA) sensed via this pathway, leading to STING activation [435]. To investigate whether the mtDNA from AML ABs caused STING activation in BM macrophages, I generated AML cells devoid of mtDNA, ρ^0 MN1 cells. Initially, I tried to achieve the depletion of mtDNA in MN1 cells by culturing the cells in media containing ethidium bromide (EtBr). To check whether mtDNA in ρ^0 MN1 cells were depleted, MN1 cells were lysed, and the DNA extracted. The mtDNA of ρ^0 MN1 and untreated MN1 cells was analysed via qPCR and normalised against genomic DNA (Figure 4.27A). The process was time consuming and using EtBr alone did not deplete the mtDNA enough to produce ρ^0 MN1 cells (Figure 2.27B). Next, I used a combination of EtBr and dideoxycytidine (ddC) to generate ρ^0 MN1 cells [470]. I cultured the cells for 20 days to deplete mtDNA and after qPCR analysis the MN1 cells were depleted of mtDNA, successfully generating ρ^0 MN1 cells (Figure 4.27C).

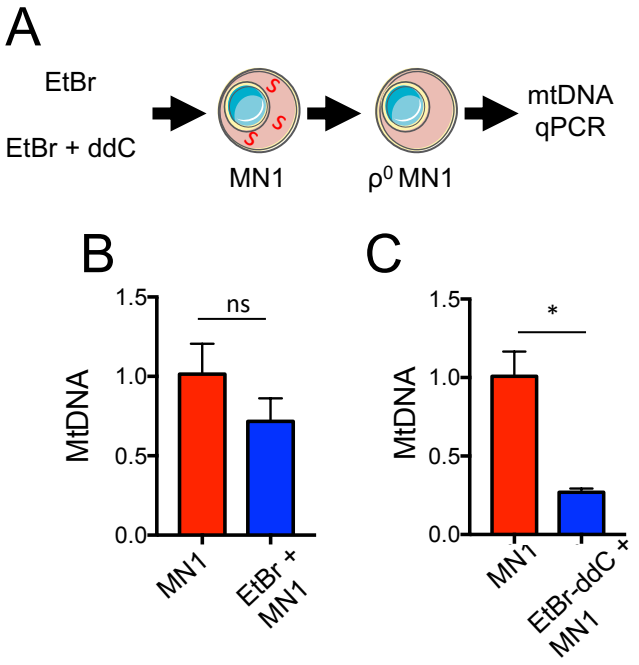

Figure 4.27. Treatment of MN1 cells with a combination of ethidium bromide and dideoxycytidine generate ρ⁰ MN1 cells depleted of mitochondrial DNA

(A) Schematic of experimental design. MN1 cells were treated with either ethidium bromide (EtBr, 1µg/ml, 40 days) alone or a combination of EtBr and dideoxycytidine (ddC; 200µM) for 20 days. DNA was extracted and the mitochondrial DNA (mtDNA) was analysed via qPCR. (B) The relative mitochondrial DNA levels of MN1 cells and MN1 cells treated with EtBr. (C) The relative mitochondrial DNA levels of MN1 cells and MN1 cells treated with EtBr and ddC. Mitochondrial DNA was normalised to genomic DNA levels using Taqman PCR and Tert and ND3 probes. n=5. Data shown are means ± SD. *p<0.05, Mann–Whitney U.

To address whether mtDNA from AML ABs caused STING activation in BM macrophages, I isolated the ABs from ρ^0 MN1 cells. Additionally, mitochondrial containing ABs (mtAB) were isolated from MN1 and LSK cells via FACS. This was achieved by culturing MN1 and LSK cells with MitoTracker Red before apoptosis induction and AB isolation. The lower levels of mitochondria in LSK cells were factored into the sorting of mtAB and as such, a reduced number of LSK mtAB were obtained. Isolated ABs were then culture with BMDM for 24 hours before the RNA was extracted, and the gene expression analysed for genes relating to STING activation (Figure 4.28A). MN1 mtAB increased the expression of STING activation genes, however, LSK ABs did not. Furthermore, ABs isolated from ρ^0 MN1 cells did not cause an increase in STING related genes (Figure 4.28B). To investigate whether the increase in STING gene activation was LAP dependent, mtAB isolated from MN1 and LSK cells were cultured with Atg16L1^{E230+} and Atg16L1^{E230-} BMDM for 24 hours. The extracted RNA was analysed for the same STING related genes (Figure 4.29A). While mtAB from MN1 cells induced STING related gene activation in LAP competent macrophages, no increased gene expression was seen in LAP deficient macrophages treated with mtAB (Figure 4.29B). Taken together, this data shows that mtDNA from AML ABs induces a STING related response in a LAP dependent mechanism.

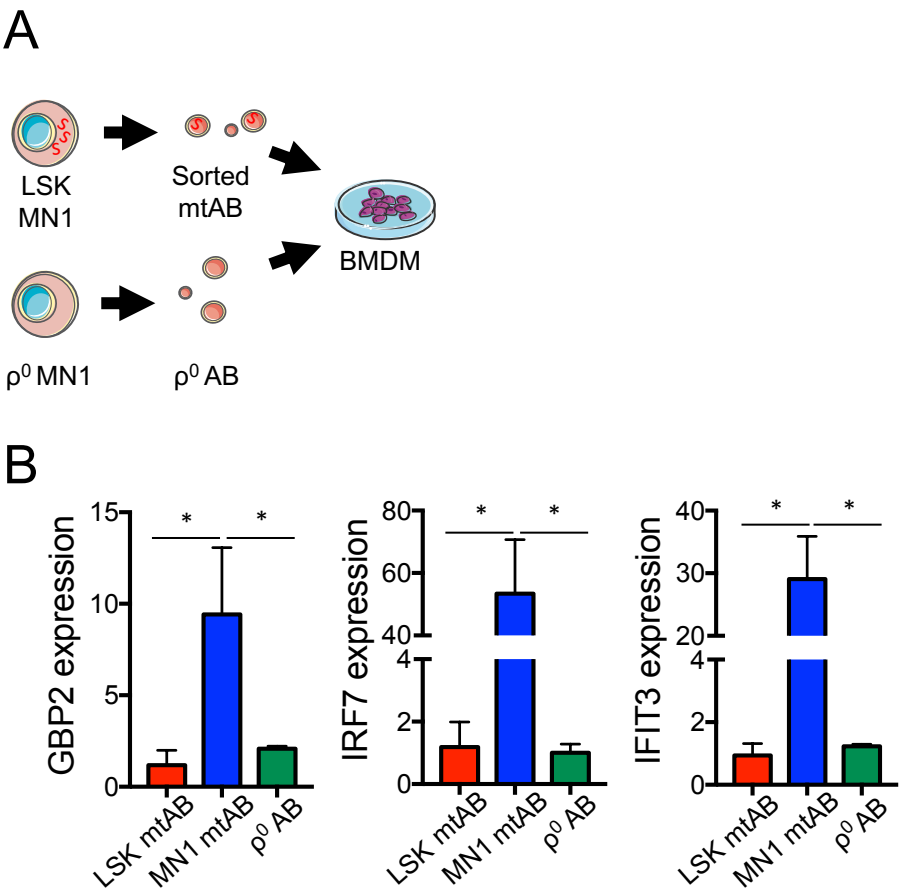

Figure 4.28. AML apoptotic bodies containing mitochondrial DNA causes increased STING related gene expression in bone marrow derived macrophages

(A) Non-malignant LSK cells and MN1 cells were stained for MitoTracker Red and the apoptotic bodies (ABs) isolated before being sorted based on positive MTR signal via FACS. ρ^0 MN1 ABs were also isolated. The ABs were cultured with BMDM from C57/BL6 mice for 24 hours and the RNA extracted to be analysed via qPCR for STING related gene expression. (B) The relative gene expression of *gbp2*, *irf7 and ifit3* of BMDM cultured with sorted mitochondria containing ABs from MN1 and LSK and ρ^0 MN1 cells ABs. n=4. Data shown are means ± SD. *p<0.05, Kruskal Wallis with Dunn's post hoc.

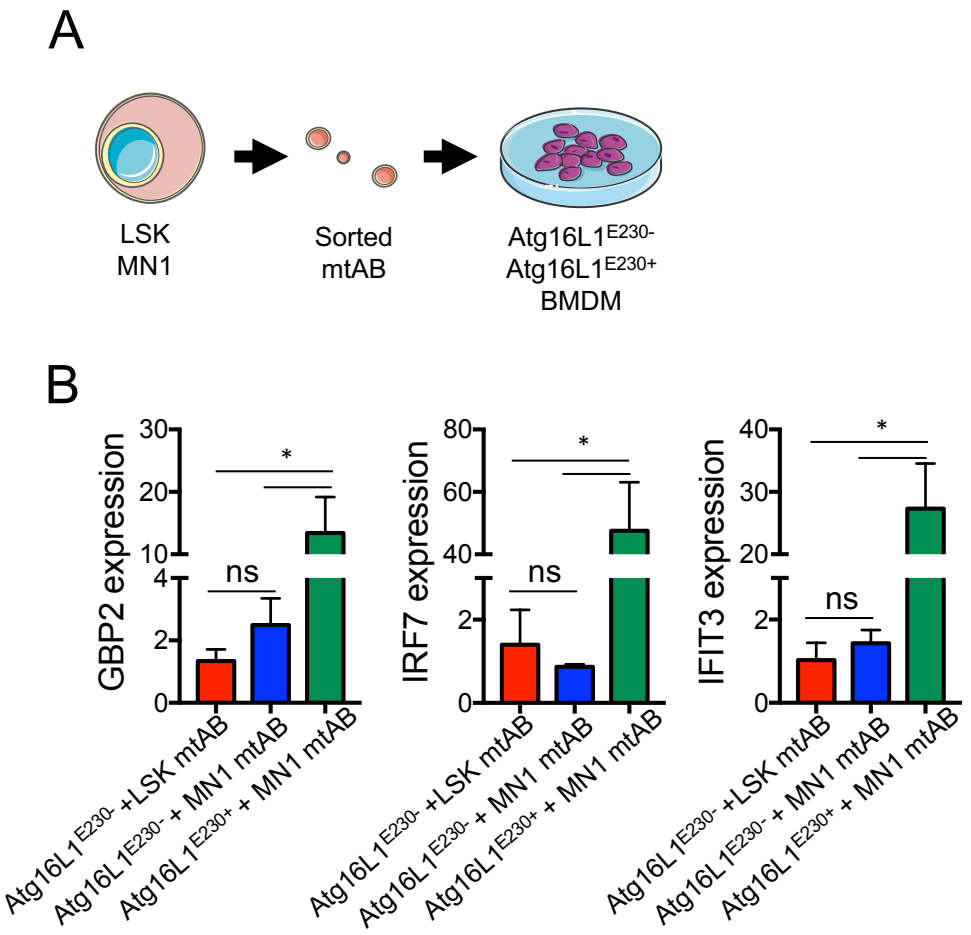

Figure 4.29. Mitochondrial containing AML apoptotic bodies causes increased STING related gene expression in bone marrow derived macrophages in a LAP dependent mechanism

(A) Non-malignant LSK cells and MN1 cells were stained for MitoTracker Red and the apoptotic bodies (ABs) isolated before being sorted based on positive MTR signal via FACS. The ABs were cultured with BMDM from Atg16L1^{E230+} and Atg16L1^{E230-} mice for 24 hours and the RNA extracted to be analysed via qPCR for STING related gene expression. (B) The relative gene expression of *gbp2*, *irf7 and ifit3* of BMDM cultured with sorted mitochondria containing ABs from MN1 and LSK. n=4. Data shown are means ± SD. *p<0.05, Kruskal Wallis with Dunn's post hoc.

4.7 Summary

In this chapter I have explored the role LAP plays in the suppression of AML in the context of phagocytosis of apoptotic AML cellular debris. I have shown that in a leukaemic microenvironment, LAP does not alter the overall polarity of BM macrophages. However, LAP is needed in order to clear AML ABs, in which LAP is responsible for the processing of AML ABs via presenting apoptotic cargo to lysosome for degradation. Furthermore, the processing of AML ABs induces STING related activation in BM macrophages via LAP, which is required for AML suppression. Interestingly, STING activation in an AML environment does not lead to cytotoxic T-cell activation. The inhibition of STING in BM macrophages leads to reduced phagocytic potential highlighting that, unlike solid tumours, STING related suppression of AML may confer increased phagocytic potential in macrophages independent of cytotoxic T-cell activation. The results show that AML ABs contain large amounts of mitochondrial content compared to non-malignant ABs. Furthermore, BM macrophages are responsible for the uptake of AML mitochondria. Depletion of mtDNA in AML cells identified that mtDNA contained in the AML ABs causes increased STING related gene expression and this process is governed by LAP. Together, these results show that apoptotic AML cells produce mitochondrial containing ABs and these mtAB are processed via BM macrophages by LAP. The mtDNA contained within the ABs leads to the activation of STING which is responsible for AML related suppression via increased phagocytic potential of BM macrophages, independent of activation of cytotoxic T-cells.

5. Investigating how bone marrow macrophage TIM4 expression affects AML progression

5.1 Introduction

In my previous two chapters I have revealed that LC3 associated phagocytosis (LAP) in bone marrow (BM) macrophages is important for the control of AML growth, specifically mtDNA in AML ABs is responsible for STING activation in BM macrophages, which is important in AML suppression and phagocytic function of macrophages. For my last chapter, I investigated how cell surface markers on macrophages affect the progression of AML. One such receptor, TIM4, has largely been studied for its ability as an apoptotic detecting receptor found on the surface of most macrophages and dendritic cells [235]. Within the context of immunity in a malignant environment, TIM4 has been shown to be over expressed in macrophages [269, 270]. Furthermore, TIM4 expression has been shown to be upregulated on macrophages in the tumour environment after chemotherapy induced apoptosis, with cancer derived DAMPs playing a role [245]. Conversely, studies have shown TIM4 expression in macrophages can be down regulated in tumour environments [273]. However, evidence in the role of TIM4 in the progression of malignancies is not fully understood, with studies suggesting that it could act as pro- or anti-tumoral, which may depend on the type of cancer or the progression of the tumour. The study of the effects of TIM4 in macrophages within a leukaemic environment has not been investigated. As such, this chapter will attempt to investigate what effect TIM4 expression in BM macrophages has on AML progression.

5.2 TIM4 is required for bone marrow macrophage phagocytosis of apoptotic bodies in vitro

The function of TIM4 is to recognise phosphatidylserine on apoptotic cells and ABs to allow phagocytosis of the dying cell. In my previous chapters I have shown the importance of phagocytosis of AML ABs in BM macrophages in AML progression. As such, I investigated what effects blocking TIM4 had on the phagocytic potential of BM macrophages. To do this, I deployed two methods to study phagocytosis. Firstly, I used human AML cells tagged with an mCherry tag (mCh-AML) to look at the uptake and processing of ABs over time. Apoptosis was induced in mCh-AML as previously described and the mCh-AB were isolated via centrifugation. The mCh-AB were cultured with BMDM from C57/BL6 mice for 24 hours with and without a TIM4 inhibitor (RMT4-54). The mCherry fluorescence was investigated by confocal microscopy at 4 and 24 hours (Figure 5.1A). At 4 hours, BMDM treated with RMT4-54 had reduced mCherry fluorescence compared to untreated BMDM (Figure 5.1B). However, at 24 hours, while the fluorescence of treated BMDM remained the same, mCherry fluorescence was reduce to similar levels of RMT4-54 treated BMDM (Figure 5.1C). This data suggests that blocking TIM4 inhibits uptake of and processing of AML ABs.

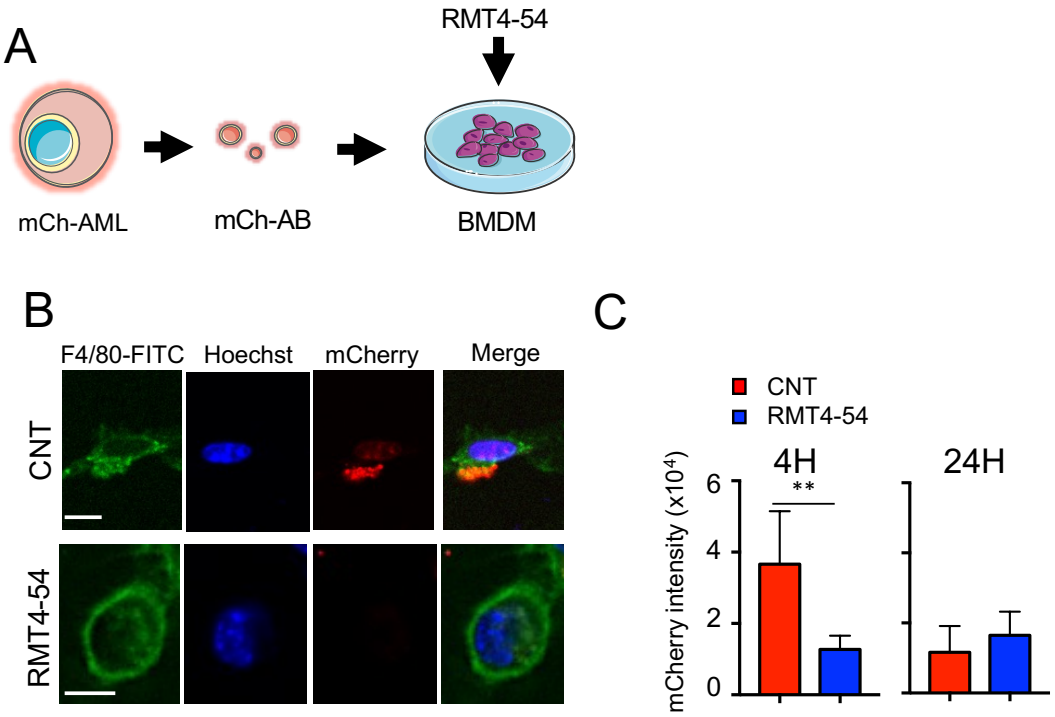

Figure 5.1. TIM4 blockade inhibits uptake and processing of AML apoptotic bodies in vitro

(A) Schematic of experimental design. Primary AML cells were transduced with rLV.EF1.mCherry mito9 lentivirus (mCh-AML), apoptosis induced, and the apoptotic bodies isolated (mCh-AB). The mCh-AB were cultured with bone marrow derived macrophages (BMDM) isolated from C57/BL6 mice pre-treated with and without RMT4-54 (30 µg/ml). Controls were untreated with RMT4-54. The BMDMs were observed via confocal microscopy at 4 hours and 24 hours. The fluorescence of mCherry was investigated post capture with ImageJ. (B) Representative confocal images of BMDM at 4 hours labelled with F4/80-FITC antibody and stained with Hoechst (magnification 63X). (C) mCherry fluorescence intensity as measured using ImageJ at 4 and 24 hours of BMDM pre-treated with and without RMT4-54. n=20. Scale bar: 10µm. Data shown are means ± SD. **p<0.01, Mann–Whitney U.

Next, I investigated whether TIM4 was important in the processing of ABs via lysosomal degradation of cargo. To do this I used pHrodo Red SE to detect pH changes after phagocytosis, allowing visualisation of lysosomal fusion with phagosome. ABs from MN1 cells were isolated and stained with pHrodo Red SE. The pHrodo ABs were incubated with BMDM either pre-treated with RMT4-54 or vehicle for 3 hours. The pHrodo fluorescence intensity was investigated by confocal microscopy (Figure 5.2A). Data showed that BMDM treated with RMT4-54 had significantly less pHrodo fluorescence compared to control BMDM (Figure 5.2B and 5.2C). This data further supports the notion that TIM4 is important in the processing of AML apoptotic cells in BM macrophages.

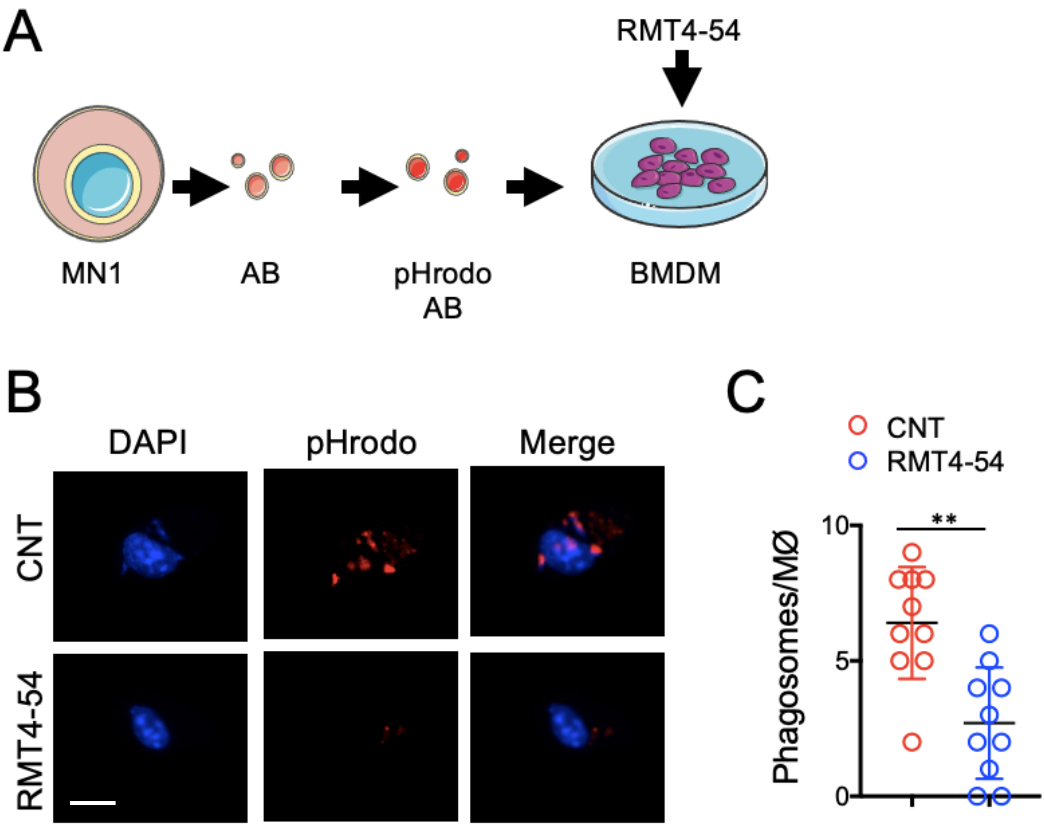

Figure 5.2. TIM4 in bone marrow macrophages is required for the formation of phagolysosome of AML apoptotic bodies

(A) Apoptotic bodies (ABs) were isolated from apoptotic MN1 cells and labelled with pHrodo Red SE. Labelled pHrodo ABs were cultured with RMT4-54 or vehicle (CNT) pre-treated BMDM from C57/BL6 mice for 3 hours before being imaged via confocal microscopy. (B) Representative image of BMDM with pHrodo Red SE labelled ABs and DAPI (magnification 63X). (C) The number of phagosomes, as identified by pHrodo fluorescence, was counted per BMDM. n=10 BMDM. Scale bar=10μm. Data shown are means ± SD. **p<0.01, Mann–Whitney U.

5.3 TIM4 expression in bone marrow macrophages is required for AML suppression

I have shown that TIM4 is an important component in BM macrophages to allow the correct processing of AML ABs. In my previous chapters I have shown that the efficient processing of AML ABs by BM macrophages is required for AML suppression. This suggest that TIM4 in BM macrophages may play a role in the control of AML progression. To investigate TIM4 in a leukaemic environment further, I looked at whether the expression of TIM4 is altered in animals with AML. As such, C57/BL6 mice were pre-treated with busulfan before being injected with 10^6 MN1-GFP cells or vehicle. At day 14, the BM was harvested and examined by flow cytometry (Figure 5.3A). The BM of control and MN1-GFP engrafted animals were analysed for the expression of TIM4 in BM macrophages as defined as $CD45^+$, $MN1\text{-}GFP^-$, $GR1^-$, $F4/80^+$, $CD115^{LOW/INT}$, $TIM4^+$ (Figure 5.3B and 5.3C). Data showed that the expression of TIM4 in BM macrophages was significantly increased in animals with AML compared to control animals (Figure 5.3D). Therefore, TIM4 expression on macrophages in an AML environment maybe important for the regulation of AML.

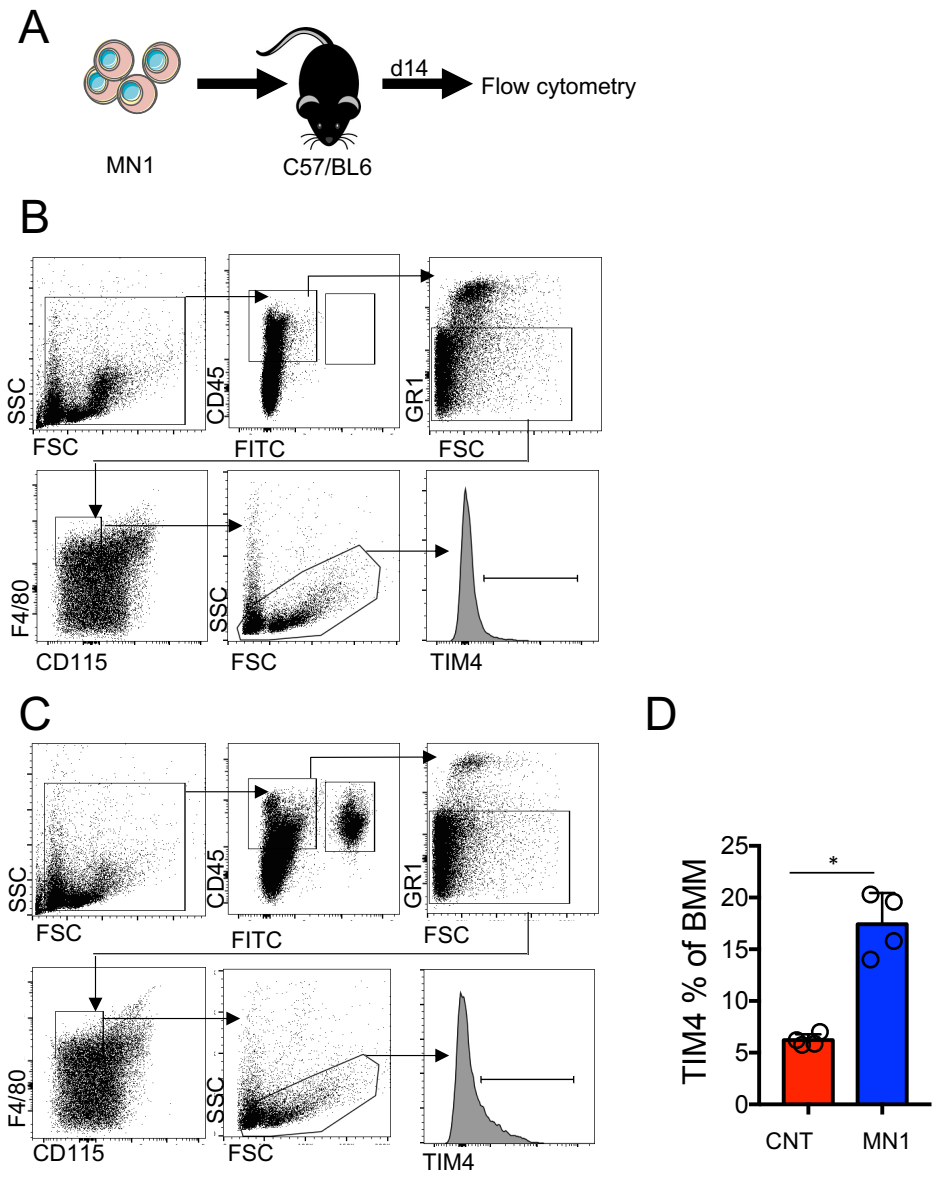

Figure 5.3. TIM4 expression in bone marrow macrophages is increased in AML engrafted mice

(A) Schematic of experimental design. 10^6 MN1-GFP cells or PBS was I.V injected into busulfan treated (25mg/kg for 2 days) C57/BL6 mice. After 14 days the animals were sacrificed, the bone marrow harvested and analysed for TIM4 expression by flow cytometry. (B) Gating strategy and typical flow plots of control animal bone marrow macrophages ($CD45^+$, MN1-GFP^-, $GR1^-$, $F4/80^+$, $CD115^{LOW/INT}$) to identify TIM4 expression. (C) Gating strategy and typical flow plots of MN1-GFP engrafted animal bone marrow macrophages to identify TIM4 expression. (D) TIM4 expression as a percentage of bone marrow macrophages. n=4. Data shown are means ± SD. *p<0.05, Mann–Whitney U. See pg. 88 for flow panel information.

To investigate the importance of TIM4 expression in the control of AML, I inhibited TIM4 in vivo using RMT4-54. C57/BL6 animals pre-treated with busulfan were engrafted with 10^6 MN1-GFP cells. Animals were then treated with 250μg of RMT4-54 or PBS on days 7, 9, 11 and 13. The animals were then sacrificed at day 14 and the BM isolated to be analysed by flow cytometry (Figure 5.4A). The BM was initially analysed for AML engrafted by identification of GFP positive cells (Figure 5.4B and 5.4C). Animals treated with the TIM4 inhibitor RMT4-54 had significantly increased MN1-GFP cells in the BM compared to control animals (Figure 5.4D). As TIM4 is required for the uptake of AML ABs, I analysed the BM of RMT4-54 treated animals for AML ABs. To do this, I looked at the BM of RMT4-54 treated and control animals for cellular debris. From the cellular debris, I investigated GFP positive debris as an indicator of AML ABs/debris (Figure 5.5A). RMT4-54 treated animals had significantly more AML debris compared to control animals (Figure 5.5B). Together, this suggests that TIM4 is required for AML suppression and inhibiting TIM4 leads to accumulation of AML ABs.

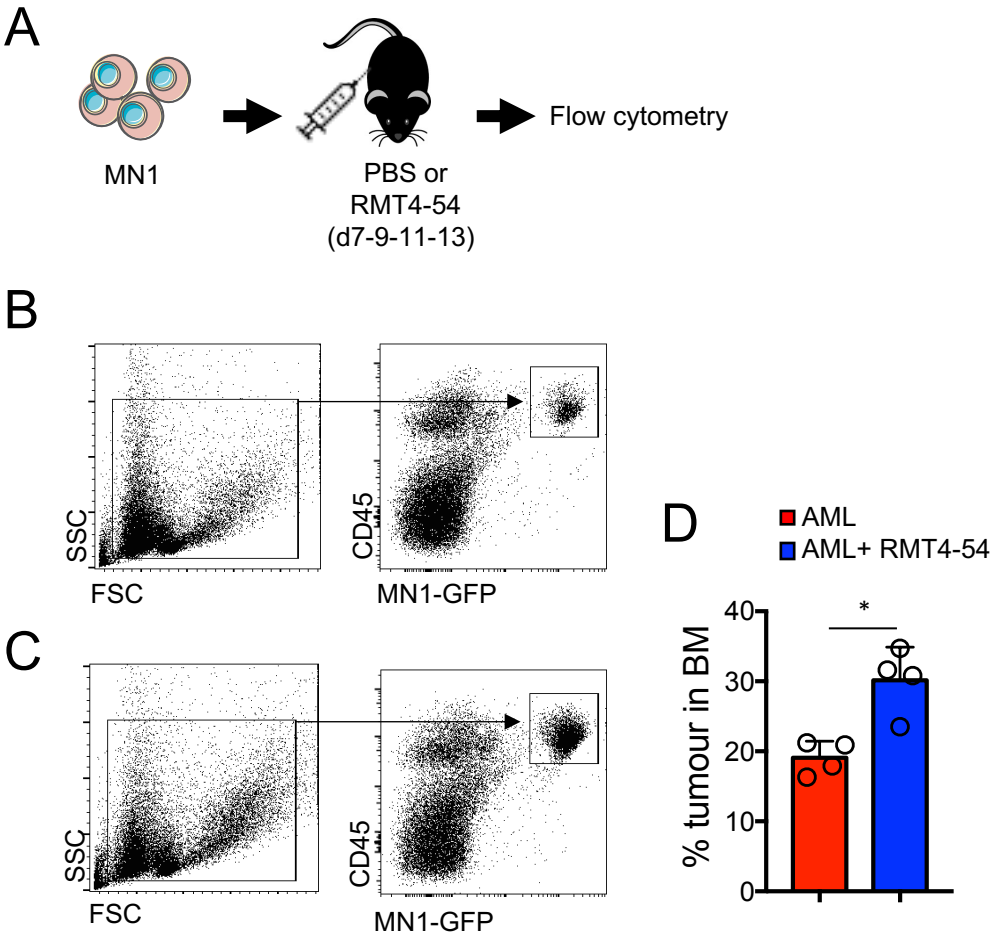

Figure 5.4. Inhibiting TIM4 in vivo leads to increased AML burden

(A) Schematic of experimental design. 10^6 MN1-GFP cells were I.V injected into busulfan treated (25mg/kg for 2 days) C57/BL6 mice. Animals were then treated with either 250µg of RMT4-54 or PBS on days 7, 9, 11 and 13. After 14 days the animals were sacrificed, the bone marrow harvested and analysed for MN1-GFP engraftment by flow cytometry. (B) Gating strategy and typical flow plots of control animals with MN1-GFP engraftment. (C) Gating strategy and typical flow plots of RMT4-54 animals with MN1-GFP engraftment. (D) MN1-GFP engraftment of AML (MN1-GFP) or AML+RMT4-54 animals as a percentage of the bone marrow. n=4. Data shown are means ± SD. *p<0.05, Mann–Whitney U. See pg. 88 for flow panel information.

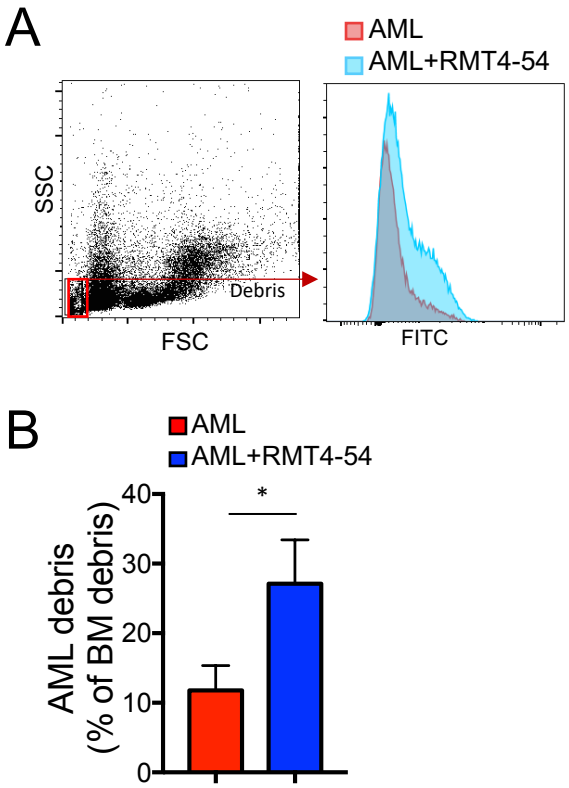

Figure 5.5. Inhibiting TIM4 in vivo leads to increased AML debris in the bone marrow

(A) Gating strategy and typical flow plots of debris (SSC^{LOW}, FSC^{LOW}) and AML debris as identified by FITC. (B) AML debris (SSC^{LOW}, FSC^{LOW}, MN1-GFP) in control and RMT4-54 treated animals as a percentage of bone marrow debris (SSC^{LOW}, FSC^{LOW}). n=4. Data shown are means ± SD. *p<0.05, Mann–Whitney U. See pg. 88 for flow panel information.

As TIM4 seems to play an important role in the clearance of AML ABs and the control of AML progression, I investigated how inhibiting TIM4 in an AML environment effected macrophages. As such, the same mice were investigated for macrophage populations, resident BM macrophages (BMM) and recruited AML associated macrophages (AAM). These macrophages, while broadly similar, have been shown to express altered surface markers and as such can be investigated independently [61, 397]. The BM of RMT4-54 or control treated mice were analysed for BMM (MN1-GFP^{-}, CD45^{+}, GR1^{-}, F4/80^{+}, CD115$^{LOW/INT}$) and AAM (MN1-GFP^{-}, CD45^{+}, Lys6G^{-}, CD11b^{+}) cell numbers. Additionally, AAM cells were isolated via FACS, and the RNA extracted to be analysed by qPCR (Figure 5.6). The data showed that animals treated with RMT4-54 had decreased BMM compared to control animals. Furthermore, RMT4-54 treated mice had significantly more AAM when compared to control mice, suggesting macrophages from TIM4 inhibited animals are more phenotypical of AAM compared to BMM (Figure 5.7A).

Next, I analysed the gene expression of the more abundant macrophage type, AAM, for pro-inflammatory markers. RMT4-54 treated mice AAM had increased gene expression of *il-1β*, *TNF-α* and *il-6* pro-inflammatory cytokines, suggesting TIM4 inhibited macrophages have an increased pro-inflammatory profile (Figure 5.7B). Previously I have investigated whether STING activation occurs after phagocytosis of AML ABs by looking at genes relating to STING. To see what effects inhibiting TIM4 has on STING activation in AAM, I looked at genes relating to STING activation. Blocking TIM4 via RMT4-54 significantly reduced the gene expression of STING related genes when compared to control AAM (Figure 5.7C). This data shows that TIM4 is an important receptor in macrophages within a leukaemic environment not only for AML suppression and pro-inflammatory regulation but may be required to efficiently activate the STING pathway via AML ABs uptake.

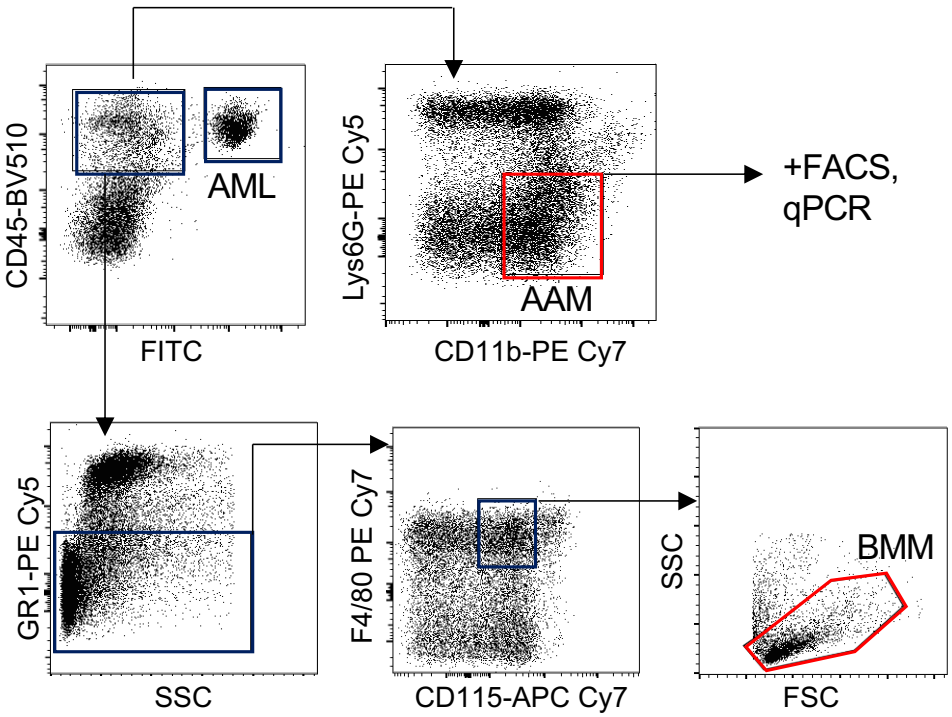

Figure 5.6. Gating strategy for the identification of macrophage sub-populations

The bone marrow of RMT4-54 (250µg) or PBS treated mice engrafted with MN1-GFP cells were analysed for resident bone marrow macrophages (BMM, MN1-GFP^{-}, CD45^{+}, GR1^{-}, F4/80^{+}, CD115$^{LOW/INT}$) and recruited AML associate macrophage (AAM, MN1-GFP^{-}, CD45^{+}, Lys6G^{-}, CD11b^{+}) via flow cytometry. AAM were isolated via FACS, and the RNA extracted to be analysed by qPCR. See pg. 88 for flow panel information.

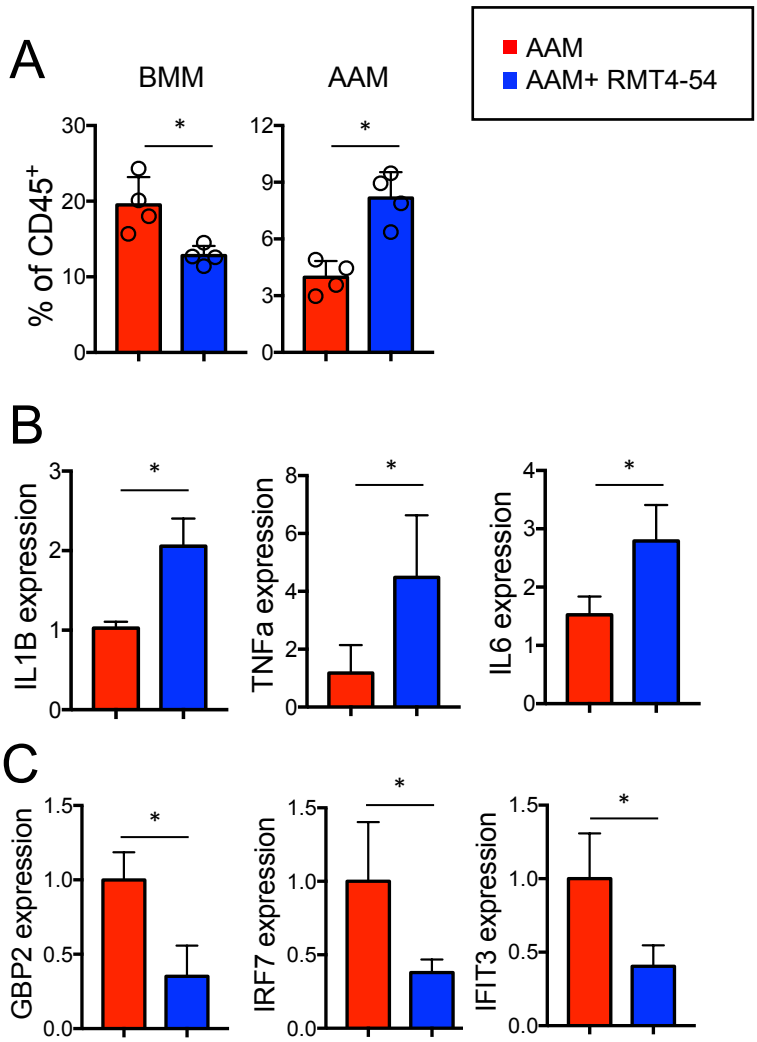

Figure 5.7. Inhibiting TIM4 in vivo alters bone marrow and recruited macrophages

(A) Bone marrow macrophages (BMM) and AML associated macrophages (AAM) cell number as a percentage of $CD45^+$ cells from RMT4-54 and control treated animals. (B) The relative gene expression of *il-1β*, *TNF-α* and *il-6* from AAM cells. (C) The relative gene expression of *GBP2*, *IRF7* and *IFIT3* from AAM cells. n=4. Data shown are means ± SD. *p<0.05, Mann–Whitney U.

I have previously demonstrated that STING activation in a leukaemic environment does not lead to activation of cytotoxic T-cells. To see if TIM4 inhibition altered the T-cell response in AML engrafted animals, I further analysed the BM of RMT4-54 and control treated animals for T-cell information. I analysed $CD4^+$ and $CD8^+$ numbers as well as cytotoxic $CD8^+$ activation via flow cytometry (Figure 5.8A). Inhibiting TIM4 led to no changes in $CD4^+$ T-cells, however, significantly decreased $CD8^+$ T-cells. Nevertheless, there were no differences in $CD8^+$ T-cell activation between RMT4-54 and control treated animals (Figure 5.8B). This information shows that whilst inhibiting TIM4 in an AML environment may alter the numbers of T-cells, it does not alter their activation. This data supports my previous findings that cytotoxic $CD8^+$ T-cell activation is not responsible for the suppression of AML growth seen both in LAP and TIM4 competent models.

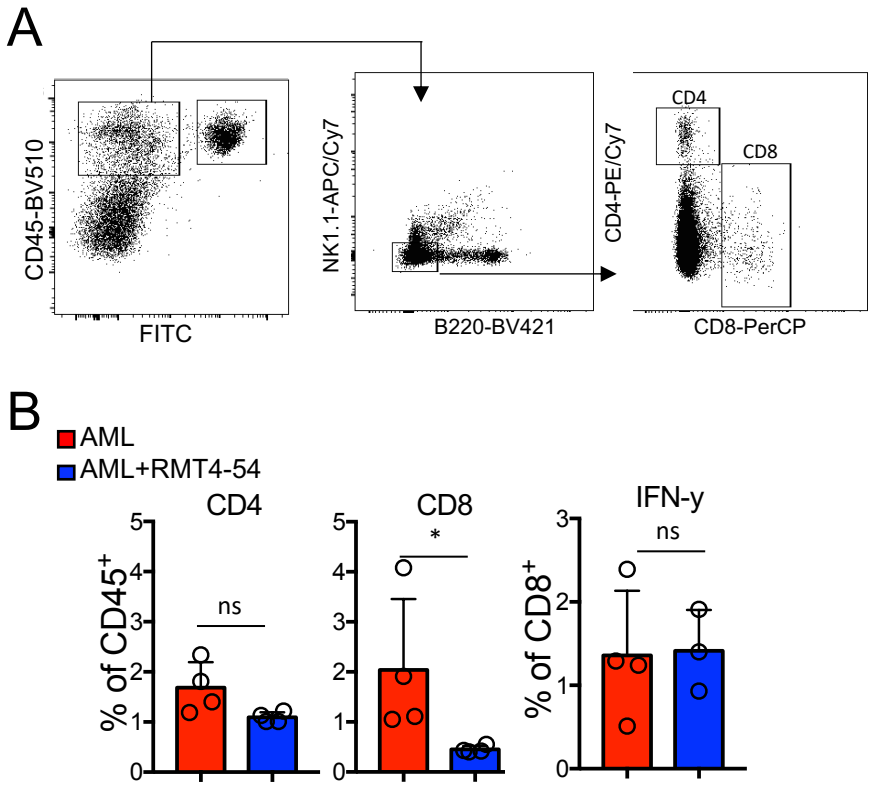

Figure 5.8. Inhibiting TIM4 in vivo alters CD8⁺ T-cell numbers but not their activation

(A) At day 14 the bone marrow from RMT4-54 and CNT treated AML engrafted mice was harvested and analysed via flow cytometry for $CD4^+$ cell numbers ($MN1\text{-}GFP^-$, $CD45^+$, $B220^-$, $NK1.1^-$, $CD4^+$), $CD8^+$ cell numbers ($MN1\text{-}GFP^-$, $CD45^+$, $B220^-$, $NK1.1^-$, $CD8^+$) and $CD8^+$ cell activation ($MN1\text{-}GFP^-$, $CD45^+$, $B220^-$, $NK1.1^-$, $CD8^+$, IFN-γ^+). (B) The percentage of $CD4^+$ and $CD8^+$ cells in the BM (of $CD45^+$ cells) as well as the percentage of IFN-γ expressing $CD8^+$ cells. n=4. Data shown are means ± SD. *p<0.05, Mann–Whitney U. See pg. 88 for flow panel information.

In my previous chapters I have uncovered that LAP in BM macrophages is important for the suppression of AML. Mechanistically, this occurs via the activation of STING in BM macrophages after LC3 associated phagocytosis of AML ABs containing mtDNA. Additionally, this process seems to rely on the upregulation of the phagocytic potential of BM macrophages independently of cytotoxic T-cell activation. This suggests that activation of STING in BM macrophages may upregulate certain components of the phagocytosis pathway. Therefore, as I have found that TIM4 in BM macrophages to be important to AML suppression and for the activation of STING related genes, I wanted to investigate if LAP deficiency in an AML environment alters TIM4 expression in BM macrophages. To do this, 10^6 MN1-GFP cells were injected into pre-treated (busulfan, 2 days, 25mg/kg) Atg16L1^{E230-} and Atg16L1^{E230+} mice. After 14 days the BM was harvested and analysed via flow cytometry (Figure 5.9A). The BM of Atg16L1^{E230-} and Atg16L1^{E230+} mice were analysed for TIM4 expression in BM macrophages (MN1-GFP^{-}, CD45^{+}, GR1^{-}, F4/80^{+}, CD115$^{LOW/INT}$, TIM4^{+}, Figure 5.9B). Data showed that LAP deficient animals had significantly less TIM4 expressing BM macrophages compared to LAP competent animals (Figure 5.9C). This data suggests that LAP in BM macrophages is required for upregulation of TIM4 in an AML environment.

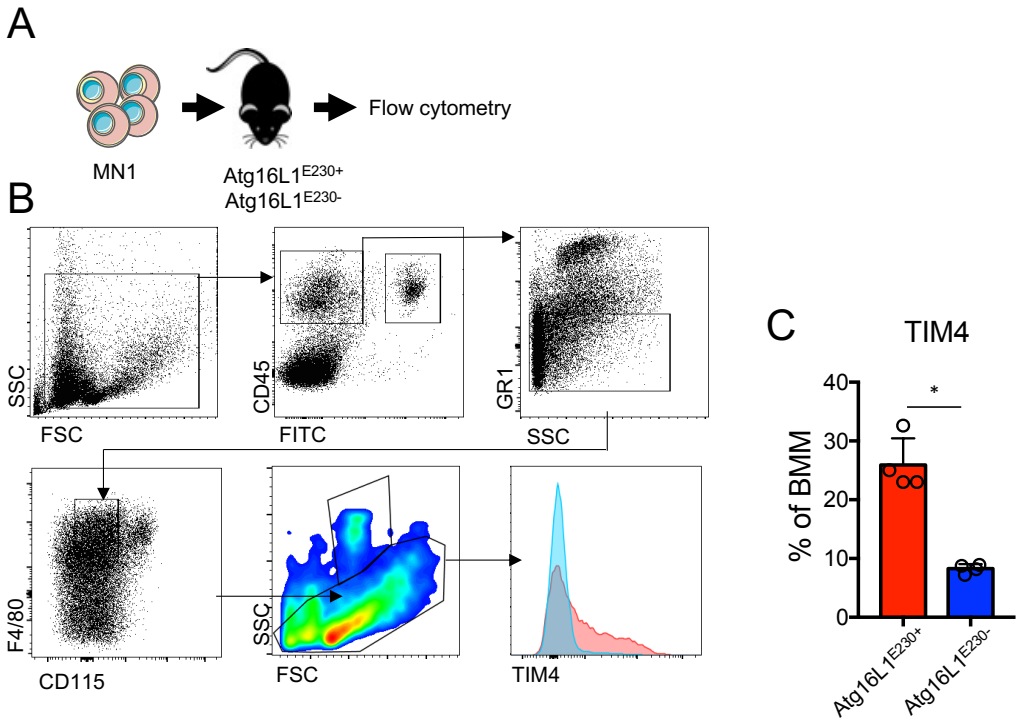

Figure 5.9. Bone marrow macrophage TIM4 expression in LAP deficient animals is altered in a leukaemic environment

(A) MN1-GFP cells ($1x10^6$) were injected into busulfan treated Atg16L1^{E230+} and Atg16L1^{E230-} mice (25mg/kg for 2 days). At day 14 the bone marrow was harvested and analysed via flow cytometry for TIM4 expressing bone marrow macrophages. (B) Representative gating strategy for the identification of TIM4 expression bone marrow macrophages (MN1-GFP$^-$, CD45$^+$, GR1$^-$, F4/80$^+$, CD115$^{LOW/INT}$, TIM4$^+$). (C) Identification of the percentage of TIM4 positive cells within the bone marrow macrophage population of Atg16L1^{E230+} and Atg16L1^{E230-} mice engrafted with MN1-GFP cells. n=4 mice in each group. Data shown are means ± SD. *p<0.05, Mann–Whitney U. See pg. 88 for flow panel information.

5.4 Summary

In the last chapter of my thesis, I have examined what role TIM4 in BM macrophages has upon AML progression. I have shown that TIM4 expressed on macrophages is required for the efficient uptake of AML ABs. Moreover, TIM4 in BM macrophages allows for lysosomal degradation of AML ABs phagosomes. I also have identified that TIM4 expression in BM macrophages is elevated in animals with AML and that inhibiting TIM4 leads to AML ABs accumulation in the BM and accelerated AML growth in vivo. Inhibiting TIM4 in AML engrafted animals led to altered macrophage numbers, of which the gene expression profile shows an increase in pro-inflammatory markers but decreased gene expression in genes relating to STING activation. However, TIM4 mediated STING activation did not lead to altered activation of cytotoxic T-cells, a phenomenon seen in LAP competent STING activation in AML engrafted animals. Lastly, I show that LAP competent animals with AML have increased TIM4 expression in BM macrophages compared to LAP deficient animals. This suggests that LAP uptake of apoptotic AML cells and debris, leading to STING related activation, may allow upregulation of TIM4, and as such, increased phagocytic compacities in BM macrophages.

6. Discussion and Conclusions

6.1 General discussion

AML is a debilitating haematological malignancy that, despite current treatment options, is an incurable cancer. Currently, intensive chemotherapy strategies are deployed for the treatment of the disease and whilst these processes can reduce the majority of malignant cells, disease relapse is common leading to disease progression and death. Specifically, several AML cells remain within special BM niches. These niches allow AML cells to be protected from chemotherapies, allowing AML cells to become resistant giving them the ability to proliferate to repopulate the BM and induce disease relapse. More recently, alterative treatment strategies have been investigated, such as B-cell lymphoma 2 (BCL-2) inhibitors in combination with hypomethylating agents (such as Venetoclax) [471]. New strategies to effectively clear AML cells that reside within the protected BM niches is envisioned to provide better outcomes for AML patients. As such, the study of how AML cells remain protected within the BM is imperative. Interactions between macrophages of the BM is one way AML can survive. Understanding the complex interactions between AML cells and macrophages may allow for novel treatment strategies.

In this thesis, I have shown how the interactions between BM macrophages and apoptotic AML cells can contribute to the survival and proliferation of AML. I have investigated the specific mechanisms in which macrophages deploy to process apoptotic AML cells which confers a tumour clearance advantage. Understanding these key mechanisms is hoped to be used as a therapeutic target in combination with current and upcoming novel treatment strategies, which may lead to increased survival and better outcomes for AML patients.

6.2 Key findings

6.2.1 LC3-associated phagocytosis in bone marrow macrophages and its importance in the AML microenvironment

In this thesis, I have shown that BM macrophages are required to inhibit the progression of AML cells. Importantly, I show that LAP is a vital mechanism that macrophages use to control AML growth.

Multiple studies have investigated the role macrophages have on cancer progression. Studies have focused on how tumour associated macrophages (TAMs) govern anti-tumour suppression, specifically, by the promotion of an M2 phenotype with the production of TGFß, IL-10, PGE2, reduction in antigen presentation and reduction of proinflammatory mediators [312, 317, 337, 338]. Moreover, TAMs can promote angiogenesis allowing metastasis in cancer [341]. Regarding AML, TAMs have been shown to be recruited to the BM, where increased AML TAMs correlates with poor outcomes in both animals and human patients [397, 398]. In conjunction with this, BM macrophage phagocytic activities are downregulated by CD47 expression in AML cells to avoid AML cell clearance [203]. Moreover, preleukaemic patients present poorly differentiated monocytes and macrophage impairment [396]. This demonstrates the important of macrophages within AML models, in which AML cells can manipulate their environment to the benefit of AML cells, by the suppression of BM macrophages and recruitment of TAMs. I find that, after BM macrophage clearance via clodronate, AML progression is enhanced. This is supported by research that showed depletion of macrophages via clodronate in a leukaemic model increased engraftment [205]. These finding supports the notion that functional BM macrophages are required for AML suppression.

The importance of functional macrophages in a leukaemic environment may largely be due to their ability to process apoptotic leukaemic cells efficiently. LAP in BM macrophages is a very efficient mechanism used to process apoptotic cells with studies identifying LAP deficiencies leading to the accumulation of unprocessed ABs [299]. Apoptosis has previously been thought of as immunologically silent or even tolerogenic death modality [472-

474]. However, a growing body of evidence suggests an important role for uncleared apoptotic debris in stimulating immunologic responses in malignancies [180, 475-478]. The correct processing of ABs by LAP leads to degradation of apoptotic cargo whereas ABs that remain unprocessed in LAP deficient models may not be efficiently degraded. I show data to support this, as when ABs from AML cells are cultured with LAP deficient macrophages, they are taken up by the phagocyte but not processed, contrastingly, LAP competent macrophages can efficiently process the ABs (4.6). Investigations into how LAP effects malignancies have largely centred on solid tumour types such as melanoma and adenocarcinoma [303]. Research showed that LAP deficiencies lead to tumour suppression which was largely dependent on T-cell activation and recruitment. In contrast, my results show that that LAP in macrophages is important to negatively regulate AML progression by altering the phagocytic capacities of macrophages, promoting increased phagocytic clearance. Moreover, there was no increase in the recruitment or activation of cytotoxic T-cells into the leukaemic BM of LAP deficient animals. These contrasting results highlights the importance of understanding the specific microenvironment of the malignancy. As such, the BM is an immuno-privileged site, which protects the process of haematopoiesis, this results in little T-cell recruitment and the absence of cytotoxic T-cells in the BM [464, 465].

The significance of LAP in AML suppression has been identified in this study via the use of a mouse model lacking the linker and WD domains of ATG16L1, via insertions of stop codons at E230 in the amino acid sequence ($Atg16L1^{E230-}$). $Atg16L1^{E230-}$ mice are LAP deficient globally, not just in the myeloid lineage, which may allow for non-myeloid cells to be implicated in the observations of this study. An additional model was used to allow for myeloid specificity, which also showed increased AML engraftment compared to controls. Other studies have used the deletion of RUBCN/Rubicon (rubcn−/-, Rubicon) [300, 303], which can be targeted to the myeloid cells. Rubicon is part of a complex upstream of ATG16L1 containing UVRAG, Beclin 1 and VPS34. As previously discussed, Rubicon is essential for LAP because it increases the class III PI3 kinase activity of VPS34 to generate PI3P on phagosomes to stabilise the NOX2 complex for the production of ROS and subsequential recruitment of

the LC3 conjugated machinery, allowing LC3 to tag the phagosome membrane [288, 289]. Rubcn−/- mouse models show inefficient clearance of pathogens and apoptotic cells as well as elevated inflammation leading to the development of autoimmune disease like systemic lupus erythematosus (SLE). Additionally, rubcn−/- mice were shown to induce a type I IFN responses in tumour infiltrating macrophages [303]. As such, both models of LAP deficiency are comparable, thus Rubcn-/- models could have been used to determine the role of LAP in AML progression. However, studies investigating Rubicon as a potential prognostic marker of cancer outcomes has shown that increased expression can lead to decrease survival in patients of various cancer types, whilst having little difference in high or low expression of Rubicon in some other cancer types. Thus, malignant specificity may alter the outcomes of how LAP regulation modifies the prognostic outcomes of cancers.

The importance of functional LAP and processing of ABs indicates that dysfunctional clearance may have adverse effects on the microenvironment. Research investigating autoimmunity and defects in apoptotic cell clearance shows eventual accumulation of secondary necrotic debris. This phenotype has been shown to represent hallmarks in the onset of chronic inflammatory and autoimmune diseases, for example SLE [260, 479, 480]. Furthermore, deficiencies in DNase II or engulfment genes in macrophages showed an accumulation of apoptotic cell debris and the development of an autoimmune phenotype, including IFN stimulation, a signature that closely resembles human SLE [457, 481]. My results show that that deficiencies of LAP in BM macrophages leads to accumulation of apoptotic AML cell and ABs, which results in a tumour supporting environment. This accumulation of apoptotic AML debris indicates that deficiencies in LAP not only leads to the ineffective processing of ABs but may incur some deficiencies in the uptake of the apoptotic debris. It has been identified that mice who are deficient in LAP, accumulate ABs in their tissues [463]. This process was linked to LAP and not canonical autophagy; thus, a feedback mechanism may exist in which LAP processing of ABs leads to an upregulation of engulfment mechanisms. Furthermore, the accumulation of apoptotic cells in a leukaemic environment

suggests that induction of secondary necrosis, or an alternative signalling stimulus, may be responsible for some of the tumour permissive environment seen in this study. More detailed investigations would be required to identify what processes contribute to AML progression in a leukaemic environment with accumulated ABs. This would be important as one of the main aims of cancer therapies is to induce apoptosis in cancer cells, understanding these processes may allow therapeutic opportunities which combines the induction of apoptosis and the efficient clearance of apoptotic cells via LAP.

LAP in macrophages have largely been investigated in mouse models of solid tumours or in vitro, however, research into how LAP interacts with AML, specifically in patients with AML, has not been investigated. AML has been shown to have increased expression of calreticulin, a pro-phagocytic signal, and while this is balanced by upregulation of CD47 on AML cells it suggests that AML in patients may use calreticulin for monocyte and macrophage recruitment [395]. In support of this, AML in patients leads to the invasion of TAMs to the BM with the overall survival rates in leukaemia patients with high levels of TAMs significantly worse compared to patients with low levels of TAMs [398]. Even so, how AML in patient's prime macrophages is unclear. In this study I have shown that monocytes derived from AML patients have significantly more LC3 density when compared to healthy controls. This information suggests that patients with AML may have monocytes that are primed towards a phagocytic profile before migration toward the malignant site. Furthermore, I showed that macrophages from AML engrafted mice have an increased capacity to phagocytose, specially via LAP. Together, it highlights that LAP in human AML patients may play an important role in AML regulation. To expand on this work, investigating how LC3 density or LAP in macrophage changes with the progression of the disease may show altered capacities.

6.2.2 Mitochondrial containing apoptotic bodies from AML cells

In this study, I have shown that AML ABs contain mitochondria, of which, the mtDNA taken up by BM macrophages is an important component in the controlled growth of AML.

The mitochondrial content of AML cells has been shown to be significantly increased when compared to non-malignant counterparts [406, 411]. Certainly, in my investigations I also found that AML cells have a large mitochondrial content. This is primarily due to the energy production of AML cells. Unlike many tumour cells that rely on the Warburg effect for energy production, that is the reliance on aerobic glycolysis even in the presence of oxygen, AML use oxidative phosphorylation for ATP production [404]. To support the demand of ATP production in the rapidly growing AML cells, studies have identified several methods that AML cells can manipulate the microenvironment, such as the hijacking of functional mitochondria from BMSC [411]. This increase in mitochondrial mass and the rapid growth of the AML cells can lead to dysfunctional mitochondria, which ultimately can lead not only to increased ROS as a by-product of oxidative phosphorylation, but initiator cascades which is required for the induction of apoptosis [482-484]. Apoptotic cells produce membrane blebs that release from the cell in the form of ABs, in which they contain cellular components, such as mtDAMPs [485]. I show that apoptotic AML ABs have a high mitochondrial content compared to non-malignant counterparts, both in murine and human AML derived ABs. Furthermore, the mitochondrial containing ABs from AML cells are processed by BM macrophages in a LAP dependent manner. This data adds to how BM macrophages process ABs and that apoptotic AML cells can encase mitochondria in ABs. This uptake of AML ABs containing mitochondrial components also highlights how this mechanism can change the phenotype of the BM macrophage via LAP.

The interactions between macrophages and apoptotic cells have been well documented, however, there is a large range of possible molecular interactions reported in the literature, which could be due to microenvironment specificity. It has been identified that residential macrophage populations, such as liver, BM and spleen are heterogeneous in their antigen expression

profile and morphology. To that extent, it has been shown that gene expression profiles are organ-specific in tissue macrophage populations [486]. Moreover, the processing of apoptotic cells is regulated via distinct pathways in different macrophage sites which seems to be microenvironment specific [487, 488]. As such, studies have shown that specific tissue resident macrophages, such as in the lung alveolar and $CX_3CR_1^+$, $CD64^+$, $MerTK^+$, $CD11c^+$ resident macrophages, are programmed for the silent clearance of apoptotic debris [489, 490]. However, apoptotic cells release a complex mixture of cellular components which can affect macrophage phenotype. Of note, CD14, expressed by monocytes and macrophages, is an early central regulator of inflammation. Research has highlighted that lipids from dying cells can induce an immune response via CD14 interactions [491]. These studies provide an opportunity to address the vast heterogeneity that macrophages possess, with environmental cues being a contributing factor of their specific polarity. The research presented in the current study highlights that AML ABs, containing mitochondria, are processed by BM macrophages via LAP. In the absence of LAP, BM macrophages cannot process the mtAB, even if the macrophages are able to recognise and associate with the ABs, presumably by the interaction with PtdSer receptors, such as TIM4. This highlights that LAP is required for the uptake of ABs in an AML environment. The uptake of mtAB also leads to activation of STING via AML mtDNA sensing. However, further investigations would be required to investigate what other signalling mechanisms may be responsible for the activation of this pathway. For example, late-stage apoptosis results in nuclear DNA degradation and is subsequentially exported in ABs. Whether nuclear DNA containing ABs leads to STING activation via LAP by BM macrophages, though it seems likely, is currently unknown. As such, future research needs to consider the immune-silence and pro-inflammatory subtypes of macrophages, the nature of the apoptotic cellular debris and targets, the LC3 status of the macrophage, as well as the clearance receptor regulation and usage as a wider spectrum of the macrophage landscape.

6.2.3 STING and AML

One of the major aims for any research project is to understand how the mechanism of an observation occurs. In my thesis, I have identified that the uptake of AML ABs by LAP in BM macrophages is important for AML suppression. The mechanisms involve require LAP processing of AML ABs containing mtDNA which leads to activation of STING. The activation of STING leads to increased phagocytic capacities in BM macrophages, where inhibition of STING leads to suppression of BM macrophage phagocytosis and increased AML progression.

The processing of the ABs allows the macromolecules of the degraded cargo to be used for recycling or potential for further downstream activators, such as antigen presentation or cGAS-STING activation. DNA and mtDNA have been shown to activate STING via cGAS-cGAMP signalling to cause downstream affects, such as type I IFN response [492]. STING activation has previously been highlighted as a mechanism to recruit and activate T-cells to suppress tumour growth. Moreover, STING activation results in the consequence of LAP deficient processing of apoptotic cells [303]. However, the types of tumours involved were reliant on solid malignancies. Consequently, not only were other cancer types not Investigated, such as haemopoietic malignancies, but the microenvironment that the macrophages reside in can confer different reactions to the apoptosis of malignant cells. This is important in tumour sites where T-cell activation does not occur, such as the BM, as the observed effects of tumour regulation via T-cell activation would not be attributed to these forms of malignancies. Previous investigation into AML STING activation has shown that AML type I IFN response is not triggered when compared to solid tumours, where STING activation is responsible for maturation of dendritic cells [493]. Using the STING inhibitor H-151, I have shown that inhibiting STING in BM macrophages leads to decreased phagocytic potential. This supports the previous findings that STING activation can lead to different phagocyte phenotypes, where increased phagocytotic capacities are the result of STING activation. Not only this, but STING inhibition also leads to increased AML progression, and this is LAP mediated. This information connects the process of LAP in BM macrophages and STING

activation that allows for AML suppression in vivo. Moreover, no changes in T-cell activation was observed, supporting the notion of tissue specificity when it comes to macrophage activation and their response to tumours. Thus, the rapid proliferation in AML cells driven by ATP occurs with the metabolic cost of increased ROS, apoptosis, and dysfunctional mitochondria. Moreover, mitochondrial released into the BM microenvironment are processed by LAP in BM macrophages which results in the activation of STING and increased phagocytotic capacities in the macrophages. These observations reveal tumour specific vulnerabilities allowing for strategic opportunities when considering novel approaches to managing patients with AML.

STING activation in tumour immune regulation is a promising new aspect of investigation for the potential treatment of malignancies. As previously discussed, sensing of tumour derived DNA by phagocytes can drive the STING response and downstream activities. As such, STING agonists are currently under investigation for cancer therapies as combinatorial agents with other therapies, such as immune checkpoint inhibitors [494]. STING-targeted treatments, such as ADU-S100 (MIW815) and E7766 (NCT04144140) have been approved for clinical trials. Ordinarily, STING activation leads to IFN-β production which leads to cytotoxic T-cell immune regulation of tumours, though the effects could be more far reaching, such as activation of phagocytes [309, 495]. The activation of STING in phagocytes has been hypothesised to be either via tumour derived DNA sensing or tumour derived cGAMP sensing [309, 496]. Here, I provide evidence that tumour derived mtDNA is a key activator of the STING response in BM macrophages. This information provides an opportunity to develop novel strategies of inducing STING activation in BM macrophages that can complement existing AML treatment strategies. Even so, increasingly, research into activating STING in cancer models shows promising results, such as inhibiting cancer cell growth, reduced tumour sizing, improved survival and reduction of metastasis in multiple of models [497-500]. Owing to the complex nature of AML disease progression and the limited reach of current treatment strategies, the best approach for novel therapies may consist of the combination of existing and new therapies.

One such candidate in the treatment of AML is blocking of the so called ‘do not eat me’ signals. Recently, CD47 has been identified as a potential target as it has been shown to be overexpressed in myeloid malignancies [202-204]. CD47 overexpression in AML cells can lead to tumour evasion, this occurs by inhibiting phagocytosis by macrophages. However, blockade of CD47 can lead to engulfment of leukaemic cells by BM macrophages and represents a potential treatment strategy. As such, in vivo experiments using monoclonal antibodies that block AML cell surface CD47 interactions with SIRPα on macrophages, enables phagocytosis of AML cells [203]. To expand on this research, further work has investigated the inhibition of CD47 in myeloid malignancies in clinical trials (NCT04778397 and NCT04912063) [501, 502]. In my research I have not investigate the effects of CD47 inhibition in combination with STING activation. However, the combination of CD47 inhibition, which will allow increased phagocytosis of AML cells, with STING activation, which also promotes phagocytosis, may present an attractive combination strategy for AML treatment.

6.2.4 TIM4 and AML

In the final part of my thesis, I investigated the PtdSer recognition receptor, TIM4. I found that TIM4 is important in the processing of AML ABs and that inhibiting TIM4 led to increased AML engraftment in vivo. Furthermore, TIM4 was upregulated in LAP competent animals with AML.

TIM4 is expressed on the surface of phagocytes and is an important mechanism in efferocytosis. However, the complete function of TIM4 is still not fully understood, with accumulating data suggesting TIM4 is involved in tumour progression. As such, the overexpression of TIM4 is a promotional aspect in the proliferation of non-small cell lung carcinoma [238]. Furthermore, TIM4 has been shown to dampen the effect of chemotherapies and increases cancer immune tolerance [269]. More recently, a study investigating the role of TIM4 in colorectal cancer showed that TIM4 is an angiogenesis promoter via upregulation of VEGF as well as recruiting TAMs via PI3K/Akt signalling, thus promoting cancer progression [274]. However, the role of TIM4 in macrophages, like the activation of STING, seems to be site specific. As such, TIM4 deficiencies has been shown to exhibit a phenotype similar to that of dysregulated processing of ABs, as such it suggests that dedicated apoptotic receptor pathways enables DNA degradation [448]. Additionally, TIM4 expression in dendritic cells of models of lung cancer in mouse models contributes to immune surveillance while in advance tumour, the expression is supressed [273]. In my research, I found that LAP deficiencies lead to the accumulation of ABs. Moreover, deficiencies in LAP led to the downregulation of TIM4 expression on BM macrophages. This suggests a link exists between LAP and TIM4 in BM macrophages. This is supported by the fact that TIM4 and LAP are both required for presenting the phagocytosed ABs to the lysosomal for degradation. Even so, previous data is conflicting and as such need further investigations to allow identification of how TIM4 operates within specific malignancies.

The loss of function of apoptotic recognition receptors, such as TIM4, has been shown to lead to the accumulation of apoptotic cells and debris in multiple tissues, leading to adverse side effects [228-231]. Furthermore, this can lead to secondary necrosis of apoptotic cells leading to the exposure of harmful

contents for neighbouring cells [283, 284]. This process can lead to inflammation resulting in cell and tissue damage [285, 286]. Furthermore, unprocessed ABs can cause macrophages to alter their polarisation [303, 307, 308]. This information highlights the importance of apoptotic clearance by macrophages. I have shown that LAP deficient macrophages also express low levels of TIM4. This is also linked to increased apoptotic AML cells and ABs in the BM microenvironment. Together, this data highlights the importance of apoptotic clearance in the microenvironment. TIM4 processing of apoptotic AML cells is required to reduce inflammation caused by secondary necrosis. Additionally, it may act as a pathway for LAP processing of apoptotic cells, in which mtDNA sensing can lead to STING activation.

Even with the development of new therapies, the main treatment of AML still relies on the use of intensive cytotoxic chemotherapy strategies in patients that can withstand the therapy. As apoptosis is a consequence of this therapy, the efficient clearance of the debris is required. It has been highlighted that damage-associated molecular patterns (DAMPs) molecules released from dying or stressed tumour cells treated with chemotherapeutics could promote TIM4 expression on macrophages. However, glycoprotein-mediated degradation of dying tumour cells can also lead to reduced antigen presentation [245]. As I have shown that TIM4 is required for efficient processing of apoptotic AML cells, increasing TIM4 expression in BM macrophages may offer a novel strategy to use in conjugation with existing chemotherapies. To date, no research has investigated the effects of upregulation of TIM4 in BM macrophages and its regulatory effect in AML cells. It can be hypothesised that the increased expression of TIM4 in BM macrophages, in combination with apoptosis induction via chemotherapies, would lead to the increased apoptotic AML clearance. Furthermore, if TIM4 and LAP are linked, this could also lead to the activation of STING which can further promote phagocytosis. It could be envisioned that a treatment strategy that combines apoptosis induction, increased TIM4 expression, blockade of CD47 expression along with a STING activator could provide a multi-layered approach to treating AML. However, much more research would be needed to

identify how these therapies work together and their suitability for human therapeutics.

6.3 Limitations

Despite the results collected in this thesis, as with any study, there are limitations that restricted this investigation. The study largely relied on the combination of in vivo, in vitro, and primary AML investigations. The amount of primary AML samples used could have been increased to allow a more robust analysis owing to the heterogeneity of the disease. Limitation on the collection of primary samples means that in certain experiments sample numbers are low. However, the data generated was investigated in multiple models and the use of a small amount of primary AML samples outweighs the reliance on the use of cell lines.

The in vivo experiments also could have been expanded. Some animal experiments had reduced numbers of animals due to animal availability, especially in the ATG16L1^{E230} models. To expand on the research, more animals could have been used to provide more statistical power when looking for significant differences in experimental groups. However, experiments were planned in accordance with the three ‘R’s’, to make experiments as efficient as possible without the excessive use of animals unnecessarily. Additionally, many animal models used were engrafted with two types of murine AML cells. This could have been expanded to include more primary AML cells or alterative murine AML models. Nevertheless, experiments using human AML in the xenograft transplant model was used to identify mitochondria uptake by macrophages. Moreover, my studies were hindered by the lack of engraftment in certain experiments. Though several factors may have contributed to this, such as missing the tail vein while injecting or having non-viable cells, this limited the amount of data able to be generate in these experiments. Also, to further investigate the effect of LAP in animals a Rubicon knockout model could have been used to add to the experimental findings in this study.

Additional models could have been used to study the effect of STING in this thesis. In my thesis I studied the effects of STING activation in BM macrophages on AML. With the combination of cytokine arrays, RNA analysis

and the use of a STING inhibitor both in vitro and in vivo I showed the importance of STING activation in the suppression of AML. The use of a STING knockout mouse model would be able to add to this work by removing the need to inhibit STING activity chemically. Furthermore, the activation of STING has been used in several studies, even in malignant models. This has been achieved through using STING agonists, such as DMXAA. This would allow investigations to see if enhance STING activities leads to further suppression of AML in this study. Additionally, to investigate the effects of the LAP response in BM macrophages to AML derived ABs, I focused on the secretion profile of chemokines and cytokines using cytokines arrays. This provided a wealth of data allowing me to identify the differences between BM macrophages that can undergo LAP and not, highlighting differences in STING related signatures. To expand on this finding the use of techniques such as RNAseq would have provided more data on the changes of the macrophage gene expression.

Another limitation of the study is the depletion of macrophages to study the effects of macrophages on AML progression. In my study I used clodronate liposomes which selectively depletes phagocytes. Whilst I showed that BM macrophages were depleted after clodronate treatment, I did not investigate the effects of clodronate on any other phagocytes, such as dendritic cells. As dendritic cells play an important role in phagocytosis and antigen presentation, it would be interesting to investigate whether dendritic cells contribute to the phenotype seen in regards to AML progression. A more selective method of macrophage and dendritic cell depletion may allow the investigation of the effect of each phagocyte type upon AML control. Furthermore, isolation of BM macrophages in some experiments relied on the isolation of cells via F4/80 surface markers on the cells. This is a marker of murine macrophages, even so, immature monocytes can express F4/80. As such, further classification of macrophages could be used to obtain specific populations.

Studying apoptosis in my thesis was important to investigate the correct induction of apoptosis to isolate ABs but also to investigate the live counts of MN1 cells after engraftment in animals. To do this, I looked for the expression of PtdSer on the surface of apoptotic cells using Annexin V. I used flow

cytometry to identify Annexin V positive cells as an indicator of apoptosis. This methodology is limited as it does not allow distinctions between necrotic cells, early-stage apoptosis, or late-stage apoptosis. To expand on this, the inclusion of PI could have been used to allow further distinctions between dying populations. However, the number of fluorophores available for each flow cytometry experiment meant some channels were occupied by other antibodies or stains. To improve the results, inclusion of PI would allow complete classification of apoptosis.

Lastly, time constraints had a limitation on the study. Like many researchers during 2020, a national lockdown due to the COVID-19 limited the capacity to undertake research in laboratories. Although, I had limited access to in vitro research, along with helping to develop COVID-19 PCR testing systems, in vivo work was extremely restricted. Furthermore, research into TIM4 and its effect on AML progression was not fully completed due to this. Moreover, investigations into T-cell activities could not be explored further. More research would be required to explore TIM4, and T-cell activaties, further in the context of AML interactions.

6.4 Future work

With the aims of this study being achieved, the next stages would be to look how to expand the information collected and what future work could be completed. I have shown that STING activation leads to increased phagocytic capacities in BM macrophages. Moreover, LAP is required for this process to occur. However, how the mechanisms occur are not known. For example, how does the activation of STING via LAP of mtAB cause upregulation of phagocytosis in BM macrophages? It has been shown that STING activation can partly function to upregulate LC3 association to phagosomes, whether or not this allows for increased phagocytic potential in BM macrophages needs to be explored. Further to this, I showed a linked between LAP and TIM4 in BM macrophages. It would be interesting to investigate how STING activation supports the expression of TIM4 in BM macrophages. It could be hypothesised that LAP processing of mtAB leads to STING activation and the increase in both LC3 association and TIM4 expression on the surface of BM macrophages, allowing for increased ABs clearance in BM macrophages. Future investigation may answer these important questions.

One important factor seen in many malignancies, such as AML, is the upregulation of CD47, the ‘do not eat me’ signal. In my research, I did not investigate CD47 in any of my experiments. Due to the nature of my research, it would be beneficial to investigate how making AML cells less resistant to phagocytosis could support my findings. Furthermore, discovering mechanisms to increase the phagocytic capacities of BM macrophages while marking AML cells for engulfment presents an attractive strategy. Future investigations combining these two approaches may be able to investigate the therapeutic potential of this specific combination.

Lastly, I have conducted my experiments at pre-defined time points. These time points, generally 14 days in vivo and 24 hours in vitro, was to allow less variation in the results obtained. However, this method does not represent the presentation of the disease clinically. As such, future research, looking at early-, mid- and late-stage disease, as well as relapse, would be able to see how the phenotype observed in this study translates. Particularly, how the constant processing of ABs by BM macrophages effects the ability of the

macrophage to continue the increased phagocytic capacities. Exhaustion in macrophages is difficult to research, this could be due to the phenotype of senescence in macrophages being complex and not well characterised. Senescent cells and macrophages share similar characteristics, such as similar secretory profiles, increased lysosome numbers and similar inflammatory mediators [503]. Nevertheless, investigating how these outcomes effect the progression of AML would be a target future research could undertake.

6.5 Conclusions

Overall, in my thesis I have reported that BM macrophages are an important cell in the control of AML, and their depletion leads to accelerated AML growth. I show that AML associated BM macrophages have an increased capacity to phagocytose compared to naïve BM macrophages and that this pathway is via LC3 associated phagocytosis (LAP). I find that LAP deficiencies in BM macrophages causes increased AML progression as well as decreased survival in animals. Furthermore, LAP deficiencies lead to the accumulation of apoptotic debris in the BM as well as a decreased ability to process ABs effectively via lysosomal degradation. Investigating how the addition of AML derived ABs to LAP deficient and competent macrophages effected their cytokine expression, I showed that cytokines and chemokines relating to STING activation was upregulated in LAP competent macrophages treated with ABs but absent from all LAP deficient macrophages. STING activation in BM macrophages was shown to occur via culture with AML derived ABs but inhibiting STING led to increased AML growth in LAP competent animals but no changes were seen in LAP deficient animals, highlighting the role of LAP in STING activation. Furthermore, STING activation in BM macrophages in an AML environment did not lead to cytotoxic T-cell recruitment or activation but conferred an increase potential for macrophages to phagocytose. I discovered that the increased mitochondrial content of AML cells leads to increase export of mitochondrial components in ABs, specifically mtDNA. The AML derived mtDNA containing ABs are processed by BM macrophages in a LAP dependent manner that allows for increased STING activation. Lastly, I showed that TIM4 is an important molecule used by BM macrophages to allow for AML suppression and that the expression of TIM4 is linked to the LAP status of the macrophage. Together, I have highlighted important mechanisms that BM macrophages utilise to control apoptotic AML cells, in which activation of STING confers a phagocytic benefit in the macrophages.

7. References

1. Gurkan, U.A. and O. Akkus, *The mechanical environment of bone marrow: a review.* Ann Biomed Eng, 2008. **36**(12): p. 1978-91.
2. Kopp, H.G., et al., *The bone marrow vascular niche: home of HSC differentiation and mobilization.* Physiology (Bethesda), 2005. **20**: p. 349-56.
3. Shafat, M.S., et al., *The bone marrow microenvironment - Home of the leukemic blasts.* Blood Rev, 2017. **31**(5): p. 277-286.
4. Travlos, G.S., *Normal structure, function, and histology of the bone marrow.* Toxicol Pathol, 2006. **34**(5): p. 548-65.
5. Jung, W.C., J.P. Levesque, and M.J. Ruitenberg, *It takes nerve to fight back: The significance of neural innervation of the bone marrow and spleen for immune function.* Semin Cell Dev Biol, 2017. **61**: p. 60-70.
6. Winkler, I.G., et al., *Bone marrow macrophages maintain hematopoietic stem cell (HSC) niches and their depletion mobilizes HSCs.* Blood, 2010. **116**(23): p. 4815-28.
7. Broome, C.S. and J.A. Miyan, *Neuropeptide control of bone marrow neutrophil production. A key axis for neuroimmunomodulation.* Ann N Y Acad Sci, 2000. **917**: p. 424-34.
8. Rameshwar, P. and P. Gascón, *Substance P (SP) mediates production of stem cell factor and interleukin-1 in bone marrow stroma: potential autoregulatory role for these cytokines in SP receptor expression and induction.* Blood, 1995. **86**(2): p. 482-90.
9. Ivanovs, A., et al., *Identification of the niche and phenotype of the first human hematopoietic stem cells.* Stem Cell Reports, 2014. **2**(4): p. 449-56.
10. Dzierzak, E. and N.A. Speck, *Of lineage and legacy: the development of mammalian hematopoietic stem cells.* Nat Immunol, 2008. **9**(2): p. 129-36.
11. Kiel, M.J. and S.J. Morrison, *Uncertainty in the niches that maintain haematopoietic stem cells.* Nat Rev Immunol, 2008. **8**(4): p. 290-301.
12. Morrison, S.J. and D.T. Scadden, *The bone marrow niche for haematopoietic stem cells.* Nature, 2014. **505**(7483): p. 327-34.
13. Nombela-Arrieta, C., et al., *Quantitative imaging of haematopoietic stem and progenitor cell localization and hypoxic status in the bone marrow microenvironment.* Nat Cell Biol, 2013. **15**(5): p. 533-43.
14. Wilson, A., et al., *Hematopoietic stem cells reversibly switch from dormancy to self-renewal during homeostasis and repair.* Cell, 2008. **135**(6): p. 1118-29.
15. Baldridge, M.T., et al., *Quiescent haematopoietic stem cells are activated by IFN-gamma in response to chronic infection.* Nature, 2010. **465**(7299): p. 793-7.
16. Pietras, E.M., et al., *Functionally Distinct Subsets of Lineage-Biased Multipotent Progenitors Control Blood Production in Normal and Regenerative Conditions.* Cell Stem Cell, 2015. **17**(1): p. 35-46.
17. Sanjuan-Pla, A., et al., *Platelet-biased stem cells reside at the apex of the haematopoietic stem-cell hierarchy.* Nature, 2013. **502**(7470): p. 232-6.
18. Laurenti, E. and B. Göttgens, *From haematopoietic stem cells to complex differentiation landscapes.* Nature, 2018. **553**(7689): p. 418-426.
19. Rieger, M.A. and T. Schroeder, *Hematopoiesis.* Cold Spring Harb Perspect Biol, 2012. **4**(12).

20. Kiel, M.J., et al., *SLAM family receptors distinguish hematopoietic stem and progenitor cells and reveal endothelial niches for stem cells.* Cell, 2005. **121**(7): p. 1109-21.
21. Görgens, A., et al., *Revision of the human hematopoietic tree: granulocyte subtypes derive from distinct hematopoietic lineages.* Cell Rep, 2013. **3**(5): p. 1539-52.
22. Ng, A.P. and W.S. Alexander, *Haematopoietic stem cells: past, present and future.* Cell Death Discov, 2017. **3**: p. 17002.
23. Notta, F., et al., *Distinct routes of lineage development reshape the human blood hierarchy across ontogeny.* Science, 2016. **351**(6269): p. aab2116.
24. Paul, F., et al., *Transcriptional Heterogeneity and Lineage Commitment in Myeloid Progenitors.* Cell, 2015. **163**(7): p. 1663-77.
25. Grün, D., et al., *De Novo Prediction of Stem Cell Identity using Single-Cell Transcriptome Data.* Cell Stem Cell, 2016. **19**(2): p. 266-277.
26. Braccini, A., et al., *Three-dimensional perfusion culture of human bone marrow cells and generation of osteoinductive grafts.* Stem Cells, 2005. **23**(8): p. 1066-72.
27. Cheng, L., et al., *Human adult marrow cells support prolonged expansion of human embryonic stem cells in culture.* Stem Cells, 2003. **21**(2): p. 131-42.
28. Pittenger, M.F., *Mesenchymal stem cells from adult bone marrow.* Methods Mol Biol, 2008. **449**: p. 27-44.
29. Sacchetti, B., et al., *Self-renewing osteoprogenitors in bone marrow sinusoids can organize a hematopoietic microenvironment.* Cell, 2007. **131**(2): p. 324-36.
30. Méndez-Ferrer, S., et al., *Mesenchymal and haematopoietic stem cells form a unique bone marrow niche.* Nature, 2010. **466**(7308): p. 829-34.
31. Wu, J., et al., *The Differentiation Balance of Bone Marrow Mesenchymal Stem Cells Is Crucial to Hematopoiesis.* Stem Cells Int, 2018. **2018**: p. 1540148.
32. Ding, L., et al., *Endothelial and perivascular cells maintain haematopoietic stem cells.* Nature, 2012. **481**(7382): p. 457-62.
33. Omatsu, Y., et al., *The essential functions of adipo-osteogenic progenitors as the hematopoietic stem and progenitor cell niche.* Immunity, 2010. **33**(3): p. 387-99.
34. Kunisaki, Y., et al., *Arteriolar niches maintain haematopoietic stem cell quiescence.* Nature, 2013. **502**(7473): p. 637-43.
35. Yu, V.W., et al., *Distinctive Mesenchymal-Parenchymal Cell Pairings Govern B Cell Differentiation in the Bone Marrow.* Stem Cell Reports, 2016. **7**(2): p. 220-35.
36. Aguila, H.L., et al., *Osteoblast-specific overexpression of human interleukin-7 rescues the bone mass phenotype of interleukin-7-deficient female mice.* J Bone Miner Res, 2012. **27**(5): p. 1030-42.
37. Yu, V.W., et al., *Specific bone cells produce DLL4 to generate thymus-seeding progenitors from bone marrow.* J Exp Med, 2015. **212**(5): p. 759-74.
38. Chitteti, B.R., et al., *Osteoblast lineage cells expressing high levels of Runx2 enhance hematopoietic progenitor cell proliferation and function.* J Cell Biochem, 2010. **111**(2): p. 284-94.

39. Chitteti, B.R., et al., *Hierarchical organization of osteoblasts reveals the significant role of CD166 in hematopoietic stem cell maintenance and function.* Bone, 2013. **54**(1): p. 58-67.
40. Asada, N., et al., *Matrix-embedded osteocytes regulate mobilization of hematopoietic stem/progenitor cells.* Cell Stem Cell, 2013. **12**(6): p. 737-47.
41. Sato, M., et al., *Osteocytes regulate primary lymphoid organs and fat metabolism.* Cell Metab, 2013. **18**(5): p. 749-58.
42. Fazeli, P.K., et al., *Marrow fat and bone--new perspectives.* J Clin Endocrinol Metab, 2013. **98**(3): p. 935-45.
43. Ambrosi, T.H., et al., *Adipocyte Accumulation in the Bone Marrow during Obesity and Aging Impairs Stem Cell-Based Hematopoietic and Bone Regeneration.* Cell Stem Cell, 2017. **20**(6): p. 771-784.e6.
44. Naveiras, O., et al., *Bone-marrow adipocytes as negative regulators of the haematopoietic microenvironment.* Nature, 2009. **460**(7252): p. 259-63.
45. Belaid-Choucair, Z., et al., *Human bone marrow adipocytes block granulopoiesis through neuropilin-1-induced granulocyte colony-stimulating factor inhibition.* Stem Cells, 2008. **26**(6): p. 1556-64.
46. Ghode, S.S., et al., *Neuropilin-1 Is an Important Niche Component and Exerts Context-Dependent Effects on Hematopoietic Stem Cells.* Stem Cells Dev, 2017. **26**(1): p. 35-48.
47. Sitnicka, E., et al., *Transforming growth factor beta 1 directly and reversibly inhibits the initial cell divisions of long-term repopulating hematopoietic stem cells.* Blood, 1996. **88**(1): p. 82-8.
48. Miharada, K., et al., *Lipocalin 2 functions as a negative regulator of red blood cell production in an autocrine fashion.* FASEB J, 2005. **19**(13): p. 1881-3.
49. Broxmeyer, H.E., et al., *Dipeptidylpeptidase 4 negatively regulates colony-stimulating factor activity and stress hematopoiesis.* Nat Med, 2012. **18**(12): p. 1786-96.
50. Itkin, T., et al., *Distinct bone marrow blood vessels differentially regulate haematopoiesis.* Nature, 2016. **532**(7599): p. 323-8.
51. Rafii, S., J.M. Butler, and B.S. Ding, *Angiocrine functions of organ-specific endothelial cells.* Nature, 2016. **529**(7586): p. 316-25.
52. Bruns, I., et al., *Megakaryocytes regulate hematopoietic stem cell quiescence through CXCL4 secretion.* Nat Med, 2014. **20**(11): p. 1315-20.
53. Zhao, M., et al., *Megakaryocytes maintain homeostatic quiescence and promote post-injury regeneration of hematopoietic stem cells.* Nat Med, 2014. **20**(11): p. 1321-6.
54. Storan, M.J., et al., *Brief Report: Factors Released by Megakaryocytes Thrombin Cleave Osteopontin to Negatively Regulate Hematopoietic Stem Cells.* Stem Cells, 2015. **33**(7): p. 2351-7.
55. Alvarez, M.B., et al., *Megakaryocyte and Osteoblast Interactions Modulate Bone Mass and Hematopoiesis.* Stem Cells Dev, 2018. **27**(10): p. 671-682.
56. Gordon, S., *Alternative activation of macrophages.* Nat Rev Immunol, 2003. **3**(1): p. 23-35.
57. Martinez, F.O., et al., *Macrophage activation and polarization.* Front Biosci, 2008. **13**: p. 453-61.

58. Crocker, P.R. and S. Gordon, *Isolation and characterization of resident stromal macrophages and hematopoietic cell clusters from mouse bone marrow.* J Exp Med, 1985. **162**(3): p. 993-1014.
59. Chasis, J.A. and N. Mohandas, *Erythroblastic islands: niches for erythropoiesis.* Blood, 2008. **112**(3): p. 470-8.
60. Chow, A., et al., *CD169^{+} macrophages provide a niche promoting erythropoiesis under homeostasis and stress.* Nat Med, 2013. **19**(4): p. 429-36.
61. Chow, A., et al., *Bone marrow CD169+ macrophages promote the retention of hematopoietic stem and progenitor cells in the mesenchymal stem cell niche.* J Exp Med, 2011. **208**(2): p. 261-71.
62. McCabe, A. and K.C. MacNamara, *Macrophages: Key regulators of steady-state and demand-adapted hematopoiesis.* Exp Hematol, 2016. **44**(4): p. 213-22.
63. Osborn, L., et al., *Direct expression cloning of vascular cell adhesion molecule 1, a cytokine-induced endothelial protein that binds to lymphocytes.* Cell, 1989. **59**(6): p. 1203-11.
64. Mevorach, D., et al., *Complement-dependent clearance of apoptotic cells by human macrophages.* J Exp Med, 1998. **188**(12): p. 2313-20.
65. Chang, K.H., et al., *p62 is required for stem cell/progenitor retention through inhibition of IKK/NF-κB/Ccl4 signaling at the bone marrow macrophage-osteoblast niche.* Cell Rep, 2014. **9**(6): p. 2084-97.
66. Broxmeyer, H.E., et al., *Rapid mobilization of murine and human hematopoietic stem and progenitor cells with AMD3100, a CXCR4 antagonist.* J Exp Med, 2005. **201**(8): p. 1307-18.
67. Christopher, M.J., et al., *Expression of the G-CSF receptor in monocytic cells is sufficient to mediate hematopoietic progenitor mobilization by G-CSF in mice.* J Exp Med, 2011. **208**(2): p. 251-60.
68. Furze, R.C. and S.M. Rankin, *The role of the bone marrow in neutrophil clearance under homeostatic conditions in the mouse.* FASEB J, 2008. **22**(9): p. 3111-9.
69. Stark, M.A., et al., *Phagocytosis of apoptotic neutrophils regulates granulopoiesis via IL-23 and IL-17.* Immunity, 2005. **22**(3): p. 285-94.
70. Casanova-Acebes, M., et al., *Rhythmic modulation of the hematopoietic niche through neutrophil clearance.* Cell, 2013. **153**(5): p. 1025-35.
71. Renehan, A.G., C. Booth, and C.S. Potten, *What is apoptosis, and why is it important?* BMJ, 2001. **322**(7301): p. 1536-8.
72. Thompson, C.B., *Apoptosis in the pathogenesis and treatment of disease.* Science, 1995. **267**(5203): p. 1456-62.
73. Ellis, R.E., J.Y. Yuan, and H.R. Horvitz, *Mechanisms and functions of cell death.* Annu Rev Cell Biol, 1991. **7**: p. 663-98.
74. Pasparakis, M. and P. Vandenabeele, *Necroptosis and its role in inflammation.* Nature, 2015. **517**(7534): p. 311-20.
75. Fuchs, Y. and H. Steller, *Live to die another way: modes of programmed cell death and the signals emanating from dying cells.* Nat Rev Mol Cell Biol, 2015. **16**(6): p. 329-44.

76. Conrad, M., et al., *Regulated necrosis: disease relevance and therapeutic opportunities.* Nat Rev Drug Discov, 2016. **15**(5): p. 348-66.
77. Galluzzi, L., et al., *Cell death modalities: classification and pathophysiological implications.* Cell Death Differ, 2007. **14**(7): p. 1237-43.
78. Vakkila, J. and M.T. Lotze, *Inflammation and necrosis promote tumour growth.* Nat Rev Immunol, 2004. **4**(8): p. 641-8.
79. Izzo, V., et al., *Mitochondrial Permeability Transition: New Findings and Persisting Uncertainties.* Trends Cell Biol, 2016. **26**(9): p. 655-667.
80. Galluzzi, L., et al., *Molecular mechanisms of cell death: recommendations of the Nomenclature Committee on Cell Death 2018.* Cell Death Differ, 2018. **25**(3): p. 486-541.
81. Vanden Berghe, T., et al., *Regulated necrosis: the expanding network of non-apoptotic cell death pathways.* Nat Rev Mol Cell Biol, 2014. **15**(2): p. 135-47.
82. Roos, W.P., A.D. Thomas, and B. Kaina, *DNA damage and the balance between survival and death in cancer biology.* Nat Rev Cancer, 2016. **16**(1): p. 20-33.
83. Czabotar, P.E., et al., *Control of apoptosis by the BCL-2 protein family: implications for physiology and therapy.* Nat Rev Mol Cell Biol, 2014. **15**(1): p. 49-63.
84. Brumatti, G., M. Salmanidis, and P.G. Ekert, *Crossing paths: interactions between the cell death machinery and growth factor survival signals.* Cell Mol Life Sci, 2010. **67**(10): p. 1619-30.
85. Green, D.R., T.H. Oguin, and J. Martinez, *The clearance of dying cells: table for two.* Cell Death Differ, 2016. **23**(6): p. 915-26.
86. Tait, S.W. and D.R. Green, *Mitochondria and cell death: outer membrane permeabilization and beyond.* Nat Rev Mol Cell Biol, 2010. **11**(9): p. 621-32.
87. Shamas-Din, A., et al., *Mechanisms of action of Bcl-2 family proteins.* Cold Spring Harb Perspect Biol, 2013. **5**(4): p. a008714.
88. Luna-Vargas, M.P.A. and J.E. Chipuk, *Physiological and Pharmacological Control of BAK, BAX, and Beyond.* Trends Cell Biol, 2016. **26**(12): p. 906-917.
89. Singh, R., A. Letai, and K. Sarosiek, *Regulation of apoptosis in health and disease: the balancing act of BCL-2 family proteins.* Nat Rev Mol Cell Biol, 2019. **20**(3): p. 175-193.
90. Chen, H.C., et al., *An interconnected hierarchical model of cell death regulation by the BCL-2 family.* Nat Cell Biol, 2015. **17**(10): p. 1270-81.
91. Dai, H., et al., *Evaluation of the BH3-only protein Puma as a direct Bak activator.* J Biol Chem, 2014. **289**(1): p. 89-99.
92. Moldoveanu, T., et al., *BID-induced structural changes in BAK promote apoptosis.* Nat Struct Mol Biol, 2013. **20**(5): p. 589-97.
93. Ren, D., et al., *BID, BIM, and PUMA are essential for activation of the BAX- and BAK-dependent cell death program.* Science, 2010. **330**(6009): p. 1390-3.
94. Luo, X., et al., *Bid, a Bcl2 interacting protein, mediates cytochrome c release from mitochondria in response to activation of cell surface death receptors.* Cell, 1998. **94**(4): p. 481-90.
95. O'Neill, K.L., et al., *Inactivation of prosurvival Bcl-2 proteins activates Bax/Bak through the outer mitochondrial membrane.* Genes Dev, 2016. **30**(8): p. 973-88.

96. Cosentino, K. and A.J. García-Sáez, *Bax and Bak Pores: Are We Closing the Circle?* Trends Cell Biol, 2017. **27**(4): p. 266-275.
97. Tait, S.W. and D.R. Green, *Mitochondrial regulation of cell death.* Cold Spring Harb Perspect Biol, 2013. **5**(9).
98. Li, P., et al., *Cytochrome c and dATP-dependent formation of Apaf-1/caspase-9 complex initiates an apoptotic protease cascade.* Cell, 1997. **91**(4): p. 479-89.
99. Julien, O. and J.A. Wells, *Caspases and their substrates.* Cell Death Differ, 2017. **24**(8): p. 1380-1389.
100. Nagata, S., *DNA degradation in development and programmed cell death.* Annu Rev Immunol, 2005. **23**: p. 853-75.
101. Naito, M., et al., *Phosphatidylserine externalization is a downstream event of interleukin-1 beta-converting enzyme family protease activation during apoptosis.* Blood, 1997. **89**(6): p. 2060-6.
102. Martin, S.J., et al., *Phosphatidylserine externalization during CD95-induced apoptosis of cells and cytoplasts requires ICE/CED-3 protease activity.* J Biol Chem, 1996. **271**(46): p. 28753-6.
103. Coleman, M.L., et al., *Membrane blebbing during apoptosis results from caspase-mediated activation of ROCK I.* Nat Cell Biol, 2001. **3**(4): p. 339-45.
104. Du, C., et al., *Smac, a mitochondrial protein that promotes cytochrome c-dependent caspase activation by eliminating IAP inhibition.* Cell, 2000. **102**(1): p. 33-42.
105. Salvesen, G.S. and C.S. Duckett, *IAP proteins: blocking the road to death's door.* Nat Rev Mol Cell Biol, 2002. **3**(6): p. 401-10.
106. Eckelman, B.P., G.S. Salvesen, and F.L. Scott, *Human inhibitor of apoptosis proteins: why XIAP is the black sheep of the family.* EMBO Rep, 2006. **7**(10): p. 988-94.
107. Eckelman, B.P. and G.S. Salvesen, *The human anti-apoptotic proteins cIAP1 and cIAP2 bind but do not inhibit caspases.* J Biol Chem, 2006. **281**(6): p. 3254-60.
108. Segawa, K., et al., *Caspase-mediated cleavage of phospholipid flippase for apoptotic phosphatidylserine exposure.* Science, 2014. **344**(6188): p. 1164-8.
109. Andersen, J.P., et al., *P4-ATPases as Phospholipid Flippases-Structure, Function, and Enigmas.* Front Physiol, 2016. **7**: p. 275.
110. Coleman, J.A. and R.S. Molday, *Critical role of the beta-subunit CDC50A in the stable expression, assembly, subcellular localization, and lipid transport activity of the P4-ATPase ATP8A2.* J Biol Chem, 2011. **286**(19): p. 17205-16.
111. Segawa, K., S. Kurata, and S. Nagata, *Human Type IV P-type ATPases That Work as Plasma Membrane Phospholipid Flippases and Their Regulation by Caspase and Calcium.* J Biol Chem, 2016. **291**(2): p. 762-72.
112. Kornberg, R.D. and H.M. McConnell, *Inside-outside transitions of phospholipids in vesicle membranes.* Biochemistry, 1971. **10**(7): p. 1111-20.
113. Whitlock, J.M. and H.C. Hartzell, *Anoctamins/TMEM16 Proteins: Chloride Channels Flirting with Lipids and Extracellular Vesicles.* Annu Rev Physiol, 2017. **79**: p. 119-143.
114. Nagata, S., *Apoptosis and Clearance of Apoptotic Cells.* Annu Rev Immunol, 2018. **36**: p. 489-517.

115. Bevers, E.M. and P.L. Williamson, *Getting to the Outer Leaflet: Physiology of Phosphatidylserine Exposure at the Plasma Membrane.* Physiol Rev, 2016. **96**(2): p. 605-45.
116. Yu, K., et al., *Identification of a lipid scrambling domain in ANO6/TMEM16F.* Elife, 2015. **4**: p. e06901.
117. Segawa, K. and S. Nagata, *An Apoptotic 'Eat Me' Signal: Phosphatidylserine Exposure.* Trends Cell Biol, 2015. **25**(11): p. 639-650.
118. Fadok, V.A., et al., *Exposure of phosphatidylserine on the surface of apoptotic lymphocytes triggers specific recognition and removal by macrophages.* J Immunol, 1992. **148**(7): p. 2207-16.
119. Krahling, S., et al., *Exposure of phosphatidylserine is a general feature in the phagocytosis of apoptotic lymphocytes by macrophages.* Cell Death Differ, 1999. **6**(2): p. 183-9.
120. Asano, K., et al., *Masking of phosphatidylserine inhibits apoptotic cell engulfment and induces autoantibody production in mice.* J Exp Med, 2004. **200**(4): p. 459-67.
121. Ashkenazi, A. and V.M. Dixit, *Death receptors: signaling and modulation.* Science, 1998. **281**(5381): p. 1305-8.
122. Flusberg, D.A. and P.K. Sorger, *Surviving apoptosis: life-death signaling in single cells.* Trends Cell Biol, 2015. **25**(8): p. 446-58.
123. Gibert, B. and P. Mehlen, *Dependence Receptors and Cancer: Addiction to Trophic Ligands.* Cancer Res, 2015. **75**(24): p. 5171-5.
124. Wajant, H., *The Fas signaling pathway: more than a paradigm.* Science, 2002. **296**(5573): p. 1635-6.
125. Mehlen, P. and D.E. Bredesen, *Dependence receptors: from basic research to drug development.* Sci Signal, 2011. **4**(157): p. mr2.
126. Aggarwal, B.B., S.C. Gupta, and J.H. Kim, *Historical perspectives on tumor necrosis factor and its superfamily: 25 years later, a golden journey.* Blood, 2012. **119**(3): p. 651-65.
127. von Karstedt, S., A. Montinaro, and H. Walczak, *Exploring the TRAILs less travelled: TRAIL in cancer biology and therapy.* Nat Rev Cancer, 2017. **17**(6): p. 352-366.
128. Fleten, K.G., et al., *hvTRA, a novel TRAIL receptor agonist, induces apoptosis and sustained growth retardation in melanoma.* Cell Death Discov, 2016. **2**: p. 16081.
129. Muzio, M., et al., *FLICE, a novel FADD-homologous ICE/CED-3-like protease, is recruited to the CD95 (Fas/APO-1) death--inducing signaling complex.* Cell, 1996. **85**(6): p. 817-27.
130. Dickens, L.S., et al., *The 'complexities' of life and death: death receptor signalling platforms.* Exp Cell Res, 2012. **318**(11): p. 1269-77.
131. Boldin, M.P., et al., *A novel protein that interacts with the death domain of Fas/APO1 contains a sequence motif related to the death domain.* J Biol Chem, 1995. **270**(14): p. 7795-8.
132. Chinnaiyan, A.M., et al., *FADD, a novel death domain-containing protein, interacts with the death domain of Fas and initiates apoptosis.* Cell, 1995. **81**(4): p. 505-12.

133. Scott, F.L., et al., *The Fas-FADD death domain complex structure unravels signalling by receptor clustering.* Nature, 2009. **457**(7232): p. 1019-22.
134. Chan, F.K., et al., *A domain in TNF receptors that mediates ligand-independent receptor assembly and signaling.* Science, 2000. **288**(5475): p. 2351-4.
135. Scaffidi, C., et al., *The role of c-FLIP in modulation of CD95-induced apoptosis.* J Biol Chem, 1999. **274**(3): p. 1541-8.
136. Fu, T.M., et al., *Cryo-EM Structure of Caspase-8 Tandem DED Filament Reveals Assembly and Regulation Mechanisms of the Death-Inducing Signaling Complex.* Mol Cell, 2016. **64**(2): p. 236-250.
137. Dickens, L.S., et al., *A death effector domain chain DISC model reveals a crucial role for caspase-8 chain assembly in mediating apoptotic cell death.* Mol Cell, 2012. **47**(2): p. 291-305.
138. Oberst, A., et al., *Inducible dimerization and inducible cleavage reveal a requirement for both processes in caspase-8 activation.* J Biol Chem, 2010. **285**(22): p. 16632-42.
139. Kallenberger, S.M., et al., *Intra- and interdimeric caspase-8 self-cleavage controls strength and timing of CD95-induced apoptosis.* Sci Signal, 2014. **7**(316): p. ra23.
140. Kavuri, S.M., et al., *Cellular FLICE-inhibitory protein (cFLIP) isoforms block CD95- and TRAIL death receptor-induced gene induction irrespective of processing of caspase-8 or cFLIP in the death-inducing signaling complex.* J Biol Chem, 2011. **286**(19): p. 16631-46.
141. Micheau, O., et al., *The long form of FLIP is an activator of caspase-8 at the Fas death-inducing signaling complex.* J Biol Chem, 2002. **277**(47): p. 45162-71.
142. Chang, D.W., et al., *c-FLIP(L) is a dual function regulator for caspase-8 activation and CD95-mediated apoptosis.* EMBO J, 2002. **21**(14): p. 3704-14.
143. Yu, J.W., P.D. Jeffrey, and Y. Shi, *Mechanism of procaspase-8 activation by c-FLIPL.* Proc Natl Acad Sci U S A, 2009. **106**(20): p. 8169-74.
144. Fricker, N., et al., *Model-based dissection of CD95 signaling dynamics reveals both a pro- and antiapoptotic role of c-FLIPL.* J Cell Biol, 2010. **190**(3): p. 377-89.
145. Hughes, M.A., et al., *Co-operative and Hierarchical Binding of c-FLIP and Caspase-8: A Unified Model Defines How c-FLIP Isoforms Differentially Control Cell Fate.* Mol Cell, 2016. **61**(6): p. 834-49.
146. Schleich, K., et al., *Molecular architecture of the DED chains at the DISC: regulation of procaspase-8 activation by short DED proteins c-FLIP and procaspase-8 prodomain.* Cell Death Differ, 2016. **23**(4): p. 681-94.
147. Barnhart, B.C., E.C. Alappat, and M.E. Peter, *The CD95 type I/type II model.* Semin Immunol, 2003. **15**(3): p. 185-93.
148. Strasser, A., et al., *Bcl-2 and Fas/APO-1 regulate distinct pathways to lymphocyte apoptosis.* EMBO J, 1995. **14**(24): p. 6136-47.
149. Jost, P.J., et al., *XIAP discriminates between type I and type II FAS-induced apoptosis.* Nature, 2009. **460**(7258): p. 1035-9.
150. Gross, A., et al., *Caspase cleaved BID targets mitochondria and is required for cytochrome c release, while BCL-XL prevents this release but not tumor necrosis factor-R1/Fas death.* J Biol Chem, 1999. **274**(2): p. 1156-63.

151. Huang, K., et al., *Cleavage by Caspase 8 and Mitochondrial Membrane Association Activate the BH3-only Protein Bid during TRAIL-induced Apoptosis.* J Biol Chem, 2016. **291**(22): p. 11843-51.
152. O'Donnell, M.A., et al., *Ubiquitination of RIP1 regulates an NF-kappaB-independent cell-death switch in TNF signaling.* Curr Biol, 2007. **17**(5): p. 418-24.
153. Li, H., et al., *Ubiquitination of RIP is required for tumor necrosis factor alpha-induced NF-kappaB activation.* J Biol Chem, 2006. **281**(19): p. 13636-13643.
154. Goldschneider, D. and P. Mehlen, *Dependence receptors: a new paradigm in cell signaling and cancer therapy.* Oncogene, 2010. **29**(13): p. 1865-82.
155. Mehlen, P. and S. Tauszig-Delamasure, *Dependence receptors and colorectal cancer.* Gut, 2014. **63**(11): p. 1821-9.
156. Liu, J., et al., *Mediation of the DCC apoptotic signal by DIP13 alpha.* J Biol Chem, 2002. **277**(29): p. 26281-5.
157. Charras, G.T., et al., *Life and times of a cellular bleb.* Biophys J, 2008. **94**(5): p. 1836-53.
158. Charras, G.T., et al., *Non-equilibration of hydrostatic pressure in blebbing cells.* Nature, 2005. **435**(7040): p. 365-9.
159. Croft, D.R., et al., *Actin-myosin-based contraction is responsible for apoptotic nuclear disintegration.* J Cell Biol, 2005. **168**(2): p. 245-55.
160. Sebbagh, M., et al., *Caspase-3-mediated cleavage of ROCK I induces MLC phosphorylation and apoptotic membrane blebbing.* Nat Cell Biol, 2001. **3**(4): p. 346-52.
161. Orlando, K.A., N.L. Stone, and R.N. Pittman, *Rho kinase regulates fragmentation and phagocytosis of apoptotic cells.* Exp Cell Res, 2006. **312**(1): p. 5-15.
162. Orlando, K.A. and R.N. Pittman, *Rho kinase regulates phagocytosis, surface expression of GlcNAc, and Golgi fragmentation of apoptotic PC12 cells.* Exp Cell Res, 2006. **312**(17): p. 3298-311.
163. Witasp, E., et al., *Bridge over troubled water: milk fat globule epidermal growth factor 8 promotes human monocyte-derived macrophage clearance of non-blebbing phosphatidylserine-positive target cells.* Cell Death Differ, 2007. **14**(5): p. 1063-5.
164. Pace, K.E., et al., *Restricted receptor segregation into membrane microdomains occurs on human T cells during apoptosis induced by galectin-1.* J Immunol, 1999. **163**(7): p. 3801-11.
165. Korb, L.C. and J.M. Ahearn, *C1q binds directly and specifically to surface blebs of apoptotic human keratinocytes: complement deficiency and systemic lupus erythematosus revisited.* J Immunol, 1997. **158**(10): p. 4525-8.
166. Navratil, J.S., et al., *The globular heads of C1q specifically recognize surface blebs of apoptotic vascular endothelial cells.* J Immunol, 2001. **166**(5): p. 3231-9.
167. Ogden, C.A., et al., *C1q and mannose binding lectin engagement of cell surface calreticulin and CD91 initiates macropinocytosis and uptake of apoptotic cells.* J Exp Med, 2001. **194**(6): p. 781-95.

168. Maas, S.L.N., X.O. Breakefield, and A.M. Weaver, *Extracellular Vesicles: Unique Intercellular Delivery Vehicles.* Trends Cell Biol, 2017. **27**(3): p. 172-188.
169. Barros, F.M., et al., *Exosomes and Immune Response in Cancer: Friends or Foes?* Front Immunol, 2018. **9**: p. 730.
170. Mashouri, L., et al., *Exosomes: composition, biogenesis, and mechanisms in cancer metastasis and drug resistance.* Mol Cancer, 2019. **18**(1): p. 75.
171. Wickman, G.R., et al., *Blebs produced by actin-myosin contraction during apoptosis release damage-associated molecular pattern proteins before secondary necrosis occurs.* Cell Death Differ, 2013. **20**(10): p. 1293-305.
172. Schiller, M., et al., *Induction of type I IFN is a physiological immune reaction to apoptotic cell-derived membrane microparticles.* J Immunol, 2012. **189**(4): p. 1747-56.
173. Lötvall, J., et al., *Minimal experimental requirements for definition of extracellular vesicles and their functions: a position statement from the International Society for Extracellular Vesicles.* J Extracell Vesicles, 2014. **3**: p. 26913.
174. Winau, F., et al., *Apoptotic vesicles crossprime CD8 T cells and protect against tuberculosis.* Immunity, 2006. **24**(1): p. 105-17.
175. Kowal, J., et al., *Proteomic comparison defines novel markers to characterize heterogeneous populations of extracellular vesicle subtypes.* Proc Natl Acad Sci U S A, 2016. **113**(8): p. E968-77.
176. Tixeira, R. and I.K.H. Poon, *Disassembly of dying cells in diverse organisms.* Cell Mol Life Sci, 2019. **76**(2): p. 245-257.
177. Kakarla, R., et al., *Apoptotic cell-derived exosomes: messages from dying cells.* Exp Mol Med, 2020. **52**(1): p. 1-6.
178. Pérez-Garijo, A. and H. Steller, *Spreading the word: non-autonomous effects of apoptosis during development, regeneration and disease.* Development, 2015. **142**(19): p. 3253-62.
179. Atkin-Smith, G.K., et al., *A novel mechanism of generating extracellular vesicles during apoptosis via a beads-on-a-string membrane structure.* Nat Commun, 2015. **6**: p. 7439.
180. Poon, I.K., et al., *Apoptotic cell clearance: basic biology and therapeutic potential.* Nat Rev Immunol, 2014. **14**(3): p. 166-80.
181. Caruso, S. and I.K.H. Poon, *Apoptotic Cell-Derived Extracellular Vesicles: More Than Just Debris.* Front Immunol, 2018. **9**: p. 1486.
182. Park, S.J., et al., *Molecular mechanisms of biogenesis of apoptotic exosome-like vesicles and their roles as damage-associated molecular patterns.* Proc Natl Acad Sci U S A, 2018. **115**(50): p. E11721-E11730.
183. Zhu, M., et al., *Mitochondria Released by Apoptotic Cell Death Initiate Innate Immune Responses.* Immunohorizons, 2018. **2**(11): p. 384-397.
184. Sierra, A., et al., *Microglia shape adult hippocampal neurogenesis through apoptosis-coupled phagocytosis.* Cell Stem Cell, 2010. **7**(4): p. 483-95.
185. Fourgeaud, L., et al., *TAM receptors regulate multiple features of microglial physiology.* Nature, 2016. **532**(7598): p. 240-244.

186. McGaha, T.L. and M.C. Karlsson, *Apoptotic cell responses in the splenic marginal zone: a paradigm for immunologic reactions to apoptotic antigens with implications for autoimmunity.* Immunol Rev, 2016. **269**(1): p. 26-43.
187. Peter, C., et al., *Dangerous attraction: phagocyte recruitment and danger signals of apoptotic and necrotic cells.* Apoptosis, 2010. **15**(9): p. 1007-28.
188. Medina, C.B. and K.S. Ravichandran, *Do not let death do us part: 'find-me' signals in communication between dying cells and the phagocytes.* Cell Death Differ, 2016. **23**(6): p. 979-89.
189. Lauber, K., et al., *Apoptotic cells induce migration of phagocytes via caspase-3-mediated release of a lipid attraction signal.* Cell, 2003. **113**(6): p. 717-30.
190. Peter, C., et al., *Migration to apoptotic "find-me" signals is mediated via the phagocyte receptor G2A.* J Biol Chem, 2008. **283**(9): p. 5296-305.
191. Gude, D.R., et al., *Apoptosis induces expression of sphingosine kinase 1 to release sphingosine-1-phosphate as a "come-and-get-me" signal.* FASEB J, 2008. **22**(8): p. 2629-38.
192. Elliott, M.R., et al., *Nucleotides released by apoptotic cells act as a find-me signal to promote phagocytic clearance.* Nature, 2009. **461**(7261): p. 282-6.
193. Truman, L.A., et al., *CX3CL1/fractalkine is released from apoptotic lymphocytes to stimulate macrophage chemotaxis.* Blood, 2008. **112**(13): p. 5026-36.
194. Yang, L.V., et al., *Gi-independent macrophage chemotaxis to lysophosphatidylcholine via the immunoregulatory GPCR G2A.* Blood, 2005. **105**(3): p. 1127-34.
195. Idzko, M., D. Ferrari, and H.K. Eltzschig, *Nucleotide signalling during inflammation.* Nature, 2014. **509**(7500): p. 310-7.
196. Haynes, S.E., et al., *The P2Y12 receptor regulates microglial activation by extracellular nucleotides.* Nat Neurosci, 2006. **9**(12): p. 1512-9.
197. Ohsawa, K., et al., *P2Y12 receptor-mediated integrin-beta1 activation regulates microglial process extension induced by ATP.* Glia, 2010. **58**(7): p. 790-801.
198. Gao, A.G., et al., *Integrin-associated protein is a receptor for the C-terminal domain of thrombospondin.* J Biol Chem, 1996. **271**(1): p. 21-4.
199. Brown, E.J. and W.A. Frazier, *Integrin-associated protein (CD47) and its ligands.* Trends Cell Biol, 2001. **11**(3): p. 130-5.
200. Oldenborg, P.A., et al., *Role of CD47 as a marker of self on red blood cells.* Science, 2000. **288**(5473): p. 2051-4.
201. Barclay, A.N. and T.K. Van den Berg, *The interaction between signal regulatory protein alpha (SIRPα) and CD47: structure, function, and therapeutic target.* Annu Rev Immunol, 2014. **32**: p. 25-50.
202. Jaiswal, S., et al., *CD47 is upregulated on circulating hematopoietic stem cells and leukemia cells to avoid phagocytosis.* Cell, 2009. **138**(2): p. 271-85.
203. Majeti, R., et al., *CD47 is an adverse prognostic factor and therapeutic antibody target on human acute myeloid leukemia stem cells.* Cell, 2009. **138**(2): p. 286-99.
204. Kim, D., et al., *Anti-CD47 antibodies promote phagocytosis and inhibit the growth of human myeloma cells.* Leukemia, 2012. **26**(12): p. 2538-45.

205. Theocharides, A.P., et al., *Disruption of SIRPα signaling in macrophages eliminates human acute myeloid leukemia stem cells in xenografts.* J Exp Med, 2012. **209**(10): p. 1883-99.
206. Chao, M.P., et al., *Anti-CD47 antibody synergizes with rituximab to promote phagocytosis and eradicate non-Hodgkin lymphoma.* Cell, 2010. **142**(5): p. 699-713.
207. Horrigan, S.K. and R.P.C. Biology, *Replication Study: The CD47-signal regulatory protein alpha (SIRPa) interaction is a therapeutic target for human solid tumors.* Elife, 2017. **6**.
208. Russ, A., et al., *Blocking "don't eat me" signal of CD47-SIRPα in hematological malignancies, an in-depth review.* Blood Rev, 2018. **32**(6): p. 480-489.
209. Martin, M. and A.M. Blom, *Complement in removal of the dead - balancing inflammation.* Immunol Rev, 2016. **274**(1): p. 218-232.
210. Kenyon, K.D., et al., *IgG autoantibodies against deposited C3 inhibit macrophage-mediated apoptotic cell engulfment in systemic autoimmunity.* J Immunol, 2011. **187**(5): p. 2101-11.
211. Hanayama, R., et al., *Identification of a factor that links apoptotic cells to phagocytes.* Nature, 2002. **417**(6885): p. 182-7.
212. Murakami, Y., et al., *CD300b regulates the phagocytosis of apoptotic cells via phosphatidylserine recognition.* Cell Death Differ, 2014. **21**(11): p. 1746-57.
213. Lemke, G., *How macrophages deal with death.* Nat Rev Immunol, 2019. **19**(9): p. 539-549.
214. Freeman, G.J., et al., *TIM genes: a family of cell surface phosphatidylserine receptors that regulate innate and adaptive immunity.* Immunol Rev, 2010. **235**(1): p. 172-89.
215. Lemke, G. and C.V. Rothlin, *Immunobiology of the TAM receptors.* Nat Rev Immunol, 2008. **8**(5): p. 327-36.
216. Lew, E.D., et al., *Differential TAM receptor-ligand-phospholipid interactions delimit differential TAM bioactivities.* Elife, 2014. **3**.
217. Stitt, T.N., et al., *The anticoagulation factor protein S and its relative, Gas6, are ligands for the Tyro 3/Axl family of receptor tyrosine kinases.* Cell, 1995. **80**(4): p. 661-70.
218. Lemke, G., *Phosphatidylserine Is the Signal for TAM Receptors and Their Ligands.* Trends Biochem Sci, 2017. **42**(9): p. 738-748.
219. Tsou, W.I., et al., *Receptor tyrosine kinases, TYRO3, AXL, and MER, demonstrate distinct patterns and complex regulation of ligand-induced activation.* J Biol Chem, 2014. **289**(37): p. 25750-63.
220. Gautier, E.L., et al., *Gene-expression profiles and transcriptional regulatory pathways that underlie the identity and diversity of mouse tissue macrophages.* Nat Immunol, 2012. **13**(11): p. 1118-28.
221. Consortium, I., *Open-source ImmGen: mononuclear phagocytes.* Nat Immunol, 2016. **17**(7): p. 741.
222. Scott, R.S., et al., *Phagocytosis and clearance of apoptotic cells is mediated by MER.* Nature, 2001. **411**(6834): p. 207-11.
223. Grabiec, A.M., et al., *Axl and MerTK receptor tyrosine kinases maintain human macrophage efferocytic capacity in the presence of viral triggers.* Eur J Immunol, 2018. **48**(5): p. 855-860.

224. Thorp, E., et al., *Mertk receptor mutation reduces efferocytosis efficiency and promotes apoptotic cell accumulation and plaque necrosis in atherosclerotic lesions of apoe-/- mice.* Arterioscler Thromb Vasc Biol, 2008. **28**(8): p. 1421-8.
225. Toda, S., K. Segawa, and S. Nagata, *MerTK-mediated engulfment of pyrenocytes by central macrophages in erythroblastic islands.* Blood, 2014. **123**(25): p. 3963-71.
226. Zagórska, A., et al., *Diversification of TAM receptor tyrosine kinase function.* Nat Immunol, 2014. **15**(10): p. 920-8.
227. Chan, P.Y., et al., *The TAM family receptor tyrosine kinase TYRO3 is a negative regulator of type 2 immunity.* Science, 2016. **352**(6281): p. 99-103.
228. Lu, Q., et al., *Tyro-3 family receptors are essential regulators of mammalian spermatogenesis.* Nature, 1999. **398**(6729): p. 723-8.
229. Lu, Q. and G. Lemke, *Homeostatic regulation of the immune system by receptor tyrosine kinases of the Tyro 3 family.* Science, 2001. **293**(5528): p. 306-11.
230. Khan, T.N., et al., *Prolonged apoptotic cell accumulation in germinal centers of Mer-deficient mice causes elevated B cell and CD4+ Th cell responses leading to autoantibody production.* J Immunol, 2013. **190**(4): p. 1433-46.
231. Rothlin, C.V., et al., *TAM receptor signaling in immune homeostasis.* Annu Rev Immunol, 2015. **33**: p. 355-91.
232. Rothlin, C.V., et al., *TAM receptors are pleiotropic inhibitors of the innate immune response.* Cell, 2007. **131**(6): p. 1124-36.
233. A-Gonzalez, N., et al., *Apoptotic cells promote their own clearance and immune tolerance through activation of the nuclear receptor LXR.* Immunity, 2009. **31**(2): p. 245-58.
234. Wallet, M.A., et al., *MerTK is required for apoptotic cell-induced T cell tolerance.* J Exp Med, 2008. **205**(1): p. 219-32.
235. Meyers, J.H., et al., *TIM-4 is the ligand for TIM-1, and the TIM-1-TIM-4 interaction regulates T cell proliferation.* Nat Immunol, 2005. **6**(5): p. 455-64.
236. Wong, K., et al., *Phosphatidylserine receptor Tim-4 is essential for the maintenance of the homeostatic state of resident peritoneal macrophages.* Proc Natl Acad Sci U S A, 2010. **107**(19): p. 8712-7.
237. Kobayashi, N., et al., *TIM-1 and TIM-4 glycoproteins bind phosphatidylserine and mediate uptake of apoptotic cells.* Immunity, 2007. **27**(6): p. 927-40.
238. Zhang, Q., et al., *TIM-4 promotes the growth of non-small-cell lung cancer in a RGD motif-dependent manner.* Br J Cancer, 2015. **113**(10): p. 1484-92.
239. Tan, X., et al., *Tim-4 promotes the growth of colorectal cancer by activating angiogenesis and recruiting tumor-associated macrophages via the PI3K/AKT/mTOR signaling pathway.* Cancer Lett, 2018. **436**: p. 119-128.
240. Dorfman, D.M., et al., *The phosphatidylserine receptors, T cell immunoglobulin mucin proteins 3 and 4, are markers of histiocytic sarcoma and other histiocytic and dendritic cell neoplasms.* Hum Pathol, 2010. **41**(10): p. 1486-94.
241. Miyanishi, M., et al., *Identification of Tim4 as a phosphatidylserine receptor.* Nature, 2007. **450**(7168): p. 435-9.
242. Kim, H.S., C.W. Lee, and D.H. Chung, *T cell Ig domain and mucin domain 1 engagement on invariant NKT cells in the presence of TCR stimulation*

enhances IL-4 production but inhibits IFN-gamma production. J Immunol, 2010. **184**(8): p. 4095-106.
243. Xu, L.Y., et al., *Tim-4 Inhibits NO Generation by Murine Macrophages.* PLoS One, 2015. **10**(4): p. e0124771.
244. Xu, L., et al., *T cell immunoglobulin- and mucin-domain-containing molecule-4 attenuates concanavalin A-induced hepatitis by regulating macrophage.* J Leukoc Biol, 2010. **88**(2): p. 329-36.
245. Baghdadi, M., et al., *TIM-4 glycoprotein-mediated degradation of dying tumor cells by autophagy leads to reduced antigen presentation and increased immune tolerance.* Immunity, 2013. **39**(6): p. 1070-81.
246. Yang, B., et al., *Probiotics SOD inhibited food allergy via downregulation of STAT6-TIM4 signaling on DCs.* Mol Immunol, 2018. **103**: p. 71-77.
247. Liu, Z.Q., et al., *Vitamin D regulates immunoglobulin mucin domain molecule-4 expression in dendritic cells.* Clin Exp Allergy, 2017. **47**(5): p. 656-664.
248. Abe, Y., et al., *TIM-4 has dual function in the induction and effector phases of murine arthritis.* J Immunol, 2013. **191**(9): p. 4562-72.
249. Mizui, M., et al., *Bimodal regulation of T cell-mediated immune responses by TIM-4.* Int Immunol, 2008. **20**(5): p. 695-708.
250. Yanagihashi, Y., et al., *Mouse macrophages show different requirements for phosphatidylserine receptor Tim4 in efferocytosis.* Proc Natl Acad Sci U S A, 2017. **114**(33): p. 8800-8805.
251. Park, D., A. Hochreiter-Hufford, and K.S. Ravichandran, *The phosphatidylserine receptor TIM-4 does not mediate direct signaling.* Curr Biol, 2009. **19**(4): p. 346-51.
252. Flannagan, R.S., et al., *The phosphatidylserine receptor TIM4 utilizes integrins as coreceptors to effect phagocytosis.* Mol Biol Cell, 2014. **25**(9): p. 1511-22.
253. Lee, J., et al., *A scaffold for signaling of Tim-4-mediated efferocytosis is formed by fibronectin.* Cell Death Differ, 2019. **26**(9): p. 1646-1655.
254. Chae, S.C., et al., *The association of the exon 4 variations of Tim-1 gene with allergic diseases in a Korean population.* Biochem Biophys Res Commun, 2003. **312**(2): p. 346-50.
255. Liu, Q., et al., *A functional polymorphism in the TIM-1 gene is associated with asthma in a Chinese Han population.* Int Arch Allergy Immunol, 2007. **144**(3): p. 197-202.
256. Cai, P.C., et al., *Association of TIM4 promoter polymorphism -1419G>A with childhood asthma in a Chinese Han population.* Tissue Antigens, 2009. **74**(1): p. 11-6.
257. Xu, L., et al., *Cockroach allergen Bla g 7 promotes TIM4 expression in dendritic cells leading to Th2 polarization.* Mediators Inflamm, 2013. **2013**: p. 983149.
258. Feng, B.S., et al., *Disruption of T-cell immunoglobulin and mucin domain molecule (TIM)-1/TIM4 interaction as a therapeutic strategy in a dendritic cell-induced peanut allergy model.* J Allergy Clin Immunol, 2008. **122**(1): p. 55-61, 61.e1-7.
259. Aprahamian, T., et al., *Impaired clearance of apoptotic cells promotes synergy between atherogenesis and autoimmune disease.* J Exp Med, 2004. **199**(8): p. 1121-31.

260. Muñoz, L.E., et al., *The role of defective clearance of apoptotic cells in systemic autoimmunity.* Nat Rev Rheumatol, 2010. **6**(5): p. 280-9.
261. Fang, X.Y., et al., *Novel insights into Tim-4 function in autoimmune diseases.* Autoimmunity, 2015. **48**(4): p. 189-95.
262. Xu, J., et al., *Genetic variation and significant association of polymorphism rs7700944 G>A of TIM-4 gene with rheumatoid arthritis susceptibility in Chinese Han and Hui populations.* Int J Immunogenet, 2012. **39**(5): p. 409-13.
263. Mosaad, Y.M., et al., *TIM-1 rs41297579 G>A (-1454) and TIM-4 rs7700944 gene polymorphisms as possible risk factor for rheumatoid arthritis: relation to activity and severity.* Int J Immunogenet, 2015. **42**(4): p. 254-64.
264. Zakeri, Z., et al., *Association between the rs7700944 polymorphism in the TIM-4 gene and rheumatoid arthritis in Zahedan, southeast Iran.* Rev Bras Reumatol, 2013. **53**(4): p. 341-5.
265. Zhao, P., et al., *Increased expression of human T-cell immunoglobulin- and mucin-domain-containing molecule-4 in peripheral blood mononuclear cells from patients with system lupus erythematosus.* Cell Mol Immunol, 2010. **7**(2): p. 152-6.
266. Miyanishi, M., K. Segawa, and S. Nagata, *Synergistic effect of Tim4 and MFG-E8 null mutations on the development of autoimmunity.* Int Immunol, 2012. **24**(9): p. 551-9.
267. Rodriguez-Manzanet, R., et al., *T and B cell hyperactivity and autoimmunity associated with niche-specific defects in apoptotic body clearance in TIM-4-deficient mice.* Proc Natl Acad Sci U S A, 2010. **107**(19): p. 8706-11.
268. Rhodes, B. and T.J. Vyse, *General aspects of the genetics of SLE.* Autoimmunity, 2007. **40**(8): p. 550-9.
269. Albacker, L.A., et al., *TIM-4, a receptor for phosphatidylserine, controls adaptive immunity by regulating the removal of antigen-specific T cells.* J Immunol, 2010. **185**(11): p. 6839-49.
270. Xu, L., et al., *Glioma-derived T cell immunoglobulin- and mucin domain-containing molecule-4 (TIM4) contributes to tumor tolerance.* J Biol Chem, 2011. **286**(42): p. 36694-9.
271. Etzerodt, A., et al., *Tissue-resident macrophages in omentum promote metastatic spread of ovarian cancer.* J Exp Med, 2020. **217**(4).
272. Baghdadi, M., et al., *Combined blockade of TIM-3 and TIM-4 augments cancer vaccine efficacy against established melanomas.* Cancer Immunol Immunother, 2013. **62**(4): p. 629-37.
273. Caronni, N., et al., *TIM4 expression by dendritic cells mediates uptake of tumor-associated antigens and anti-tumor responses.* Nat Commun, 2021. **12**(1): p. 2237.
274. Chow, A., et al., *Tim-4.* Cancer Cell, 2021. **39**(7): p. 973-988.e9.
275. Rabinovitch, M., *Professional and non-professional phagocytes: an introduction.* Trends Cell Biol, 1995. **5**(3): p. 85-7.
276. Uribe-Querol, E. and C. Rosales, *Phagocytosis: Our Current Understanding of a Universal Biological Process.* Front Immunol, 2020. **11**: p. 1066.
277. Freeman, S.A. and S. Grinstein, *Phagocytosis: receptors, signal integration, and the cytoskeleton.* Immunol Rev, 2014. **262**(1): p. 193-215.

278. Levin, R., S. Grinstein, and J. Canton, *The life cycle of phagosomes: formation, maturation, and resolution.* Immunol Rev, 2016. **273**(1): p. 156-79.
279. Elliott, M.R. and K.S. Ravichandran, *The Dynamics of Apoptotic Cell Clearance.* Dev Cell, 2016. **38**(2): p. 147-60.
280. Hochreiter-Hufford, A. and K.S. Ravichandran, *Clearing the dead: apoptotic cell sensing, recognition, engulfment, and digestion.* Cold Spring Harb Perspect Biol, 2013. **5**(1): p. a008748.
281. Henson, P.M., D.L. Bratton, and V.A. Fadok, *Apoptotic cell removal.* Curr Biol, 2001. **11**(19): p. R795-805.
282. Gheibi Hayat, S.M., et al., *Efferocytosis: molecular mechanisms and pathophysiological perspectives.* Immunol Cell Biol, 2019. **97**(2): p. 124-133.
283. Vandivier, R.W., P.M. Henson, and I.S. Douglas, *Burying the dead: the impact of failed apoptotic cell removal (efferocytosis) on chronic inflammatory lung disease.* Chest, 2006. **129**(6): p. 1673-82.
284. Sarode, G.S., *Efferocytosis in oral squamous cell carcinoma.* J Oral Maxillofac Pathol, 2016. **20**(2): p. 170-2.
285. Tao, H., et al., *Macrophage SR-BI mediates efferocytosis via Src/PI3K/Rac1 signaling and reduces atherosclerotic lesion necrosis.* J Lipid Res, 2015. **56**(8): p. 1449-60.
286. Proto, J.D., et al., *Regulatory T Cells Promote Macrophage Efferocytosis during Inflammation Resolution.* Immunity, 2018. **49**(4): p. 666-677.e6.
287. Kinchen, J.M. and K.S. Ravichandran, *Phagosome maturation: going through the acid test.* Nat Rev Mol Cell Biol, 2008. **9**(10): p. 781-95.
288. Kinchen, J.M., et al., *A pathway for phagosome maturation during engulfment of apoptotic cells.* Nat Cell Biol, 2008. **10**(5): p. 556-66.
289. Gorvel, J.P., et al., *rab5 controls early endosome fusion in vitro.* Cell, 1991. **64**(5): p. 915-25.
290. Simonsen, A., et al., *The Rab5 effector EEA1 interacts directly with syntaxin-6.* J Biol Chem, 1999. **274**(41): p. 28857-60.
291. Chen, Y.A. and R.H. Scheller, *SNARE-mediated membrane fusion.* Nat Rev Mol Cell Biol, 2001. **2**(2): p. 98-106.
292. Flannagan, R.S., V. Jaumouillé, and S. Grinstein, *The cell biology of phagocytosis.* Annu Rev Pathol, 2012. **7**: p. 61-98.
293. Harrison, R.E., et al., *Phagosomes fuse with late endosomes and/or lysosomes by extension of membrane protrusions along microtubules: role of Rab7 and RILP.* Mol Cell Biol, 2003. **23**(18): p. 6494-506.
294. Li, B., et al., *The melanoma-associated transmembrane glycoprotein Gpnmb controls trafficking of cellular debris for degradation and is essential for tissue repair.* FASEB J, 2010. **24**(12): p. 4767-81.
295. Yin, C. and B. Heit, *Cellular Responses to the Efferocytosis of Apoptotic Cells.* Front Immunol, 2021. **12**: p. 631714.
296. Sanjuan, M.A., et al., *Toll-like receptor signalling in macrophages links the autophagy pathway to phagocytosis.* Nature, 2007. **450**(7173): p. 1253-7.
297. Ellson, C.D., et al., *Phosphatidylinositol 3-phosphate is generated in phagosomal membranes.* Curr Biol, 2001. **11**(20): p. 1631-5.

298. Asare, P.F., et al., *LC3-Associated Phagocytosis (LAP): A Potentially Influential Mediator of Efferocytosis-Related Tumor Progression and Aggressiveness.* Front Oncol, 2020. **10**: p. 1298.
299. Martinez, J., et al., *Noncanonical autophagy inhibits the autoinflammatory, lupus-like response to dying cells.* Nature, 2016. **533**(7601): p. 115-9.
300. Martinez, J., et al., *Molecular characterization of LC3-associated phagocytosis reveals distinct roles for Rubicon, NOX2 and autophagy proteins.* Nat Cell Biol, 2015. **17**(7): p. 893-906.
301. Bhargava, H.K., et al., *Structural basis for autophagy inhibition by the human Rubicon-Rab7 complex.* Proc Natl Acad Sci U S A, 2020. **117**(29): p. 17003-17010.
302. Wong, S.W., P. Sil, and J. Martinez, *Rubicon: LC3-associated phagocytosis and beyond.* FEBS J, 2018. **285**(8): p. 1379-1388.
303. Cunha, L.D., et al., *LC3-Associated Phagocytosis in Myeloid Cells Promotes Tumor Immune Tolerance.* Cell, 2018. **175**(2): p. 429-441.e16.
304. Rai, S., et al., *The ATG5-binding and coiled coil domains of ATG16L1 maintain autophagy and tissue homeostasis in mice independently of the WD domain required for LC3-associated phagocytosis.* Autophagy, 2019. **15**(4): p. 599-612.
305. Joseph, S.B., et al., *Reciprocal regulation of inflammation and lipid metabolism by liver X receptors.* Nat Med, 2003. **9**(2): p. 213-9.
306. Heming, M., et al., *Peroxisome Proliferator-Activated Receptor-γ Modulates the Response of Macrophages to Lipopolysaccharide and Glucocorticoids.* Front Immunol, 2018. **9**: p. 893.
307. Zhong, X., et al., *Myc-nick promotes efferocytosis through M2 macrophage polarization during resolution of inflammation.* FASEB J, 2018. **32**(10): p. 5312-5325.
308. Zhou, Y., et al., *Blockade of the Phagocytic Receptor MerTK on Tumor-Associated Macrophages Enhances P2X7R-Dependent STING Activation by Tumor-Derived cGAMP.* Immunity, 2020. **52**(2): p. 357-373.e9.
309. Woo, S.R., et al., *STING-dependent cytosolic DNA sensing mediates innate immune recognition of immunogenic tumors.* Immunity, 2014. **41**(5): p. 830-42.
310. Mosmann, T.R., et al., *Two types of murine helper T cell clone. I. Definition according to profiles of lymphokine activities and secreted proteins.* J Immunol, 1986. **136**(7): p. 2348-57.
311. Mosmann, T.R. and R.L. Coffman, *TH1 and TH2 cells: different patterns of lymphokine secretion lead to different functional properties.* Annu Rev Immunol, 1989. **7**: p. 145-73.
312. Mantovani, A., et al., *Macrophage polarization: tumor-associated macrophages as a paradigm for polarized M2 mononuclear phagocytes.* Trends Immunol, 2002. **23**(11): p. 549-55.
313. Guha, M. and N. Mackman, *LPS induction of gene expression in human monocytes.* Cell Signal, 2001. **13**(2): p. 85-94.
314. Trinchieri, G., *Interleukin-12 and the regulation of innate resistance and adaptive immunity.* Nat Rev Immunol, 2003. **3**(2): p. 133-46.

315. Martinez, F.O., et al., *Transcriptional profiling of the human monocyte-to-macrophage differentiation and polarization: new molecules and patterns of gene expression.* J Immunol, 2006. **177**(10): p. 7303-11.
316. Mantovani, A., A. Sica, and M. Locati, *Macrophage polarization comes of age.* Immunity, 2005. **23**(4): p. 344-6.
317. Mantovani, A., et al., *The chemokine system in diverse forms of macrophage activation and polarization.* Trends Immunol, 2004. **25**(12): p. 677-86.
318. Gruenheid, S. and P. Gros, *Genetic susceptibility to intracellular infections: Nramp1, macrophage function and divalent cations transport.* Curr Opin Microbiol, 2000. **3**(1): p. 43-8.
319. MacMicking, J., Q.W. Xie, and C. Nathan, *Nitric oxide and macrophage function.* Annu Rev Immunol, 1997. **15**: p. 323-50.
320. Janeway, C.A. and R. Medzhitov, *Innate immune recognition.* Annu Rev Immunol, 2002. **20**: p. 197-216.
321. Mukhopadhyay, S., L. Peiser, and S. Gordon, *Activation of murine macrophages by Neisseria meningitidis and IFN-gamma in vitro: distinct roles of class A scavenger and Toll-like pattern recognition receptors in selective modulation of surface phenotype.* J Leukoc Biol, 2004. **76**(3): p. 577-84.
322. Mukhopadhyay, S., et al., *MARCO, an innate activation marker of macrophages, is a class A scavenger receptor for Neisseria meningitidis.* Eur J Immunol, 2006. **36**(4): p. 940-9.
323. Stein, M., et al., *Interleukin 4 potently enhances murine macrophage mannose receptor activity: a marker of alternative immunologic macrophage activation.* J Exp Med, 1992. **176**(1): p. 287-92.
324. Wang, J., et al., *Cytokine regulation of human immunodeficiency virus type 1 entry and replication in human monocytes/macrophages through modulation of CCR5 expression.* J Virol, 1998. **72**(9): p. 7642-7.
325. Chizzolini, C., et al., *Th2 cell membrane factors in association with IL-4 enhance matrix metalloproteinase-1 (MMP-1) while decreasing MMP-9 production by granulocyte-macrophage colony-stimulating factor-differentiated human monocytes.* J Immunol, 2000. **164**(11): p. 5952-60.
326. Gratchev, A., et al., *Alternatively activated macrophages differentially express fibronectin and its splice variants and the extracellular matrix protein betaIG-H3.* Scand J Immunol, 2001. **53**(4): p. 386-92.
327. Töröcsik, D., et al., *Identification of factor XIII-A as a marker of alternative macrophage activation.* Cell Mol Life Sci, 2005. **62**(18): p. 2132-9.
328. Modolell, M., et al., *Reciprocal regulation of the nitric oxide synthase/arginase balance in mouse bone marrow-derived macrophages by TH1 and TH2 cytokines.* Eur J Immunol, 1995. **25**(4): p. 1101-4.
329. Hesse, M., et al., *Differential regulation of nitric oxide synthase-2 and arginase-1 by type 1/type 2 cytokines in vivo: granulomatous pathology is shaped by the pattern of L-arginine metabolism.* J Immunol, 2001. **167**(11): p. 6533-44.
330. Sutterwala, F.S., et al., *Reversal of proinflammatory responses by ligating the macrophage Fcgamma receptor type I.* J Exp Med, 1998. **188**(1): p. 217-22.

331. Bowie, A. and L.A. O'Neill, *The interleukin-1 receptor/Toll-like receptor superfamily: signal generators for pro-inflammatory interleukins and microbial products.* J Leukoc Biol, 2000. **67**(4): p. 508-14.
332. Anderson, C.F. and D.M. Mosser, *A novel phenotype for an activated macrophage: the type 2 activated macrophage.* J Leukoc Biol, 2002. **72**(1): p. 101-6.
333. Wu, W., R.D. Mosteller, and D. Broek, *Sphingosine kinase protects lipopolysaccharide-activated macrophages from apoptosis.* Mol Cell Biol, 2004. **24**(17): p. 7359-69.
334. Edwards, J.P., et al., *Biochemical and functional characterization of three activated macrophage populations.* J Leukoc Biol, 2006. **80**(6): p. 1298-307.
335. Bogdan, C., et al., *Contrasting mechanisms for suppression of macrophage cytokine release by transforming growth factor-beta and interleukin-10.* J Biol Chem, 1992. **267**(32): p. 23301-8.
336. Valledor, A.F. and M. Ricote, *Nuclear receptor signaling in macrophages.* Biochem Pharmacol, 2004. **67**(2): p. 201-12.
337. Allavena, P., et al., *The chemokine receptor switch paradigm and dendritic cell migration: its significance in tumor tissues.* Immunol Rev, 2000. **177**: p. 141-9.
338. Sica, A., A. Saccani, and A. Mantovani, *Tumor-associated macrophages: a molecular perspective.* Int Immunopharmacol, 2002. **2**(8): p. 1045-54.
339. Klimp, A.H., et al., *Expression of cyclooxygenase-2 and inducible nitric oxide synthase in human ovarian tumors and tumor-associated macrophages.* Cancer Res, 2001. **61**(19): p. 7305-9.
340. Vicari, A.P. and C. Caux, *Chemokines in cancer.* Cytokine Growth Factor Rev, 2002. **13**(2): p. 143-54.
341. Hotchkiss, K.A., et al., *Mechanisms by which tumor cells and monocytes expressing the angiogenic factor thymidine phosphorylase mediate human endothelial cell migration.* Cancer Res, 2003. **63**(2): p. 527-33.
342. Drolle, H., et al., *Hypoxia regulates proliferation of acute myeloid leukemia and sensitivity against chemotherapy.* Leuk Res, 2015. **39**(7): p. 779-85.
343. Mayani, H., *Hematopoietic and microenvironment alterations in bone marrow from patients with multiple myeloma.* Leuk Res, 2013. **37**(2): p. 228-9.
344. Hazlehurst, L.A., et al., *Genotypic and phenotypic comparisons of de novo and acquired melphalan resistance in an isogenic multiple myeloma cell line model.* Cancer Res, 2003. **63**(22): p. 7900-6.
345. Hideshima, T., et al., *Advances in biology of multiple myeloma: clinical applications.* Blood, 2004. **104**(3): p. 607-18.
346. Kawano, Y., et al., *Targeting the bone marrow microenvironment in multiple myeloma.* Immunol Rev, 2015. **263**(1): p. 160-72.
347. Vacca, A., et al., *Endothelial cells in the bone marrow of patients with multiple myeloma.* Blood, 2003. **102**(9): p. 3340-8.
348. Döhner, H., D.J. Weisdorf, and C.D. Bloomfield, *Acute Myeloid Leukemia.* N Engl J Med, 2015. **373**(12): p. 1136-52.
349. Behrmann, L., J. Wellbrock, and W. Fiedler, *Acute Myeloid Leukemia and the Bone Marrow Niche-Take a Closer Look.* Front Oncol, 2018. **8**: p. 444.

350. Tesfai, Y., et al., *Interactions between acute lymphoblastic leukemia and bone marrow stromal cells influence response to therapy.* Leuk Res, 2012. **36**(3): p. 299-306.
351. Iwamoto, S., et al., *Mesenchymal cells regulate the response of acute lymphoblastic leukemia cells to asparaginase.* J Clin Invest, 2007. **117**(4): p. 1049-57.
352. Sipkins, D.A., et al., *In vivo imaging of specialized bone marrow endothelial microdomains for tumour engraftment.* Nature, 2005. **435**(7044): p. 969-73.
353. Vilchis-Ordoñez, A., et al., *Bone Marrow Cells in Acute Lymphoblastic Leukemia Create a Proinflammatory Microenvironment Influencing Normal Hematopoietic Differentiation Fates.* Biomed Res Int, 2015. **2015**: p. 386165.
354. NHS. *Overview of Acute myeloid leukaemia*. 2019 [cited 2022 June 2022].
355. Juliusson, G., et al., *Acute myeloid leukemia in the real world: why population-based registries are needed.* Blood, 2012. **119**(17): p. 3890-9.
356. Institution, N.C. *SEER Statistics*. [cited 2022.
357. Ley, T.J., et al., *Genomic and epigenomic landscapes of adult de novo acute myeloid leukemia.* N Engl J Med, 2013. **368**(22): p. 2059-74.
358. Ding, L., et al., *Clonal evolution in relapsed acute myeloid leukaemia revealed by whole-genome sequencing.* Nature, 2012. **481**(7382): p. 506-10.
359. Bennett, J.M., et al., *Proposals for the classification of the acute leukaemias. French-American-British (FAB) co-operative group.* Br J Haematol, 1976. **33**(4): p. 451-8.
360. Bloomfield, C.D. and R.D. Brunning, *FAB M7: acute megakaryoblastic leukemia--beyond morphology.* Ann Intern Med, 1985. **103**(3): p. 450-2.
361. Lee, E.J., et al., *Minimally differentiated acute nonlymphocytic leukemia: a distinct entity.* Blood, 1987. **70**(5): p. 1400-6.
362. Duchayne, E., et al., *Diagnosis of acute basophilic leukemia.* Leuk Lymphoma, 1999. **32**(3-4): p. 269-78.
363. Society, A.C. *Acute Myeloid Leukemia (AML) Subtypes and Prognostic Factors*. 2018 [cited 2022.
364. Vardiman, J.W., N.L. Harris, and R.D. Brunning, *The World Health Organization (WHO) classification of the myeloid neoplasms.* Blood, 2002. **100**(7): p. 2292-302.
365. Estey, E. and H. Döhner, *Acute myeloid leukaemia.* Lancet, 2006. **368**(9550): p. 1894-907.
366. Döhner, H., et al., *Diagnosis and management of acute myeloid leukemia in adults: recommendations from an international expert panel, on behalf of the European LeukemiaNet.* Blood, 2010. **115**(3): p. 453-74.
367. Harris, N.L., et al., *World Health Organization classification of neoplastic diseases of the hematopoietic and lymphoid tissues: report of the Clinical Advisory Committee meeting-Airlie House, Virginia, November 1997.* J Clin Oncol, 1999. **17**(12): p. 3835-49.
368. Dombret, H. and C. Gardin, *An update of current treatments for adult acute myeloid leukemia.* Blood, 2016. **127**(1): p. 53-61.
369. Koreth, J., et al., *Allogeneic stem cell transplantation for acute myeloid leukemia in first complete remission: systematic review and meta-analysis of prospective clinical trials.* JAMA, 2009. **301**(22): p. 2349-61.

370. Thol, F., *What to use to treat AML: the role of emerging therapies.* Hematology Am Soc Hematol Educ Program, 2021. **2021**(1): p. 16-23.
371. Stone, R.M., et al., *Midostaurin plus Chemotherapy for Acute Myeloid Leukemia with a FLT3 Mutation.* N Engl J Med, 2017. **377**(5): p. 454-464.
372. Roboz, G.J., et al., *Updated safety of midostaurin plus chemotherapy in newly diagnosed.* Leuk Lymphoma, 2020. **61**(13): p. 3146-3153.
373. DiNardo, C.D., et al., *Safety and preliminary efficacy of venetoclax with decitabine or azacitidine in elderly patients with previously untreated acute myeloid leukaemia: a non-randomised, open-label, phase 1b study.* Lancet Oncol, 2018. **19**(2): p. 216-228.
374. Huntly, B.J. and D.G. Gilliland, *Leukaemia stem cells and the evolution of cancer-stem-cell research.* Nat Rev Cancer, 2005. **5**(4): p. 311-21.
375. Civini, S., et al., *Leukemia cells induce changes in human bone marrow stromal cells.* J Transl Med, 2013. **11**: p. 298.
376. Sansone, P. and J. Bromberg, *Targeting the interleukin-6/Jak/stat pathway in human malignancies.* J Clin Oncol, 2012. **30**(9): p. 1005-14.
377. Nefedova, Y., T.H. Landowski, and W.S. Dalton, *Bone marrow stromal-derived soluble factors and direct cell contact contribute to de novo drug resistance of myeloma cells by distinct mechanisms.* Leukemia, 2003. **17**(6): p. 1175-82.
378. Xia, B., et al., *c-Myc plays part in drug resistance mediated by bone marrow stromal cells in acute myeloid leukemia.* Leuk Res, 2015. **39**(1): p. 92-9.
379. Heasman, S.A., et al., *Protection of acute myeloid leukaemia cells from apoptosis induced by front-line chemotherapeutics is mediated by haem oxygenase-1.* Oncotarget, 2011. **2**(9): p. 658-68.
380. Bendall, L.J., et al., *Bone marrow adherent layers inhibit apoptosis of acute myeloid leukemia cells.* Exp Hematol, 1994. **22**(13): p. 1252-60.
381. Garrido, S.M., et al., *Acute myeloid leukemia cells are protected from spontaneous and drug-induced apoptosis by direct contact with a human bone marrow stromal cell line (HS-5).* Exp Hematol, 2001. **29**(4): p. 448-57.
382. Abdul-Aziz, A.M., et al., *MIF-Induced Stromal PKCβ/IL8 Is Essential in Human Acute Myeloid Leukemia.* Cancer Res, 2017. **77**(2): p. 303-311.
383. Yilmaz, O.H., et al., *Pten dependence distinguishes haematopoietic stem cells from leukaemia-initiating cells.* Nature, 2006. **441**(7092): p. 475-82.
384. Han, J., et al., *Adipose tissue is an extramedullary reservoir for functional hematopoietic stem and progenitor cells.* Blood, 2010. **115**(5): p. 957-64.
385. Ye, H., et al., *Leukemic Stem Cells Evade Chemotherapy by Metabolic Adaptation to an Adipose Tissue Niche.* Cell Stem Cell, 2016. **19**(1): p. 23-37.
386. Das, S.K., et al., *Adipose triglyceride lipase contributes to cancer-associated cachexia.* Science, 2011. **333**(6039): p. 233-8.
387. Tabe, Y., et al., *Bone Marrow Adipocytes Facilitate Fatty Acid Oxidation Activating AMPK and a Transcriptional Network Supporting Survival of Acute Monocytic Leukemia Cells.* Cancer Res, 2017. **77**(6): p. 1453-1464.
388. Lee, E.A., et al., *Targeting Mitochondria with Avocatin B Induces Selective Leukemia Cell Death.* Cancer Res, 2015. **75**(12): p. 2478-88.
389. Liu, Z., et al., *Mature adipocytes in bone marrow protect myeloma cells against chemotherapy through autophagy activation.* Oncotarget, 2015. **6**(33): p. 34329-41.

390. Duong, M.N., et al., *Adipose cells promote resistance of breast cancer cells to trastuzumab-mediated antibody-dependent cellular cytotoxicity.* Breast Cancer Res, 2015. **17**: p. 57.
391. Shafat, M.S., et al., *Leukemic blasts program bone marrow adipocytes to generate a protumoral microenvironment.* Blood, 2017. **129**(10): p. 1320-1332.
392. Drusbosky, L., et al., *Bone Marrow Endothelial Cells Protect Acute Myeloid Leukemia From Chemotherapy By Direct Contact: The BCAM/Laminin/VLA5 Axis As a Potential Therapeutic Target.* Blood, 2013. **122**(21): p. 2546.
393. Tran, J., et al., *A role for survivin in chemoresistance of endothelial cells mediated by VEGF.* Proc Natl Acad Sci U S A, 2002. **99**(7): p. 4349-54.
394. Gong, Y., et al., *Megakaryocyte-derived excessive transforming growth factor β1 inhibits proliferation of normal hematopoietic stem cells in acute myeloid leukemia.* Exp Hematol, 2018. **60**: p. 40-46.e2.
395. Chao, M.P., et al., *Calreticulin is the dominant pro-phagocytic signal on multiple human cancers and is counterbalanced by CD47.* Sci Transl Med, 2010. **2**(63): p. 63ra94.
396. Ha, Y., H. Wang, and Z. Shao, *Monocyte-Derived Macrophages Are Impaired in Myelodysplastic Syndrome.* Journal of Immunology Research, 2016.
397. Al-Matary, Y.S., et al., *Acute myeloid leukemia cells polarize macrophages towards a leukemia supporting state in a Growth factor independence 1 dependent manner.* Haematologica, 2016. **101**(10): p. 1216-1227.
398. Zhou, X., et al., *Tumor-Associated Macrophages Maybe Associated with Acute Myeloid Leukemia Survival and Prognosis.* Blood, 2017. **130**(Suppl 1): p. 5090.
399. Simsek, T., et al., *The distinct metabolic profile of hematopoietic stem cells reflects their location in a hypoxic niche.* Cell Stem Cell, 2010. **7**(3): p. 380-90.
400. Ito, K., et al., *Regulation of oxidative stress by ATM is required for self-renewal of haematopoietic stem cells.* Nature, 2004. **431**(7011): p. 997-1002.
401. Kohli, L. and E. Passegué, *Surviving change: the metabolic journey of hematopoietic stem cells.* Trends Cell Biol, 2014. **24**(8): p. 479-87.
402. Suda, T., K. Takubo, and G.L. Semenza, *Metabolic regulation of hematopoietic stem cells in the hypoxic niche.* Cell Stem Cell, 2011. **9**(4): p. 298-310.
403. WARBURG, O., *On the origin of cancer cells.* Science, 1956. **123**(3191): p. 309-14.
404. Suganuma, K., et al., *Energy metabolism of leukemia cells: glycolysis versus oxidative phosphorylation.* Leuk Lymphoma, 2010. **51**(11): p. 2112-9.
405. Skrtić, M., et al., *Inhibition of mitochondrial translation as a therapeutic strategy for human acute myeloid leukemia.* Cancer Cell, 2011. **20**(5): p. 674-88.
406. Boultwood, J., et al., *Amplification of mitochondrial DNA in acute myeloid leukaemia.* Br J Haematol, 1996. **95**(2): p. 426-31.
407. Papa, L., M. Djedaini, and R. Hoffman, *Mitochondrial Role in Stemness and Differentiation of Hematopoietic Stem Cells.* Stem Cells Int, 2019. **2019**: p. 4067162.
408. Kroemer, G., L. Galluzzi, and C. Brenner, *Mitochondrial membrane permeabilization in cell death.* Physiol Rev, 2007. **87**(1): p. 99-163.

409. Sakamuru, S., M.S. Attene-Ramos, and M. Xia, *Mitochondrial Membrane Potential Assay.* Methods Mol Biol, 2016. **1473**: p. 17-22.
410. Wiley, C.D., et al., *Mitochondrial Dysfunction Induces Senescence with a Distinct Secretory Phenotype.* Cell Metab, 2016. **23**(2): p. 303-14.
411. Marlein, C.R., et al., *NADPH oxidase-2 derived superoxide drives mitochondrial transfer from bone marrow stromal cells to leukemic blasts.* Blood, 2017. **130**(14): p. 1649-1660.
412. Phinney, D.G., et al., *Mesenchymal stem cells use extracellular vesicles to outsource mitophagy and shuttle microRNAs.* Nat Commun, 2015. **6**: p. 8472.
413. Davis, C.H., et al., *Transcellular degradation of axonal mitochondria.* Proc Natl Acad Sci U S A, 2014. **111**(26): p. 9633-8.
414. Moschoi, R., et al., *Protective mitochondrial transfer from bone marrow stromal cells to acute myeloid leukemic cells during chemotherapy.* Blood, 2016. **128**(2): p. 253-64.
415. Spees, J.L., et al., *Mitochondrial transfer between cells can rescue aerobic respiration.* Proc Natl Acad Sci U S A, 2006. **103**(5): p. 1283-8.
416. Dong, L.F., et al., *Horizontal transfer of whole mitochondria restores tumorigenic potential in mitochondrial DNA-deficient cancer cells.* Elife, 2017. **6**.
417. Hayakawa, K., et al., *Transfer of mitochondria from astrocytes to neurons after stroke.* Nature, 2016. **535**(7613): p. 551-5.
418. Plotnikov, E.Y., et al., *Cytoplasm and organelle transfer between mesenchymal multipotent stromal cells and renal tubular cells in co-culture.* Exp Cell Res, 2010. **316**(15): p. 2447-55.
419. Griessinger, E., et al., *Mitochondrial Transfer in the Leukemia Microenvironment.* Trends Cancer, 2017. **3**(12): p. 828-839.
420. Rustom, A., et al., *Nanotubular highways for intercellular organelle transport.* Science, 2004. **303**(5660): p. 1007-10.
421. Abounit, S. and C. Zurzolo, *Wiring through tunneling nanotubes--from electrical signals to organelle transfer.* J Cell Sci, 2012. **125**(Pt 5): p. 1089-98.
422. Lu, J., et al., *Tunneling nanotubes promote intercellular mitochondria transfer followed by increased invasiveness in bladder cancer cells.* Oncotarget, 2017. **8**(9): p. 15539-15552.
423. Onfelt, B., et al., *Structurally distinct membrane nanotubes between human macrophages support long-distance vesicular traffic or surfing of bacteria.* J Immunol, 2006. **177**(12): p. 8476-83.
424. Bénard, M., et al., *Structural and functional analysis of tunneling nanotubes (TnTs) using gCW STED and gconfocal approaches.* Biol Cell, 2015. **107**(11): p. 419-25.
425. Liu, K., et al., *Mesenchymal stem cells rescue injured endothelial cells in an in vitro ischemia-reperfusion model via tunneling nanotube like structure-mediated mitochondrial transfer.* Microvasc Res, 2014. **92**: p. 10-8.
426. Ahmad, T., et al., *Miro1 regulates intercellular mitochondrial transport & enhances mesenchymal stem cell rescue efficacy.* EMBO J, 2014. **33**(9): p. 994-1010.

427. Islam, M.N., et al., *Mitochondrial transfer from bone-marrow-derived stromal cells to pulmonary alveoli protects against acute lung injury.* Nat Med, 2012. **18**(5): p. 759-65.
428. Falchi, A.M., et al., *Astrocytes shed large membrane vesicles that contain mitochondria, lipid droplets and ATP.* Histochem Cell Biol, 2013. **139**(2): p. 221-31.
429. Wang, J., et al., *Extracellular vesicle cross-talk in the bone marrow microenvironment: implications in multiple myeloma.* Oncotarget, 2016. **7**(25): p. 38927-38945.
430. Corrado, C., et al., *Exosome-mediated crosstalk between chronic myelogenous leukemia cells and human bone marrow stromal cells triggers an interleukin 8-dependent survival of leukemia cells.* Cancer Lett, 2014. **348**(1-2): p. 71-6.
431. Nomura, S., et al., *Microparticles as Biomarkers of Blood Coagulation in Cancer.* Biomark Cancer, 2015. **7**: p. 51-6.
432. Ratajczak, J., et al., *Membrane-derived microvesicles: important and underappreciated mediators of cell-to-cell communication.* Leukemia, 2006. **20**(9): p. 1487-95.
433. Lamichhane, T.N., et al., *Emerging roles for extracellular vesicles in tissue engineering and regenerative medicine.* Tissue Eng Part B Rev, 2015. **21**(1): p. 45-54.
434. Surman, M., et al., *Deciphering the role of ectosomes in cancer development and progression: focus on the proteome.* Clin Exp Metastasis, 2017. **34**(3-4): p. 273-289.
435. Ablasser, A. and Z.J. Chen, *cGAS in action: Expanding roles in immunity and inflammation.* Science, 2019. **363**(6431).
436. Ablasser, A., et al., *cGAS produces a 2'-5'-linked cyclic dinucleotide second messenger that activates STING.* Nature, 2013. **498**(7454): p. 380-4.
437. Diner, E.J., et al., *The innate immune DNA sensor cGAS produces a noncanonical cyclic dinucleotide that activates human STING.* Cell Rep, 2013. **3**(5): p. 1355-61.
438. Gao, P., et al., *Cyclic [G(2',5')pA(3',5')p] is the metazoan second messenger produced by DNA-activated cyclic GMP-AMP synthase.* Cell, 2013. **153**(5): p. 1094-107.
439. Ishikawa, H. and G.N. Barber, *STING is an endoplasmic reticulum adaptor that facilitates innate immune signalling.* Nature, 2008. **455**(7213): p. 674-8.
440. Ergun, S.L., et al., *STING Polymer Structure Reveals Mechanisms for Activation, Hyperactivation, and Inhibition.* Cell, 2019. **178**(2): p. 290-301.e10.
441. Shang, G., et al., *Cryo-EM structures of STING reveal its mechanism of activation by cyclic GMP-AMP.* Nature, 2019. **567**(7748): p. 389-393.
442. Dobbs, N., et al., *STING Activation by Translocation from the ER Is Associated with Infection and Autoinflammatory Disease.* Cell Host Microbe, 2015. **18**(2): p. 157-68.
443. Gui, X., et al., *Autophagy induction via STING trafficking is a primordial function of the cGAS pathway.* Nature, 2019. **567**(7747): p. 262-266.
444. Schoggins, J.W., et al., *A diverse range of gene products are effectors of the type I interferon antiviral response.* Nature, 2011. **472**(7344): p. 481-5.

445. Liu, S., et al., *Phosphorylation of innate immune adaptor proteins MAVS, STING, and TRIF induces IRF3 activation.* Science, 2015. **347**(6227): p. aaa2630.
446. Honda, K. and T. Taniguchi, *IRFs: master regulators of signalling by Toll-like receptors and cytosolic pattern-recognition receptors.* Nat Rev Immunol, 2006. **6**(9): p. 644-58.
447. Wu, J., et al., *Interferon-Independent Activities of Mammalian STING Mediate Antiviral Response and Tumor Immune Evasion.* Immunity, 2020. **53**(1): p. 115-126.e5.
448. Decout, A., et al., *The cGAS-STING pathway as a therapeutic target in inflammatory diseases.* Nat Rev Immunol, 2021. **21**(9): p. 548-569.
449. Hou, Y., et al., *Non-canonical NF-κB Antagonizes STING Sensor-Mediated DNA Sensing in Radiotherapy.* Immunity, 2018. **49**(3): p. 490-503.e4.
450. Bakhoum, S.F., et al., *Chromosomal instability drives metastasis through a cytosolic DNA response.* Nature, 2018. **553**(7689): p. 467-472.
451. Kopitar-Jerala, N., *The Role of Interferons in Inflammation and Inflammasome Activation.* Front Immunol, 2017. **8**: p. 873.
452. Schmeisser, H., et al., *Identification of alpha interferon-induced genes associated with antiviral activity in Daudi cells and characterization of IFIT3 as a novel antiviral gene.* J Virol, 2010. **84**(20): p. 10671-80.
453. Liu, X.Y., et al., *IFN-induced TPR protein IFIT3 potentiates antiviral signaling by bridging MAVS and TBK1.* J Immunol, 2011. **187**(5): p. 2559-68.
454. Saitoh, T., et al., *Atg9a controls dsDNA-driven dynamic translocation of STING and the innate immune response.* Proc Natl Acad Sci U S A, 2009. **106**(49): p. 20842-6.
455. Liu, D., et al., *STING directly activates autophagy to tune the innate immune response.* Cell Death Differ, 2019. **26**(9): p. 1735-1749.
456. Prabakaran, T., et al., *Attenuation of cGAS-STING signaling is mediated by a p62/SQSTM1-dependent autophagy pathway activated by TBK1.* EMBO J, 2018. **37**(8).
457. Kawane, K., et al., *Chronic polyarthritis caused by mammalian DNA that escapes from degradation in macrophages.* Nature, 2006. **443**(7114): p. 998-1002.
458. Martinez, J., et al., *Microtubule-associated protein 1 light chain 3 alpha (LC3)-associated phagocytosis is required for the efficient clearance of dead cells.* Proc Natl Acad Sci U S A, 2011. **108**(42): p. 17396-401.
459. West, A.P., et al., *Mitochondrial DNA stress primes the antiviral innate immune response.* Nature, 2015. **520**(7548): p. 553-7.
460. Abdul-Aziz, A.M., et al., *Acute myeloid leukemia induces protumoral p16INK4a-driven senescence in the bone marrow microenvironment.* Blood, 2019. **133**(5): p. 446-456.
461. Livshits, M.A., et al., *Isolation of exosomes by differential centrifugation: Theoretical analysis of a commonly used protocol.* Sci Rep, 2015. **5**: p. 17319.
462. Mistry, J.J., et al., *ROS-mediated PI3K activation drives mitochondrial transfer from stromal cells to hematopoietic stem cells in response to infection.* Proc Natl Acad Sci U S A, 2019. **116**(49): p. 24610-24619.

463. Heckmann, B.L., et al., *LC3-Associated Phagocytosis and Inflammation.* J Mol Biol, 2017. **429**(23): p. 3561-3576.
464. Di Rosa, F. and R. Pabst, *The bone marrow: a nest for migratory memory T cells.* Trends Immunol, 2005. **26**(7): p. 360-6.
465. Fujisaki, J., et al., *In vivo imaging of Treg cells providing immune privilege to the haematopoietic stem-cell niche.* Nature, 2011. **474**(7350): p. 216-9.
466. Yamamoto, A., et al., *Bafilomycin A1 prevents maturation of autophagic vacuoles by inhibiting fusion between autophagosomes and lysosomes in rat hepatoma cell line, H-4-II-E cells.* Cell Struct Funct, 1998. **23**(1): p. 33-42.
467. Li, A., et al., *Activating cGAS-STING pathway for the optimal effect of cancer immunotherapy.* J Hematol Oncol, 2019. **12**(1): p. 35.
468. Luo, W., et al., *Critical Role of Cytosolic DNA and Its Sensing Adaptor STING in Aortic Degeneration, Dissection, and Rupture.* Circulation, 2020. **141**(1): p. 42-66.
469. Honda, K., et al., *IRF-7 is the master regulator of type-I interferon-dependent immune responses.* Nature, 2005. **434**(7034): p. 772-7.
470. Khozhukhar, N., et al., *Elimination of Mitochondrial DNA from Mammalian Cells.* Curr Protoc Cell Biol, 2018. **78**(1): p. 20.11.1-20.11.14.
471. Lai, C., K. Doucette, and K. Norsworthy, *Recent drug approvals for acute myeloid leukemia.* J Hematol Oncol, 2019. **12**(1): p. 100.
472. Hanayama, R., et al., *Autoimmune disease and impaired uptake of apoptotic cells in MFG-E8-deficient mice.* Science, 2004. **304**(5674): p. 1147-50.
473. Ferguson, T.A., et al., *Uptake of apoptotic antigen-coupled cells by lymphoid dendritic cells and cross-priming of CD8(+) T cells produce active immune unresponsiveness.* J Immunol, 2002. **168**(11): p. 5589-95.
474. Hugues, S., et al., *Tolerance to islet antigens and prevention from diabetes induced by limited apoptosis of pancreatic beta cells.* Immunity, 2002. **16**(2): p. 169-81.
475. Casares, N., et al., *Caspase-dependent immunogenicity of doxorubicin-induced tumor cell death.* J Exp Med, 2005. **202**(12): p. 1691-701.
476. Obeid, M., et al., *Calreticulin exposure dictates the immunogenicity of cancer cell death.* Nat Med, 2007. **13**(1): p. 54-61.
477. Bondanza, A., et al., *Inhibition of phosphatidylserine recognition heightens the immunogenicity of irradiated lymphoma cells in vivo.* J Exp Med, 2004. **200**(9): p. 1157-65.
478. Condeelis, J. and J.W. Pollard, *Macrophages: obligate partners for tumor cell migration, invasion, and metastasis.* Cell, 2006. **124**(2): p. 263-6.
479. Herrmann, M., et al., *Impaired phagocytosis of apoptotic cell material by monocyte-derived macrophages from patients with systemic lupus erythematosus.* Arthritis Rheum, 1998. **41**(7): p. 1241-50.
480. Baumann, I., et al., *Impaired uptake of apoptotic cells into tingible body macrophages in germinal centers of patients with systemic lupus erythematosus.* Arthritis Rheum, 2002. **46**(1): p. 191-201.
481. Cohen, P.L., et al., *Delayed apoptotic cell clearance and lupus-like autoimmunity in mice lacking the c-mer membrane tyrosine kinase.* J Exp Med, 2002. **196**(1): p. 135-40.

482. Jensen, P.K., *Antimycin-insensitive oxidation of succinate and reduced nicotinamide-adenine dinucleotide in electron-transport particles. II. Steroid effects.* Biochim Biophys Acta, 1966. **122**(2): p. 167-74.
483. Sies, H., *Oxidative stress: oxidants and antioxidants.* Exp Physiol, 1997. **82**(2): p. 291-5.
484. Redza-Dutordoir, M. and D.A. Averill-Bates, *Activation of apoptosis signalling pathways by reactive oxygen species.* Biochim Biophys Acta, 2016. **1863**(12): p. 2977-2992.
485. West, A.P., G.S. Shadel, and S. Ghosh, *Mitochondria in innate immune responses.* Nat Rev Immunol, 2011. **11**(6): p. 389-402.
486. Lavin, Y., et al., *Tissue-resident macrophage enhancer landscapes are shaped by the local microenvironment.* Cell, 2014. **159**(6): p. 1312-26.
487. Cummings, R.J., et al., *Different tissue phagocytes sample apoptotic cells to direct distinct homeostasis programs.* Nature, 2016. **539**(7630): p. 565-569.
488. A-Gonzalez, N., et al., *Phagocytosis imprints heterogeneity in tissue-resident macrophages.* J Exp Med, 2017. **214**(5): p. 1281-1296.
489. Roberts, A.W., et al., *Tissue-Resident Macrophages Are Locally Programmed for Silent Clearance of Apoptotic Cells.* Immunity, 2017. **47**(5): p. 913-927.e6.
490. Baratin, M., et al., *T Cell Zone Resident Macrophages Silently Dispose of Apoptotic Cells in the Lymph Node.* Immunity, 2017. **47**(2): p. 349-362.e5.
491. Zanoni, I., et al., *By Capturing Inflammatory Lipids Released from Dying Cells, the Receptor CD14 Induces Inflammasome-Dependent Phagocyte Hyperactivation.* Immunity, 2017. **47**(4): p. 697-709.e3.
492. Bode, C., et al., *Human plasmacytoid dentritic cells elicit a Type I Interferon response by sensing DNA via the cGAS-STING signaling pathway.* Eur J Immunol, 2016. **46**(7): p. 1615-21.
493. Curran, E., et al., *STING Pathway Activation Stimulates Potent Immunity against Acute Myeloid Leukemia.* Cell Rep, 2016. **15**(11): p. 2357-66.
494. Mullard, A., *Can innate immune system targets turn up the heat on 'cold' tumours?* Nat Rev Drug Discov, 2018. **17**(1): p. 3-5.
495. Fuertes, M.B., et al., *Type I interferon response and innate immune sensing of cancer.* Trends Immunol, 2013. **34**(2): p. 67-73.
496. Marcus, A., et al., *Tumor-Derived cGAMP Triggers a STING-Mediated Interferon Response in Non-tumor Cells to Activate the NK Cell Response.* Immunity, 2018. **49**(4): p. 754-763.e4.
497. Karaolis, D.K., et al., *3',5'-Cyclic diguanylic acid (c-di-GMP) inhibits basal and growth factor-stimulated human colon cancer cell proliferation.* Biochem Biophys Res Commun, 2005. **329**(1): p. 40-5.
498. Li, T., et al., *Antitumor Activity of cGAMP via Stimulation of cGAS-cGAMP-STING-IRF3 Mediated Innate Immune Response.* Sci Rep, 2016. **6**: p. 19049.
499. Demaria, O., et al., *STING activation of tumor endothelial cells initiates spontaneous and therapeutic antitumor immunity.* Proc Natl Acad Sci U S A, 2015. **112**(50): p. 15408-13.
500. Corrales, L., et al., *Direct Activation of STING in the Tumor Microenvironment Leads to Potent and Systemic Tumor Regression and Immunity.* Cell Rep, 2015. **11**(7): p. 1018-30.

501. Chao, M.P., et al., *Therapeutic Targeting of the Macrophage Immune Checkpoint CD47 in Myeloid Malignancies.* Front Oncol, 2019. **9**: p. 1380.
502. Liu, J., et al., *Pre-Clinical Development of a Humanized Anti-CD47 Antibody with Anti-Cancer Therapeutic Potential.* PLoS One, 2015. **10**(9): p. e0137345.
503. Behmoaras, J. and J. Gil, *Similarities and interplay between senescent cells and macrophages.* J Cell Biol, 2021. **220**(2).

8. Appendix

Number	Age	Sex	WHO diagnosis
AML1	77	M	AML not otherwise categorised
AML2	89	M	AML with maturation
AML3	72	M	AML with myelodysplasia-related changes
AML4	80	M	AML with monoblastic/monocytic lineage differentiation
AML5	58	M	AML with biallelic mutations of CEBPA
AML6	73	M	AML with minimal differentiation
AML7	37	M	AML without maturation
AML8	61	M	AML with mutated NPM1
AML9	54	M	AML with mutated NPM1
AML10	67	M	AML with mutated NPM1
AML11	58	M	AML with biallelic mutations of CEBPA
AML12	78	M	Acute monoblastic and monocytic leukaemia
AML13	54	F	Acute myeloid leukaemia with t(9;11)(p21.3;q23.3); KMT2A-MLLT3

Table 8.1. AML patient information from AML samples used.